

**PROBABILISTIC MICROMECHANICS OF CLAY COMPRESSION  
AND CONSOLIDATION**

**By**

**Rajab A. AL-Geroushi**

A thesis submitted to the Faculty of Graduate Studies and Research  
in partial fulfillment of the requirements for the degree of  
Doctor of Philosophy

Department of Civil Engineering and Applied Mechanics

McGill University

Montreal, Quebec

April, 1988

© AL-Geroushi Rajab (1988)

## ABSTRACT

In the light of new studies of physico-chemical analysis, fabric, and particle interaction, the consideration of the actual constitution of the soil media is required for actual prediction of the soil media performance under loads. This study has been restricted to the prediction of clay performance under compression loading.

A micromechanics approach has been used in this research; a microelement scale has been introduced and a set of formulations (i.e, stress transfer, fluid flow equation, and volumetric constitutive equation) has been developed for this scale. The passage from the microelement to the global scale has been established by using evolution equations. These equations have been solved by using numerical techniques (finite difference and finite element). The prediction of the developed models is discussed.

# ETUDE PROBABILISTIQUE DES MICROMECHANIQUES DE LA COMPRESSION ET DE LA CONSOLIDATION DE L'ARGILE

## RESUME

A la lumière de récentes études sur l'analyse physico-chimique, la fabrique et l'interaction des particules, il paraît fondamental de considérer de façon adéquate la constitution d'un sol pour prédire la performance de ce sol sous l'effet de charges. La présente étude a été axée sur la prédiction de la performance de l'argile sous l'effet de charges de compression.

Dans cette étude, une approche basée sur la micromécanique a été utilisée. Une échelle microélémentaire a été introduite et une formulation complète (transfert de contraintes, équation d'écoulement des fluides et équation constitutive de volume) a été développée pour cette échelle. Le passage de l'échelle microélémentaire à l'échelle globale a été établi à l'aide des équations d'évolution. Ces équations ont été résolues en utilisant les techniques de calcul numérique (éléments finis et différences finies). La prédiction des modèles développées est discutée.

## ACKNOWLEDGEMENTS

This work was carried out in the Department of Civil Engineering and Applied Mechanics under the direction of Dr. Raymond N. Yong, William Scott Professor of Civil Engineering and Applied Mechanics, and Director, Geotechnical Research Centre, to whom the author wishes to express his deepest gratitude for his inspiring motivation and brilliant guidance as well as his constant encouragement and valuable advice throughout this study.

In addition, the author is greatly indebted to Professor Axelrad of the Department of Mechanical Engineering, McGill University, for his stimulating discussions.

The author gratefully acknowledges the assistance of his colleagues in the Geotechnical Research Centre; especial thanks are due to Mr. A. M. O. Mohamed, Department of Civil Engineering and Applied Mechanics, and to Mr. E. Turcott-Rios, Department of Mechanical Engineering.

Special acknowledgement is due to the Scholarship Department of Garyounis University, Benghazi, Libya, for financial support and leave of absence for Ph.D. studies at McGill University.

The author extends his sincere appreciation to all the members of his family and all his friends, for their encouragement and moral support.



## TABLE OF CONTENTS

ABSTRACT	i
ACKNOWLEDGMENTS	iii
Table of Contents	iv
List of Figures	viii
List of Tables	xi
List of Flowcharts	xi
List of Symbols	xii
 <b>1-INTRODUCTION</b>	 1
1-1 FORWARD	1
1-2 PROBLEM DEFINITION	4
1-2-1 Objective	10
1-3 POINT OF VIEW AND THE BASIC PHILOSOPHY	11
1-4 THE PROGRAM STRATEGY AND ACTION PLAN	13
 <b>2-FABRIC ANALYSIS AND THE PHYSICS OF CLAY COMPRESSION</b>	 17
2-1 FABRIC ANALYSIS	17
2-1-1 Fabric Formation	18
2-1-1-1 Review	19
2-1-1-2 Identification I	21
2-1-1-3 Identification II	25
2-1-2 Fabric Scale For Soil Performance Prediction	31
2-2 THE PHYSICS OF CLAY COMPRESSION	35
2-2-1 Review	35
2-2-2 The Mechanism	37
2-2-2-1 The Mechanism Of Compression Under a Single Fixed Load	37
2-2-2-2 The Mechanism Of Compression Under Multiple Loads	49
2-3 SUMMARY	50
 <b>3- KINEMATICS OF DEFORMATION OF THE CLAY-WATER SYSTEM</b>	 52
3-1 OBJECTIVE	52
3-2 THE KINEMATICS OF DEFORMATION OF PARTICULATE SYSTEM	53
3-2-1 The Types of Deformations of Particulate Systems	54
i- Simple Deformation	54
ii- Constrained Generalized Deformation	55
ii-1 First Kind of Deformation Type B1	55

ii-1-a Two-Particles (Two-Clusters) Unit	55
ii-1-b Complete Fabric System	57
ii-1-c Two-Particle System Idealization	60
ii-2 Second Kind of Deformation Type B2	63
iii- Generalized Deformation	66
3-3 THE CONCEPT OF THE DIRECTOR THEORY	65
3-4 MATHEMATICAL MODELLING OF MICROSTRAIN	74
3-4-1 The Kinematics of Deformation of the First Region	78
3-4-1-1 Microstrain Formulation	83
3-4-2 The Kinematics of Deformation of the Second Region	99
3-4-2-1 Microstrain Formulation	101
3-5 VOLUMETRIC AND WEIGHT RELATIONSHIPS	107
3-5-1 The Concept of "the Compression Zone"	111
3-5-2 Void Ratio of the Macrostructural unit	117
3-6 FLUID KINEMATICS AND FLOW EQUATION	126
3-6-1 Review	130
3-6-2 Flow Equation Development	133
3-6-2-1 Mathematical Formulation	136
3-7 SUMMARY	144
<b>4- STRESS-COMPRESSIBILITY RELATIONSHIP</b>	146
4-1 FORWARD	146
4-2 LOCAL STRESS BALANCE	148
4-2-1 Calculation Of $\sigma^*$ from the Interaction Potential	154
4-2-1-1 General	154
4-2-1-2 Mathematical Formulation	157
4-2-2 Measurements of the Pore Water Pressure	161
4-3 CONSTITUTIVE MODELLING OF THE MACROSTRUCTURAL UNIT	165
4-3-1 General	165
4-3-2 Objective and Method of Approach	167
4-3-2-1 Intrinsic Time Measure	170
4-3-2-2 The First Region of Compression	172
4-3-2-3 The Second Region of Compression	179
4-3-3 Constitutive Equation	184
4-4 SUMMARY	190
<b>5- PASSAGE TO THE CONTINUUM (GLOBAL)</b>	192
5-1 GENERAL	192
5-2 REVIEW	193
5-3 AXIOMATIC RELATIONS FOR THE PASSAGE TO CONTINUUM	200

5-4 PROBABILISTIC APPROACH	209
5-4-1 Evolution Equation	212
5-4-2 Evolution Equation for the First Region	219
5-4-2-1 Calculation of the coefficients	224
5-4-3 Evolution Equation For the Total Region of Compression	230
5-5 MATHEMATICAL MODELLING OF THE OVERLAPPED REGION	233
5-5-1 The Intensity Parameter C	237
5-5-2 Implementation-Evolution Equation of the Overlapped Region	241
5-6 SUMMARY-THE EVOLUTION EQUATIONS	246
<b>6- THE FEASIBILITY OF APPLICATION OF THE EVOLUTION MODELS</b>	251
6-1 FORWARD	251
6-2 SUMMARY-EVOLUTION EQUATIONS USED	252
6-2-1 Geometrical Parameters	252
6-2-2 Stress-Modulus Parameters	259
6-3 APPLICATION-EVOLUTION EQUATIONS	260
6-3-1 Calculation Procedures of the Parameters	261
6-3-2 Discussion	266
<b>7-CONCLUSION, CONTRIBUTION AND RECOMMENDATIONS</b>	278
7-1 FORWARD	278
7-2 SUMMARY	279
7-3 CONCLUSION	284
7-4 CONTRIBUTION	287
7-5 RECOMMENDATIONS FOR FUTURE RESEARCH	289
<b>REFERENCES</b>	291
<b>Appendix A</b>	311
A-1 The Relation Between the Moments of Observed and Calculated Cluster Size Distribution	311
A-2 Numerical Technique for Solving Equation 3.37	314
<b>Appendix B</b>	316
B-1 The Development of the Conduit Flow Equation	316
B-2 The Development of the Hydraulic Radius (R)	319
<b>Appendix C</b>	321
C-1 The Computer Program for the Evolution Model of the First Region	321
C-2 The Computer Program for the Evolution Model of the Total Region of Compression	332

**Appendix D**  
D- Monte Carlo Simulation

335  
335

**Appendix E**  
E- Experimental Data

344  
344

## LIST OF FIGURES

No.	Caption	page
Fig. 1	Old fabric models	22
Fig. 2	Schematic clay particle arrangement	23
Fig. 3	Photomicrograph of St. Marcel Clay, on a vertical plane (a, x 3000; b, x 7000; c, x 15000) on a horizontal plane (d, X 3000; e, X 7000) (intact sample, natural water content 80%, cluster size=5 $\mu$ m) Delage et al. (1984)	26
Fig. 4	Photomicrographs of clay arrangement	27
Fig. 5	Schematic view of particulate system	32
Fig. 6	Schematic view of the consolidation process of the first region	40
Fig. 7	Schematic view of the creep process of the second region	46
Fig. 8	Time deformation for a clay soil showing first region, second region, and overlapped region	48
Fig. 9	The mechanism of type B1 deformation (two units)	58
Fig. 10	The mechanism of type B1 deformation (complete system)	61
Fig. 11	Two cylindrical shaped system idealization	62
Fig. 12	The definition and the mechanism of type B2 deformation for particulate system	64
Fig. 13	Schematic view of the topological structure of the clay medium	77
Fig. 14	Kinematics of deformation (type B1)	81
Fig. 15	The mechanics of deformation (type B1)	89
Fig. 16	Deformation field and sliplines	92
Fig. 17	Kinematics of deformation (type B2)	102

Fig. 18	Schematic view of the new fabric definition	124
Fig. 19	Computational flow scheme of probability distribution of $e_m$ , $w_m$ and $\rho_m$	127
Fig. 20	The mechanism of fluid flow	131
Fig. 21	Geometrical models for the flow equation	135
Fig. 22	Different channel conditions between two neighbor MSUs	137
Fig. 23	Schematic view of channels connected with the macropores	140
Fig. 24	The stress balance for the MSU	152
Fig. 25	Fabric formation	158
Fig. 26	Pore water pressure distribution	162
Fig. 27	The intrinsic time measure of the macrostructural unit	173
Fig. 28	The intrinsic time scale for the first region of compression	180
Fig. 29	Continuum experimental analysis	195
Fig. 30	Schematic view of the axiomatic structure of the passage to continuum	204
Fig. 31	Computational flow scheme of Monte-Carlo Finite Difference analysis (MFD)	209
Fig. 32	The plotting of Eq. 5.29 for different values of the intensity parameter( $\bar{C}_0$ )	229
Fig. 33	Computational flow scheme for modelling the total region of compression	238
Fig. 34	The probability distribution of macrostructural void ratio (photomicrograph from, Troucett 1988)	247
Fig. 35	Schematic view of the method of finding the initial tangent modulus of the first region	257
Fig. 36	The steps for finding the parameters of the second region of compression	263
Fig. 37	Schematic view of the solution	265

	technique for the overlapped region	267
Fig. 38-a	The average microconsolidation coefficient Monte Carlo Finite Difference Analysis(MFD) (100 Monte-Carlo run)	270
Fig. 38-b	The average excess pore water pressure (half length of the sample) MFD 100 run.	271
Fig. 38-c	The average excess pore water pressure for time-variable $\bar{C}_v$ and constant $\bar{C}_v$ (MFD, for constant $\bar{C}_v$ the subroutine UPDATE is excluded, 100 run).	272
Fig. 38-d	The average microstrain for different values of D (first region, MFD, 100 run)	273
Fig. 38-e	The average microstress for different values of D (MFD, 100 run)	274
Fig. 39-a	The average macrostructural void ratio for different values of D	275
Fig. 39-b	The average microstrain (it is calculated by two different numerical techniques; finite difference and finite element. Note: the computer time for FE is relatively larger than FD time, 70 run).	276
Fig. 39-c	The average microstrain for the total region of compression: first region, overlapped region and second region. Note: the computer time mainframe 25 minutes.	277

## LIST OF TABLES

No.	Caption	Page
Table 1	Volumetric-weight relationships of the MSU	110
Table 2	Compression zones formulation for different shapes	116
Table 3	Different stress balance equations for saturated soils	149
Table 4	Summary-evolution equations	249
Table 5	Summary-evolution equations	253
Table 6	Values for models prediction	268

## LIST OF FLOW CHARTS

No.	Caption	Page
Flow Chart 1	The program strategy	16
Flow Chart 2	Fabric scale for soil performance prediction	34
Flow Chart 3	The summary of the program strategy	280



## LIST OF SYMBOLS

SYMBOL	NAME
<b>Chapter 3</b>	
$a$	the cross sectional area of the channel
$\underline{a}$	the vector triad for the compression zone
$A$	the area enclosed between the two cluster units
$\underline{b}$	the vector triad for the compression zone
$\underline{c}$	a vector at right angle with plane of the two vectors $\underline{a}$ and $\underline{b}$
$c_s$	the shape factor of the channels
$\hat{c}$	$(3 \pi/4)^{1/3}$
$\underline{D}^{\wedge \Gamma}$	the vector joins the centre of the MSU( $\wedge$ ) and the centre of MSU( $\Gamma$ )
$E(r)$	the expected value of the radius $r$
$E(r)^n$	the $n$ -th moment of the radius $r$
$e_m$	the macrostructural void ratio
$e$	bulk void ratio
$\hat{e}_c$	the cluster void ratio
$f(y)$	probability density function of the observed radius of the spherical cluster unit

$f(v)$	probability density function of the volume of the cluster unit
$\tilde{g}(r)$	probability density function of the calculated radius of the spherical cluster unit
$g(r)$	function relationship between the radius and the volume
$K$	the permeability coefficient
$N_c$	the number of the cluster units in the MSU
$N_m$	the number of the MSU in the ensemble
$\tilde{N}^{\alpha\Lambda}$	the vector joins the centre of the cluster( $\alpha$ ) with contact( $i$ ) in the MSU( $\Lambda$ )
$P^\pi$	the excess pore water pressure in the MSU
$q_i$	the rate of flow per channel( $i$ )
$q_{net}$	the net of flow stored in the cavity
$R$	the hydraulic radius
$\tilde{r}_i(\tilde{r}_{22})$	the vector which describes the internal configuration of the individual particles
$S_v$	the average specific surface area
$\underline{S}_i(\underline{S}_i)$	unit vector
$S$	the degree of saturation of the MSU
$\underline{Y}^{\alpha\Lambda}$	the vector joins the centre of the cluster and the reference frame
$\underline{Y}^\Lambda$	the vector joins the centre of the MSU( $\Lambda$ ) and the reference frame
$\underline{Y}^{i\Lambda}$	the vector joins the contact( $i$ ) and the reference frame for MSU( $\Lambda$ )

$u$	unit vector at right angle to the plane of the two units
${}^{\alpha\wedge}U(t)$	the total displacement of the centre of the cluster unit( $\pi$ ) within MSU( $\wedge$ ) w.r.t. the centre of the MSU( $\wedge$ )
${}^{\alpha\wedge}U(t)$	the total displacement of the centre of the cluster unit( $\alpha$ ) within MSU( $\wedge$ ) with respect to the reference frame
$\Delta U_1$	the incremental displacement due to the top cluster unit displacement
$\Delta U_2$	the incremental displacement of the system (SU)
$\Delta U_3$	the incremental displacement due to the rotation of the SU
$\Delta U_4$	the incremental displacement due to the rotation of the top cluster unit
$\Delta U$	the total incremental change of position of the centre of the cluster unit( $\alpha$ ) within MSU( $\wedge$ )
$U$	the total displacement of the MSU
$V_m$	the volume of the MSU
$V_c$	the volume of the cluster
$v$	the volume enclosed by triad directors
$V_s$	the volume of solids(plates) within the cluster unit
$w_m$	the water content of the MSU
$w$	bulk water content of the soil sample
${}^{\alpha\wedge}Z$	the vector joins the centre of the cluster unit and the centre of the MSU
${}^{i\wedge}Z$	the vector joins the centre of the MSU to the point of the contact of the cluster

units

- $\omega$  the rotation vector at right angles with plane of motion and located at the centre of the bottom cluster unit
- $\omega'$  the rotation vector at right angles with plane of motion and located at the contact point of the two cluster units
- $\omega''$  the angular velocity of the vector at right angles of the plane of motion
- $\epsilon(t)$  the microstrain of the MSU (first region)
- $\epsilon'(t)$  the microstrain of the MSU (second region)
- $\psi^m$  the deformation gradient of the MSU (first region)
- $\psi'^m$  the deformation gradient of the MSU (second region)
- $\rho_m$  the saturated density of the MSU
- $\rho_w$  the density of water
- $\bar{\rho}_s$  the density of the cluster unit
- $\mu$  the average rate of number of the cluster units in the MSU
- $\zeta$  experimental fitting parameter
- $\tau_w$  the unit weight of water
- $\eta$  the coefficient of absolute viscosity

---

#### Chapter 4

- $\hat{a}, \hat{a}$  constants for the constitutive equation of the first region
- $dz_0$  intrinsic time scale (deviatoric)

$dz_H$	intrinsic time scale (volumetric)
$d\epsilon_D$	path length in deviatoric strain space (distortion measure)
$d\epsilon_H$	path length in volumetric strain space (volumetric measure)
$dc_1$	volumetric strain for the first region
$dc_2$	volumetric strain for the second region
$f_i$	the interaction forces between pair of particles
$F_i$	the interaction forces between two adjacent clusters
$m_1$	the tangent modulus of the compressibility of the MSU (first region)
$m_2$	the tangent modulus of the compressibility of the MSU (second region)
$sb_1, sb_2$	constants for the constitutive equation of the second region
$\sigma_a^m$	the total stress applied to the MSU
$\sigma_a^c$	the intercluster stress (mechanical stress)
$\sigma_a^{IP}$	the stress due to the interaction potential
$\sigma_a^m$	the applied stress which is taken by the solid part.
$\phi$	the interaction potential between two neighbor cluster units
$\phi$	the interaction potential between pair of clay particles
$\kappa_{10}$	material properties which represent the volume change

due to the over all shear  
(dilatancy)

$k_v$  material properties which  
represent the cavity volume  
decrease due to shear at the  
contacts (overall volume change)

$v$  constant parameter for the  
constitutive equation

$v_I$  structural viscosity of the MSU  
(first region)

$v_{II}$  structural viscosity of the MSU  
(second region)

---

## Chapter 5

$\tilde{C}_v$  microconsolidation coefficient

$C_v$  Terzaghi coefficient of  
consolidation

$\tilde{C}_0$  the intensity parameter for  
the overlapped region

$\tilde{C}$  drift coefficient  $= \langle \Delta w / \Delta t \rangle$

$\tilde{\tilde{C}}$  diffusion coefficient =  
 $\langle (\Delta w)^2 / \Delta t \rangle$

$j$  the number of the MSUs which  
behave as type B1

$K_{(j), (k), \dots}$  the coefficients of the  
differential equation

$N_m$  the number of the MSUs per  
ensemble

$Pr(.)$  probability distribution

$Pr(.|..)$  the conditional probability  
distribution

$t$  local time

$w$  random variable

$x(t)$  denotes the number of survival  
in time interval  $(0, t)$ , i.e., the  
number of the MSUs which behave  
as type B1

$\alpha_i$  constant parameter

$\beta$	constant which relates the rate of change of the excess pore water pressure to the rate of change of the effective stress
$\epsilon_{ov}$	the volumetric microstrain for the overlapped region
$\tau(t)$	input to the microelement system (e.g. stress)
$u(t)$	response of the microelement system (e.g. strain)
$f$	represents the mapping from the input to the response for the microelement
$\gamma$	subset in the banach space (for the input)
$\zeta$	subset in the banach space (for the response)
$\Omega$	the total subset in the banach space
$\Pi$	the mapping from the local to the global
$\theta$	an element in the banach space (e.g. local strain at time $t$ )
$\theta$	an element in the banach space (e.g. local strain at time $t + \tau$ )
$\tau(t)$	input to the ensemble (e.g. stress)
$u(t)$	response of the ensemble (e.g. strain)
$f$	represents the mapping from the input to the response for the ensemble
$\gamma$	subset in the banach space (for the input)
$\zeta$	subset in the banach space (for the response)
$\Omega$	the total subset in the banach space

$\chi$

an element in the banach space  
(e.g. stress, global)

Banach  
space

is the set which has properties  
very useful in construction of the  
function relationship between the  
input and the response of a system

---

## Chapter 6

$\bar{b}$

constant parameter

H

the height of the test sample

$\bar{m}$

the initial tangent modulus of  
the global test sample

$T_1$

the test time for the first  
region and the overlapped region

$T_2$

the test time for the second region

---

## Mathematical Symbols

$\sim$

denotes vector quantity

$\approx$

denotes tensor quantity

$\langle \rangle$

denotes the average

$\epsilon$

element of

$\cup$

union

$\Delta$

denotes increment



Mapping



## CHAPTER 1

### INTRODUCTION

#### 1-1 FORWARD:

Today's increasing demands for better capability in design and analysis in geotechnical engineering practices are reflected in corresponding requirements for more accurate predictions of the performance of soils under load. To respond to these needs and requirements, soils have to be treated according to **their actual physical constitution.**

Actual soil is not really a continuum, but a collection of 'particles.' Information about the arrangement and the interaction of these particles is **fundamental** to describe soil performance. The problem of soil stability under different boundary conditions has been considered mainly from the continuum mechanics point of view. Therefore the difficulty in this approach is that particle arrangements and interactions are not expressible in terms of continuum theories.

Soil stability can be defined as the integrity of the soil system against a physical disturbance to prevent shear failure or excessive settlement. These are all tied into the mechanistic picture of the shear

strength, compressibility, and permeability. Different soil stability problems have been dealt with by different continuum theories.

Continuum mechanics is based on the idea that all material bodies possess continuous mass densities, and that the laws of motion and the axioms of constitution are valid for every part of the body regardless of its size. Continuous media are dense collections of point masses; i.e., concentrated infinitesimal masses devoid of internal structure.

As a physical theory, continuum mechanics has found wide acceptance, especially in the geotechnical engineering discipline. However, inherent in the continuum viewpoint are drastic limitations on the extent to which continuum descriptions of macroscopic behaviour can successfully mirror the soil structure. The limitations become more acute as more refined and more complete descriptions of soil behaviour and performances are sought.

Hence, in order to describe and model the physics of soil performance under different boundary conditions, geometrical arrangement of the particles and voids and particle interaction should be included in establishing the mathematical model. In modern soil mechanics, the geometrical arrangement and the particle interaction can be put under the heading "soil

structure". We include the soil structure in mathematical modelling by using the micromechanics approach.

The term "micromechanics" for the purposes of the present investigation is introduced to relate the observable macroscopic response behaviour of the network of the soil system to the microstructural characteristics of such a network. Within the framework of this mechanics, the system under consideration is regarded as a discrete ensemble of microelements.

An attempt to consider the soil structure in the modelling of soil performance under applied load was done by Baker, in his thesis (Baker, 1971). He has modified the continuum theory in such a way that it is capable of including the concept of soil structure. Baker has used the concept of "directors" in a deterministic way. He did not solve a particular problem, but he incorporated a body of knowledge on the nature of the interparticle forces and the particle arrangement into continuum theory.

Numerous attempts to develop micromechanics theories for different materials have been considered in the literature. For example, the foundations of the micromechanics of fibers and polycrystal metals have been established by Axelrad (1978 and 1984). Bazant and

his coworkers (Zubelewicz et al. (1987), and Bazant et al. (1985 and 1986)) have introduced different micromechanics concepts for development of constitutive equations for geomaterials (such as soils, rocks and concrete). Nemat-Nasser and his coworkers (Oda (1972 and 1977), and Nemat-Nasser et al. (1980 and 1983)) have worked at the microlevel in the mechanics of the granular materials.

These works and others will be discussed in detail in the following chapters. Further in this study, the foundations of the micromechanics of clay soil under compression loading will be established. In this chapter, the problem definition, the objective of this study and the method of approach will be discussed.

## **1-2 PROBLEM DEFINITION:**

The general problem which this work addresses is the performance of fully saturated clay under compression loading. The compressibility describes the volumetric response behaviour of the soil mass. It is not restricted to the volume change due to the extrusion of pore water but includes the volume change due to the particle rearrangement and interaction without measurable water extrusion.

Since Terzaghi developed his consolidation theory, two global mechanisms of clay performance under applied

load have been discussed in the literature:

**a- Mechanism I (Terzaghi, 1925):** The sole cause of delay in compression is the time required for the water to be squeezed out, i.e., the permeability of the clay. According to this concept clay compression is divided into three regions; primary compression, consolidation, and secondary compression. Terzaghi's theory is the consolidation part of the compression process. In this mechanism, the consolidation period of soil layers of various thicknesses will be proportional to the squares of the thicknesses of these layers.

**b- Mechanism II (Taylor and Marchent, 1940):** The total resistance to volume change or clay compression comes partly from permeability and partly from the structural resistance of the clay itself, i.e., the structure of the clay itself possesses a time dependent resistance to compression. According to this concept, there is no division between consolidation and secondary compression. The consolidation periods of soil layers with various thicknesses will no longer be proportional to the squares of the thicknesses of these layers.

Mechanism II is realistic in representing the physics of the compression performance of clay soil because it includes the internal state of the material, i.e., the structural resistance of the clay. Therefore,

it represents the process of compression as one complete process, without division between the consolidation and secondary compression. This structural resistance can be represented by the soil structure.

A large amount of work has been done on consolidation and compression following both mechanistic routes (Mechanism I and Mechanism II). These developments have been mostly in the continuum direction and for the second mechanism, continuum rheological models are considered. In the following sections, we will discuss the research works which have attempted to include the soil structure.

De Josselin de Jong (1968) has developed a consolidation model from two separate models, namely the concept of the viscoelastic analysis and cavity channel networks. He has shown that both models gave the same effect of time-delay on compressibility. However, the definition of the excess pore water pressure for the cavity channel model is not clear. Furthermore, an explicit definition of the soil structure is, also, not clear. On the other hand, using modern test techniques, for example scanning electron microscopy, Yong and Sheeran (1973), and Yong and Warkentin (1975) have explained the compression performance of clay soil through the fabric unit interaction and rearrangement. This compression is

classified in terms of dominant drainage characteristics which depend on the pore size distribution. They classify the flow into two kinds which are not separable: the flow through the macropores, and from the micropores into the macropores. Hence, their description has been from the mechanics of fluid flow.

Meanwhile, by experimentally using electron microscopy and thin section analysis, McConnachie(1974) has demonstrated that reorientation of the fabric units as well as the changes of the pore size are caused by the applied load. Furthermore, he has found that the fabric changes its size when the load is beyond  $0.15 \text{ Kg/cm}^2$ . In recent work with natural clay, Delage and Lefebvre (1984) have performed scanning electron microscopy and mercury porosimetry on samples of Champlain clay from Quebec. They have demonstrated that the micropores within the fabric unit and the macropores (interfabric voids) contribute 30% and 70% of the total void ratio respectively. In addition, during the process of consolidation, the macropores will close first.

Several works on the probabilistic analysis of clay consolidation have been introduced in the literature. These works, in general, support the concept of including more information about the local properties of the clay soil i.e., soil structure, in

modelling the clay consolidation and compression. In the following section, we will discuss some of these works.

Freeze (1977) used a general diffusion equation to predict the consolidation of clay soil. However, he has considered soil properties such as the coefficient of compressibility, permeability and porosity as random variables, multivariate normal. He used the Monte Carlo Simulation to predict the pore pressure and settlement. This paper has not considered the clay structure and its intrinsic stability. However, its analysis offers some kind of understanding of the variability of the continuum parameters. This work supports the idea of including more information about the internal properties of the material which can reflect the variability of the continuum parameters and the heterogeneity of the soil.

Marsal (1965), and Athanasiou-Grivas and Harr (1978) have considered the compression of the clay (consolidation part only) from the theory of probability. They have implemented the simple random walk for grain particles to advance under compression loads. They have demonstrated that the final formulation is similar to Terzaghi's equation. These papers did not explain the physics of compression. Furthermore, their approach is a continuum approach and there were no constitutive laws governing the grain



particle advances. However, this approach provided an initial step towards including more information about the local properties of the soil (i.e., soil structure).

Chang(1985) has considered the consolidation of clay soil from Terzaghi's equation for one layer and for multilayers, but he inputs the soil property (coefficient of consolidation), as random variable, specifically, as Gamma distribution.. He has demonstrated that the variability in the coefficient of consolidation has a high impact on the prediction of the true excess pore water pressure.

Among others, Kitamura (1978, 1981 and 1985) has considered the local properties of granular materials. In his analysis, he has proposed the Markov theory to describe the deformation process of granular materials under loads. He has also used the generalized Fokker-Planck equation for the development of the stress-strain law. The state parameters which are used in the Fokker-Planck equation are the direction cosines of the normals at the contacts between the particles.

Hence, from the above discussion, the fundamental importance of including the "soil structure" in modelling clay performance under compression loads becomes clear. This inclusion not only gives a realistic description and a better prediction of the

compression process of clay systems than classical theories, but also solves two fundamental problems. First, the performance prediction of a highly compressible clay system in which its macropores (pores between the aggregate of clay particles) contribute more than 50% of the total pore voids, and therefore, the description of the collapse state of the macropores, under applied loads, is essential. Secondly, when environmental changes can alter the properties and the status of the material, (i.e., the status of soil structure), the performance of the clay system under compression loads can change in sympathy to the environmental changes.

From an engineering point of view, the above two problems (i.e., the supportability of highly compressible clay for land development, and the variation of geotechnical properties of clay soil under the environmental changes) are facing the geotechnical engineer in everyday engineering practice. Hence the work described in this thesis is the development of the **fundamental aspects** of the performance of clay soil under compression loading.

#### 1-2-1 Objective:

The objective of this research is to develop a mathematical model for saturated clay compression and consolidation, in which the concept of soil structure (the local state of the clay) plays its natural central

role. Such models should be able to give a better representation of the behaviour of actual soil under different status of loading and environmental conditions.

### 1-3 POINT OF VIEW AND THE BASIC PHILOSOPHY:

The preceding discussion highlights the importance of including the soil structure in modelling clay compression performance. In this section, we will give our point of view of the mathematical technique that can reconcile the actual physics of the compression performance.

The probabilistic nature of the properties should be recognized and accounted for because of the following: 1- the inherent variability of the soil properties and conditions; 2- the difficulty in the portrayal of the relative importance of a given set of local parameters which describe these properties and conditions; 3- our inability to predict global behaviour when the microelement performance is developed.

The basic philosophy of the probabilistic input and response of soil system can be considered in the following two conditions:

a-When the emphasis is in the uncertainty and

variability of the system properties, the input should be put in deterministic form. Therefore, the consequence of these variabilities can be seen in the output variability. It helps in identifying the important parameters of the system that are essential in the modelling and prediction of the overall performance of the system.

b-When the emphasis is in the variability and the uncertainty of the input, the system properties should be put in deterministic form. Therefore, the consequence of these variabilities can be seen in the output. It also helps in identifying the important parameters for modelling. In our work the emphasis is on the variability of the soil system properties, and therefore, the input loads will be put in a deterministic form.

In discussing the basic philosophy and the procedures for the development of the micromechanics approach, we include two environments, namely; the deterministic environment (D.E.) and the probabilistic environment (P.E.). The procedure for working in the former environment (D.E.) consists of:

1. Establishing a physical scale (microelement) for the discrete system.
2. Development of a mathematical model (state function) to describe the "law of performance" of the physical model.

Finally, the latter environment (P.E.) can be considered by establishing the following two steps:

1. Randomness of the state function. If the randomness of the process is a point in time and/or space, then the process can be represented by a random variable. If the randomness of the process is "history" in time and/or space, then it can be represented by a stochastic process.
2. Passage of the microelement performance to the global (ensemble of microelements). This is done by using an evolution equation.

It should be noted that there is a link between the two environments. This link gives one of the peculiar features of our micromechanics theory. These two environments will be discussed in the following chapters.

#### **1-4 THE PROGRAM STRATEGY AND ACTION PLAN:**

The thesis is divided into the following major portions(see Flow Chart 1):

**I- Fabric analysis and the physics of clay compression:**  
the following points will be discussed:

a- The definition of the fabric and geometric parameters, and the local scale that have meaningful

description and can model the global clay behaviour.

b- The postulation of the mechanism of clay compression in light of modern soil mechanics of fabric formation, and the substantiation of this postulate, through existing experimental test programs.

## **II- The kinematics of deformation of the clay water system:**

Once the local scale or microelement from the above analysis is established, the following points will be developed:

a- The kinematics and deformations of the microelement under applied stress. The concept of the directors will be employed.

b- Volumetric-mass relationship. The volume-mass relationship for the microelement and the ensemble of microelements will be discussed as well as how to develop the void ratio. The water content of the microelement will be also developed.

c- The fluid movement from the microelement. Newton's law of fluid movement will be applied.

**III- Stress-Compressibility relationship:** In discussing the internal stress applied to the microelement, the following two points will be established:

a- Local stress balance of the microelement, and its components.

b- Local stress-strain relationship.

#### IV- Passage to the continuum:

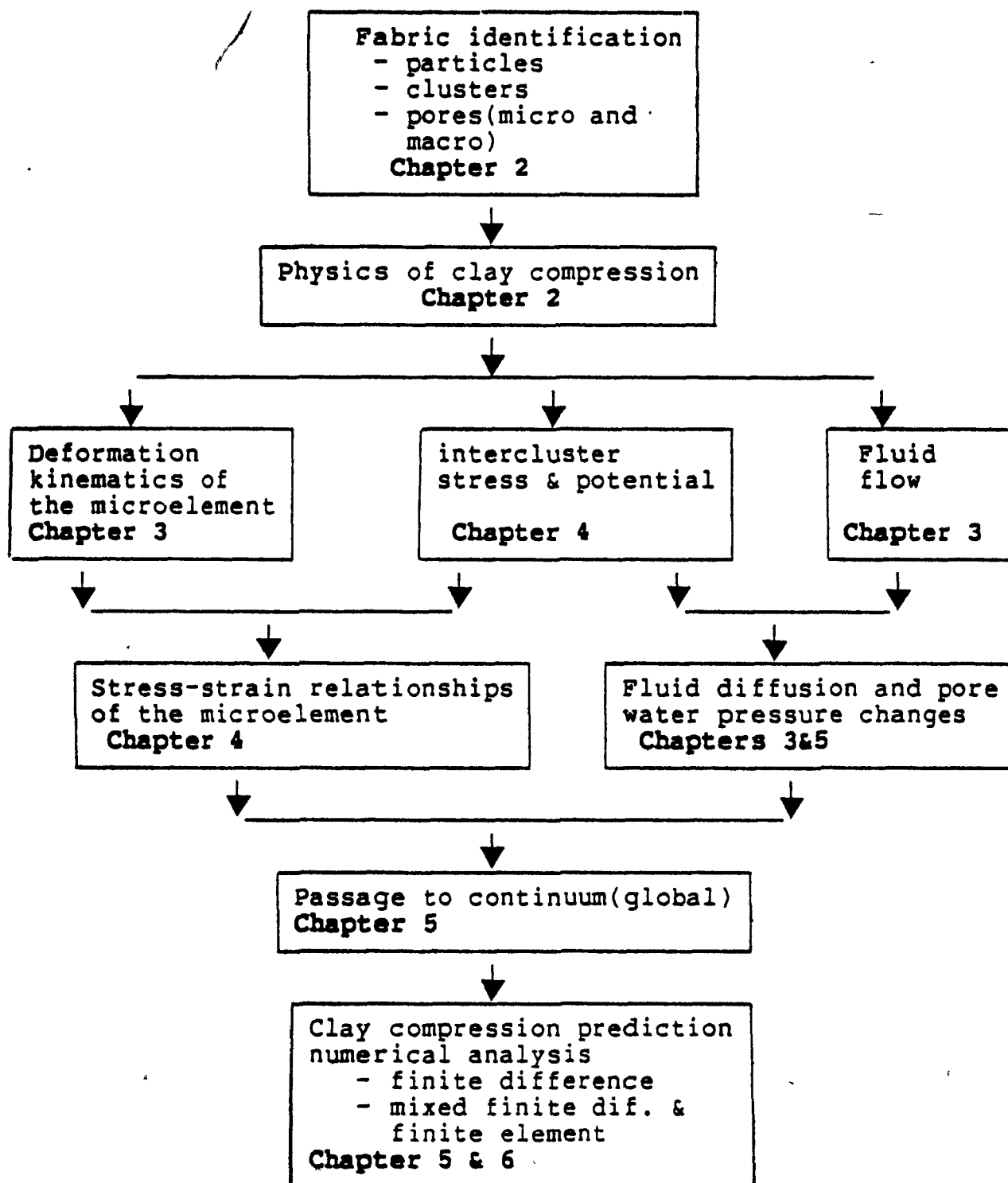
The passage from clay-water microelement performance to the global clay-water mass performance will be done by using the evolution equation in the probabilistic sense. To do that, the following two points will be established:

- a- The axiomatic structure of the passage.
- b- The concept of the "intrinsic soil structure variability".

V-An analytical model will be developed for the overlapped region of the compression time process.

The feasibility of application of the developed models will be discussed.

The thesis is composed of seven chapters, and five appendices which provide all supporting materials. All the above parts are divided into four chapters.



Flow Chart 1 The program strategy



## CHAPTER 2

## FABRIC ANALYSIS AND THE PHYSICS OF CLAY COMPRESSION

## 2-1 FABRIC ANALYSIS:

In the introductory chapter, we have stated that in order to develop the compression performance of the clay system, internal physical parameters which reflect the physics of the material should be included. These parameters are established from the internal structure and the fabric of the clay system. Soil structure as a property includes two elements, fabric and forces.

A-Fabric: i) the gradation and the arrangement of the particles, and the configuration of this arrangement; ii) pore size distribution and the interpore connections between the individual particles and particle groups. The clay system is viewed as liquid-in-solid not solid-in-liquid. Hence the solid material must be sufficiently close to develop the fabric or geometric system. We assume the fluid is a continuum substance, i.e., it has no fabric or structure. But, the dipolar character of the fluid and the properties of the adsorbed water must be considered, as they affect the behaviour of the clay via the interaction forces.

B-Forces: i) the forces which originate from the interaction potential (intercluster forces and interparticle forces) between the clay particles. These forces depend on the clay-water-electrolyte system of the medium. ii) The forces which arise from the friction and/or the adhesion between the clay particles. These forces depend on the surface properties of clay particles. The forces will be considered in detail in Chapter 4.

An assessment of soil structure and fabric is required for proper evaluation of soil performance. It will help in:

- 1- determination and establishment of the pertinent soil properties and characteristics, and
- 2- formulation of a physical model that can describe the interaction of the various physical components, and that can predict the integrity of the soil mass system under various stages of loading that impact on the boundary of the system.

#### **2-1-1 Fabric Formation:**

For natural soils, the fabric formation and soil structure depend on a complex interaction of a large number of factors operating at the time of deposition. Some of these factors are:

- a- Clay content, organic content and minerology.

b- Silt and sand content, and the shape and the size of the particles.

c- The rate and the mode of sedimentation, and facies models (sedimentation models) for sabkha deposits.

d- State of agitation, depth of water and seasonal drying out of the subsoil.

e- Electrolyte concentration at deposition.

f- The concentration of sediment being deposited (overburden pressure).

It must be noted that the dynamic equilibrium of soil structure and fabric at the time of formation is not necessarily the same as that at a later date.

#### 2-1-1-1 Review:

The history of development of models for soil fabric started when Terzaghi(1925) realized that the interpretation of certain phenomena in soil, (the clay sensitivity and the origin of cohesion), must include the concept of fabric. No techniques for observation, however, were available at that time. As a result, purely ad-hoc models were devised and used to interpret certain clay properties.

These types of models included, first, Terzaghi's concept of a honeycomb structure where the clay particles stick to each other at the point of contact to build up this structure. Second, the Casagrande

model (1932) postulated that the "honeycomb" structure existed in sensitive marine soils (see Fig. 1a). Goldschmidt(1926) was of the opinion that the clay particles in highly sensitive clays were arranged in unstable "cardhouse" arrangements.

In later years, developments were made which involved the consideration of the double layer theory. Lambe (1953,1958) examined the fabric of inorganic soils, and he presented clay mineral arrangements associated with deposition in a range of electro-chemical environments from fresh water to marine (see Fig. 1b). Van Olphen (1963) summarized the various modes of particle association in clay suspension edge-to-edge and edge-to-face flocculated systems.

Tan (1957) presented a schematic picture of a clay particle network. He then suggested that the three-dimensional clay platelet arrangements were one of the contacts between one clay platelet and the plane of another (see Fig. 1c).

When the observation of soil fabric has been examined by using the transmission and scanning electron microscopy, much information on fabric viewing has been obtained: See Barden et al.(1971), Collins and McGown (1974), Pusch(1970,1973 a,b,c), Smart(1969), Yong (1971), Yong and Sheeran (1972) and others.

We can conclude, generally, that in natural and in synthetic clay soil, the single clay particle can be easily distinguished. We note that, by-and-large, the clay particles tend to form identifiable groups (group units) or aggregations. These group units can be identified as fabric units (see Figs. 2 and 3).

}

In this work, the fabric unit will be considered as the first order of identification. The geometrical arrangement of single particles within each fabric unit will be considered as the second order of identification.

From these identifications, we can distinguish between different types of pore space distribution. The total arrangement of all particles, fabric units and voids compose the total fabric of the clay soil system. The fabric features observed can be divided into two levels of viewing.

#### 2-1-1-2 Identification I:

In this scale of viewing, the fabric unit arrangements and the pore space between them are observed. In the case of clays, single particles will not be distinguishable at this level of viewing. The fabric units identified consist of several particles or groups of particles. These fabric units are defined as **clusters**, which have definable physical boundaries and a specific mechanical function. They act effectively as

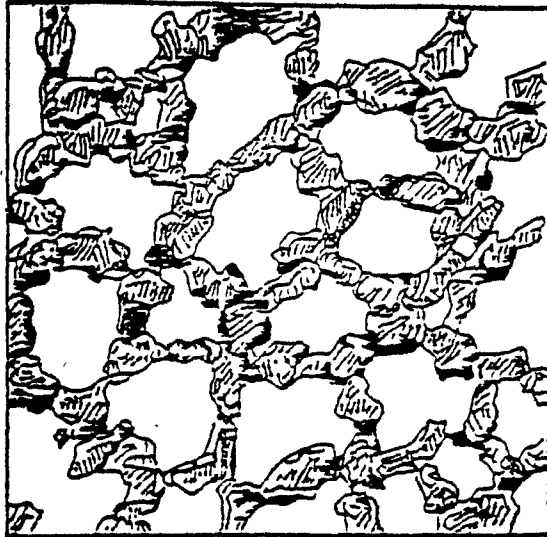


Fig. 1-a The Honeycomb Structure

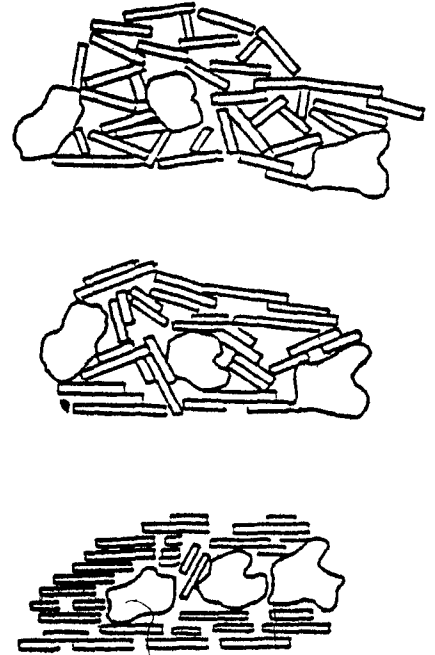


Fig. 1-b Structure of Natural Soil  
(Lambe 1958)

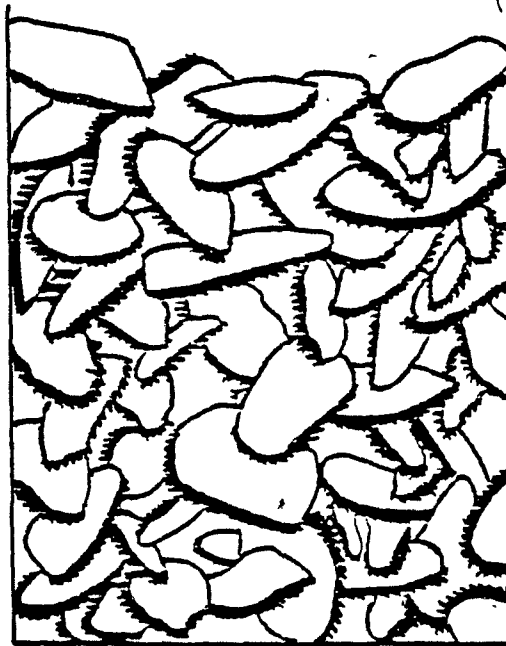
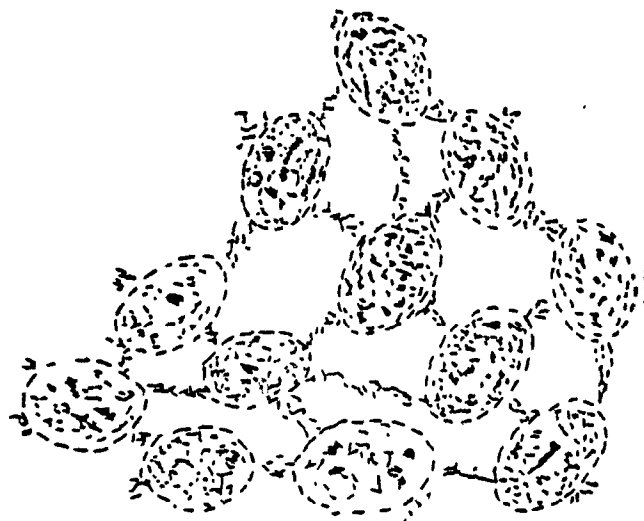
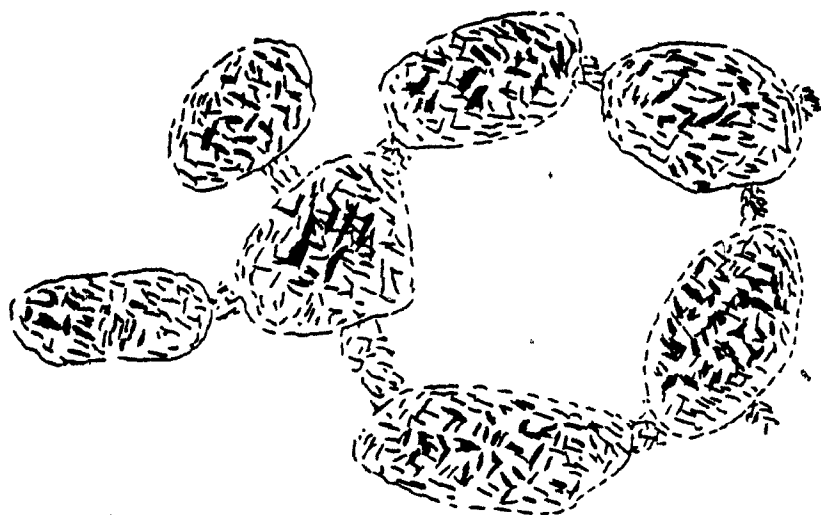


Fig. 1-c Clay Network (Tan 1957)

Fig. 1 Old Fabric Models



**Fig. 2-a Clay deposited in fresh water**  
(Pusch, 1973)



**Fig. 2-b Marine clay with**  
**large, dense aggregates separated by large voids**  
(Pusch, 1973)

**Fig2 Schematic clay particle arrangement**

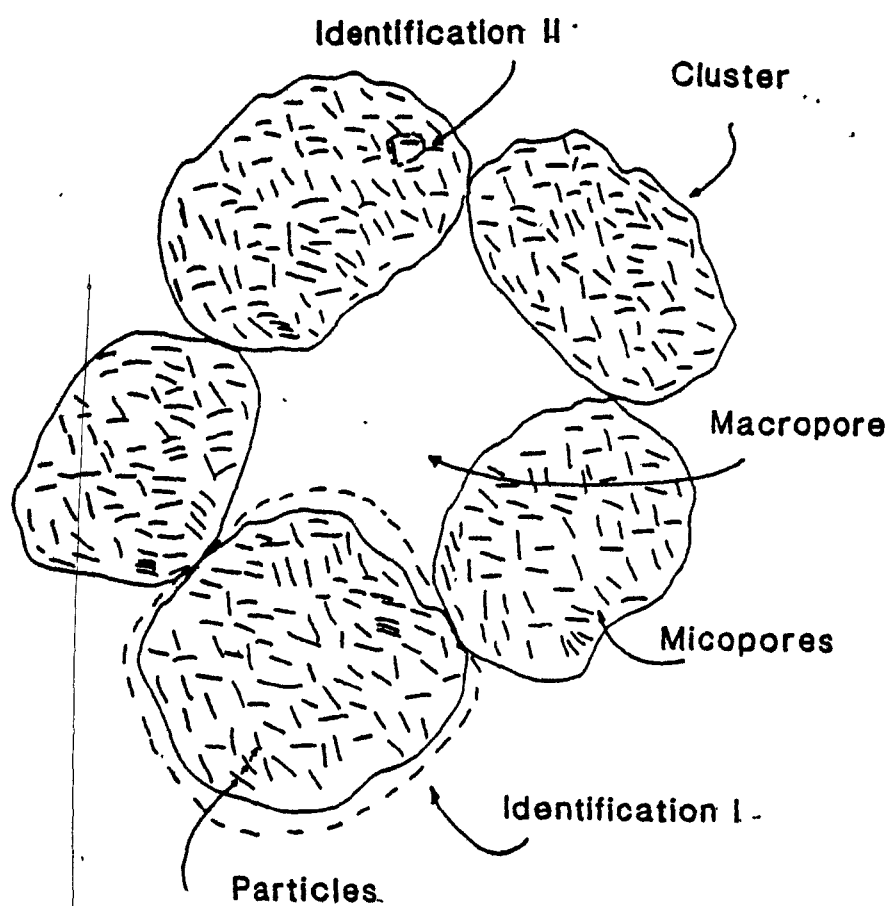


Fig. 2-c Schematic View of Clay Identification



individual units. These clusters can be combined to form peds (group of clusters).

The pore space between fabric units can be observed, depending on the shape and the arrangement of the fabric units. We define this pore space as a **macropore**. In identifying and characterizing the network of fabric units, it is necessary to take into account the fabric unit's pore space.

#### 2-1-1-3 Identification II/

In this scale of viewing, the arrangement of particles within the fabric unit, and the pore space between particles within the fabric unit are observed. Single or individual clay particles can be distinguished at this level of viewing. The small fabric units or the subfabric units can also be observed and distinguished at this level of viewing. Domain units consisting of two or more particles, can act as one unit. Several domains could combine to form a cluster.

The pore space within the cluster is defined as a **micropore**. The micropore distribution, shape and size depend on the arrangement of the particles, in edge-to-edge, edge-to-face and face-to-face associations.

Figures 2, 3 and 4 show the schematic and

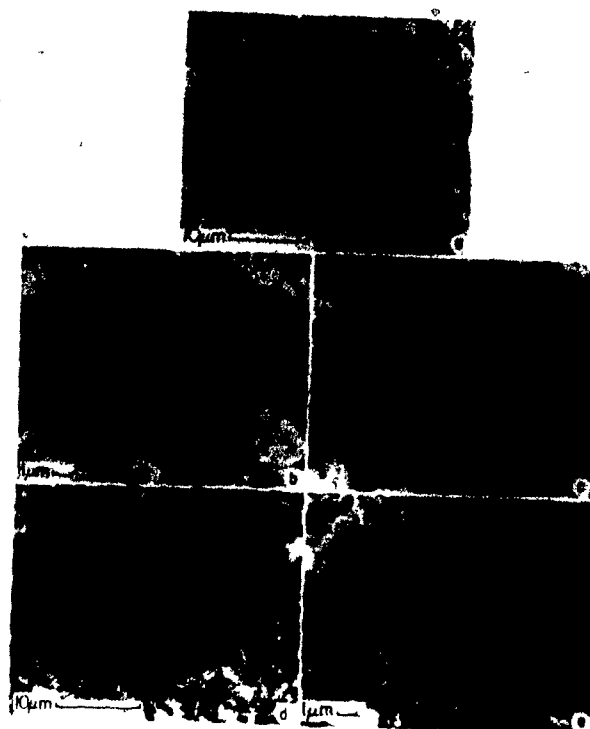
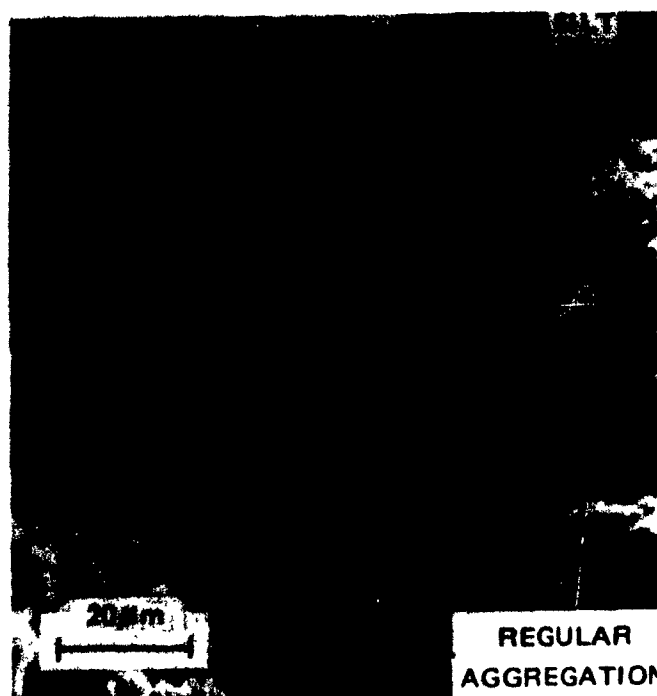


Fig. 3 Photomicrograph of St. Marcel Clay, on a Vertical Plane  
(a, x 3000; b, x 7000; c, x 15,000) on a Horizontal Plane  
(d, x 3000; e, x 7000) (intact sample, natural water  
content 80%, cluster size = 5 µm)

Delage et al. (1984)



a. Natural Silty Clay Sample (Collins and McGown 1974)

Fig. 4 Photomicrographs of Clay Arrangement



6600 x

b. Synthetic Clay (UF) (Turcott 1988)

Fig. 4 Photomicrographs of Clay Arrangement (Cont.)



c. Synthetic Clay (UF) (Turcott 1988)

Fig. 4 Photomicrograph of Clay Arrangement (Cont.)



8000 ×

d. Synthetic Clay (UF) (Turcott 1988)

Fig. 4 Photomicrographs of Clay Arrangement (Cont.)

photomicrographic view of both identifications.

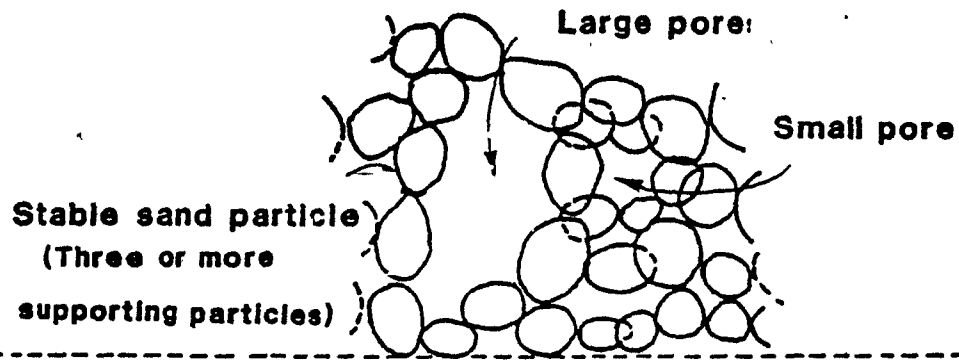
There is no unique relationship between the composition of the soil mass and the fabric of the system. However, some simple conditions arise from the compositional analysis: the dispersion of soil particles and fabric units, can be due to low salt content, high pH, or fresh water deposition, and a flocculated soil system can be due to high salt content.

In order to complete the picture of the fabric analysis, a schematic picture of fabric (packing) formations of different materials is shown in Fig. 5. Fig. 5a shows a random arrangement of loose sand which is different from an ordered arrangement of sand system; i.e., it is different from ideal packings of uniform spheres (simple cubic, cubical tetrahedral, tetragonal sphenoidal, pyramidal and tetrahedral).

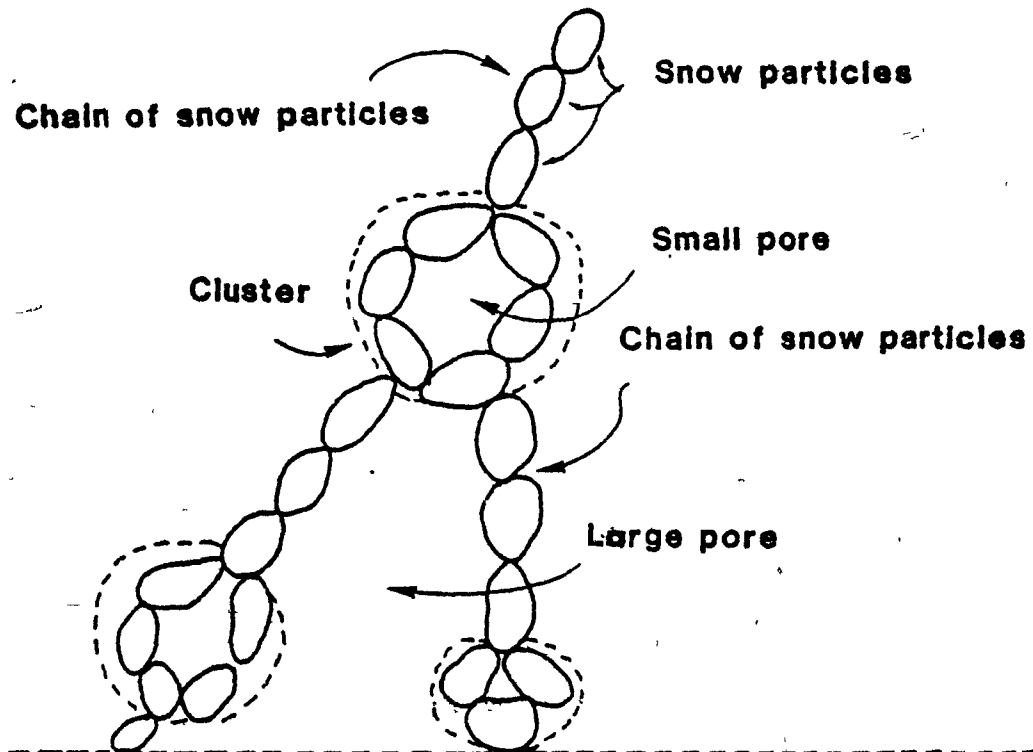
#### **2-1-2 Fabric Scale For Soil Performance Prediction:**

The following question is raised: what level of fabric viewing is suitable for soil behaviour evaluation, analysis and prediction, specifically, for clay compression performance? The answer to this question can be viewed in Flow Chart 2.

Identification II of fabric viewing is seen to be tied into the analyses concerned with the integrity and



a. Random fabric of sand system



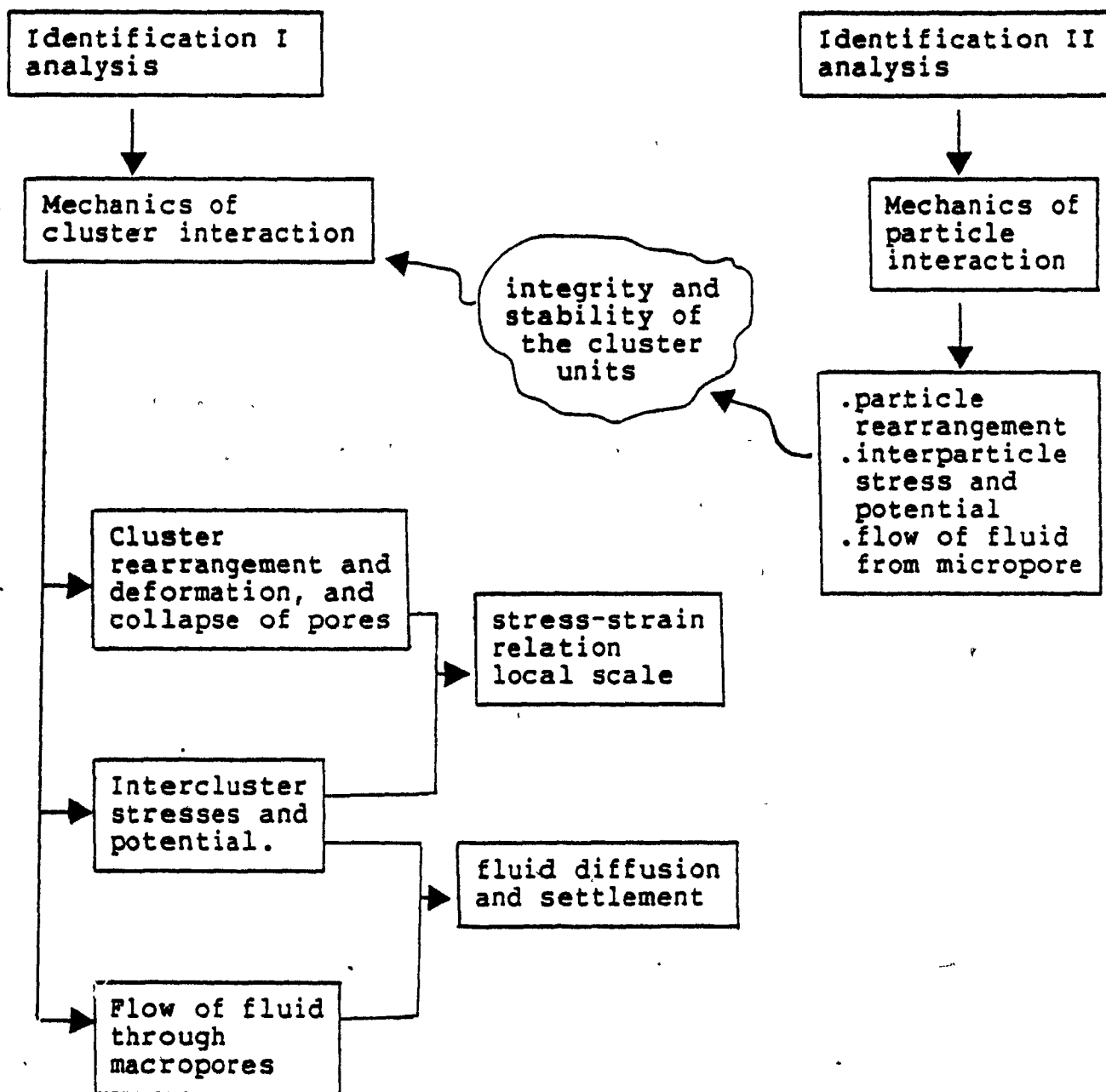
b. Fabric of soft snow system

Fig. 5 Schematic View of Particulate System



stability of individual particle arrangement within the fabric unit. Therefore, the organic and inorganic bonds, and the cement bonding between the particles should describe the properties of the cluster units and their connection with each other. Hence, the scale of Identification II cannot by itself give the complete prediction of the global behaviour of the system. Therefore, much larger scales, which should be linked with Identification II viewing, ought to be used for soil behaviour prediction.

Moreover, not all of the detailed information in the scale of two or three particle systems is necessary for soil performance prediction. The scale of Identification I of fabric viewing can be used in the analysis. Therefore, the smallest scale which ought to be used for analytical and physical modelling, is the **cluster unit**. This agrees with the suggestion by Yong (1971) that single plate theory is relevant only to dilute colloidal suspensions, and that natural consolidated clays require consideration of a multiple plate unit, i.e., cluster unit.



Flow Chart 2 Fabric scale for soil performance prediction

## 2-2 THE PHYSICS OF CLAY COMPRESSION:

### 2-2-1 Review:

Terzaghi was the first to make a serious attempt to understand the mechanisms controlling the compressibility of clay. He had previously postulated the existence of a semi-solid layer of adsorbed water on clay surfaces. He had used this hypothesis only to explain the low permeability of clays and their secondary consolidation.

Leonards and Altschaeffl (1964), and Kenney et al. (1967), concluded that the resistance against deformation which a soil exhibits during a consolidation test, is a manifestation of the shear resistances. These resistances can be mobilized at the contacts between individual particles. Therefore the displacements between the particles are controlled by the bond strength between them. Bolt (1956) explained and concluded that compressibility will essentially be a function of the double layer repulsive force. This force is primarily dependent on the type of clay and the electrolyte content of the system.

Olson et al. (1970) have done several one-dimensional consolidation experiments for different clay minerals with different chemical solutions. They have discussed their experiments qualitatively in terms of two postulated models of behaviour: the mechanical

model, which represents the shape, surface friction and geometric arrangement of the particles; the physico-chemical model, which represents particle shape, geometric arrangement and chemical variables, such as adsorbed water, cation, dielectric constant, etc. One of their conclusions is that the mechanical model governs the volume change behaviour of the kaolinite.

Sridharan et al. (1973,1979) have postulated two mechanisms for a clay system. In the first mechanism, the volume change is controlled by the shearing resistance at the interparticle level. In the second mechanism, it is controlled primarily by the long range diffuse double layer repulsive forces. They have concluded that the first mechanism primarily governs the volume change behaviour of non-expanding lattice-type clays like kaolinite, while the second mechanism governs that of expanding lattice-type clays like montmorillonite.

These descriptions of the clay compression mechanisms do not require that the clay particles form cluster units. These units, however, do have a physical boundary and a mechanical function. Hence, in the following, we will base the description of the mechanism on the modern view of fabric analysis.

### 2-2-2 The Mechanism:

The mechanism of clay compression which will be described here, is divided into two descriptions. The first is under a single fixed load, and the observation of the compression evolution is with time. The second is the description under multiple loads, with the observation on the compression-stress evolution.

#### ~~2-2-2-1~~ The Mechanism Of Compression Under a Single Fixed Load:

The principle of clay compression can be viewed in terms of the physical phenomena of the deformation of the skeleton of the clay system, fluid movement, and the stress transfer from the fluid to the skeleton which are acting simultaneously and depend on each other.

The fluid flow and the clay skeleton deformation are combined mechanisms and depend on the clay structure. Some aspects of the structure have a more significant influence on one of these two mechanisms than others. These mechanisms depend on the type, the capacity and the duration of loading as well as the condition of the soil system. Therefore, the total resistance to the volume change or clay compression comes partly from the permeability and partly from the structural resistance of the clay itself, i.e., the structure of clay itself possesses a time dependent

resistance to compression.

We may postulate that the compression mechanism of the clay can be divided into two overlapping regions. With the compression in the first region, rearrangement and reorientation of the clusters will take place, and the fluid will flow primarily through the interconnected macropores.

As the compression process takes place with time, the clusters will start to translate and rotate without any significant distortion of these units, and the volume of the cavities (macropores) which are formed between the cluster units will decrease. As a result, the fluid will squeeze out from the cavities and move through the macropores.

The relative motion of the cluster units depends on three aspects: first, the physico-chemical aspects of the soil-water system. The chemical variables which influence the system are: Dielectric constant, electrolyte concentration, cation exchange capacity and specific surface area, cation valence, pH value, and temperature. Secondly, the sliding resistance between the cluster units which is due to friction and/or viscous action at the contacts. Finally, the surface features of the cluster units, i.e., the cluster units may be coated by amorphous materials such as alumina, silica and iron.

The relative motion of a group of cluster units can produce local deformation in the sense of changes in the geometry and size of macropores. This deformation can be linked with the local stress acting on this group of cluster units through a material modulus.

Water extrusion from and through the cavities (macropores) depends on the macropore size distribution of the clay system and the excess pore fluid pressure in the macropores. The local velocity of fluid movement from the cavity can be linked with the pore fluid pressure gradient through a conductivity operator. As the water is extruded from the cavities in the compression process, the excess pore fluid pressure in the cavity will decrease, resulting in a transfer of the applied stress. This can be viewed as an intercluster force and potential.

As we can see this first region of compression represents a consolidation process. Throughout this study we use the term "first region" for this consolidation part, see Fig.6.

The results of the experimental work of Pusch (1970 and 1981) and Delage et al. (1984) substantiate this postulate. Pusch made a series of unconfined compression tests and creep tests on marine quick clay and natural Illitic clay, and he made also observations

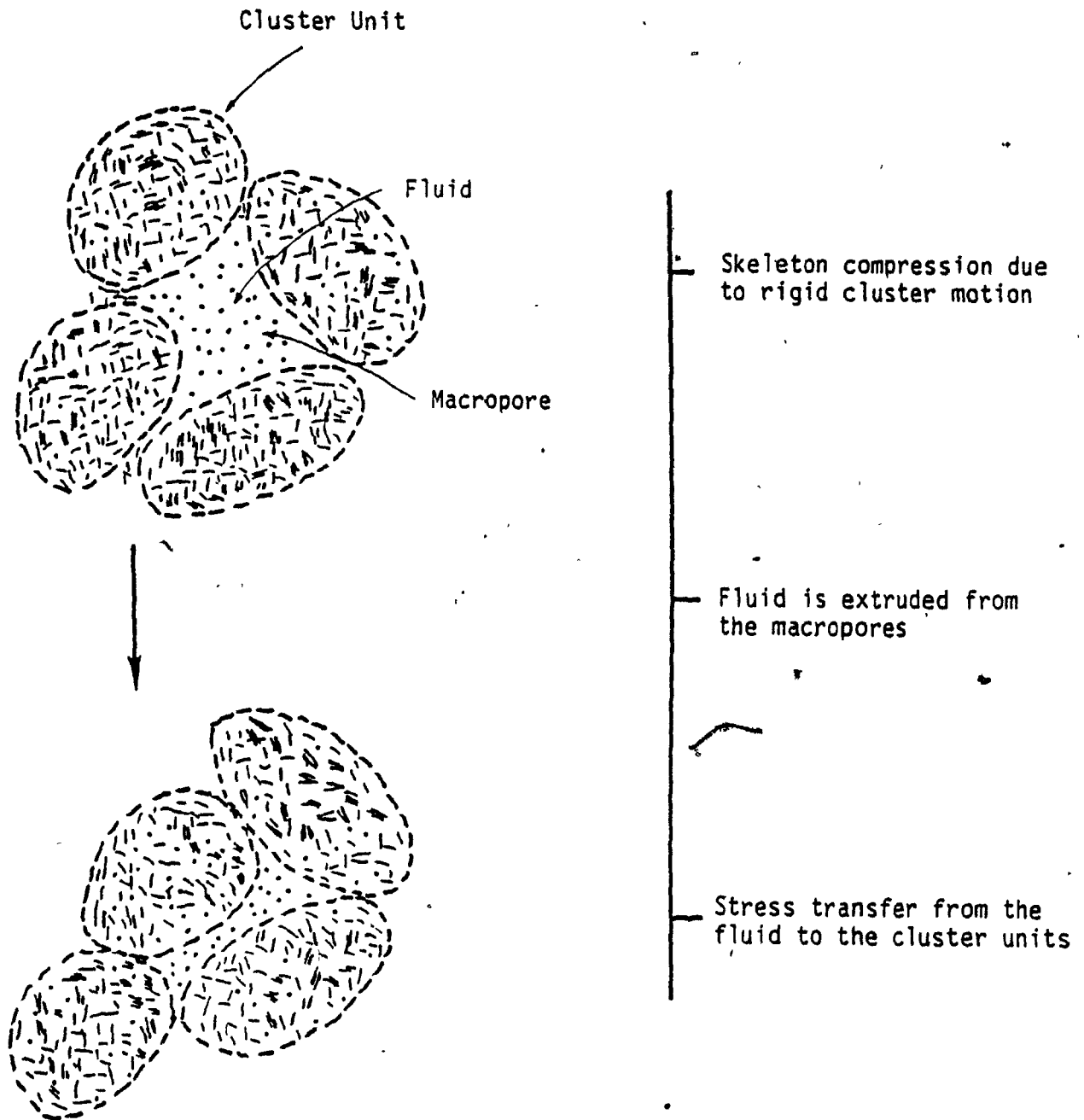


Fig. 6 Schematic View of the Consolidation Process of the First Region



using an ultra thin section technique and transmission electron microscopy. He concluded that aggregates (cluster units) behaved as rigid bodies up to a certain stress level during the shear process. Delage et al. concluded that a collapse of an interaggregate pore (macropore) will take place first during consolidation without any significant distortion of the aggregate.

**Compression in the overlapped region:** Not all the cavities are equally affected by the load at the same time, due to, firstly, the position of the macropores, secondly, the perturbation of the local stresses and pore water pressure, and thirdly, the random nature of the internal properties of the material. Therefore, more orientation of the cluster units will take place. These orientations will cause the pore water pressure to build up in some of the macropores affected, and hence, an average pore water pressure can be measured on the boundary of the sample. This measurement of pore water pressure at the surface for this overlapped region (for fairly large load increment ratios) can be approximately at a degree of consolidation between 80 percent and 100 percent.

On the other hand, the particles within some of the fabric units which are already oriented in the first region try to slide at their points of contact. This sliding can be very small and can occur through a lubricated surface such as a layer of adsorbed water.

It has characteristics that are different from free water.

This mechanism of particle movement within the cluster unit will be explained in the second region of compression since the overlapped region is the start portion of the second region, and the end portion of the first region. The fluid flow is through interconnected macropores, and interconnected micro- and macropores.

For the compression in the second region, no relative movement of the clusters can take place. However, more movement of the particles within the fabric units can take place. This movement is governed by several resistance forces that exist at the contact between particles.

The conditions of the contacts depend on, a) the adsorbed layer of water and layer of cations which are responsible for the forces of attraction and repulsion between particles. These forces depend on the size of the fabric units and the mode of association of the particles within the fabric unit, b) amorphous material within the cluster unit which is responsible for viscous/friction forces, c) the friction between the particles which is responsible for friction forces.

It is not clear which of these resistance forces

contribute more to the bond strength between the particles. The bond strength can be defined as the forces required to resist displacement of the two particles at a point of contact with each other. We believe that all of these forces participate in the bond strength of the contacts of the particle with its neighbors. It should be noted that at any contact, there is a weak plane and strong plane of resistance which depends on the contributing resistance forces and their directions.

If we assume that these resistance forces are contributing in an additive way to bond strength, the physics which generate the variability of the bond strength within the cluster unit can be modelled as a Gaussian distribution in terms of forces. Hence, the integrity of the cluster unit under a stress system which is transmitted at the contact points with neighbor cluster units depends on the mean and the variance of the Gaussian distribution.

Once the resistance forces are exceeded, sliding occurs at most of the particles' contact. The sliding can result in an increase or decrease in a particular bond strength. If the net effect tends toward an over-all increase in bond strength, sliding will gradually decay, and this sliding will result in a volume change of the cluster unit. The change in the size of a group of cluster units can produce local

deformation. This deformation can be linked with the local applied stress on this group through a material modulus.

The change in the size of the cluster units can build up pore water pressure inside these units, but these changes in the size of the cluster units are not sufficient to build up measurable pore water pressure in the macropores. The pore water pressure which is built inside the cluster units cannot be measured at the surface of the sample, but this excess pore water pressure is sufficient to drain some of the water to the macropores through the interconnected micropores inside these cluster units.

The characteristics of the flow within the cluster units depend on the particles' arrangement, orientation within the fabric units, the interparticle forces, and potential. Therefore the driving forces for flow must exceed the force tending to hold water to the soil particles.

We can conclude that the flow through micropores should be characterized by, first, the strong interaction between permeant and the soil particles, and second, the geometry of interconnected micropores. This geometry is not a channel of impermeable boundaries, but interconnected roots with complex geometry.

As we can see this second region can be represented as a creep process, we will use the term "second region" for this creep process, see Fig.7. Throughout this study, the term "overlapped region" will be used for the overlapped part of the compression.

The occurrence of these two overlapped regions and their time duration in one specific soil, synthetic or natural, depend on many factors.

i) Some of them belong to the initial and boundary conditions such as load system, load increment ratio, drainage condition, etc. For example, under light load, the material may exhibit the behaviour of the overlapped and the second region.

ii) Some other factors belong to the soil system such as the geometrical factors including the depth of the layer, and the location of layer in the soil profile system; also the soil property factor which is presented from the clay type, type of cementations, organic matter, and amorphous material. Organic clay soil may exhibit the behaviour of the second region.

iii) Other factors are environmental; for example, man-made industrial waste disposals and sanitary land fills; and natural, geological evolutions over short spans of time such as sabkha deposition, and fresh

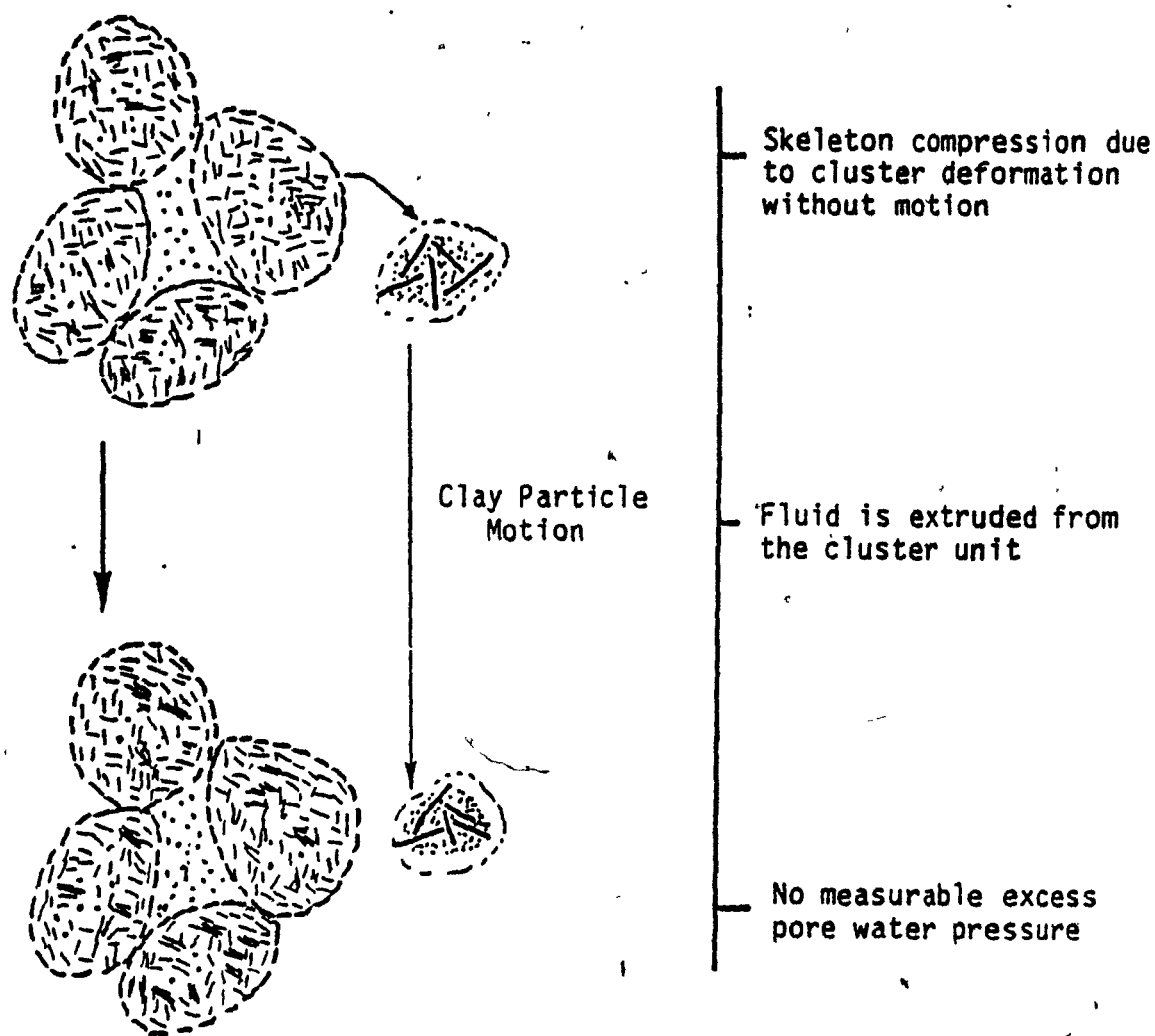
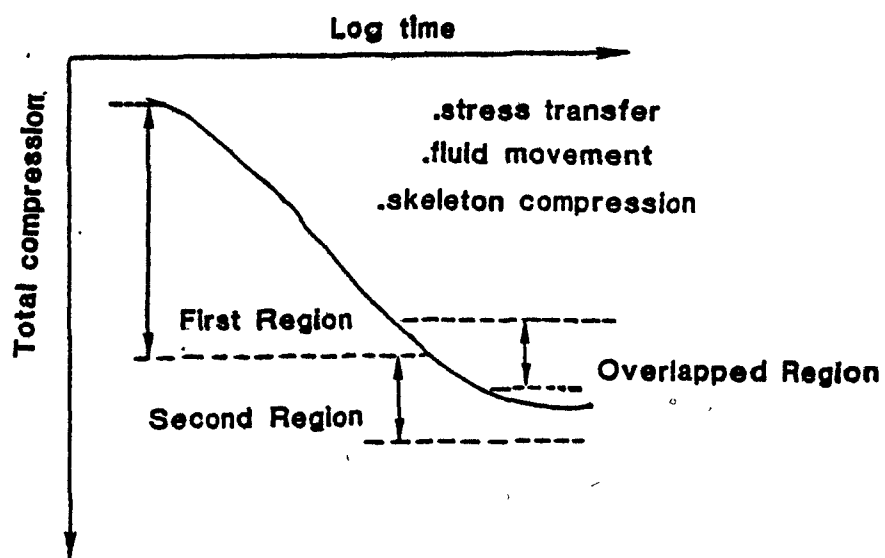


Fig. 7 Schematic View of the Creep Process of the Second Region

water leaching of a soil layer. Chemically contaminated soil may exhibit the behaviour of the second region.

In the above physics description, we benefit from several documented test programs which have been done by different investigators. These include Newland et al. (1960) who studied over 100 consolidation tests under varied conditions on a natural soil to assess the effect of the load system on the secondary compression. Wu et al. (1966) have done a consolidation test, and a triaxial creep test in the consolidated-undrained condition with pore water pressure measurements. Gibson et al. (1961) and Lo (1961) have performed fifty consolidation tests on natural and synthetic clay. Crawford (1964,1965) has performed constant rate of strain tests on natural clay soils. Yong et al. (1970) have studied the creep test for clay system. Sridharan et al. (1981) have done several consolidation tests on natural and synthetic clay with different fluid chemistries using eight different chemicals. The experiments of Delage et al. (1984) and McConnachie (1974) are discussed in Chapter 1.

Fig.8 shows a schematic view of the clay compression under single fixed load.



**Fig. Time deformation for a clay soil**

**showing first region , second region , and overlapped region.**



## 2-2-2-2 The Mechanism Of Compression Under Multiple Loads:

The mechanism of compression depends on the type of loading applied to the sample, i.e., strain controlled, stress controlled, or incremental loading. For incremental loading, there are two fundamental experimental procedures that affect the mechanism: first, the duration of the load and secondly, the load increment ratio.

The mechanism of compression of the clay system under multiple load will follow a sequential pattern as follows:

a-Rearrangement and reorientation of fabric units (clusters units) which can take place without any significant distortion of the units. This distortion depends on the load applied. In case of very large loads the fabric units may collapse.

b-Increased load application would cause a greater degree of orientation of fabric units. At this stage, some particle rearrangement within the fabric units can occur. This rearrangement will depend on the time duration of the load.

c-Further loading will cause more orientation of the fabric units and particles within the fabric units. When the load increment ratio is small, the slippage

between particles within the cluster units occurs only at a limited number of contact points.

d-At high loads, the sliding of the particles over each other has a tendency toward overall decrease in the bond strength. Shear failure of the clusters will eventually occur causing clusters to fuse together to form a homogenous soil mass system.

Delage et al. (1984) have shown that the compression under load is due to the collapsing of the structure in a progressive way, the largest interaggregate pores (macropores) being the first affected. As the consolidation proceeds, smaller and smaller pores are affected. For a given pressure increment, only the largest existing pores are affected.

## 2-3 SUMMARY:

In this chapter, we have described in detail the physics of saturated clay performance under compression loading. We postulated that the mechanism of clay compression under a single fixed load consists of two overlapped regions. In the first region, the clusters will move relative to each other and the fluid will move through macropores. In the second region, the clusters will not move but they will deform and the flow will be through the micropores. In the overlapped

region, both mechanisms work together.

These postulated mechanisms will be used for the mathematical modelling in the following chapters.

## CHAPTER 3

## KINEMATICS OF DEFORMATION OF THE CLAY-WATER SYSTEM

## 3-1 OBJECTIVE:

Our objective in this chapter is to develop the kinematics of deformation of the first and the second regions of clay compression, and to establish a macropore fluid flow model for the first region of compression.

The kinematics of the particulate system is mainly described and modelled in literature, on the principles of continuum mechanics. In the next section, we will describe the kinematics of deformation of the particulate media (granular or clay media) based on the principles of micromechanics.

Furthermore, we will introduce a new concepts in kinematics. These concepts will be used for the development of the kinematics of deformation of clay soil under compression loading.

### 3-2 THE KINEMATICS OF DEFORMATION OF PARTICULATE SYSTEM:

Kinematics describes the changes that occur with time in the quantities that describe the geometry of the body. Kinematical analysis in its widest meaning comprises the recognition and recording of stress-induced movements of the individual physical units of a compound material system, and the subsequent construction of the appropriate strain pattern for the whole system. Therefore, it can be considered as that branch of fabric analysis which is particularly interested in stress-induced fabric changes of microscopical dimension.

The deformation kinematic is the most essential aspect of mechanics. It is not a great surprise that in classical, geotechnical engineering, the kinematics of soil has been neglected, even from the continuum point of view (e.g. limit equilibrium).

In the following section, we will consider the various types of deformation.

### 3-2-1 The Types Of Deformations Of Particulate Systems:

According to the mechanics of material, the deformation of soil media can be classified into three idealized types:

- i- simple deformation,
- ii-constrained generalized deformation,
- iii-generalized deformation.

The last two types of deformations (ii and iii) will be described for the particulate system either granular (sand) or clay. Hence, the individual units which describe these types of deformation can be defined as a particle (sand) or cluster (sand or clay).

#### i- Simple Deformation:

In this case, the material of the soil mass is assumed to be continuous; hence, the deformation is established from the measurement of the boundary movement of the soil sample. Non-homogeneous deformation or shear deformation in narrow bands within the soil sample cannot be considered examples of this type of deformation. The continuum mechanics principles are applied to this type. This type of deformation has been used in soil elasticity and plasticity modelling. We will call this type of deformation type A.

## **ii- Constrained Generalized Deformation:**

This type of deformation will be called type B. In this type, we have two kinds of deformation which are:

### **ii-1 First Kind of Deformation Type B1:**

The material of the soil system is considered from the physical point of view, which means that the motion of the individual units is appreciated. These individual units comprise the material system. The units move relative to each other, their motion consisting of rotation and translation, but the units are assumed to be rigid; hence, gross deformation of the system is equal to unit motion with interaction (rotation and translation). The physical mechanism of deformation of this system can be viewed in the following.

#### **ii-1-a Two-Particles (Two-Clusters) Unit:**

By using the concept of vector analysis, we have the following vector positions for the two-particle unit:

$\vec{r}_1$  and  $\vec{r}_2$  are vectors which describe the internal configuration of the two particles.

$\vec{r}_1$  and  $\vec{r}_2$  are vectors which connect  $\vec{r}_1$  and  $\vec{r}_2$  to the reference frame.

$\underline{r}_n$  is the vector which connects the contact point with centroid of the particle

$\underline{r}$  is the vector which connects the contact point with the reference frame.

$\underline{S}_1$  and  $\underline{S}_2$  are unit vectors. See Fig 9.

The choice of position vectors depends on the two factors:

1) The shape of the particles (or the clusters): For example in the spherical shaped system, the vectors  $\underline{r}$  and  $\underline{r}_n$  are not significant, but the vector which connects the contact point with centroid is important. For a cylindrical shaped system, the vector which connects the centroid of the two-particle unit to the centroid of each particle is valuable.

2) The modes of motion of the particles which depend on the boundary conditions and the surface condition of the particles: We will describe these modes of motion below.

**Case(1) Sliding and Rotation:** In this case, the particles will slide and rotate simultaneously on top of each other. The mechanism of deformation can be viewed from the displacement due to sliding and rotation. We have two important vectors: one connects the centroid of the two particles, and the second



vector describes the internal configuration of the individual particles. See Fig.9a.

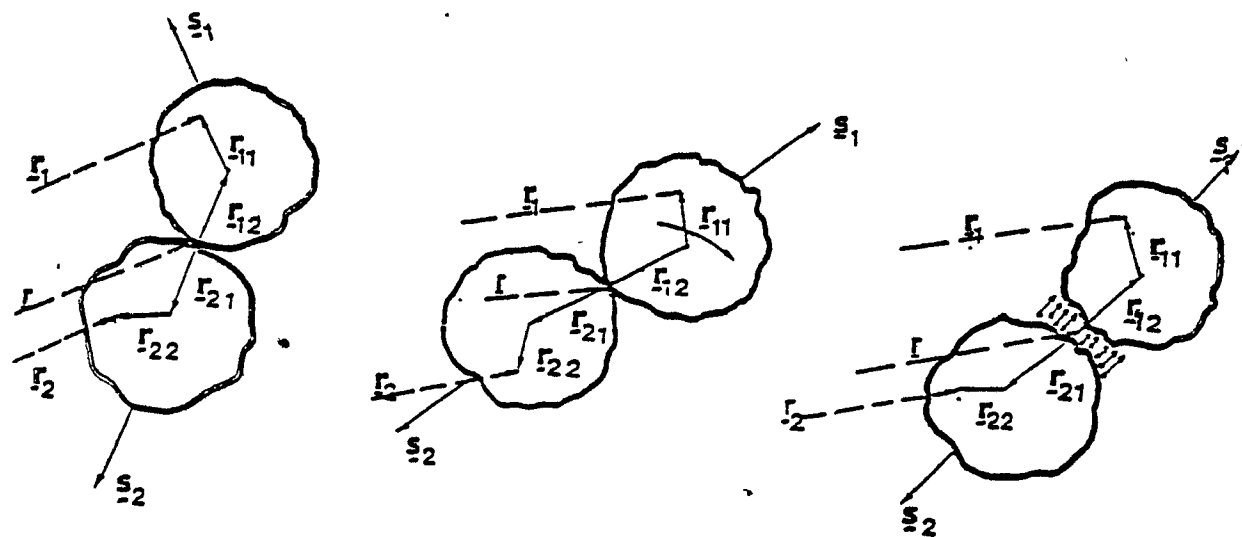
**Case(2) Rotation only:** In this case, one particle will rotate on top of the other particle. The mechanism of deformation can be viewed from the displacement due to rotation only. The vector which describes the internal configuration of the individual particles is very important. See Fig. 9b.

**Case(3) Sliding Without Rotation:** In this case, the particles will slide over each other, and the mechanism of deformation can be established from a vector connecting the centroid of the two particles. Therefore, the rotation will be the rotation of this vector. See Fig. 9c.

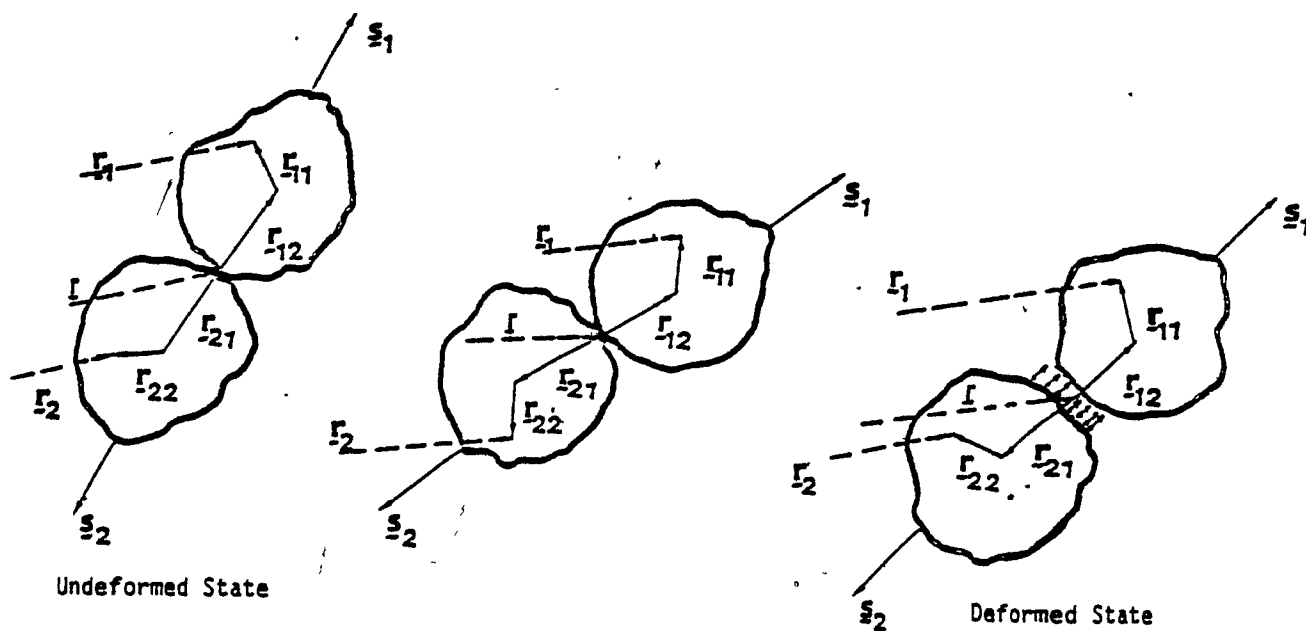
For all three cases, when the surface forces predominate, the interaction between the two particles and their movements may be relative to each other.

#### **ii-1-b Complete Fabric System:**

**Case(1)** When the collapse of the pores between the units occurs, these units will move closer to each other, but they will stay in the same order as before deformation. In the deformed state of the system, the coordination number (the number of contacts per particle) may be higher than in the undeformed state. This case can be viewed as an ordered state of

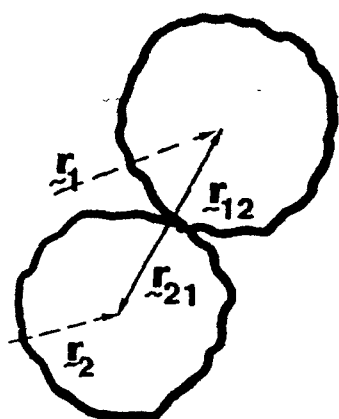


a. Case 1

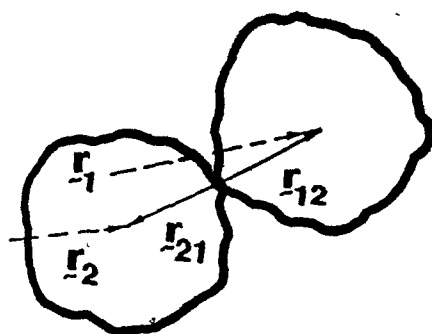


b. Case 2

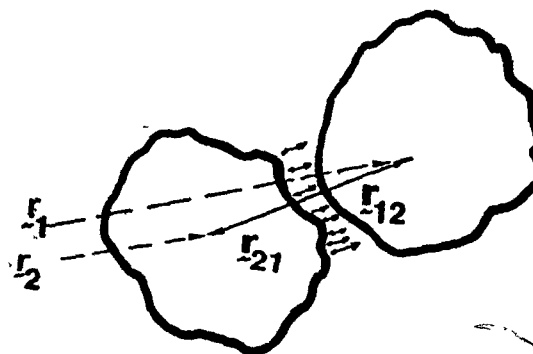
Fig. 9 The Mechanism of Type B1 Deformation (Two Units)



Undeformed State



c case 3



Deformed State

Fig. 9 The mechanism of type B1 deformation (two units)

Cont.

deformation.

Case(2) When the collapse of the pores between the units occurs, these units will move relative to each other, but they will not stay in the same order as before deformation. This case can be viewed as a disordered state of deformation. See Fig.10.

#### ii-1-c Two-Particle System Idealization:

There are several cases when the particles, cluster, or group of units can be idealized as two cylindrical or rodlike elements. For example, in the case of a group of units which have strong bonds between them and other bonds that are very weak, this group can be idealized as a cylindrical shaped system as shown in Fig.11a. For the cylindrical shaped unit system, the individual units may rotate and translate under applied load, and the centroid of the system can change.

The mechanism of deformation can be established from the vector position shown in Fig.11b. The configurations of the two-particle system are: i) edge-face, ii) face-face, or iii) edge-edge. These configurations with separations between the units exist in cases where the surface forces between the units predominate. The compressible zone between the units can be represented by the vector cross product concept, which will be discussed in later sections.

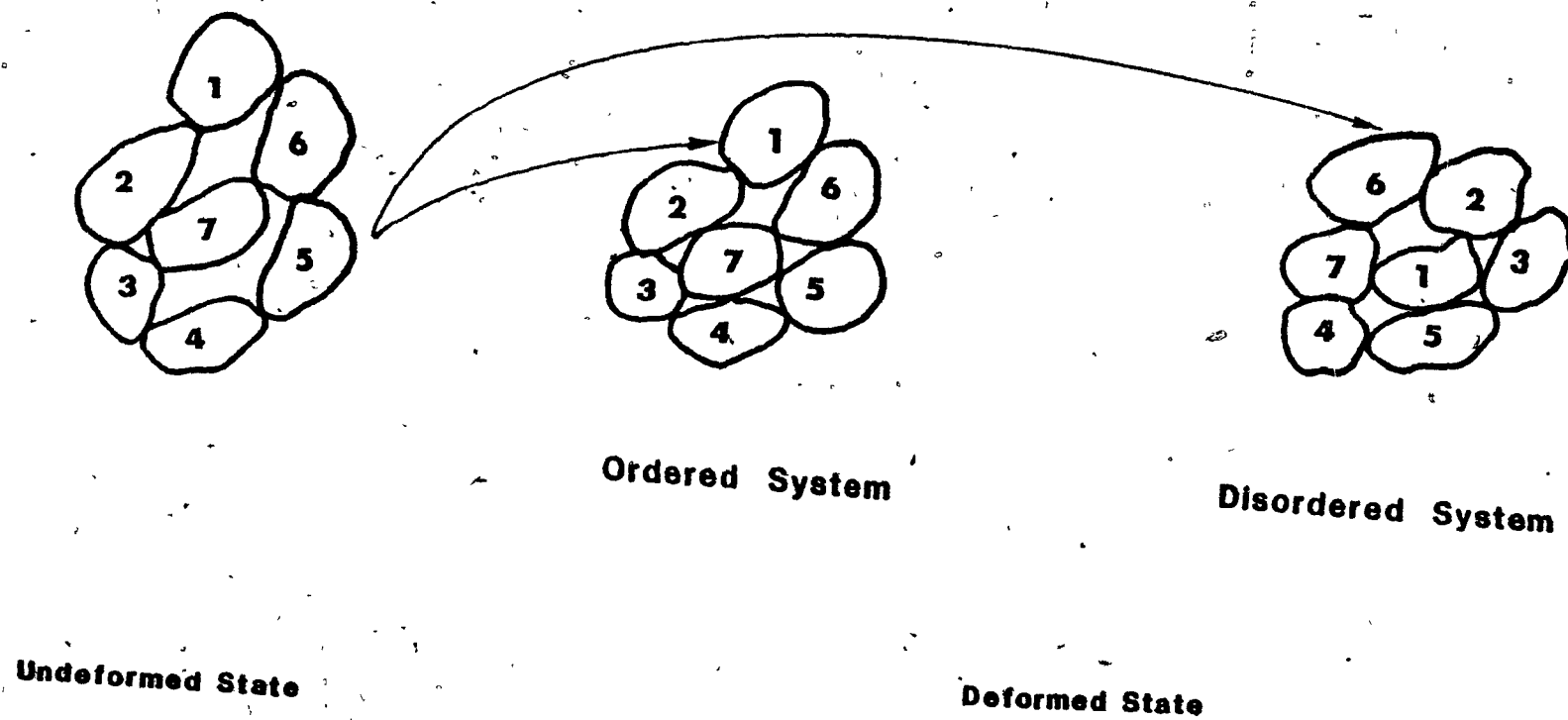
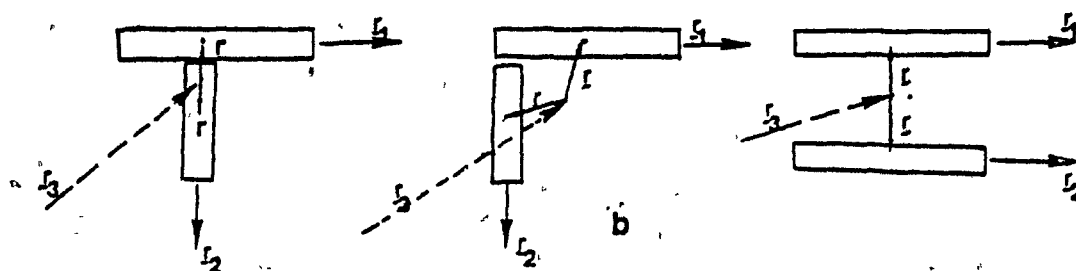
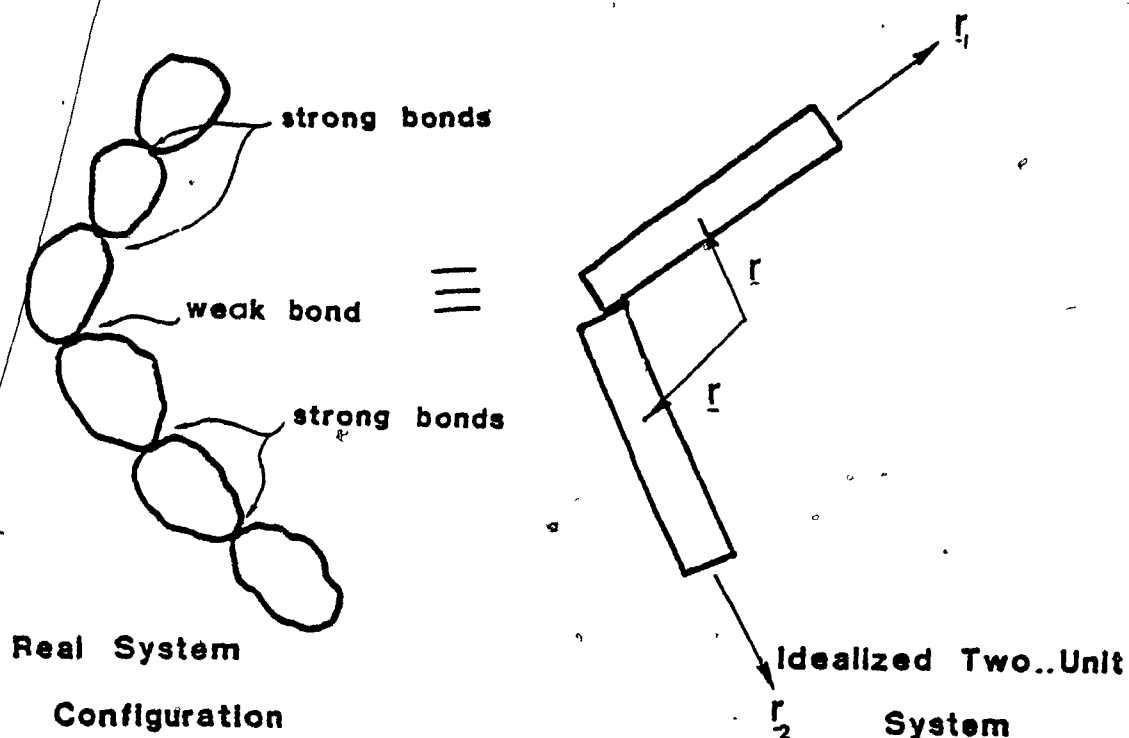


Fig. 10 The Mechanism of Type B1 Deformation (complete system)



**Different configurations**

**Fig. 11 Two Cylindrical Shaped System Idealizations**

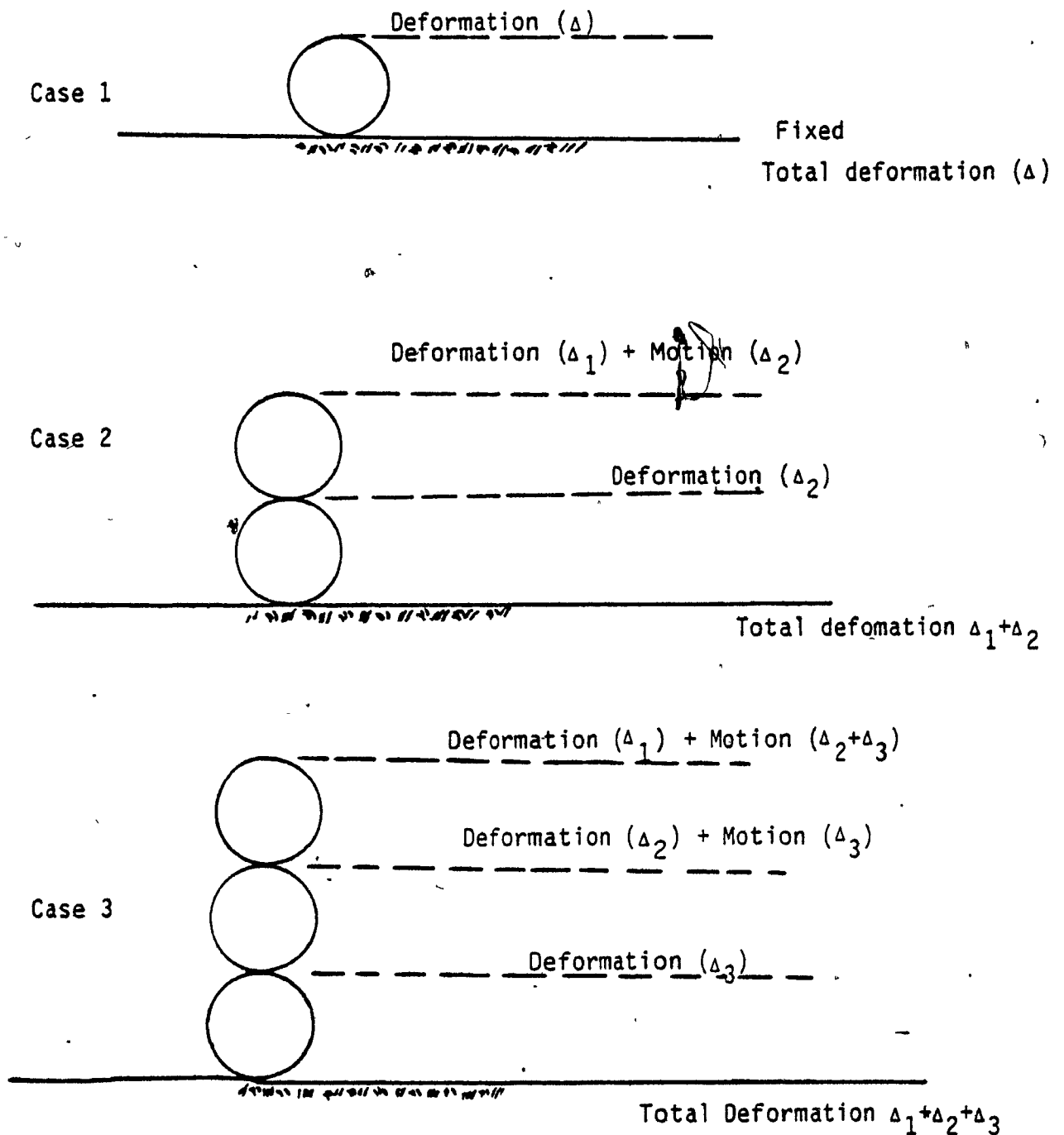
## ii-2 Second Kind Of Deformation Type B2:

In this kind of deformation, the units are allowed to deform, but they are constrained from rotation and translation. The physical mechanism of this kind of deformation is viewed and analyzed by the deformation of the contact between the two particle units.

From the cases in Fig. 12a, we will illustrate the fundamental concept of the type B2 deformation. For case 1, the amount of deformation is equal to  $\Delta$ . For case 2, the amount of deformation is equal to  $\Delta_1 + \Delta_2$ , but the top particle is moved a distance equal to  $\Delta_2$ . This distance cannot contribute to the deformation of the system, i.e., the system deformation must be equal to  $\Delta_1 + \Delta_2$ . For case 3, the total system deformation is equal to  $\Delta_1 + \Delta_2 + \Delta_3$ . The top particle is moved a distance equal to  $\Delta_2 + \Delta_3$ . Again this distance must not be used for deformation analysis.

Hence, the type B2 deformation considers only the deformation of the units without their movements. The movements of the units are caused by other units' deformation which are already accounted for.

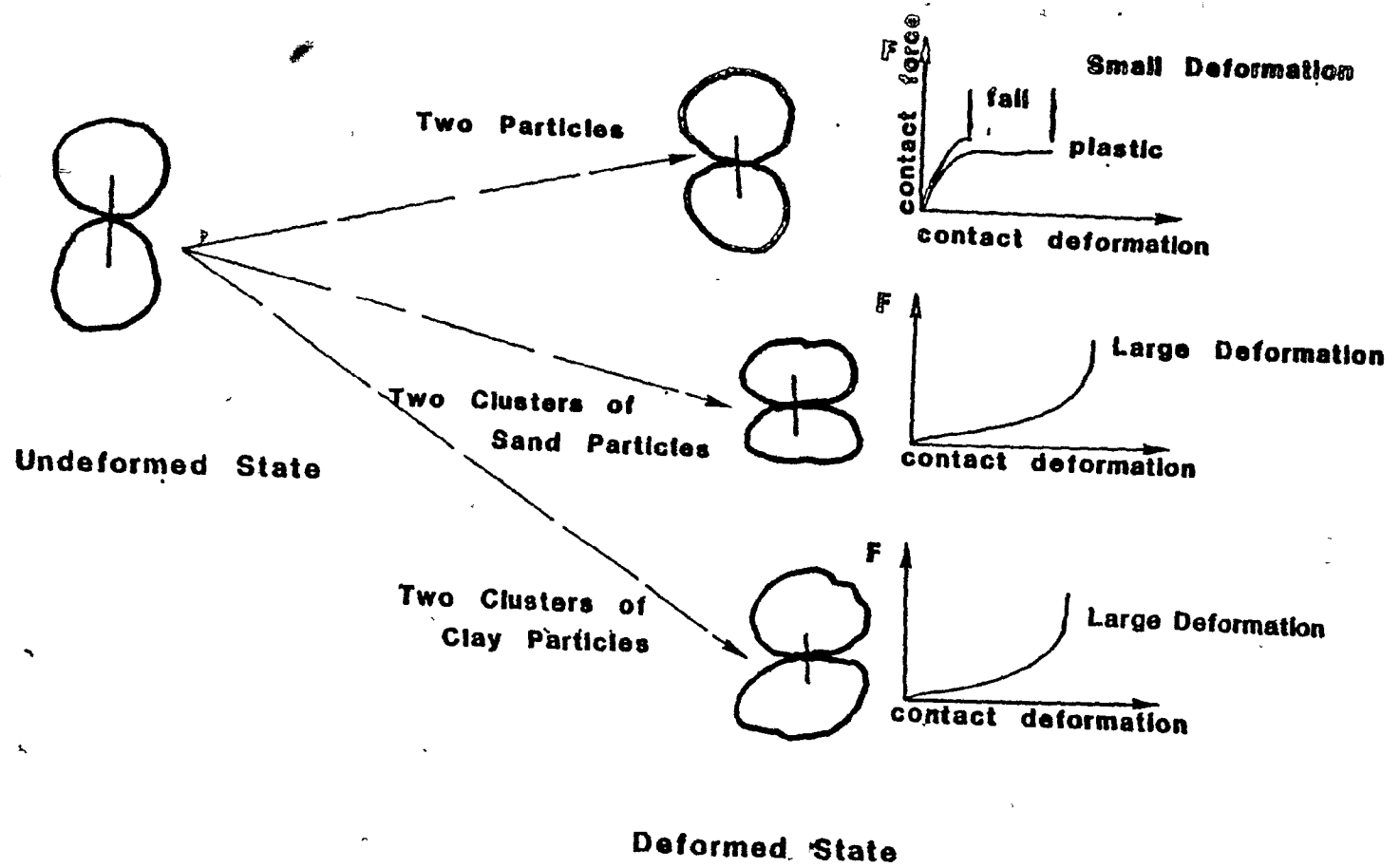
The contact deformation depends on the deformability of the particles or clusters. For instance, a brittle particle (cluster) can undergo small elastic deformations and fail, and a ductile material can deform into the plastic range. Highly



a. The definition of the constrained deformation

Fig. 12 The Definition and the Mechanism of Type B2 Deformation for Particulate System





b. The mechanism of type B2 deformation

compressible clusters may have a large deformation under very small load; and in the case of very large cluster units, these units may collapse under a small load. See Fig.12b.

### iii- Generalized Deformation:

In this type of deformation, the internal physical description, soil fabric, and the structure of the material are considered. The mechanism of deformation can consist of the motion of the units relative to each other (rotation and translation of the units) **simultaneously with deformation** of the units themselves. Hence, the gross deformation is equal to the units' motion with interaction (translation and rotation) plus continuum behaviour of the units. The two mechanisms of deformation are coupled.

The physical mechanism of this type of deformation is viewed as a particle (sand particle) or cluster deformation, and this deformation is either small elastic or large collapsible. It depends on the compressibility of the particles, and the types of their movements relative to each other. This type of deformation is called type C.

There are many physical situations encountered in practice which can be explained by type C deformation. Granular medium where the particles tend to group into clusters is an example. The cluster deformation can be

viewed from the movement of the cluster and its deformation (i.e., type C).

**Discussion:**

The preceding section highlights the following fundamental points:

1- The kinematics of deformation based on the continuum mechanics cannot describe and model accurately the deformation process of the particulate media.

2- The identification and the description of the modes and the process of deformation are required for better development of the analytical models which are capable of predicting the performance of the particulate system.

3- In the preceding section, we have introduced two types of deformations, i.e., type B (B1 and B2) and type C. These types are capable of describing different deformation processes of particulate systems. In the following sections, we will use type B deformation for the development of the deformation kinematics of a clay soil system. In this case, the individual unit is represented by the cluster unit.

### 3-3 THE CONCEPT OF THE DIRECTOR THEORY:

In this section, we discuss the director theory and how we implement it in our kinematic modelling. This theory has been given various names by different authors (for example, micropolar by Eringen (1964) and couple stress by Toupin (1964), etc.). However, we have chosen the term "director" over the others as it holds in its fundamental argument a director (vector or tensor).

E. and F. Cosserat (1909) developed the theory by introducing the concept of a rigid triad which is amenable to a simple and beautiful geometrical interpretation of the motion. Therefore, two sets of kinematic quantities are developed: macro deformation of the continuum point, and micro rotation of rigid triad. However, the assumption of the mathematical point, i.e., continuum concept was used in the development.

More than forty years after Cosserat's paper, a revival of interest in this subject has been demonstrated by authors who have taken different routes in the development of their theories. However, they have begun with principles which were laid out by the Cosserat brothers. The kinematics of deformation in some of these theories will be viewed below.

Ericksen and Truesdell (1958) and Kaloni and DeSilva (1970) used Cosserat's concept, but they allowed the deformation of the triads (vectors) which are attached to a point. Thus, they obtained macromotion which is caused by continuum deformation, and micromotion which is caused by the rotation and deformation of the vector triad. The former authors used this theory for rods and shells, and the latter authors for idealized behaviour of dilute suspension of both rigid and deformable substructure units.

Mindlin (1964) extended the work of Ericksen et al. (1958) and formulated a theory for linear elastic material with microstructure. He also presented kinematics in terms of macro and micro motion, and applied the theory for microwave propagation. His notion of microstructure is represented by a cubic cell.

Eringen et al. (1964, 1966 and 1972) have advanced two theories. The first is micropolar theory which holds that every material point of the polar medium is phenomenologically equivalent to a rigid body. Therefore, macromotion is seen as translation, and micromotion as rotation. The micromotion is represented by an orthogonal tensor. This theory may not be dissimilar to Cosserat's original theory.

Eringen et al.'s second theory is the micromorphic

theory, in which a micromorphic body is imagined as a body whose material point consists of small deformable bodies or particles. Therefore, they have macromotion as the translation, and micromotion as rotation and deformation.

For both theories, Eringen et al. used the concept of macrovolume and microvolume. Their first theory has been applied to shear flow of liquid crystals between parallel plates; and the second, for propagation of surface waves in a microelastic half space.

Although the microvolume concept has been introduced, the size of this microvolume has never been considered as a property in the calculation. Hence the microvolume is actually a point which has mass and density. It simulates the Newton particle which has no size, but has property of mass. See Kafadar et al. (1971).

For highly deformable microvolume elements, nonhomogenous deformation could exist. Therefore, Eringen et al. chose to use micromorphic theory with higher grades. Using some properties of the partial differential equations, they introduced the condition of strain compatibility for simply connected regions.

There are some similarities between the micromorphic concepts of Eringen and the deformable

triads of Ericksen et al. For example Eringen's assumption of affine (homogenous) microelement deformation can be uniquely determined by the motion of any three linearly independent vectors (director triad), (Toupin(1964) and Eringen(1971)).

Allen et al. (1967), and Kline and Allen(1971) presented a theory governing the flow of fluids which contain regular and irregularly shaped, deformable, suspended particles. They took the volume average of the moment of inertia tensor of the suspended particles to account for micro structure orientation. The changes in moment of inertia were interpreted as a measure of microelement deformation.

Green and Rivlin(1964) introduced a theory based on a generalization of classical continuum concepts. This theory is known as multipolar continuum mechanics. The kinematics of this theory lies in their postulated concept of generalized velocities, where  $(V_{i,j})$  is introduced as an arbitrary velocity gradient. The physical motivation for their theory is the mechanics of rigid particle theory.

Since 1970, little development has taken place to test the basic tenets of director theory; but rather, a search for the potential application of the theory to different fields has been pursued. Some of the most widely pursued fields are: In fluid mechanics,

anisotropic fluid and suspension in fluid; and in solid mechanics, diffusion of dislocation in crystal lattice and wave propagation in the presence of dispersion effects.

The application of the director theory in the compression and consolidation of clay does not exist, but a general application of the theory to clay soil as generalized continuum theory can be found in the work of Baker (1971). He used the director theory for a clay system. Three vectors (directors) were used to describe the configuration state of two clay plates with respect to their centroid (as one unit). The generalized coordinates of the analytical mechanics were used in the development. Baker's development is not different from the work of Green and Rivlin (1968). The application of the director theory to the granular media can be seen in work of Oshima(1953), and Kanatani(1979).

#### Discussion:

Common concepts in the kinematics of deformation found in the director theories are:

a- The material points are considered geometrical points. The geometrical point has no size at all, but some triads are ascribed to it to characterize its degree of freedom in motion and deformation.

b- The continuum concept: all the director



theories view the media as a continuum. Therefore, all the functions are continuous.

c- The introduction of at least two sets of deformation: the macrodeformation which represents the motion of the centre of the continuum, and the microdeformation which represents the micromotion of the media.

Although there are only two sets of deformation (macro- and micro-deformation), several deformation gradient measures are advanced for the director theories. They may or may not have a physical relevance.

#### **The Implementation of the Director Concept:**

The director concept will be used in the following section. First we will develop our model of kinematics by establishing the mechanical configuration state of the physical unit. Secondly, we will establish the deformation kinematics, microdeformation gradient, and microstrain. Once these parameters are established, the collective deformation of the physical units can be constructed. Therefore, the macroscopic deformation is the manifestation of the microscopic deformation of the physical units. Hence, we have only "one set" of kinematics of deformation, instead of "two sets" of kinematics of deformation as described in director theories. This is the exact procedure for establishing

the micromechanics approach.

We also use the director concept for developing the area of the compression zone in the clay system; which is done by director cross product.

### **3-4 MATHEMATICAL MODELLING OF MICROSTRAIN:**

In order to develop a mathematical model of the kinematics, some basic assumptions will be accepted. First, the shape of the cluster units are assumed to be spherical; secondly, the fluid has no structure, and therefore, the mean velocity of flow characterizes the kinematics of the fluid. Finally, the microelement or the physical unit which is considered in the modelling consists of a group of cluster units, and we define this physical unit as the macrostructural unit (MSU).

By using simple set theory, we can define the topological structure of the body and the measuring scale of the clay soil system with different sets. We shall introduce some coherence (geometrical structure) to the elements of these sets so that these sets can be organized into a space. Thus, these sets are a substitute for the mathematical point which is considered in classical continuum mechanics.

### i- Cluster unit

$$\text{Set A} = \{ \alpha : 1, 2, 3, \dots, n \}$$

Set A is a set of pairs of clay particles. Each member of the set represents a pair of clay particles.

### ii- Structural Unit

$$\text{Set B} = \{ B_1, B_2 \}$$

Set B is a closed set of two cluster units.

### iii- Macrostructural Unit

$$\text{Set C} = \{ B_1, B_2, B_3, B_4, \dots, B_n \}$$

Set C is a finite set of cluster units i.e, each member of the set represents a cluster unit.

### iv- Statistical ensemble

$$\text{Set M} = \{ C_1, C_2, C_3, C_4, \dots, C_n \}$$

Set M is defined as a countable set of macrostructural units. This set is identical to the Gibbs ensemble and the mesodomain of Axelrad (Axelrad, 1984).

### v- Total Domain of the Body

$$\text{Set p} = \{ E_1, E_2, E_3, E_4, \dots, E_n \}$$

Set  $p$  is the union of disjoint statistical ensembles, and represents the macroscopic material body. The body is the clay soil medium which is influenced by the boundary conditions, e.g., by the stressed region of the clay soil under structures.

Fig. 13 shows a schematic view of the topological structure of the clay soil medium.

We will develop our kinematics of deformation for the macrostructural unit (set C) as our microelement, and we can benefit from the structural unit (set B) for stress evaluation between the clusters. We will employ set A for evaluating the integrity of the cluster unit. Set M is used for the passage from the microelement to the ensemble of microelements.

In light of the description of the physics of clay compression in chapter two, the kinematics of deformation is divided into two overlapped regions. In the first region we have relative movement of the cluster units without physical distortion of the cluster units. Hence, this region can be simulated by type B1 deformation which has been described in the previous sections.

In the second region we have deformation of cluster units due to the small relative movement of the particles within these cluster units themselves.

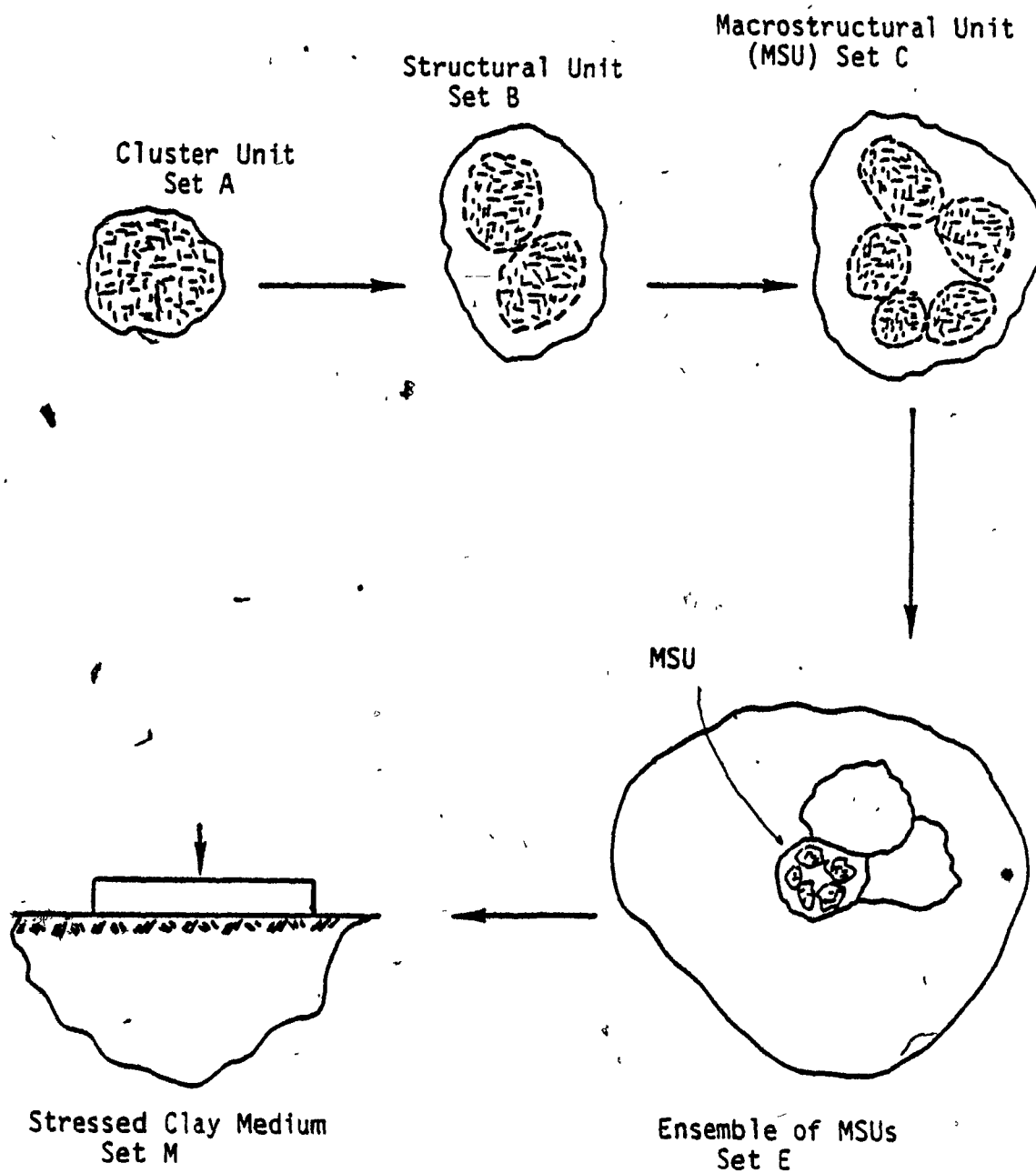


Fig. 13 Schematic View of the Topological Structure of the Clay Medium

Therefore this region can be simulated by type B2 deformation. The overlapped region will be investigated later on. In the following, we will start with the deformation of the first region.

### 3-4-1 The Kinematics of Deformation of the First Region:

In order to describe the configuration state of the macrostructural unit (MSU) and its evolution with time, position vectors of the two phases of clay soil system will be introduced. These vectors will be referred to a fixed coordinate system.

The position vector of the clay-water system will be as follows:

Undeformed state: clay system

$$\hat{\underline{Y}}(y,t) = \hat{\underline{Y}}(y,t) + \hat{\underline{Z}}(y,t) \quad (3.1a)$$

$$\hat{\underline{D}}(y,t) = \hat{\underline{Y}}(y,t) - \hat{\underline{Y}}(y,t) \quad (3.1b)$$

$$\hat{\underline{N}}(y,t) = \hat{\underline{Z}}(y,t) - \hat{\underline{Z}}(y,t) \quad (3.1c)$$

Water system:

Since the water is assumed to have no structure or fabric, its position vector is represented by the centre of the macrostructural unit. The following equation describes the discrete configuration of the cavity which encloses the water system.

$$\underline{\hat{Y}}^i(y,t) = \underline{\hat{Y}}(y,t) + \underline{\hat{Z}}^i(y,t) \quad (3.1d)$$

Deformed state: Clay system

$$\underline{\hat{Y}}^{\alpha\Lambda}(y,t) = \underline{\hat{Y}}(y,t) + \underline{\hat{Z}}^{\alpha\Lambda}(y,t) \quad (3.2a)$$

$$\underline{\hat{D}}^{\Lambda r}(y,t) = \underline{\hat{Y}}(y,t) - \underline{\hat{Y}}^r(y,t) \quad (3.2b)$$

$$\underline{\hat{N}}^{i\alpha\Lambda}(y,t) = \underline{\hat{Z}}^i(y,t) - \underline{\hat{Z}}^{\alpha\Lambda}(y,t) \quad (3.2c)$$

Water system

$$\underline{\hat{Y}}^i(y,t) = \underline{\hat{Y}}(y,t) + \underline{\hat{Z}}^i(y,t) \quad (3.2d)$$

where

$\underline{\hat{Y}}^{\alpha\Lambda}$  = the vector joining the centre of the cluster and the reference frame, and  $\alpha=1,2,\dots,n$  where  $n$ : the number of the cluster units within the macrostructural unit( $\Lambda$ ).

$\underline{\hat{Y}}^{\Lambda}$  = the vector joining the centre of the MSU( $\Lambda$ ) and the reference frame.

$\underline{\hat{Z}}^{\alpha\Lambda}$  = the vector joining the centre of the cluster unit and the centre of the macrostructural unit.

$\underline{\hat{D}}^{\Lambda r}$  = the vector joining the centre of the M.S.U.( $\Lambda$ ) and the centre of the neighbor M.S.U.( $r$ ).

$\underline{\hat{N}}^{i\alpha\Lambda}$  = the vector joining the centre of the cluster( $\alpha$ ) with contact( $i$ ) in the macrostructural

unit( $\wedge$ ). See Fig. 14.

Note: the two indices  $i$  and  $j$  should be numbered in the same way, since there is only one director (vector) for each cluster unit to describe the kinematics of deformation.

Equation 3.1b represents the configuration state of the two adjacent macrostructural units. This state represents the collapsibility condition of the adjacent macrostructural units and the fluid flow between these two adjacent macrostructural units. (See the discussion in chapter six.) Eq. 3.2c is restricted by the condition  $|N^i| = |n^i| = r$  the radius of the cluster unit.

$\underline{z}^i$  = The vector joining the centre of the MSU. to the point of the contact of the cluster units ( $i: 1, 2, 3, \dots, m$ )  $m$  is the number of contacts per MSU.

$\underline{y}^j$  = the vector joining the contact and the reference frame. (Or vector joins the centre of the structural unit and the reference frame.)

The time rate of change of these position vectors:

$$\dot{\underline{y}}^{a\wedge}(y, t) = \dot{\underline{y}}^{\wedge}(y, t) + \dot{\underline{z}}^{a\wedge}(y, t) \quad (3.3a)$$

$$\dot{\underline{d}}^{a\wedge}(y, t) = \dot{\underline{y}}^{\wedge}(y, t) - \dot{\underline{y}}^r(y, t) \quad (3.3b)$$



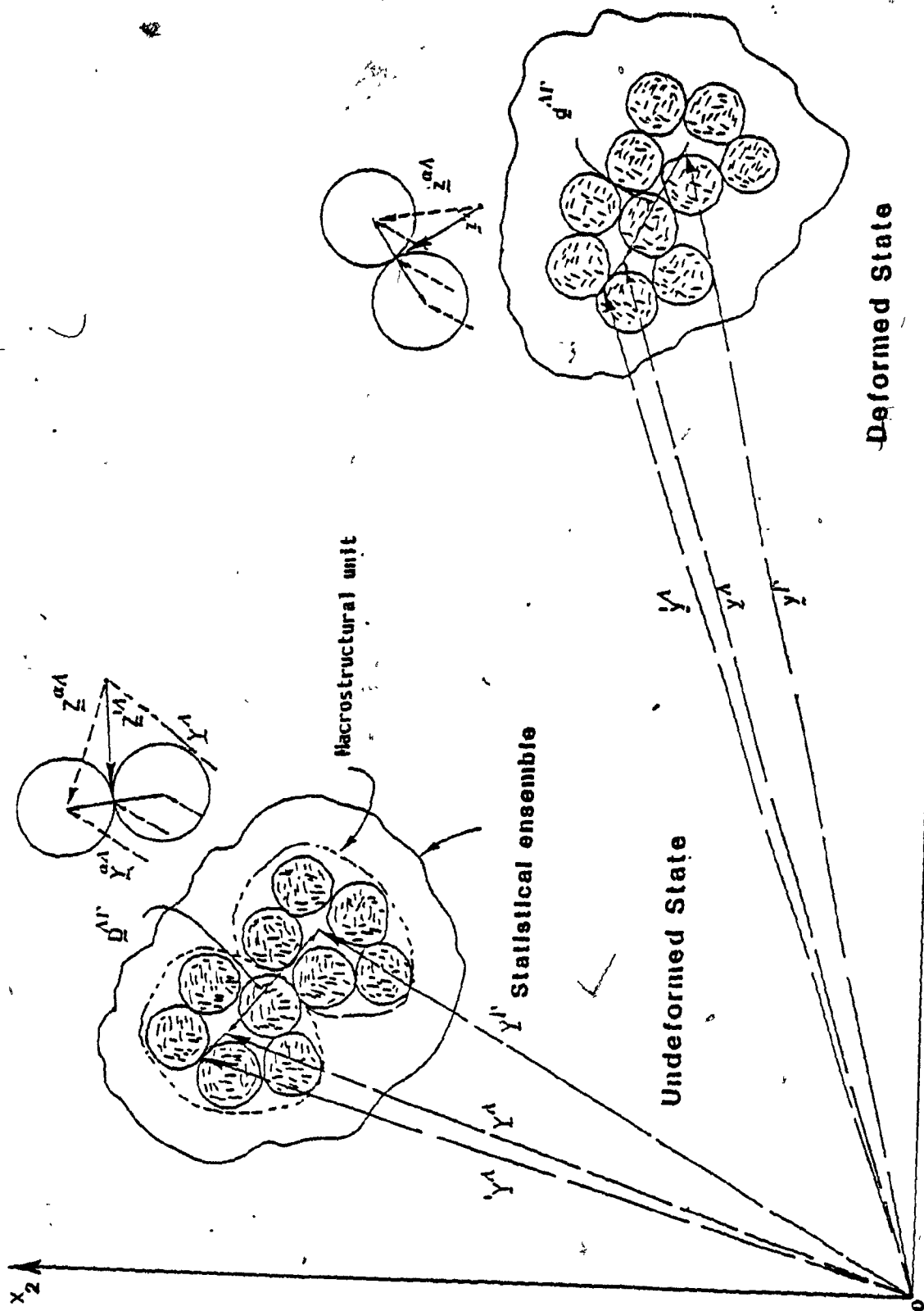


Fig. 14 Kinematics of Deformation (Type B1)

$$\ddot{\underline{z}}^{ia\Lambda}(y,t) = \ddot{\underline{z}}^{i\Lambda}(y,t) - \ddot{\underline{z}}^{a\Lambda}(y,t) \quad (3.3c)$$

$$\ddot{\underline{y}}^{ia\Lambda}(y,t) = \ddot{\underline{y}}^{i\Lambda}(y,t) + \ddot{\underline{z}}^{i\Lambda}(y,t) \quad (3.3d)$$

In which the dot denotes a time derivative ( $dy/dt$ ).

Eq. 3.3a represents the velocity of the clusters within the macrostructural unit. Eq. 3.3b represents the rate of the collapsibility of the adjacent macrostructural units. Eq. 3.3d represents the rate of change of the fluid velocity from the cavity.

The accelerations can be as follows:

$$\ddot{\underline{y}}^{a\Lambda}(y,t) = \ddot{\underline{y}}^{a\Lambda}(y,t) + \ddot{\underline{z}}^{a\Lambda}(y,t)$$

$$\ddot{\underline{d}}^{a\Lambda}(y,t) = \ddot{\underline{y}}^{a\Lambda}(y,t) - \ddot{\underline{y}}^{i\Lambda}(y,t)$$

$$\ddot{\underline{z}}^{ia\Lambda}(y,t) = \ddot{\underline{z}}^{i\Lambda}(y,t) - \ddot{\underline{z}}^{a\Lambda}(y,t)$$

$$\ddot{\underline{y}}^{ia\Lambda}(y,t) = \ddot{\underline{y}}^{i\Lambda}(y,t) + \ddot{\underline{z}}^{i\Lambda}(y,t)$$

When the process is very slow, the acceleration terms can be dropped; however they can be used for the dynamic case.

### 3-4-1-1 Microstrain Formulation:

We will consider a structural unit(S.U.) of two clusters within  $MSU(\lambda)$ , and we will trace the movement of these units. The deformations resulting from the rotation, sliding and displacement of these units can be seen in their effect on the values of the vector parameters ( $\underline{z}^i$  and  $\underline{z}^a$ ), because these vectors connect the cluster unit( $\alpha$ ) to the centroid of the macrostructural unit.

The procedures for the development of the microstrain are as follows:

i- analysis of the vector positions of the two states (undeformed and deformed) of the structural unit with respect to the centroid of the macrostructural unit( $\lambda$ ) by using vector analysis, and

ii- establishment of the incremental displacement of the structural unit (two clusters) within the macrostructural unit( $\lambda$ ), by using analytical mechanics,

iii) establishment of the deformation gradient and the strain of the macrostructural unit( $\lambda$ ) by using smoothness assumption and averaging theorem.

### i- Analysis of the Vector Positions:

The result of the motion of the cluster units will cause a change in the value of  $(\underline{\hat{z}}^{\alpha\Lambda})$ , since  $\underline{\hat{z}}^{\alpha\Lambda}$  connects the cluster unit( $\alpha$ ) with centre of the MSU( $\Lambda$ ). Hence, in terms of the total displacement of the centre of the cluster unit, we have the following equation:

$$\underline{\hat{U}}^{\alpha\Lambda}(t) = \underline{\hat{z}}^{\alpha\Lambda}(t) - \underline{\hat{z}}^{\alpha\Lambda}(t) \quad (3.4)$$

Where:

$\underline{\hat{U}}^{\alpha\Lambda}(t)$  = the total displacement of the centre of the cluster unit( $\alpha$ ) within MSU( $\Lambda$ )

$\underline{\hat{z}}^{\alpha\Lambda}(t)$  = the position vector of the cluster unit( $\alpha$ ) in undeformed state. It connects the centre of cluster to the centre of MSU( $\Lambda$ )

$\underline{\hat{z}}^{\alpha\Lambda}(t)$  = the position vector of the cluster unit( $\alpha$ ) in deformed state.

From simple vector analysis, Eq. 3.4 can take the following general form:

$$\underline{\hat{U}}^{\alpha\Lambda}(t) = \{\underline{\hat{y}}^{\alpha\Lambda}(t) - \underline{\hat{Y}}^{\alpha\Lambda}(t)\} - \{\underline{\hat{n}}^{\alpha\Lambda}(t) - \underline{\hat{N}}^{\alpha\Lambda}(t)\} - \{\underline{\hat{y}}^{\alpha\Lambda}(t) - \underline{\hat{Y}}^{\alpha\Lambda}(t)\} \quad (3.5)$$

(All these symbols are defined in the previous sections, see Fig.14.)

If we consider the displacement of the centre of the cluster unit( $\alpha$ ) with respect to the reference frame, we get the following expression:

$$\hat{\underline{U}}^{\alpha\Lambda}(t) = \hat{\underline{y}}^{\alpha\Lambda}(t) - \hat{\underline{Y}}^{\alpha\Lambda}(t) \quad (3.6)$$

From simple vector analysis, Eq. 3.6 can take the following general form:

$$\hat{\underline{U}}^{\alpha\Lambda}(t) = \hat{\underline{y}}^i(t) - \hat{\underline{Y}}^i(t) - \hat{\underline{n}}^{i\alpha\Lambda}(t) - \hat{\underline{N}}^{i\alpha\Lambda}(t) \quad (3.7)$$

Where:

$\hat{\underline{U}}^{\alpha\Lambda}(t)$  = the displacement of the cluster unit with respect to the reference frame, i.e., the displacement of the cluster unit( $\alpha$ ) due to the rigid body motion of the MSU is included.

The relation between  $\hat{\underline{U}}^{\alpha\Lambda}(t)$  and  $\hat{\underline{U}}^{\alpha\Lambda}(t)$  can be expressed as:

$$\hat{\underline{U}}^{\alpha\Lambda}(t) = \hat{\underline{U}}^{\alpha\Lambda}(t) - \{\hat{\underline{y}}^i(t) - \hat{\underline{Y}}^i(t)\} \quad (3.8)$$

The last term contributes to the rigid body motion of the macrostructural unit( $\Lambda$ ).  $\hat{\underline{U}}^{\alpha\Lambda}(t)$  represents the displacement of the cluster unit( $\alpha$ ) which causes the deformation of the MSU( $\Lambda$ ), i.e., the displacement of cluster unit( $\alpha$ ) due to the rigid body motion of the MSU is excluded.

It should be noted that the condition  $|\underline{N}|^{ia\Lambda} = |\underline{N}|^{ia\Lambda}$  should be held. However, the vector  $\underline{N}^{ia\Lambda}$  contributes in the displacement of the cluster units by its rotational mode only. This contribution will be included in our development of the incremental displacement by introducing a rotation vector  $\omega$  at right angles with vector  $\underline{N}^{ia\Lambda}$ .

### ii- Incremental displacement:

This can be established by considering "how" the structural unit changes from the undeformed state to the deformed state. This change is a result of the translation and the rotation of the system. Therefore, this incremental displacement consists of displacements due to displacement of the system, rotation of the system, sliding of the top cluster, and rotation of the top cluster. See Fig. 15.

1- The displacement of the system: From Fig. 15a, we have the following equation which represents a simple translation:

$$\Delta \underline{U}_1^{s\Lambda} = \Delta \underline{U}^{i\Lambda} \quad (3.9a)$$

Where:

$\Delta \underline{U}^{i\Lambda}$  = the incremental displacement of the contact point, i.e., the displacement of the Structural unit (SU)

2- The incremental displacement due to the rotation of the Structural unit: From Fig. 15b, and from the analytical mechanics point view, we get the following equation:

$$\Delta \underline{U}_2^{sA} = \Delta(\omega \underline{XN}^{iaA}) \quad (3.9b)$$

Where:

$\omega$  = the rotation vector at right angle with plane of motion (i.e., at right angle with  $\underline{N}^{iaA}$ ), and it is located at the contact point, see Fig. 15b.

3- The incremental displacement due to the rotation of the top cluster unit: If the rotation vector is at the centre of the bottom cluster unit, the incremental displacement  $\Delta \underline{U}^{aA}$  has the following form:

$$\Delta \underline{U}_3^{sA} = 2 \Delta(\omega \underline{XN}^{iaA}) \quad (3.9c)$$

Where:

$\omega$  = rotation vector at right angle with plane of motion and is located at the centre of the bottom cluster unit, see Fig. 15c.

4- The incremental displacement due to the displacement of the top cluster can be formulated as simple translation as follows:

$$\Delta \underline{U}_4^{a\wedge} = \Delta \underline{U}^{a\wedge} \quad (3.9d)$$

Where:

$\Delta \underline{U}^{a\wedge}$  = the displacement of the top cluster (L.C. of U).

This displacement can be expressed from the rotation vector which is located at the bottom cluster unit. See Fig. 15d.

Hence, the resulting incremental deformation is as follows:

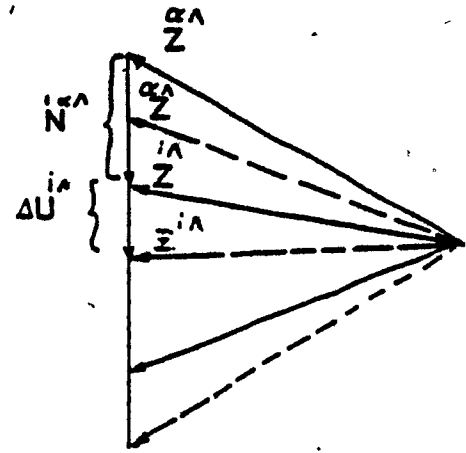
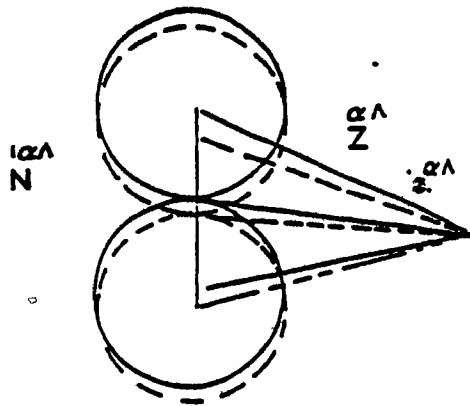
$$\Delta \underline{U}^{a\wedge} = \Delta \underline{U}_1^{a\wedge} + \Delta \underline{U}_2^{a\wedge} + \Delta \underline{U}_3^{a\wedge} + \Delta \underline{U}_4^{a\wedge} \quad (3.10)$$

Where:

$\Delta \underline{U}^{a\wedge}$  = the total incremental change of position of the centre of the cluster unit (a.) within MSU( $\wedge$ ).

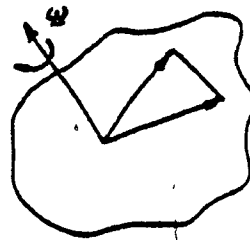
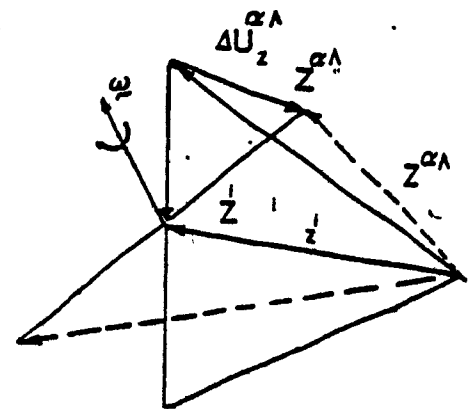
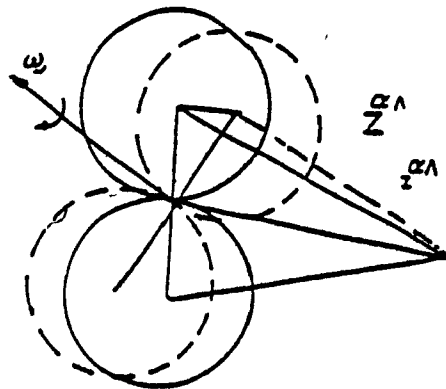
Eq. 3.10 is the outcome of the development from the mechanics of material point of view. Oda et al. (1982) have reported experimentally on the last two terms for granular media i.e., the displacement (sliding) of the top cluster (particle) and rotation (rolling) of the top cluster. (For more details see Oda et al. (1982).) The contribution of each one of the above kinematics (Eq. 3.10) depends on the surface characteristics and properties of the cluster units at





$$\Delta U_1^{\alpha\Lambda} = \Delta U^{i\Lambda}$$

a. Displacement of System

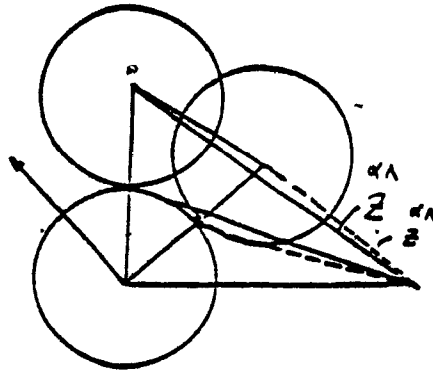


plane of motion

$$\Delta U_2^{\alpha\Lambda} = \Delta(\omega \times \underline{N}^{i\Lambda})$$

b. Rotation of the System

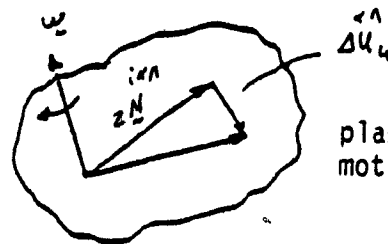
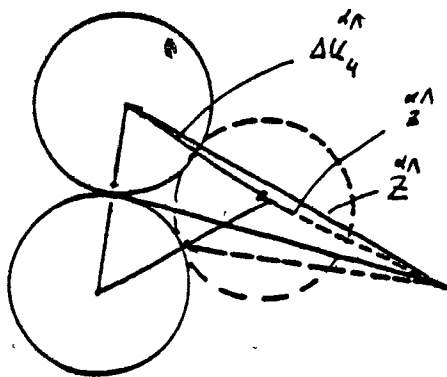
Fig. 15 The Mechanics of Deformation (Type B1)



plane of motion

$$\Delta u_3^{\alpha\lambda} = \Delta(\underline{\omega} \times 2 \underline{N}^{\alpha\lambda})$$

c. Rotation of the Top Cluster Unit



plane of motion

$$\Delta u_4^{\alpha\lambda} = \Delta u_4^{\alpha\lambda}$$

d. Sliding of the Top Cluster

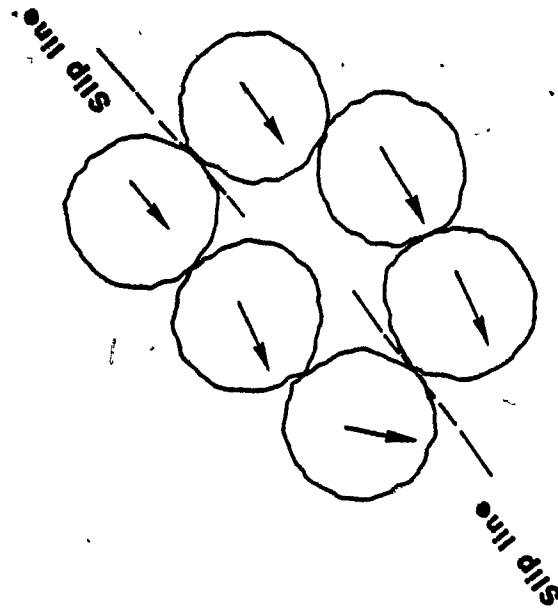
Fig. 15 The Mechanics of Deformation (Type B1) (Cont.)

the contacts and the geometrical configuration of the system.

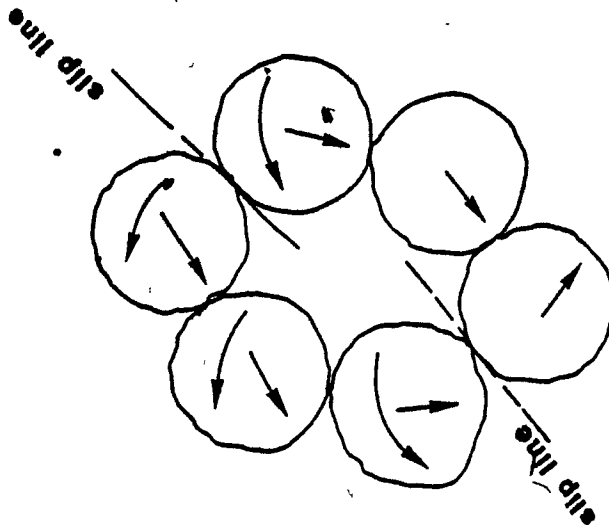
It is interesting to note that the slippage line crossing over macrostructural units can be the result of slipping or sliding and rotation of the contacts on that line. This slippage represents the shear in the macrostructural unit, (see Fig.16). It may be noted also here that when the slippage line is caused by sliding only without rotation, no dilatancy can take place in the line of shear. This slippage lines may be similar to the De Jong concept of free rotation from the continuum analysis point of view, (De Jong(1971)), and the Nemat-Nasser concept of microscopic shear plane, (Nemat-Nasser(1980)).

### **iii- Establishing of the deformation gradient and strain:**

"Strain" is the key element of the kinematics of deformation of particulate media. The best criterion for describing this strain is the deformation gradient. In general, the gradient can be defined as the partial derivative of a vector function. In our case, we have a discrete system of the macrostructural unit. Therefore, we are faced with the problem of finding the deformation gradient. In the following, we will describe two methods to find the deformation gradient:



**Deformation Field  
(without rotation)**



**Deformation Field  
(with-rotation)**

Fig. 16 Deformation Field and Sliplines

- 1- The method of theory of distribution.
- 2- The method of smoothness assumption and average theorem.

Although the second method will be used for its simplicity, a summary review of the both methods will be provided.

**1- Theory of Distribution:** The concept of this theory arises in mathematical physics where the ordinary theory of functions prove inadequate. In our case, the vector positions  $\underline{z}^{a\Lambda} (a=1,2,\dots,n)$  cannot be described by an ordinary function since vectors  $\underline{z}^{a\Lambda}$  describe distributed centres of cluster units within the macrostructural unit. If we map all the centres of the cluster units into a circle of macrostructural unit diameter, we get the vectors  $\underline{z}^{a\Lambda} (a=1,2,3,\dots,n)$  that have values in discrete points within the surface of the circle. Hence,  $\underline{z}^{a\Lambda} (a=1,2,3,\dots,n)$  can be simulated as impulses over the surface of the circle.

Therefore,  $\underline{z}^{a\Lambda}$  should be represented by a generalized distribution function. Once the distribution is described for  $\underline{z}^{a\Lambda} (a=1,2,3,\dots,n)$ , the derivative can be developed and a generalized microstrain can be established. The passage of this generalized microstrain to the global strain may require a special mathematical treatment. The complete

treatment of the theory of distribution is given in Schwartz(1960) and Gel'fand and Shilov(1958).

**2- The smoothness assumption and averaging theorem:** First an ordinary function of the concerned argument should be considered and then the smoothness assumption should be implemented. The smoothness assumption permits the derivative to exist and be continuous. The advantage of this assumption is that it is possible to get a vector gradient which puts the strain formulation in a simple form. The smoothness assumption has been used in granular mechanics by Christoffersen et al. (1981), for the total granular medium. We have applied the smoothness assumption over the macrostructural unit for this study.

The average theorem has been introduced by Rice (1971) as an average of a function over a "specific region" of the material. Rice (1971 and 1975) has used this theorem to find the global plastic strain increment from the internal state parameters in metal constitutive modelling.

#### **Implementation of the second method:**

If we apply the smoothness assumption to Eq. 3.4, we get the following equation:

$$U = z(t) - Z(t) \quad (3.11)$$

The partial derivative of Eq. 3.11 takes the following form:

$$\frac{\partial z}{\partial Z} = \frac{\partial U}{\partial Z} + 1 \quad (3.12)$$

Where:

$\partial z / \partial Z$  = The deformation gradient (Malvern 1969). We will use  $\psi$  for the deformation gradient.

$\partial U / \partial Z$  = The displacement gradient (Malvern 1969).

$U$  = The total displacement of the macrostructural unit.

Note: the gradients are based on the Lagrangian coordinate system.

The incremental form of Eq. 3.12 can be expressed as follows:

$$\frac{\Delta z}{\Delta Z} = \frac{\Delta U}{\Delta Z} + 1 \quad (3.13)$$

Eq. 3.13 is considered from Taylor approximation (i.e.,  $\Delta z = (\partial z / \partial Z) \Delta Z + \dots$ ). It is called a difference equation in the parlance of numerical analysts.

By using the average theorem, it may be possible to put the displacement gradient in terms of the average over the macrostructural unit (i.e., the average over the index  $\alpha$ ). Hence, Eq. 3.13 can be expressed as follows:

$$\frac{\Delta z}{\Delta Z} = \left\langle \frac{\Delta \bar{U}^{\alpha \Lambda}}{\Delta Z^{\Lambda}} \right\rangle + 1 \quad (3.14)$$

From Eq. 3.10, we get the following expression:

$$\left\langle \frac{\Delta \bar{U}^{\alpha \Lambda}}{\Delta Z^{\Lambda}} \right\rangle = \left\langle \frac{\Delta \bar{U}_1^{\alpha \Lambda}}{\Delta Z^{\Lambda}} + \frac{\Delta \bar{U}_2^{\alpha \Lambda}}{\Delta Z^{\Lambda}} + \frac{\Delta \bar{U}_3^{\alpha \Lambda}}{\Delta Z^{\Lambda}} + \frac{\Delta \bar{U}_4^{\alpha \Lambda}}{\Delta Z^{\Lambda}} \right\rangle \quad (3.15)$$

Note: The angular brackets define the mean values of the enclosed quantities.

Several strain measures have been used, but we will use the following form which simulates the conventional continuum one.

$$\epsilon^m(t) = (1/2) (\dot{\psi}^m \dot{\psi}^{mT} - \delta_2) \quad (3.16)$$

$\dot{\psi}^m$  = the deformation gradient, the superscript  $m$  refers to the macrostructural unit.

$\delta_2$  = two-dimensional Kronecker delta.



This form of strain is suitable for passage to the global strain and easy to operate to find the stress.

The strain of the macrostructural unit (Eq.3.16) can be expressed in terms of the modes of motion of the cluster units within this MSU as follows:

$$\epsilon^m(t) = 1/2 \left[ \frac{\Delta \dot{U}^m}{\Delta Z^m} + \frac{\Delta \dot{U}^m}{\Delta Z^m} \right] + 1/2 \left[ \frac{\Delta \dot{U}^m}{\Delta Z^m} \times \frac{\Delta \dot{U}^m}{\Delta Z^m} \right] \quad (3.17)$$

Note: the above addition and multiplication should be done in terms of vector components.

Eq.3.17 represents the strain-displacement relationship for the macrostructural unit. When the total displacement is very small, the last product term can be neglected.

The fundamental difference between the conventional continuum strain and Eq. 3.17 is that the strain in Eq.3.17 contains in its argument the internal state parameter, which is the director  $N^{ia}$ , where  $N^{ia}$  has been described by equation 3.1c.

### Discussion:

The kinematics of deformation of particulate media is a hybrid of the kinematics of two fields. The first field is the kinematics of deformation from continuum mechanics, in which the fundamental concepts are the strain of two distinct points and the continuum motion. These two concepts are built on the premises of the deformation gradient. The second field is the analytical mechanics, in which the fundamental concept is the motion of rigid particles. This motion is described by two modes i.e., rotation and translation in the generalized coordinate system.

Hence, the deformation gradient is the principal concept for the development of the kinematics of deformation of the particulate media. This deformation gradient is constructed from the concept of motion of the rigid particles (Eq.3.17), and therefore the directors  $N^{\alpha}$  play key roles as internal state parameters of the deformation gradient.

Rice (1971) and Bishop (1951 a,b) have considered the internal state parameter for continuum body rather than for microelement. Their state parameter is derived from thermodynamics, and therefore this state parameter is difficult to reconcile to the actual mechanics of the material. In the present study, it is represented from the point of view of the mechanics of cluster motion.

The difference between our theory and the director theory is that in addition to the introduction of the microelement scale, the rotation mode in our theory is transferred into displacement by introducing the rotation vector. Hence, we have only one set of deformations.

### 3-4-2 Kinematics of Deformation of the Second Region:

The deformation of the cluster is a result of the rearrangement of the particles within the cluster unit. We will not consider the kinematics of a two-particle system since the scale is too small and a lot of detailed information can emerge. These details might not be necessary for the prediction of global deformation. Hence, we will consider the deformation of the cluster unit as a continuum body.

In the analysis of this deformation, we will consider first the configuration state which can be described by the following vector positions, (see Fig.17a):

Undeformed state:

$$\underline{\dot{y}}^{aA}(y,t) = \underline{\dot{y}}^{iA}(y,t) - \underline{\dot{N}}^{iA}(y,t) \quad (3.18)$$

Deformed state:

$$\underline{\dot{y}}^{aA}(y,t) = \underline{\dot{y}}^{iA}(y,t) - \underline{\dot{n}}^{iA}(y,t) \quad (3.19)$$

$\dot{\mathbf{N}}^{ia\wedge}(\mathbf{y}, t)$  - vector joins the centre of the cluster / with the contact point(i) within  $MSU(\wedge)$ .

Note: L.C. of  $\mathbf{N}$  (i.e.,  $\mathbf{n}$ ) represents the deformation and not the rotation of this vector (there is no movement of the clusters in type B2 deformation, i.e., the cluster movements are accounted for by the deformation of the other clusters, see the definition of type B2 deformation in previous sections).

The rate of change of Eq. 3.18 has the following form:

$$\dot{\mathbf{y}}^{a\wedge}(\mathbf{y}, t) = \dot{\mathbf{y}}^{ia}(\mathbf{y}, t) - \dot{\mathbf{n}}^{ia\wedge}(\mathbf{y}, t) \quad (3.20)$$

If we take the contact point(i) as a "reference point", i.e., the rate of change of the position vector of the contact point equal to zero ( $\dot{\mathbf{y}}^i = 0$ ), the rate of change in Eq. 3.20 represents the real deformation rate of the cluster units( $\alpha$ ). The real deformation rate is defined as the deformation rate which accounts for the deformation of the cluster unit without its motion, since its motion is accounted for by the deformation of other cluster units. Hence, the deformation rate of the clusters is:

$$\dot{\mathbf{y}}^{a\wedge}(\mathbf{y}, t) = - \dot{\mathbf{n}}^{ia\wedge}(\mathbf{y}, t) \quad (3.21)$$

The acceleration, in general, can have the following

form:

$$\ddot{\underline{y}}^{\alpha\Lambda}(y,t) = \ddot{\underline{y}}^i(y,t) - \ddot{\underline{n}}^i \epsilon^{\alpha\Lambda}(y,t)$$

The cluster deformation can be viewed in terms of the deformability of the vector  $\underline{N}^{\Lambda}$  without its rotation. In other words, the deformation of the pair of clusters at the contact will be considered. The small deformations of the cluster units do not mean a small deformation of the MSU, since the MSU is a collection of several cluster units.

#### 3-4-2-1 Microstrain Formulation:

We define the scalar product of the vectors  $\underline{N}^{12}$  and  $\underline{N}^{13}$  for the MSU( $\Lambda$ ) (the indices given in  $\underline{N}^{\Lambda}$  are considered for simplicity in the development, see Fig. 17b) by

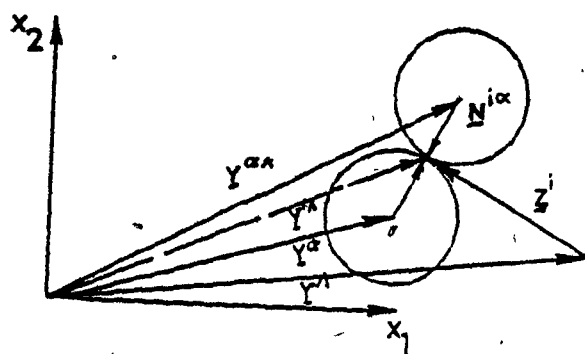
$$W = \underline{N}^{12} \cdot \underline{N}^{13} = |\underline{N}^{12}| |\underline{N}^{13}| \cos \theta \quad (3.22)$$

where  $|\underline{N}^{12}|$  and  $|\underline{N}^{13}|$  are given in Fig. 17b, and  $\theta$  is the angle between the two vectors.

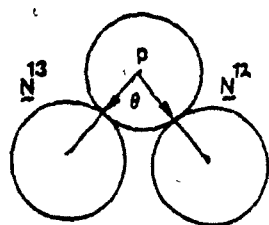
After deformation,  $W$  will have the value

$$W' = \underline{N}^{12} \cdot \underline{N}^{13} = |\underline{N}^{12}| |\underline{N}^{13}| \cos \theta'$$

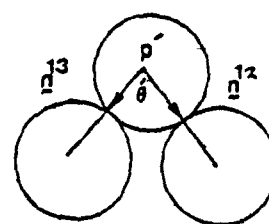
The difference is as follows:



a



Undeformed State



Deformed State

b

Fig. 17 Kinematics of Deformation (Type B2)

$$\underline{W} - \underline{W} = \underline{\dot{n}}^1 \cdot \underline{\dot{n}}^1 - \underline{\dot{N}}^1 \cdot \underline{\dot{N}}^1 = |\underline{\dot{n}}^1|^2 \cos \theta - |\underline{\dot{N}}^1|^2 \cos \theta \quad (3.23)$$

If we assume the smoothness field of deformation over the macrostructural unit, we can expand Eq. 3.20 into McLaurin's series at the contact, i.e., at the reference point.

$$(\underline{\dot{y}}^1 - \underline{\dot{n}}^1)^2 = \underline{\dot{y}}^1 + \frac{\partial \underline{\dot{n}}^1}{\partial \underline{N}^1} (\underline{\dot{Y}}^1 - \underline{\dot{N}}^1 - \underline{\dot{y}}^1) + \frac{\partial^2 \underline{\dot{n}}^1}{\partial \underline{N}^1^2} (\underline{\dot{Y}}^1 - \underline{\dot{N}}^1 - \underline{\dot{y}}^1)^2 \quad (3.24)$$

At the reference point, we have  $\underline{\dot{y}}^1 = \underline{\dot{Y}}^1$ .

Hence:

$$\underline{\dot{n}}^1 = \frac{\partial \underline{\dot{n}}^1}{\partial \underline{N}^1} \underline{\dot{N}}^1 + \frac{\partial^2 \underline{\dot{n}}^1}{\partial \underline{N}^1^2} (\underline{\dot{N}}^1)^2 \quad (3.25a)$$

and similarly for other vector,

$$\underline{\dot{n}}^2 = \frac{\partial \underline{\dot{n}}^2}{\partial \underline{N}^2} \underline{\dot{N}}^2 + \frac{\partial^2 \underline{\dot{n}}^2}{\partial \underline{N}^2^2} (\underline{\dot{N}}^2)^2 \quad (3.25b)$$

If we substitute Eqs. 3.25 a and b in Eq. 3.23, we get the following:

$$\dot{W} - W = \left( \frac{\partial \underline{n}^{12}}{\partial \underline{N}^{12}} \underline{N}^{12} + \frac{\partial \underline{n}^{212}}{\partial \underline{N}^{12^2}} (\underline{N}^{12})^2 \right) \left( \frac{\partial \underline{n}^{13}}{\partial \underline{N}^{13}} \underline{N}^{13} + \frac{\partial \underline{n}^{213}}{\partial \underline{N}^{13^2}} (\underline{N}^{13})^2 \right) - \underline{N}^{12} \underline{N}^{13}$$

$$\dot{W} - W = \left\{ \begin{array}{cc} \frac{\partial \underline{n}^{12}}{\partial \underline{N}^{12}} & \frac{\partial \underline{n}^{13}}{\partial \underline{N}^{13}} \\ \frac{\partial \underline{n}^{12}}{\partial \underline{N}^{12}} & \frac{\partial \underline{n}^{13}}{\partial \underline{N}^{13}} \end{array} \right\} - \underline{\delta} \quad \underline{N}^{12} \underline{N}^{13} + \dots \quad (3.26)$$

If  $p$  (in Fig. 17b) represents a rigid-body motion of the cluster units of center  $p$ , then  $\dot{W}$  will be equal to  $W$  for any choice of a configuration state. Therefore, this fact suggests that the term in parentheses (Eq. 3.26) is a reasonable measure of the deformation concept for the M.S.U.

Thus the strain measure in this case can have the same form as for the first region.

$$\underline{\epsilon}^n(t) = (1/2) (\underline{\psi}^n \underline{\psi}^{nT} - \underline{\delta}) \quad (3.27)$$

Where

$\underline{\psi}^n$  = The deformation gradient of the MSU (second region), and it is equal to  $\partial n / \partial N$ .

The fundamental difference between the conventional continuum strain and Eq. 3.27 is that the strain in Eq. 3.27 contains in its argument the internal state parameter which is the director  $\underline{N}^{i\alpha}$ , in



which its deformation represents the development of this strain.

#### Discussion:

The following points are important for developments in the coming chapters:

1- As can be viewed in Equations 3.17 and 3.27 the microdeformation gradient and the microstrain are produced from different elements of kinematics of deformation. Therefore, the microstrain of particulate media depends on the types of deformation (type B and type C) which are induced in these media. Therefore, the development procedures of the constitutive equations will depend on the types of deformation.

2- In micromechanics of soil, the microstrain-displacement relation has advantages over the similar relation in continuum mechanics; the microstrain can be developed from the displacement which is a direct result of the mechanism of the local cluster motion or deformation. Therefore, the establishment of the microstrain-displacement relationship requires a certain experimental program in microlevel of the clay sample to get the cluster kinematics behaviour.

Hence, under a specific load the displacement of

the cluster units can be traced by an experiment in the microlevel, and this displacement can be transferred into microstrain by a computer program ( using Eqs. 3.17 and 3.27) built in with test data acquisition.

The experimental micromechanics is beyond the objective of this study. Therefore, in the following chapters we develop the constitutive equations in terms of the "microstrain", instead of using the displacement. Further discussion of this point will be given in Chapter 4.

3- The consideration of the randomness of the microstrains over the ensemble of the macrostructural units is the subject of Chapter 5.

4- In the previous sections we have discussed the kinematics of deformation of particulate media and the director concepts, and the developments of the microstrains of the first region and the second region of the clay compression. We can now address the concept that the kinematics of deformation of particulate media may follow different "views and methodology" than the classical continuum mechanics and particle dynamics.

### 3-5 VOLUMETRIC AND WEIGHT RELATIONSHIPS:

In the last section, we developed the microstrain measures. In this section, we will develop the volumetric and mass parameters which are essential for time evolution of deformation.

There are three important relationships of volume: porosity, void ratio, and degree of saturation. Porosity is the ratio of void volume to total volume; and void ratio is the ratio of void volume to the solid volume.

The void ratio represents one of the fundamental state parameters in stability analysis. It is one of the parameters that describes the initial state of the soil media, (loose as opposed to dense condition). These conditions are fundamental in describing the mechanical behaviour of the soil system. Void ratio can be linked with a constitutive operator to find stress-compressibility relations. Moreover, it contributes to the modelling of the hydraulic conductivity of the soil system.

The bulk void ratio has often been related to the coordination number (the number of the contacts per particle) for granular media, see Smith et al. (1929), Field (1963), Gray (1968), and Oda (1972).

The most useful relationship in terms of weight is water content which is the weight of water divided by the weight of solid in a soil element. The relationship between water content and void ratio for the microelement (MSU) will be given in this section. The pore space system of the clay mass has been divided into micropores and macropores (intra- and inter-cluster). Therefore, the void ratio and water content can be defined for the inter cluster pores and intra cluster pores.

Table 1 shows some definitions of the volumetric and weight relationships for the microelement scale which is proposed in the present analysis. The phase diagram which is shown in the table indicates in the left side the volume relations and on the right side the mass relations. From this table, we can obtain the following relationships for the MSU.

$$e_m = \frac{\text{Vol. of the intercluster pores in MSU}}{\text{Vol. of the cluster units in MSU}} \quad (3.28)$$

and

$$S e_m = w \frac{\bar{\rho}_s}{\rho_w} \quad (3.29)$$

For Fully saturated macrostructural unit ( $S=1$ ),  
Eq. 3.29 can be reduced to the following form:

$$e_m = w_m \frac{\bar{\rho}_s}{\rho_w}$$

and the following expression for the saturated density:

$$\rho_{(m) \text{ sat.}} = \frac{\bar{\rho}_s + \rho_w e_m}{(1 + e_m)} \quad (3.30)$$

Where

$S$  = the degree of saturation of the macrostructural unit.

$e_m$  = the void ratio of the macrostructural unit based on the macropores, i.e., the micropores are included in the volume of the solids. This void ratio plays an essential role in the present analysis.

$\rho_{(m) \text{ sat.}}$  = the saturated density of the MSU

$w_m$  = the water content of the macrostructural unit based on the intercluster fluid. The other terms are defined in Table 1.

For the cluster unit, the void ratio( $e_c$ ) has the following form:

Table 1 Volume-weight relationship of the macrostructural unit

# Macrostructural unit

$V_i$	intercluster water
$V_a$	intracluster water
$V_s$	solid

$W_i$

=

$W_a$

$W_s$

## Volume Relationship

$V_i$  = volume of water  
(intercluster)

$V_a$  = volume of water  
(intracluster)

$V_s$  = volume of solid

$V_c$  = the volume of the  
cluster

$$e_m = \frac{V_i}{V_i + V_s} = \frac{V_i}{\Sigma V_c}$$

$\Sigma$  = summation over set C

## Weight Relationship

$W_i$  = weight of water  
(intercluster)

$W_a$  = weight of water  
(intracluster)

$W_s$  = weight of solid

$W_c$  = the weight of the cluster

$$w_m = \frac{W_i}{W_i + W_s} = \frac{W_i}{\Sigma W_c}$$

$$\rho_m = \frac{W_i + W_a + W_s}{V_i + V_a + V_s}$$

$$\bar{\rho} = \frac{W_i + W_s}{V_i + V_s}$$

$$\hat{e}_c = \frac{\text{Vol. of the intracluster (micro) pores}}{\text{Vol. of the solids within the cluster units}} \quad (3.31)$$

It should be noted here that  $e$  and  $w$  are local parameters which are different from the bulk parameters  $e$  and  $w$ . However, the average of  $e_m$  plus the average of  $\hat{e}_c$  can be equal to  $e$  (bulk void ratio), i.e.,  $e = \langle e_m \rangle + \langle \hat{e}_c \rangle$  (as an example, the Champlain clay of Quebec at specific sites has  $e = 2.28$ ,  $\langle e_m \rangle = 1.6$ ,  $\langle \hat{e}_c \rangle = .68$ . These values are developed from data of Delage et al. (1984)).

### 3-5-1 The concept of "The Compression Zone":

Compressibility as defined in the introduction is the volumetric response of the soil system. It depends on the voids in the solid system. As an example, the compressibility of a gas is greater than the compressibility of a liquid, because the voids between the molecules of gases are larger than the voids between the molecules of liquids.

Soil is a three-phase system: solid phase, water phase and air phase. If the voids of soil can be filled either with water or air, the soil will be two-phase system. Hence, the compression zone of the particulate system can be defined as the volume of the voids between particles or fabric units. The shape and the

size of the compression zone depend on the fabric and the pack of the system. For plate and rodlike particle (fabric unit) shapes, the compression zone depends on the mode of association of these particles, i.e., edge-to-edge, face-to-face and edge-to-face.

Bolt(1956) and later Sirdaran(1979) have related the compression zone of the parallel clay particles to the void ratio of the total system. They consider the compression zone in terms of the distance between two clay particles.

In the second chapter, we defined the clay system as having two different pores: macro- and micro- pores. These pores have been generated by different solid clay particle arrangements. The macropores are formed by the cluster units which have idealized spherical shapes. The micropores are formed by the particle arrangements within the cluster units. The clay particles have platelet shapes.

We will consider the compression zone for different solid shapes. The concept of the director theory which has been used for the development of microstrain is used here. One of the advantages of using the directors for the development of the compression zone is that it puts the system change as material frame indifference, i.e., the volumes and areas (and their rates) as an objective quantities.



By utilizing the director product concept, the directors are vectors which describe the shape of the compression zone. In the following, we will use this concept for three different shapes: cylindrical, spherical, and platelet.

#### Mathematical development:

From the concept of cross-product, we get the following expression:

$$\underline{a} \times \underline{b} = 2A\underline{u} \quad (3.32)$$

where

$\underline{u}$  = unit vector at right angle to the plane of the two units.

$\underline{a}$  and  $\underline{b}$  = directors which describe the shape of the compression zone between two units

$A$  = the area enclosed between the two units

Hence,

$$|\underline{a} \times \underline{b}| = 2A$$

in which  $|\underline{u}|=1$ .

If we take the time rate of change of Eq. 3.32 we get:

$$\dot{\underline{a}} \times \underline{b} + \underline{a} \times \dot{\underline{b}} = 2 (\dot{A} \underline{u} + A \dot{\underline{u}})$$

in which the dot denotes a time derivative ( $du/dt$ )

From the Schwartz inequality, we can get:

$$| \dot{\underline{a}} \times \underline{b} | + | \underline{a} \times \dot{\underline{b}} | \geq | \dot{\underline{a}} \times \underline{b} + \underline{a} \times \dot{\underline{b}} |$$

Hence,

$$| \dot{\underline{a}} \times \underline{b} | + | \underline{a} \times \dot{\underline{b}} | \geq 2 (\dot{A} \underline{u} + A \dot{\underline{u}})$$

where

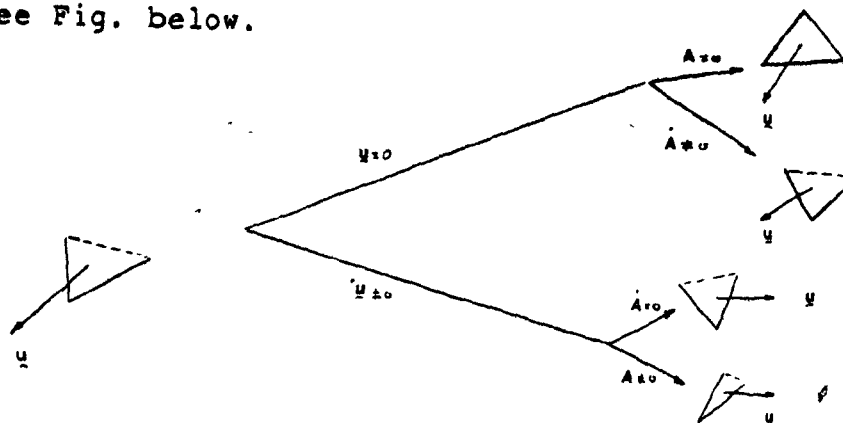
$$\dot{\underline{u}} = \dot{\omega} \times \underline{u}$$

$\dot{\omega}$  = the angular velocity of the vector which is at right angles to the plane of the two units.

If we restrict the motion of the clusters in the plane at right angles to the unit vector  $\underline{u}$ , i.e.,  $\dot{\underline{u}}=0$ , we get

$$| \dot{\underline{a}} \times \underline{b} | + | \underline{a} \times \dot{\underline{b}} | = 2 |\dot{A}| \quad (3.33)$$

See Fig. below.



For volumetric analysis, we have the triad director product,

$$V = \underline{c} \cdot | \underline{a} \times \underline{b} | \quad (3.34)$$

$\underline{c}$  = a vector at right angles with plane of the two vectors  $\underline{a}$  and  $\underline{b}$ .

$V$  = the volume enclosed by the triad directors.

The time rate of change of Eq. 3.34 is,

$$\frac{dV}{dt} = \frac{dc}{dt} \cdot |\underline{a} \times \underline{b}| + c \cdot \left( \left| \frac{d\underline{a}}{dt} \times \underline{b} \right| + \left| \underline{a} \times \frac{d\underline{b}}{dt} \right| \right) \quad (3.35)$$

For restricted motion, we get the following expression:

$$\frac{dV}{dt} = 2 \left( \frac{dc}{dt} \cdot |A| + c \cdot \left| \frac{dA}{dt} \right| \right) \quad (3.36)$$

Table 2 gives the formulations for different shapes with appropriate director definitions. In light of the mechanism of deformation of the first region, we have the cluster motion (no particle motion, i.e., rigid clusters). Hence, the compression zone between the clusters is the one which will be affected under applied load. In fact, the compression zone formed by the clusters is the generated cavity in the MSU.

In light of the mechanism of deformation and the physics of compression of the second region, we have cluster deformation without motion, i.e., particle displacement within these clusters. The compression zone between the particles is the one which will be affected under applied load. Therefore, some of these formulations will be used for the appropriate deformation regions in Chapter 4.

$$|\dot{\underline{a}}_1 \times \underline{a}_2| + |\underline{a}_1 \times \dot{\underline{a}}_2| = 2 |\dot{\lambda}|$$

$$\frac{dv}{dt} = \dot{\underline{a}}_3 \cdot |\underline{a}_1 \times \underline{a}_2| + \underline{a}_3 \cdot \left\{ |\dot{\underline{a}}_1 \times \underline{a}_2| + |\underline{a}_1 \times \dot{\underline{a}}_2| \right\}$$

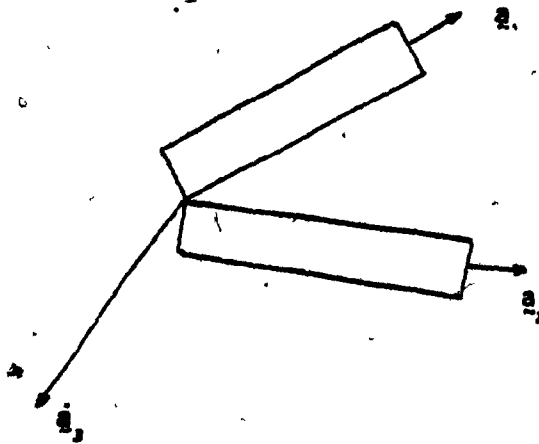
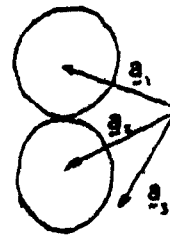
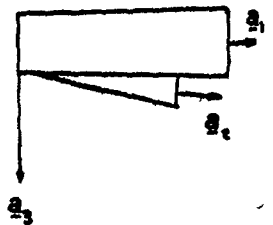
CYLINDRICAL  
SHAPESPHERICAL  
SHAPEPLATELET  
SHAPE

Table 2 Compression zone formulation for different shapes

In the last section, we developed the area and volume of the compression zone. In the following section, we will develop a model for the macrostructural void ratio by using the geometrical probability.

### 3-5-2 Void Ratio of the Macrostructural Unit:

The concept of the probability which will be used here is geometrical probability. This probability is concerned with random variables which are geometrical objects taking values in some set of possibilities on which there is a defined non-negative measure, satisfying certain required conditions which enable us to interpret it as a probability.

Part of this probability is explained in terms of intrinsic fabric variability concept (see Chapter 5 for more detail). The following steps are necessary for the development of the void ratio:

#### i- Finding the cluster diameter from the observed diameter:

If we cut a test sample, we can observe the cluster units and the pores by scanning electron microscopy. The probability distribution of the observed diameter of the cluster units can be found and called  $F(y)$ . Hence, from this distribution of diameters, we can find the actual probability distribution of the

diameter of clusters.

To do that, we will consider the integral equation model which is presented by different authors including Kendall and Moran(1963), and Tallis(1970). It was originally developed by Wicksell (1925,1926). It represents one of the fundamental equations of geometrical probability. The integral equation can have the following form:

$$f(y) = \frac{y}{E(r)} \int_y^{\infty} \frac{g(r)}{(r-y)^{1/2}} dr \quad (3.37)$$

where

$$f(y) = dF(y)/dy$$

$f(y)$  = probability density function of the observed radius of spherical cluster

$g(r)$  = probability density function of the calculated radius of the cluster.

$E(r)$  = the mean value of the radius of the clusters.

Eq. 3.37 represents relationship between the observed probability density of the cluster radius  $f(y)$ , and the calculated probability density function of the cluster radius  $g(r)$ . In the Appendix A-2, we have simplified the integration of Eq. 3.37 and have solved it by using numerical technique.

For equal size spheres, the governing equation is:

$$f(y) = \frac{y}{(r^2 - y^2)^{1/2}}$$

In the Appendix A-1, we developed the relationships between the moments of observed and calculated cluster size distribution. The expressions for the moments are:

$$E(y) = \frac{\pi}{4} \frac{E(r^2)}{E(r)} \quad (3.38)$$

$$E(y^2) = \frac{2}{3} \frac{E(r^3)}{E(r)} \quad (3.39)$$

where

$E(r)$  = The expected value of the radius  $r$ .

$E(y)$  = The expected value of the observed radius  $y$ .

$E(r^2)$  = The second moment of the function  $g(r)$ .

$E(r^3)$  = The third moment of the function  $g(r)$

(Axelrad (1978) and Benjamin et al. (1971)).

These moments are used for several applications, such as the formulation of the average specific surface area, the hydraulic radius ( $R$ ) and the cross sectional area of the channels ( $a$ ). The formulation of the last two parameters ( $R$  and  $a$ ) are considered in chapter six.

The average specific surface area of the cluster unit can have the following form (see App. A-1):

$$S_v = 3 \frac{E(r^2)}{E(r^3)} \quad (3.40)$$

Equation 3.40 will be used in Chapter 6.

## ii- Calculation of the probability distribution of volume of spheres:

We have a function relationship between the volume of the cluster and radius of the following form:

$$V = \bar{g}(r)$$

$$V = (4/3) \pi r^3$$

$$r = \bar{c} V^{1/3}$$

Where

$$\bar{c} = (3 \pi / 4)^{1/3}$$

Papoulis (1967), Ang et al. (1975) and Benjamin et al. (1971) present methods for deriving the distribution of random variables which are functionally dependent upon random variables whose distributions are known. In general, one should seek the probability distribution of the dependent random variable  $V$  (volume). For any particular value  $V$ ,  $F(V)$  is found by calculating in the sample space of  $r$  (radius) the



probability of all those events where  $g(r)$  is less than or equal to  $v$ . Hence:

$$f(v) = \left| \frac{d\bar{g}}{dv} \right|^{-1} f(\bar{g})^{-1}$$

$$f(v) = \left| \frac{c}{3v} \right|^{-1} f\left(\frac{c}{3v}\right)^{1/3} \quad (3.41)$$

Once we calculate the distribution of the diameter, we can find the probability distribution of the volume of the cluster from Eq. 3.41.

### iii- Void ratio formulation:

The probability distribution of the number of cluster units in a macrostructural unit is assumed to be a poisson distribution. It has the capability to model the possible occurrences of events at any point in space and it has the following form:

$$Pr(N_c = n_c) = \frac{\left( \mu \frac{E(V_m)}{E(v_c)} \right)^{n_c}}{n_c!} \exp - \left( \mu \frac{E(V_m)}{E(v_c)} \right) \quad (3.42)$$

where

$E(V_m)$  = the average volume of the MSU

$E(v_c)$  = the average volume of the cluster unit

$\mu$  = average rate of number of cluster units in the macrostructural unit.

$n_c$  = the number of the cluster units in the

MSU.

The macrostructural void ratio formulation can be developed from the above steps and from its definition. Hence, it can have the following form

$$E(v_c) \cdot n_c = V_m \frac{1}{1 + e_m} \quad (3.43a)$$

$$e_m = \frac{V_m - E(v_c) n_c}{E(v_c) n_c} \quad (3.43b)$$

Where  $V_m$  = the total volume of M.S.U.

The volume of the macrostructural units and the number of the cluster units( $n_c$ ) are treated as random variables according to Eqs. 3.41 and 3.42. Hence, the void ratio of macrostructural unit will have probability distribution over the ensemble of the macrostructural units. Further from this distribution and Eqs. 3.29 and 3.30, we get the probability distributions of  $w_m$  and  $\rho_m$ .

#### **New Fabric Definition:**

The void ratio of the macrostructural unit is introduced as a new fabric definition for clay soil (and sand soil). This fabric definition can describe and model the macropore size distribution and the arrangements which are essential for the following

points:

1. To describe the initial state of the system, i.e., loose state as opposed to dense state. This description is very important for modelling the constitutive equation of the soil medium.

2. To describe and model the fluid flow through the soil medium. Further, the macrostructural void ratio can be used as a state parameter to describe and model the stress-deformation equation of the soil medium. In the present analysis, we will use  $e$  for modelling the fluid flow equation. Fig. 18 shows a schematic view of this new fabric definition.

#### Calculation Procedures for $e_m$ , $w_m$ , $A_m$

The steps for calculation of the probability distribution of the macrostructural void ratio are as follows:

1- Calculate the probability distribution of the radius of clusters and the macrostructural units by using Eq. 3.37 with input data: observed radius of the clusters and MSUs in distribution form (from scanning electron microscopy soil samples).

2- Calculate the probability distribution of volume of the units by using Eq. 3.41 where the input is the calculated probability distribution of the radius.

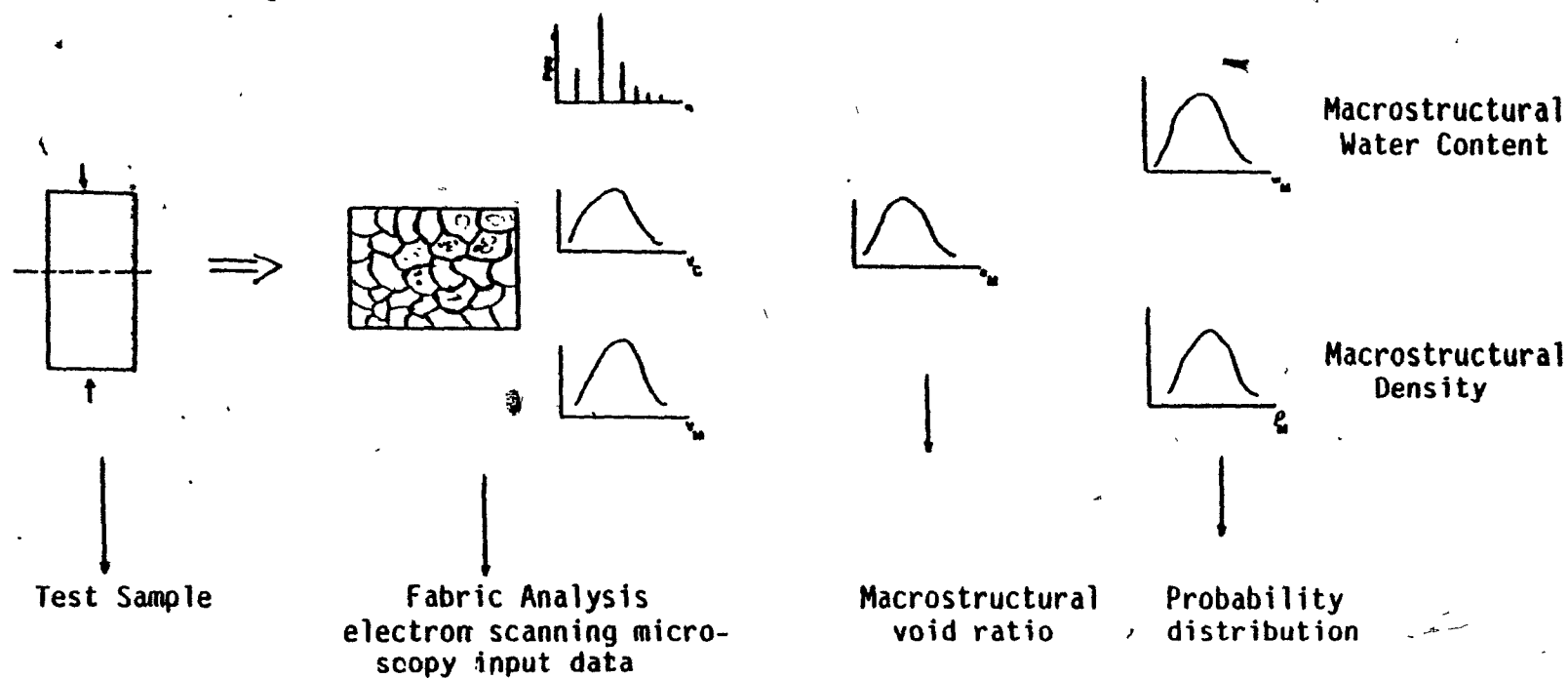


Fig. 18 Schematic View of the New Fabric Definition

3- Calculate the probability distribution of the number of the cluster units per MSU by using Eq. 3.42.

4- Calculate the probability distribution of  $e_m$  by using the above steps. This is done by applying the Monte Carlo simulation technique on Eq. 3.43, where the inputs are the probability distribution of the number of clusters in the MSU, and the probabilities of volumes of the clusters and the MSUs. The Monte Carlo technique is explained in the Appendix D.

Once we calculate the probability distribution of the macrostructural void ratio from Eq. 3.43, we are able to find the probability distribution of the water content and density by using Eqs. 3.29 and 3.30. It can be noted, interestingly, that in classical geotechnical engineering we measure mass, and calculate water content, and thus calculate the void ratio, and density ( $\rho$ ). However, in the above procedures, we are doing just the opposite.

A computer program was developed to calculate the probability distribution of the void ratio, density and water content of the macrostructural unit. The flow chart is given in Fig.19, and the numerical technique is discussed in Appendix A.

**Discussion:**

The mass-volume relationships represent the basic relations in the classical geotechnical engineering, we have extended them to cover the microelement scale, i.e., the macrostructural unit. The new mass-volume relationships have the capability to describe the macropore size distribution and the subregion(MSU) water content distribution.

The cross product of the triad directors has the capability to model the compression zones between the clusters (or particles).

The macrostructural void ratio is the key parameter for the description and modelling of the fluid flow behaviour which will be discussed next.

**3-6 FLUID KINEMATICS AND FLOW EQUATION:**

In the previous sections, we dealt with kinematics of deformation of the clay skeleton. In this section, we will develop the fluid kinematics and flow equation.

The fluid flow through soil depends on many properties and characteristics of the soil and the permeant. Those which are related to soil are the pore size distribution, tortuosity (the channel of flow), fabric and the surface characteristics of the

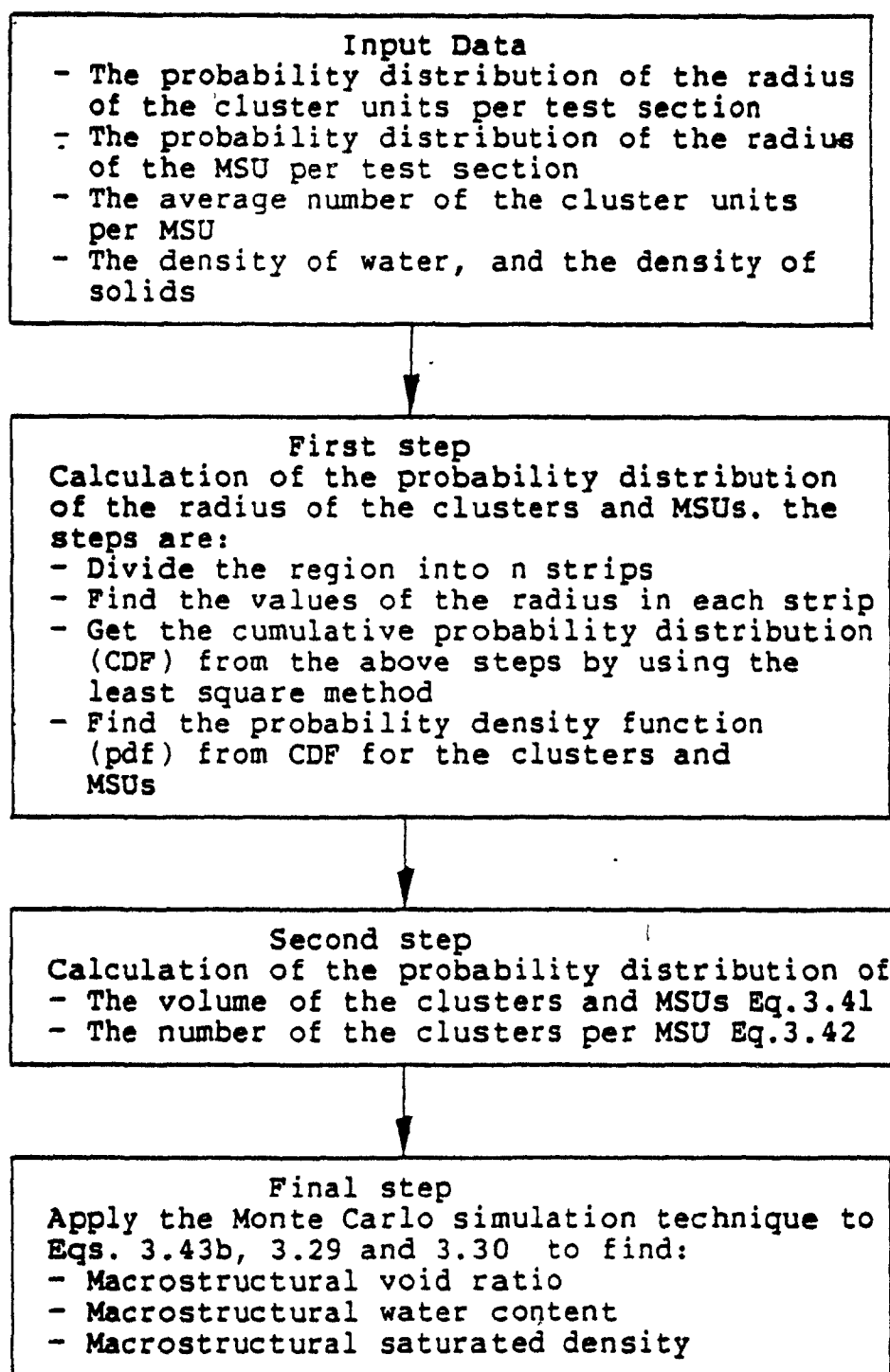


Fig. 19 Computational flow scheme of probability distribution of  $e_m$ ,  $w_m$  and  $\rho_m$

particles; and those which are related to the permeant are the viscosity, temperature, density, and its free energy. In addition, we have the soil-water interaction factors which depend on the pore fluid chemistry such as the dielectric constant, pH value, etc.

It is difficult to assess the relative importance of each of the factors, since many of them are interdependent. The effect of temperature on liquid transfer is not fully known, since temperature affects both the permeant and clay-water interaction (Yong et al. (1975)).

#### **Physics of Fluid Flow:**

The physical description of clay compression which is introduced in the second chapter reveals that in the first region, the fluid will move out from and through the cavities (macropores). The water volume which will be transferred out from the concerned soil mass is measurable as far as the excess pore water pressure can be measured.

The excess pore water pressure is measurable until the macrostructural void ratio reaches a certain value. We call this void ratio as the equilibrium void ratio. In the overlapped region, not all the macrostructural units reach equilibrium void ratio. Hence, the fluid will move out from the macrostructural units which have not reached the equilibrium void ratio. Therefore, some



surface flux of fluid (volume) can be measured.

For the second region, all macrostructural units have reached the equilibrium void ratio. Therefore, the flow from micropores to macropore will be with no surface flux of fluid. For this region, self-organization of the soil-water system can take place.

It should be noted that when the macrostructural unit reaches the equilibrium value, it does not mean that the bulk void ratio has reached the equilibrium void ratio. The equilibrium bulk void ratio has been defined in the literature as the void ratio at which 100% consolidation of the sample takes place. It concerns itself with both micropores and macropores. Therefore, the equilibrium bulk void ratio may cause confusion, since when it reaches the equilibrium, some of the micropores will be caused to change, and these micropores do not have a relation with the excess pore water pressure measurements. Micropores changes cause small pore water pressure to build up, but it is not significant to be of measurable value.

It is worth noting that our definition of equilibrium void ratio indicates that the excess pore water pressure can be measured until the macrostructural unit void ratio reaches its equilibrium value.

We summarized the above discussion in Fig.20 which shows a schematic view of surface water flux from a soil mass system; the ordinate represents the volume change and the abscissa the log time. We will develop the flow equation for the first region where the surface water flux (volume) can be measured.

### 3-6-1 Review:

From the continuum point of view, a flow equation based on experiment has been developed by Darcy. This equation relates the velocity of the flow with pressure gradient. This relationship is linked with the coefficient of permeability. Extensive investigations have been confirmed the validity of the law, and the fundamental factors controlling the permeability coefficient. See for example, Olsen(1965), Hansbo(1960), and Mesri and Olson(1971b).

Lambe(1954), Michael et al.(1954) and Olsen(1962) have demonstrated that the Kozeny-Carman equation which has frequently been used to predict permeability is not suitable for predicting the permeability of fine-grained soils.

Many empirical relationships have been established from experimental data relating the permeability to the void ratio (see Tavenas et al. (1983), Olson et al. (1981) and Juarez-Badillo(1981)). These relations can have a general function as follows:

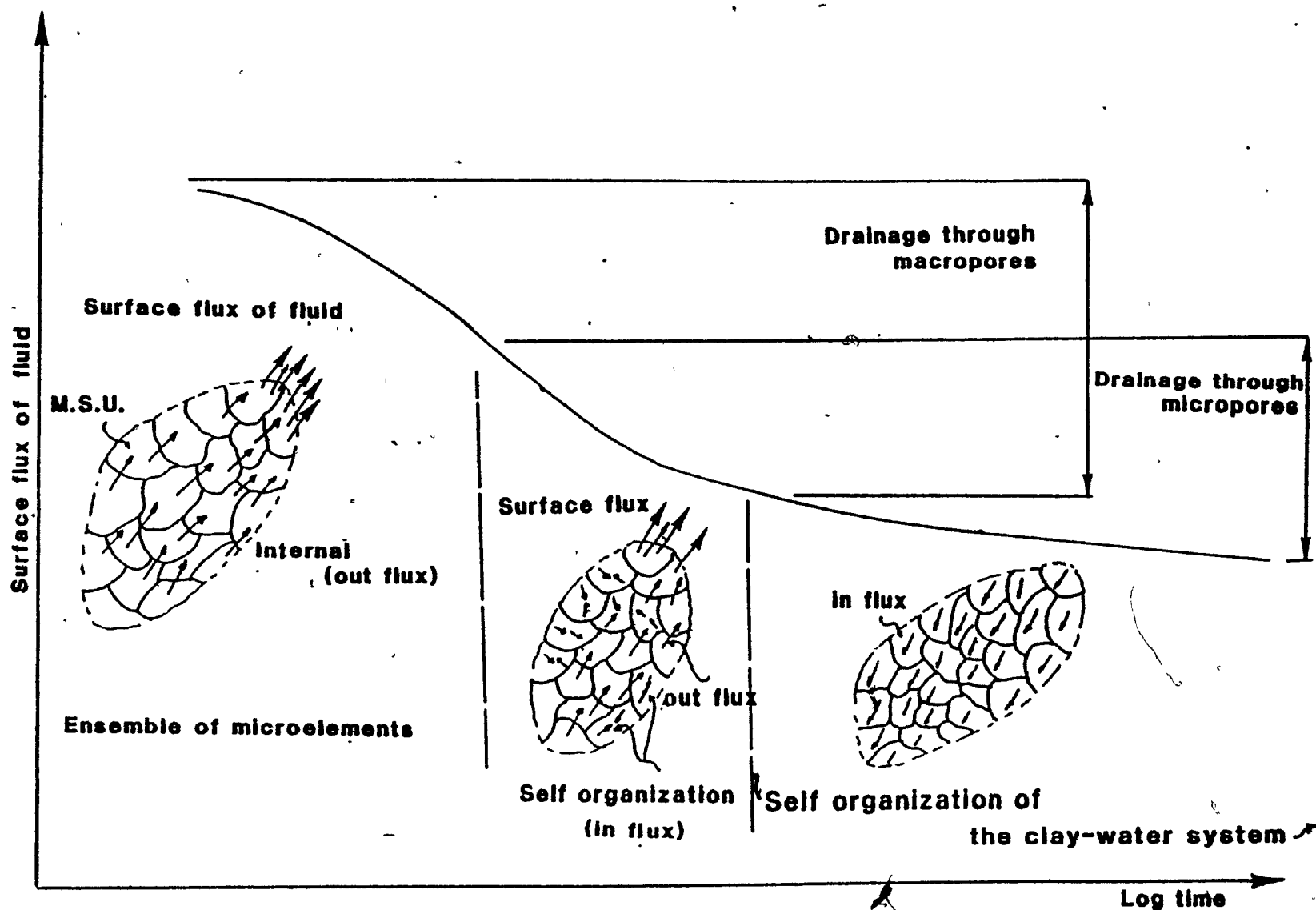


Fig. 20 The Mechanism of Fluid Flow

$$K = f(e, \zeta)$$

where

$K$  = the permeability coefficient

$e$  = bulk void ratio

$\zeta$  = experimental fitting parameter

In order to use these empirical formulations, one has to be aware of their limitations and applicability. These formulations may be suitable for a certain types of soil under certain specific fabric conditions. If two samples from the same soil with same bulk void ratios are subjected to the same external stimuli, the prediction from empirical formulations may give the same results, while the actual response could give different results since the bulk void ratio does not reflect the "soil fabric" of the system. In other words, for same bulk void ratio a medium composed of numerous small pores is likely to exhibit a lower saturated permeability than a medium composed of fewer large pores. Hence, other parameters besides the bulk void ratio which reflect the soil fabric should be considered for better representation of the actual soil-water performance.

From the discrete point of view; Leonards(1962) has developed Hagen-Poiseuille equations for different equivalent capillary channels model. Scheidegger(1974) has examined the hydraulic radius of channels model derivation from the Hagen-Poiseuille equation, and he

has presented a critique of the model. Further, Scheidegger has suggested that the preferred model of a porous medium should be based on probabilistic concepts.

With the view of using pore size distribution to predict the permeability of siltyclay, Garcia-Bengochea et al. (1979) have classified different models which are introduced by several investigators (such as Childs and Collis-George (1950) and Marshall (1958)) into capillary models and hydraulic models, all of them based on the premises of Hagen-Poiseuille equation. (See also the work of Juang and Holtz (1986)).

### 3-6-2 Flow Equation Development:

Below, we will develop a flow equation which can take into consideration the material characteristics of the media.

The mechanism of flow can be viewed as the flow through a channel connecting two adjacent macrostructural units. There are two conditions of flow between the two adjacent macrostructural units. These conditions are: a) conduit flow type and b) flow around a submerged object. These types of flow depend on the size of the macropores which in turn depend on the local and bulk void ratios.

When the cavities are very large, the conduit type

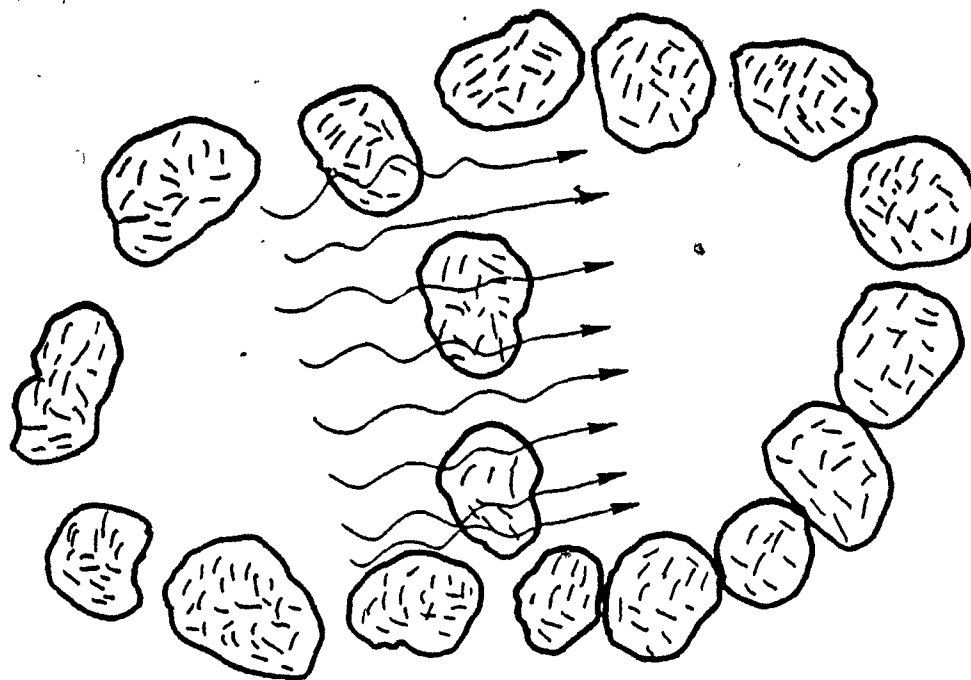
flow concept will break down. Because the flow will move around the cluster units, the friction drag mechanism will represent an increasingly higher portion of the resistance to flow as compared with the viscous shear mechanism which determines the friction in conduit flow.

The case of flow around submerged object type relates more to the physics of sedimentation and the compression of a very high void ratio clay system, and therefore it will not be considered in the present analysis. Fig. 21 shows the schematic view of the two cases. In the following pages, we will develop the flow equation for the second case, i.e., the conduit flow type.

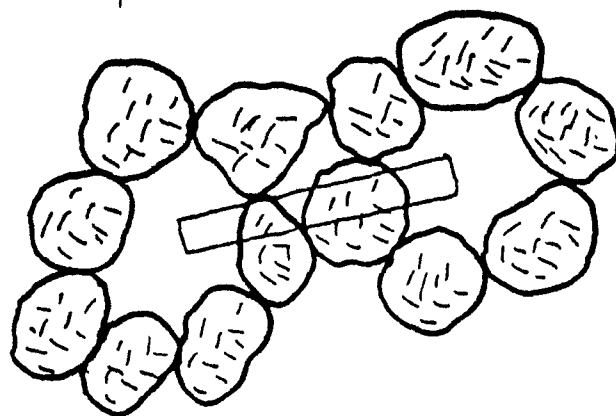
The path of the fluid between two adjacent macrostructural units is likely to be tortuous, the arrangement of the cluster units would obviously determine the degree of tortuosity. Fig. 22 shows schematic view of different cases of the channels between two adjacent macrostructural units.

**case 1:** Simple channel connects between two adjacent MSUs. The generated forces between the fluid and the channel are the viscous shear forces.

**Case 2 :** Simple channel but the existing forces



**a-Flow around submerged object type model**



**b-Conduit flow type model**

**Fig. 21 Geometrical Models for the Flow Equation**

are the physico-chemical forces and viscous shear forces. The physico-chemical forces are generated because of the presence of clay particles in the perimeter of the channels. These forces and their interactions with the media are very important in case of chemically active fluids.

**Case 3:** a network of channels connect the two adjacent macrostructural units. This is suggesting that the pore geometry is not a channel of impermeable boundaries, but interconnected roots with complex geometry. The forces which can be existed are the physico-chemical forces and viscous shear forces.

### **3-6-2-1 Mathematical Formulation:**

The conduit flow type can accommodate the development of these cases. It should be noted that in these cases the channels' variabilites and uncertainties over the ensemble of macrostructural units can be considered. Thus, the conduit flow type will be used in the following anaylsis. For simplicity in development, we will use Case 1.

For the conduit flow, we apply the concept of Hagen-Poiseuille which uses the Newton's law and force equilibrium of fluid element, (see Appendix C-1 for the development of the equation of the flow). The formulation can be as follows:



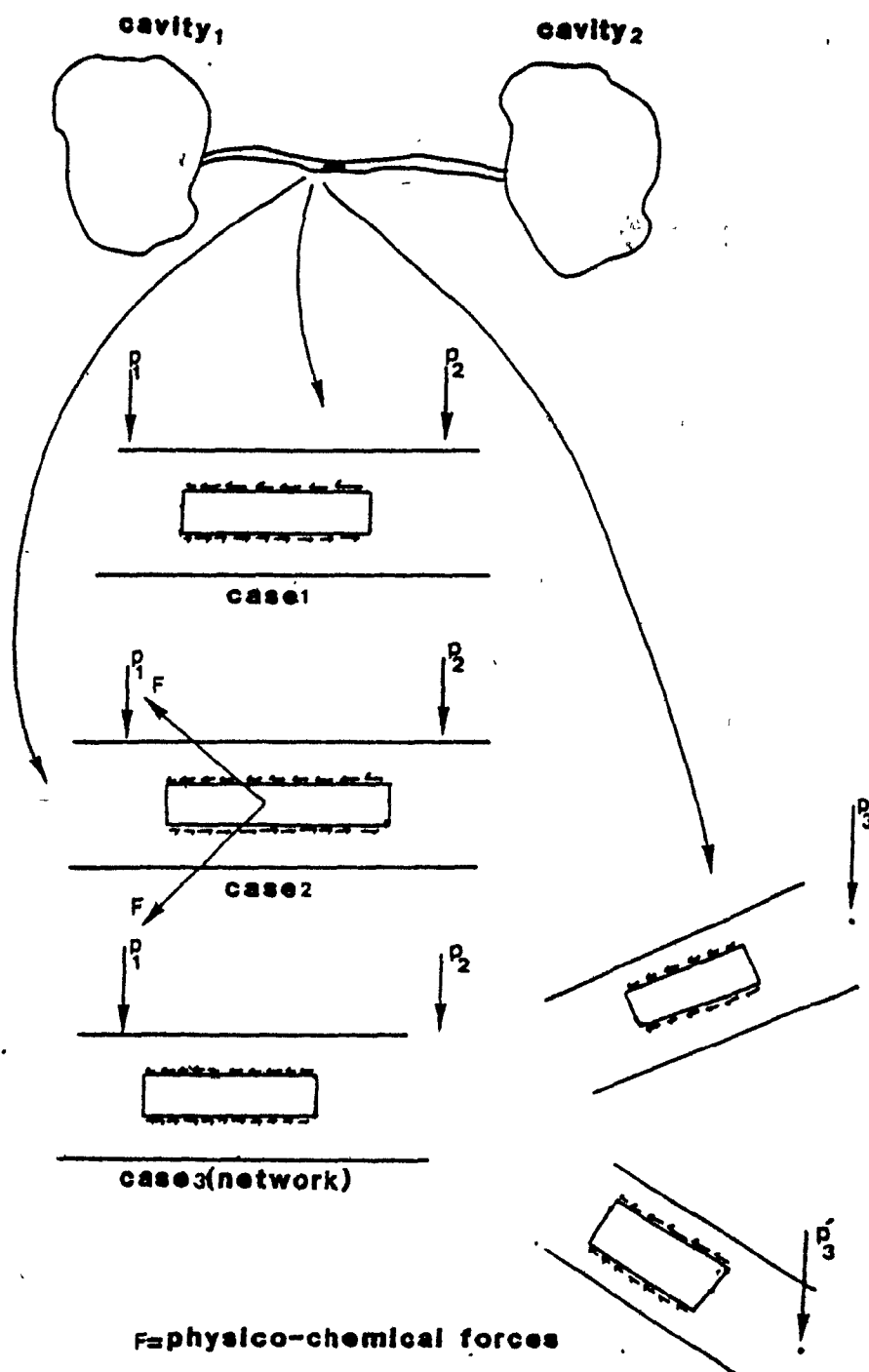


Fig. 22 Different Channel Conditions Between Two Neighbor MSUs

$$q = \frac{C_s \gamma_w}{\eta} \frac{R^2 a}{D} (P_\Lambda^\pi - P_\Gamma^\pi) \quad (3.44)$$

Where

$C_s$  = shape factor

$\gamma_w$  = the unit weight of water

$R$  = the hydraulic radius

$a$  = the cross sectional area of the channel

$P_\Lambda^\pi$  = the pore water pressure build in the cavity of MSU  $\Lambda$  with superscript  $\pi$

$P_\Gamma^\pi$  = the pore water pressure build in the cavity of MSU  $\Gamma$  with superscript  $\pi$

$D$  = the length of the channel connecting the two MSU

$q$  = the rate of flow per channel

$\eta$  = coefficient of absolute viscosity.

If we consider the continuity of the fluid flow for a reference macrostructural unit ( $r$ ), i.e., the total quantity of flow in and out from the MSU  $r$ , we get the following form:

$$\sum_i q_{i \text{ net}} = \frac{C_s \gamma_w}{\eta} \sum_i \frac{R_i^2 a_i}{D_i} (P_i^\pi - P_r^\pi) \quad (3.45)$$

Where

$q_i$  = the rate of flow per channel( $i$ ), in or out, of

the cavity in the MSU  $r$

$q_{\text{net}}$  = the net of flow stored in the cavity in the MSU  $r$ .

The summation  $\sum$  is performed over the number of the channels connected directly with the MSU( $r$ ).  $i$  represents the number of channels, and  $P_i^\pi$  and  $P_r^\pi$  are the terminals' pressure, see Fig. 23b.

$q_{\text{net}}$  is equal to the time rate of change of volume of the MSU ( $V_m$ ).

$$q_{\text{net}} = \frac{\partial V_m}{\partial t} = \frac{\partial}{\partial t} (1 + e_m) \sum V_c \quad (3.46)$$

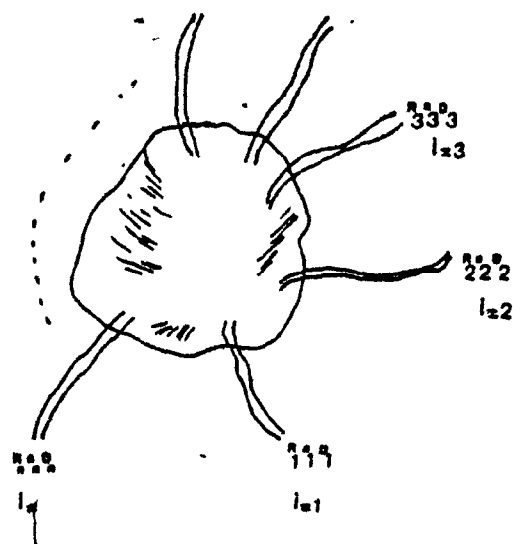
Where

$\sum V_c$  = the total volume of clusters in the MSU, i.e., the summation is performed over the number of the cluster units within the MSU.

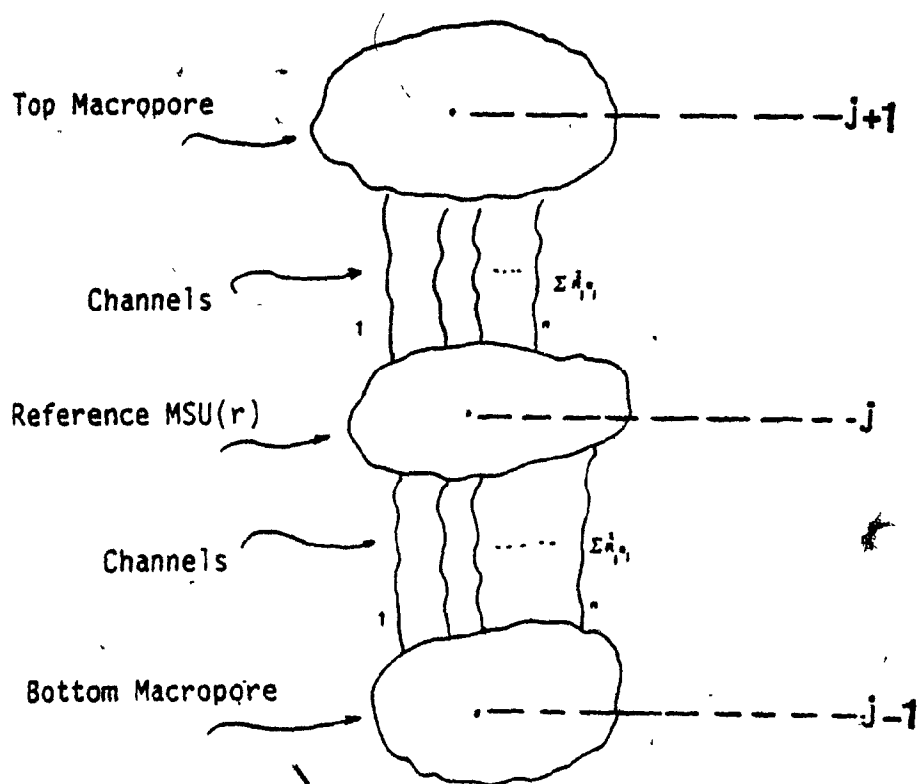
$V_m$  = the total volume of the macrostructural unit.

$$q_{\text{net}} = \sum V_c \frac{\partial e_m}{\partial t} + (1 + e_m) \frac{\partial \sum V_c}{\partial t} \quad (3.47)$$

Hence:



a. Channels Connected with Macropore



b. The Channel Connections Between the Macropores

Fig. 23 Schematic View of Channels Connected with the Macropores

$$\frac{\partial e_m}{\partial t} = \frac{1}{\Sigma V_c} \left[ \frac{\partial v_m}{\partial t} - (1 + e_m) \frac{\partial \Sigma V_c}{\partial t} \right] \quad (3.48)$$

We will assume as a first approximation that the rate of change of the number of cluster units within the macrostructural unit is negligibly small. In actual fact, this is one of the fundamental assumptions in the development of the finite consolidation theory. See Monte et al. (1976). Therefore:

$$q_{net} = \Sigma V_c \frac{\partial e_m}{\partial t} = \frac{C_s \gamma_w}{n} \sum_i \frac{R_i^2 a_i}{D_i} (p_i^\pi - p_r^\pi) \quad (3.49)$$

Hence:

$$\frac{\partial e_m}{\partial t} = \frac{C_s \gamma_w}{n \Sigma V_c} \sum_i \frac{R_i^2 a_i}{D_i} (p_i^\pi - p_r^\pi) \quad (3.50)$$

Equation 3.5 is very general and can be applied for three-dimensional analysis. However, to demonstrate the analysis, the case of one-dimensional flow will be considered here and will be used in subsequent chapters. It should be noted that one-dimensional fluid flow has been recognized experimentally in some types of clay soil. See Yong et

al. (1975).

Hence, Eq. 3.50 can be simplified in the following form:

$$\frac{\partial e_m}{\partial t} = \frac{C_s \tau_w}{n \sum V_c} \left[ K_1 P_1^\pi - (K_1 + K_2) P_r^\pi + K_2 P_2^\pi \right] \quad (3.51)$$

Where

$$K_1 = \bar{\bar{L}}_r (R_{i1}^2 a_{i1}) / D$$

$$K_2 = \bar{\bar{L}}_b (R_{i1}^2 a_{i1}) / D$$

The summations ( $\bar{\bar{L}}$  and  $\bar{\bar{L}}$ ) are performed over the channels connected from the top to macropore(r) and the channels connected to its bottom respectively. Fig 23b shows these definitions.

If the channels parameters are similar, we can assume that  $K_1 = K_2$ , and  $D_1 = D$ . Hence:

$$\frac{\partial e_m}{\partial t} = \frac{C_s \tau_w}{n \sum V_c} \frac{\sum R_{i1}^2 a_{i1}}{D} (P_{j-1}^\pi - 2 P_j^\pi + P_{j+1}^\pi) \quad (3.52)$$

The excess pore water pressure in the cavities (j, j-1, j+1) can be represented by three finite difference nodes, (see Fig. 23b). Hence, Eq. 3.52 can

be simulated as a partial differential equation with finite difference increment  $\Delta x = D$ . Thus, with some mathematical simplification, we get the following equation:

$$\frac{\partial e_m}{\partial t} = \frac{C_s \gamma_w D}{n \Sigma V_c} \left\{ \sum R_i^2 a_i \right\} \frac{\partial^2 p'}{\partial x^2} \quad (3.53)$$

Eq. 3.53 represents a model which describes the fluid flow from one macropore to the adjacent ones. The basic parameters of this model are the void ratio of the MSU, and the excess pore water pressure.

Eq. 3.53 by itself cannot describe the law of performance of the macrostructural unit under compression loading. It requires an expression to model the stress transfer, and another expression to model the compressibility of the clay skeleton (cluster units). We will try to fulfill these requirements in the next chapter.

### 3-7 SUMMARY:

In this chapter, we have developed several concepts in the kinematics of deformation of clay-water system. The summary of these developments are as follows:

1- For soil media, we described three types of deformation, i.e., type A, type B and type C. We reviewed the literature of the director theory and modified it to model the kinematics of deformation.

2- We introduced the microelement(MSU) which consists of a group of cluster units. Furthermore, we developed the kinematics of deformation of the first region which is simulated by type B1 deformation, and the kinematics of deformation of the second region which is simulated by type B2 deformation.

3- For the macrostructural unit, we developed the weight-volume relationships such as  $e$ ,  $w$ ,  $\rho$ . A computer program has been developed to find the probability distribution of these parameters over the ensemble of the macrostructural units.

4- We introduced the concept of the compression zone which is the volume enclosed between two



units (clusters or particles).

5- We discussed the physics of fluid movement from cavities and showed that there are two different types of fluid flow models: the conduit flow type and the flow around submerged object type. We have used the conduit flow type model and have established an analytical model for fluid flow from a given cavity to the adjacent ones.

In Chapter 4, we will use the kinematics of deformation of the clay system and the concept of the compression zone to develop the constitutive equations for the first and the second regions.

In Chapter 5, we will use the analytical model of the fluid flow (Eq. 3.53) to link with the constitutive equation for the establishment of the state function of the first region.

## CHAPTER 4

## STRESS-COMPRESSIBILITY RELATIONSHIP

## 4-1 FORWARD:

In order to provide a link between the stress applied and the compression induced in the material, the constitutive properties of the material should be studied. In this chapter, a discussion of the stress applied to the macrostructural unit will be provided. Moreover, attention will be focused on its components in terms of the stresses carried by different phases and local stress balance. Last but not least, a discussion of the formulation of the stress-compressibility relationship will be provided.

Before we start the program, the following question should be raised; is there a coupled stress in soil media? The answer to this question will be discussed in the following section

In our micromechanics theory, we have stated and developed the kinematics of deformation by using the director concept and we concluded that the kinematics can be represented by one set of deformation. In the case of the stress field, there cannot be any coupled

stress existing in the soil media. In the following we will substantiate this idea by describing two major works in the field of soil mechanics.

Mehrabadi and Nemat-Nasser (1983) stated, for the stress field which exists in granular media, as follows:

" Let the sample be divided into a finite number of subregions (or neighborhoods) (Note this is the same as our MSU). ..... Consider a typical subregion  $r$ , and let the 'local stress measure' in this region be  $2A_{ij} \dots$ "

As observed experimentally in the work of Oda et al. (1982), rolling and sliding exist in the granular media on the microscopic scale. However, the stress field developed in these media has no consideration of coupled stresses (i.e., the stress  $A_{ij}$  is Cauchy stress).

Yong et al. (1985) have not considered the coupled stress for anisotropic clay. In their development, they consider the orientation of the plate shaped particles with basal planes aligned in a direction normal to the axis of the major principal formational stress. In their constitutive development the orientation angle is presented but the stress is a Cauchy stress (no coupled stresses).

We conclude from the above major works in soil mechanics (see also works of Bazant et al. (1975 and 1986)) that although the director concept has been included in the kinematics, the couple stress does not exist.

#### 4-2 LOCAL STRESS BALANCE:

Terzaghi was the first engineer who introduced a stress balance as effective stress principal. The basic point of the equation is that the applied stress is taken partly by the fluid phase and partly by the solid phase.

Several balance stress equations (Table 3) have been introduced. They take into account the repulsion and the attraction forces between the particles. These equations have been applied to a scale of assemblage of particles, mostly of two-particles system.

Although the balance equations (see Table 3) are almost the same, the choice of the part of the stress which is carried by the solid system is not clear, and the terminology of using the effective stress as opposed to contact stress is less defined.

We think that when the distance between the two-particles is small in the Angstrom scale, the behaviour of the joint can be both mechanical and

Table 3 Different stress balance equations for saturated soils:

$\bar{\sigma}$ = mineral to mineral stress. $\sigma$ = total stress applied. $a_m$ = fraction of the total area. $R$ = repulsion force. $A$ = attraction force. $u$ = pore water pressure.		
Author	General Equation	Contact stress
Terzaghi (1925)	$\sigma = \bar{\sigma} + u$	effective stress $\bar{\sigma} = \sigma - u$
Lambe (1960)	$\sigma = \bar{\sigma} a_m + \bar{u} + R - A$	effective stress $\bar{\sigma} = \sigma - \bar{u} = \bar{\sigma} a_m + R - A$
Sridharan (1973)	$\sigma = \bar{\sigma} a_m + \bar{u} + R - A$	effective contact stress $\bar{\sigma} = \bar{\sigma} a_m + \bar{u} - R + A$ $\bar{u} = \bar{\sigma} + \bar{u}$
Chattopodhyay (1972)	$\sigma = \bar{\sigma} + u_m + R - A$	true effective normal stress $\bar{\sigma} = \sigma - u_m - R + A$
Mitchell (1976)	$\sigma = \sigma_i + R - A + u_o$	the intergranular stress $\sigma_i = \sigma + A - u_o - R$

physico-chemical. The meaning of the mechanical behaviour is that the space between the particles will be filled with cations and adsorbed water, and these cations and the water will work as a lubricated system over the two particle surfaces, thus giving viscous action. At the same time, the cations have positive charges and the clay surfaces have negative charges. Therefore, the physico-chemical action and reaction are responsible for the attraction and the repulsion forces between the particles.

In our work, the local stress balance is not applied for a scale of two-particles system, but it will be applied for the macrostructural unit scale (i.e., the cluster size is the smallest scale to be used) for reasons given in the second chapter (Flow Chart 2). The total stress applied to the macrostructural unit is taken by the fluid and the cluster units. The formulation which is proposed in the present analysis can be as follows:

$$\sigma_z^m = \sigma_z^{i.p.} + \sigma_z^c + P^r \delta_z \quad (4.1)$$

$$\sigma_z^m = \sigma_z^m + P^r \delta_z$$

where

$$\sigma_z^m = \sigma_z^{i.p.} + \sigma_z^c \quad (4.2)$$

$\sigma_z^m$  = The total stress applied to the macrostructural

unit

$\sigma^c$  = The intercluster stress or the mechanical stress which can be taken by the intercluster contact.

$\sigma^{i.p.}$  = The stress due to electrical interaction potential between the clusters. This stress is due to active particles near the contact of the cluster units.

$P$  = Pore water pressure which builds up in the cavity within the macrostructural unit.

Eq. 4.1 represents the stress field for the macrostructural unit, see Fig. 24.

#### The Mechanism of the Stress Balance:

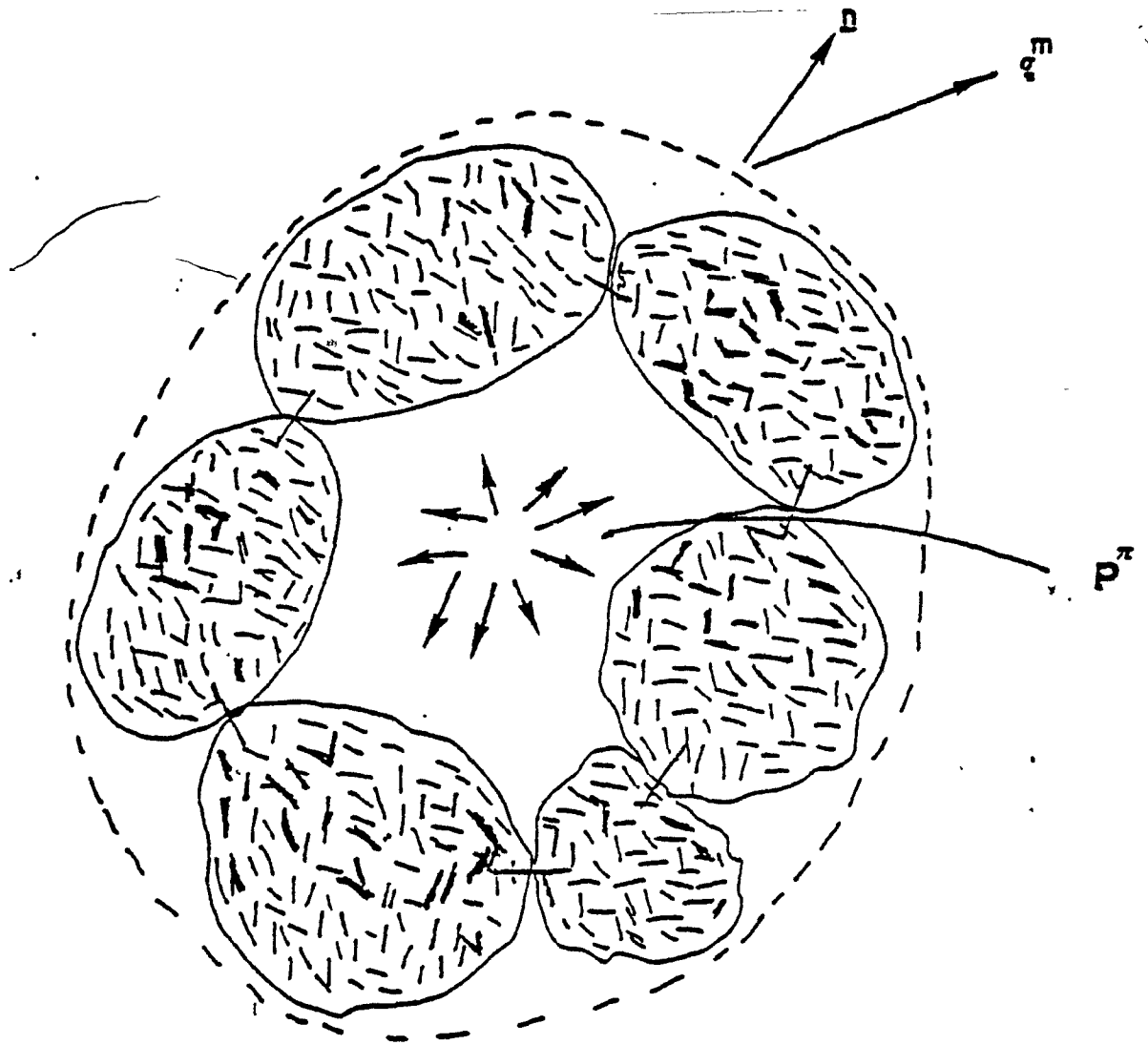
There are various conditions or physical mechanisms of the local stress balance which is controlled by the  $(\sigma^{i.p.})$ . These mechanisms are:

1- When  $\sigma^{i.p.} = 0$ . This condition can be reached either at equilibrium or at the condition of no interaction potential between the cluster units.

Hence,

$$\sigma^c = \sigma^m - P \quad (4.3)$$

In such a case, the condition of material compressibility is governed by the resistance to shear displacement at the intercluster contact. This resistance can be viscous and/or friction with no interaction potential.



$$\bar{\sigma}_n = \bar{\sigma}_c + p_n \bar{\sigma}_c$$

Fig. 24 The Stress Balance for the MSU



2- When  $\frac{i \cdot P}{\underline{g}} > 0$ . In this case, the repulsive forces will be dominant and the intercluster stresses may take the form:

$$\underline{g}^c = ( \underline{g}^m - \frac{i \cdot P}{\underline{g}} ) - P^r \underline{g} \quad (4.4)$$

In such a case, the material compressibility performance can be expressed in a mathematical form by using the Double Layer theory. In addition, the performance depends on the separation distance between the participating particles near the contacts of neighbor clusters.

3- When  $\frac{i \cdot P}{\underline{g}} < 0$ . In this case, the attractive forces will be dominant and the intercluster stresses may take the form:

$$\underline{g}^c = ( \underline{g}^m - ( - \frac{i \cdot P}{\underline{g}} ) ) - P^r \underline{g} \quad (4.5)$$

In such a case, the shear resistance at the intercluster contacts governs the material compressibility, and this shear depends on the direction of the strong plane of resistance at the contact of the cluster units. This plane is different for the Case 1 and Case 3. Therefore, the compressibility performance of Case 1 and 3 can be different.

The performance of the clay system for any of the above cases depends on the type of clay minerals (e.g. kaolinite, illite, and montmorillonite), pore water chemistry, and the size of the cluster units. Environmental alteration of the pore water chemistry of the system which was in case 1, 2 or 3, may cause this system to behave differently than before alteration.

In the following sections, a demonstration of how one can find the components of the local stress balance is given.

#### 4-2-1 Calculation of $\phi_{\text{I.P.}}$ From the Interaction Potential:

##### 4-2-1-1 General:

Clay particles have very small size. Therefore, the specific surface area is very large. Hence, a large proportion of the total number of atoms making up the particles form at the surface of the clay particles. This makes the clay particles very active electrically.

The atomic structure of the clay system includes two types of sheet structure such as tetrahedral or silica sheet, and octahedral or alumina sheet. The surface can allow isomorphous substitution phenomena to take place, i.e., substitution of ions of one kind by ions of another type, with the same or different

valence, but with retention of the same crystal structure. The isomorphous substitution and the imperfection in the crystal lattice may contribute in causing the clay surface to have a negative charge.

The properties which are responsible for the fabric formation, its stability, and the performance of the clay-water system are as follows:

i- for the soil system; they are represented by base exchange capacity, surface area, amorphous material, and cementation bonding material (organic and inorganic);

ii- for the fluid system; they are ion concentration ( $n$ ), cation, valence, dielectric constant, temperature, pH value and dipolar character of the fluid.

These properties of the clay-water system can interact to form different modes of particle associations (i.e., face-to-face, edge-to-edge, and face-to-edge configurational states). These modes of associations form a stable or metastable system which depends on the net potential of the interaction between the pair of clay particles as well as on the bond condition (i.e, cemented or uncemented condition).

This net potential can be calculated by different

mathematical models. The formation of the cluster units which are aggregations of clay particles in different depositional environments is due to local thermodynamic equilibrium.

The distance between the clay particles within the cluster units ranges between 100-250 Å, which gives a water content range between 15% → 30%. The thermodynamic properties of this water are different from normal water; it has a high viscosity, and its free energy is less than that of normal water. Therefore, the particles tend to cluster together to form a configurational state of minimum free energy.

These local equilibria of the configurational states of the cluster units may not render the total system equilibrant. Hence, an interaction between the cluster units through their contacts may exist, and the free water in the cavity is formed by a number of cluster units. Within each cluster unit, different modes of particle association can be developed.

The interaction between the cluster units can be developed through mechanical behaviour at the region of contact and through physico-chemical behaviour at the region near the contacts where the electrical forces of the interaction can be calculated. It should be noted here that the joint between the cluster units is not really a physical contact as there is actually a very

small distance between these units. Fig. 25 shows a schematic view of the physico-chemical process of the cluster formation.

#### **4-2-1-2 Mathematical Formulation:**

We will first develop the calculation procedures of the pair potential. There are two methods to find the pair potential:

##### **a- The statistical mechanics approach:**

Taylor et al.(1968) used the statistical mechanics theory of liquids and radial distribution function together with an experimental technique of small angle X-ray diffraction. The results of the X-ray scattering data are usually interpreted in terms of the average distance of separation between clay plates. He computed the pair potential for Na-montmorillonite clay suspensions.

##### **b- The Double Layer Theory:**

Clay particle interaction has been considered in terms of Gouy-Chapman double layer repulsion and van der Waals attraction for the case of parallel plates only. For other particle configurations, Flegmann et al.(1969) resorted to different computational procedures to obtain interparticle energies. He incorporated the measured zeta potential to obtain energies for edge-to-edge, face-to-face, and edge-to-face configurations.

Ions (anions, cations)

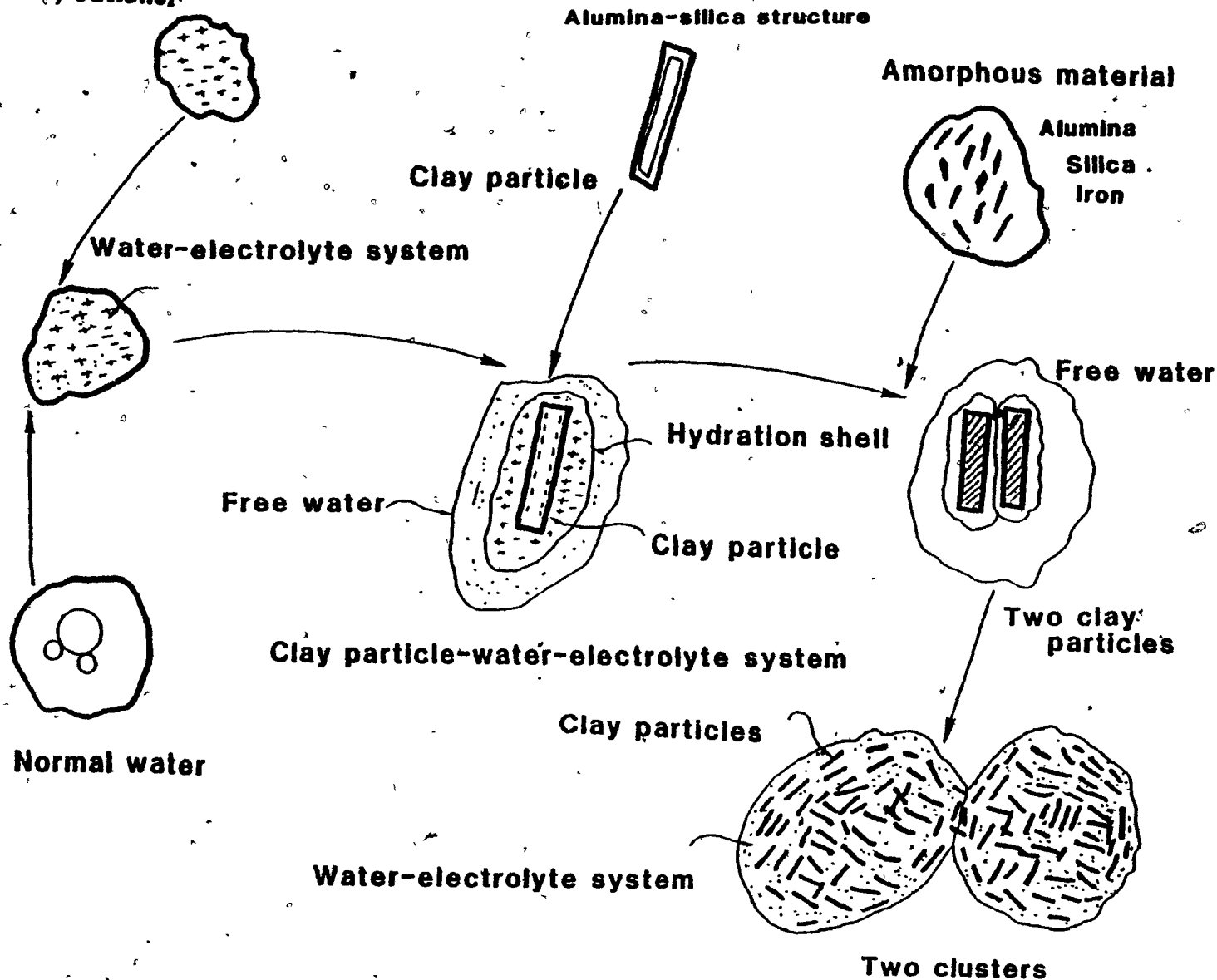


Fig. 25 Fabric Formation

In the following analysis, the Double Layer theory will be considered. Extensive details of this theory are given in Flegmann et al.(1969), Low(1961) and Van olphen(1963). In geotechnical engineering, see Yong et al.(1975 and 1978).

We assume that at the region near the contact of the two cluster units there are N number of clay particles and that they have pair potential of  $\phi$ . This potential results from surface forces which emanate from the clay particles. Yong et al. (1985) have calculated the pair potential for different clay minerals interactions, and they have used them to explain the swelling process of an expansive soil. The total N-body configurational energy which represents the interaction potential between the two neighbor cluster units can be formulated by the sum of pair-interactions as follows:

$$\phi_{c_1 c_2}(1,2,3,4,\dots,n) = \sum_{i,j} \phi(i,j) \quad (4.6)$$

where

$\phi_{c_1 c_2}$  = The interaction potential between two neighbor cluster units.

$\phi$  = The interaction potential between two particles.

Eq. 4.6 is an exact formulation of the interaction. Therefore, the interaction forces between

the two cluster units can be derived from Eq.4.6 by differentiating (with respect to distance (Yvon(1969) and Hamaker (1937))). It should be noted that it is very difficult to define the rate of change of the interaction potential(†) with respect to the cluster units displacements. Because the relative displacement between the cluster units is larger than the distance between the pair of particles, i.e., the particle which is interacted with its neighbor will have a new neighbor after the cluster units displacements.

However, the other method is as follows:

1- Find the interaction forces between the pair of clay particles by differentiating the pair interaction potential with respect to the distance separation between these particles. These particles are located at the region of the two clusters contact. The calculation procedures of these forces are given by Baker (1969) and Yong et al. (1985).

2- Make the summation of all the forces generated at cluster contact region for a "specific" region configuration, i.e.,

$$F = \sum [f] \quad (4.7)$$

Where,

$f$  = interaction forces between pair of particles

$F$  = interaction forces between two adjacent clusters.

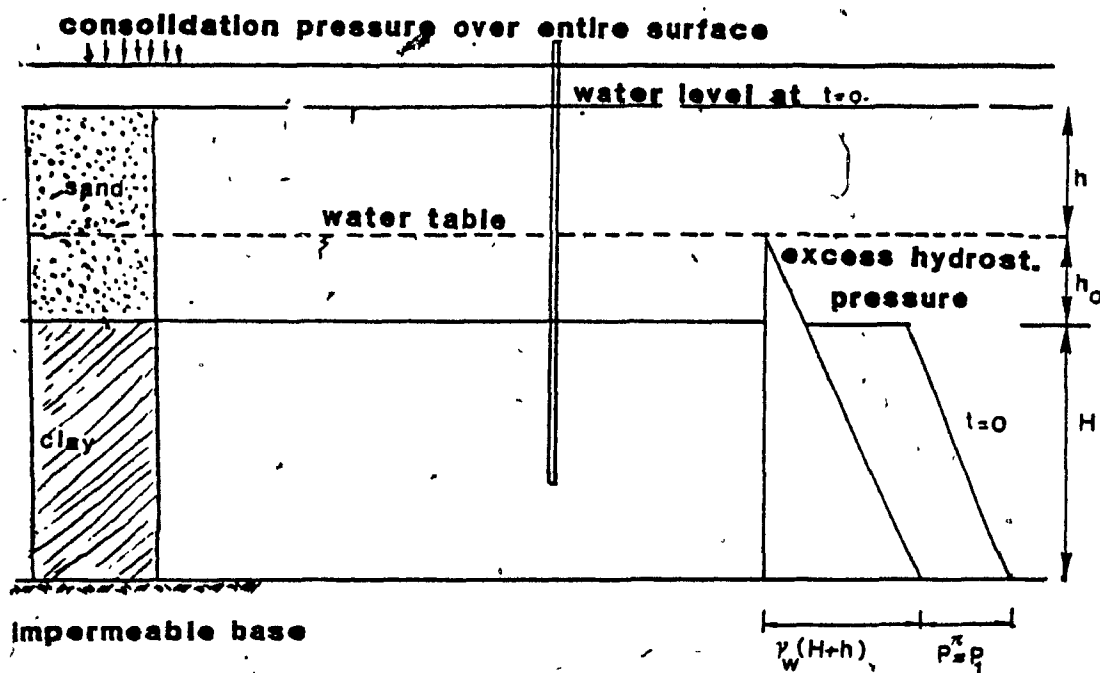


#### 4-2-2 Measurements of the Pore Water Pressure:

The pore water pressure is a volumetric pressure. It is very difficult to measure the pore water pressure  $P^p$  in each cavity within the macrostructural unit since the diameter of the cavity, comprising only a few micrometers, is so small that the piezometer cannot be fitted into the cavity. Consequently, the measurement of pore pressure in so many cavities is very difficult if at all possible. Therefore, the piezometer can only sense some kind of average of the pore water pressure in an ensemble of macrostructural units.

This problem has been faced by De Jong (1968). He proposed a theoretical local excess pore water pressure. This theoretical concept cannot reconcile to the actual excess pore water pressure in the microelement (MSU). In the following section, we will demonstrate how, in a simply way, the initial excess pore water pressure can be established.

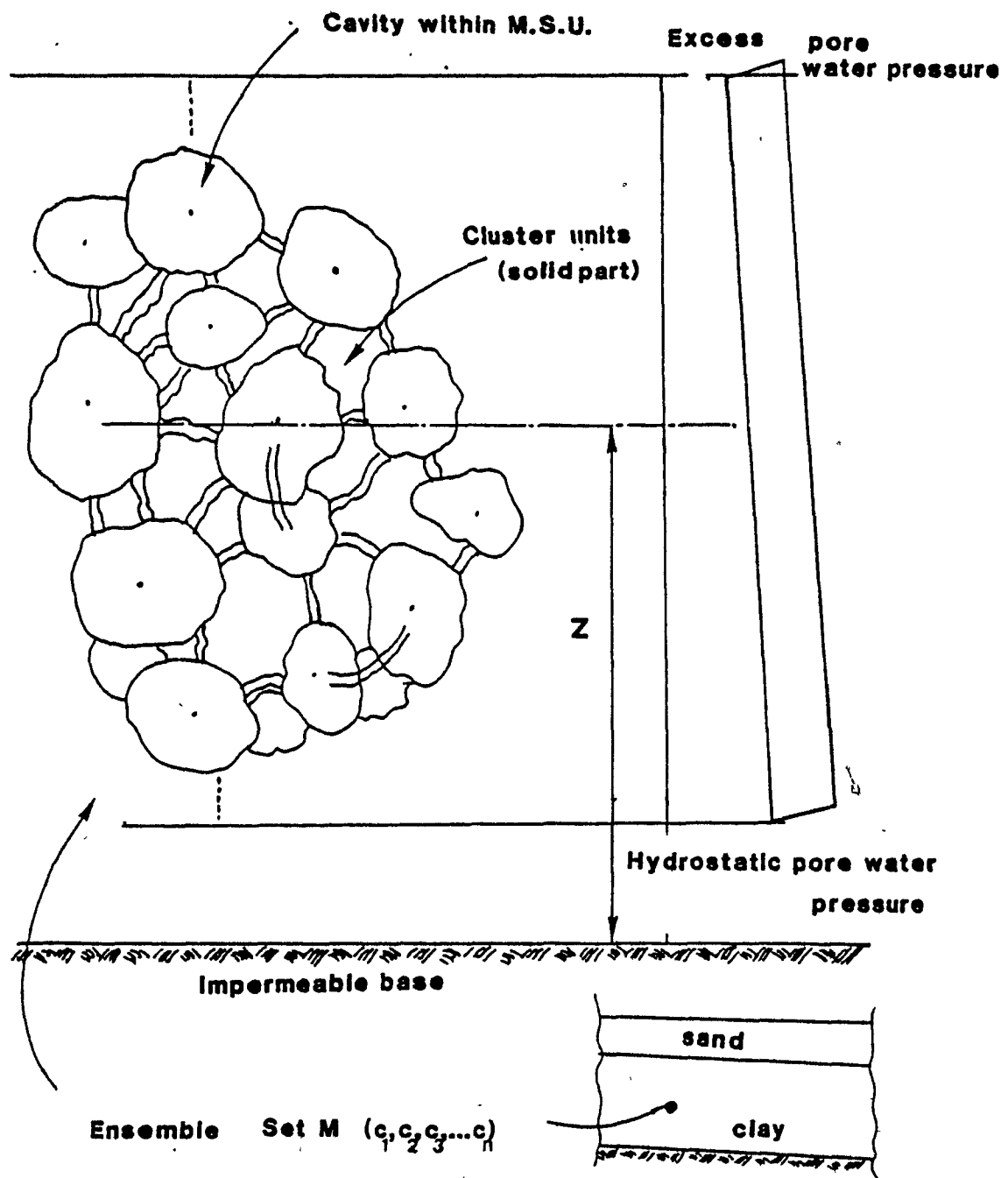
We consider the total soil system profile as shown in Fig. 26, (Tezaghi, 1943). This soil system consists of a clay layer which is buried beneath a bed of highly permeable sand, and the water is located at height ( $h_0$ ) above the clay surface, see Fig. 26a. The water will rise in a piezometric tube to the height  $h$ , and the static water pressure at any level X-X equal to the height  $(H+h_0-\langle z \rangle)$ , where  $\langle z \rangle$  represents the average height of the ensemble of macrostructural units from



d. Pore water pressure distribution at  $t=0$

(Terzaghi, 1943)

Fig. 26 Pore Water Pressure Distribution



**b. Pore water pressure distribution in the ensemble of microelements**

**Fig. 26 Pore Water Pressure Distribution (Cont.)**

the impermeable base. The height in the piezometer tube represents the average static pore water pressure of the ensemble.

If we apply a uniformly distributed surcharge load ( $P_1$ ) per unit area of the surface of sand, the pore water pressure on each level of the clay system will increase by an amount ( $P_1$ ) which is in excess to the hydrostatic pressure. Hence, the excess hydrostatic pressure in each cavity is equal to  $P_1$  (i.e.,  $P^{\pi} = P_1$ ), at the initial condition (i.e., at  $t=0.0$ ). Consequently, the water rises in a piezometric tube to the height  $h_2 = P_1 / \gamma_w$ . A schematic view of the clay system with the piezometric tube is shown in Figs. 26a and 26b. It should be noted that the assumption of  $P^{\pi} = P_1$  (at  $t=0$ ) plays a key role in the present analysis.

#### Discussion:

The stress which is transmitted to the cluster units as mechanical or physico-chemical forces controls certain aspects of clay soil behaviour, notably compression and strength. In the following section, we will discuss and model the constitutive equation of the macrostructural unit based on this stress which will be called an effective stress.

#### 4-3 CONSTITUTIVE MODELLING OF THE MACROSTRUCTURAL UNIT:

##### 4-3-1 General:

Most of the works in the consolidation of clay soil which introduce some micromechanics concepts have not considered in detail the constitutive equation of the soil. They only introduce the elastic constant and/or viscosity parameter which are not based on micromechanics modelling.

Materials having identical geometry respond differently to the same external effects. The internal constitutions of bodies are responsible for this behaviour. The constitutive characteristics of bodies are brought into play by means of the cause and effect relationships.

For modelling the clay compression performance, the constitutive modelling of the clay system under applied load is essential. And in order to develop the constitutive equation, the procedures for identification of the clay properties and characteristics should be viewed.

The material properties and characteristics which produce the physics phenomena (such as the dilatancy, the stress and strain history-dependent, and time-dependent, etc.) should be identified by testing a representative sample in the laboratory or in the field

under controlled boundary conditions. Hence, the characterization testing is essential for obtaining the material parameters and factors under different boundary conditions.

Several continuum analytically predicted models which exist in the literature ( see the survey by Scott 1985) may not reconcile with the actual physics of the clay performance. However, they can meet the actual testing boundary conditions for which they are modelled. In these models, the working parameters are only two: the stress and the strain, and the set of so-called material parameters, which are defined from the characterization testing. It is sometimes impossible to attach a clear physical meaning to each of these material constants because there is no consideration of the internal conditions of the soil (i.e., the soil structure). Furthermore, micromechanical foundations of these continuum models are lacking.

It is now widely agreed that further advances in the formulation of a realistic and broadly applicable constitutive equation for soil has to be based on the micromechanics of deformation and description of the physical processes involved in the microlevel.

#### 4-3-2 Objective and Method of Approach:

The ultimate objective of this section is to develop the microconstitutive equation which links the microstrain with microstress ( the stress applied on the macrostructural unit). The works of Bazant and his coworkers have the same objective as this section. Therefore, we will now critically review their works.

For concrete materials, Zubelewiz and Bazant (1987) introduced the concept of the active plane in order to describe the macrostrain softening of the concrete due to cracking. They attribute the macrostrain softening to a decrease of the resisting area fraction of the material on the active plane. They developed a microconstitutive equation based on the classical elasticity and plasticity theories. Six constant parameters describe this equation. The concept of the passage from the microlevel to the macrolevel of this constitutive equation will be discussed in the following chapter.

No micromechanics experiment has been used to identify or verify the parameters of the developed constitutive equation. Further advances of this model are required to clarify the following points: the size of the active plane area, and the verification of Drucker's stability postulates on the microlevel.

For clay soil, Bazant et al. (1975) developed a

microconstitutive equation (creep in shear) by modelling a triangular cell of the three straight-line particles sliding over each other at a rate determined by activation energy. This is done according to the shear force transmitted by the interparticle contact. Hence, the microconstitutive equation is based on the rate process theory.

One micromechanics experiment, X-ray scattering test, is used to identify one of the constitutive parameters (i.e., clay plate orientations). Bazant et al. (1986) drew attention to some of the serious drawbacks of this model. One of these drawbacks is that the triangular cell implies that every clay particle slips over its neighbor. This may not be realistic for clay microdeformation.

To overcome the drawbacks of the above model, Bazant et al. (1986) introduced the concept of the microplane. This concept represents an analog of the earlier slip theory of plasticity (Taylor 1938). Bazant et al. developed the microconstitutive equation which is based on the rate process theory where a derivation of viscosity tensor is introduced. One of their basic assumptions is that the sliding between the particles which are at the region of clusters contact is small. This means that large local relative displacements cannot be predicted. Although this assumption may be true for metals at the microlevel, it is difficult to



justify it for clusters displacement (see Pusch 1980). Furthermore, this model is difficult to extend to volumetric strain formulation.

The X-ray scattering is also used for finding the orientations of the microplanes. It is difficult to verify a micromechanics model by only using the X-ray scattering test. However, we feel that the concepts and the approach which have been used by Bazant are promising in that we generally benefit a great deal from his work in the mechanics of material.

#### **The Fundamental Concept:**

We need a certain "conceptual gauge" to measure the response of the clay medium under an applied load, i.e., to measure spatial and/or temporal fabric changes. This measure can be easily established for a non-dissipated system. For example, for ideal elastic material, it is the strain and for ideal viscous material, it is the time. However, for a dissipated system this measure is difficult to establish. As a starting point, we will introduce the intrinsic time measure which is similar to the one which is introduced in the endochronic theory.

From this intrinsic time measure, we can develop a microconstitutive equation which does not require identification of a yield surface or the definition of loading and unloading. This feature makes it

particularly attractive for a particulate medium which develops the rearrangement of the fabric units from the onset of loading.

The endochronic theory which has been developed by Valanis has been applied to modelling soil behaviour by Bazant and Krizek(1975), Ansal et al. (1979), Bazant et al. (1982), and Valanis and Read (1979,1982). The modelling and the application of this theory is based upon continuum mechanics.

In order to highlight the fundamentals of the constitutive equation, the intrinsic time measure will be introduced first.

#### **4-3-2-1 Intrinsic Time Measure:**

The intrinsic time measure is the corner stone for the constitutive equation. It may be defined as the length of the path traced by successive mechanical states of the material in a vector space. The mechanical states represent the accumulation of microstructural changes as deformation develops.

The reason for using intrinsic time measure in our analysis is because the fundamental concept of the intrinsic time measure is to model the local rearrangement and dislocation of the system. Hence, by using the intrinsic time measure; the first region of

compression, the rearrangement and reorientation of the cluster units within the macrostructural unit, can be considered and the second region, the rearrangements of the particles within the cluster units, can also be considered.

However, the intrinsic time measure which has been introduced in the literature has several continuum constant parameters. These parameters are obtained by experimental fitting programs as semi-empirical functions. Hence, by using these semi-empirical functions, the essence of using the intrinsic time measure has been lost.

#### Mathematical Formulation:

The general equation of the intrinsic time measure considers that in the process of deformation of microelements, the succession of strain states traces two paths namely, one in deviatoric microstrain space and another, in volumetric microstrain space. A two-dimensional intrinsic time space is then defined as one into which the previous spaces are mapped by the transformation:

$$\begin{bmatrix} dz_D^2 \\ dz_H^2 \end{bmatrix} = \begin{bmatrix} \kappa_D^2 & \kappa_H^2 \\ 0 & 1 \end{bmatrix} \begin{bmatrix} d\xi_D^2 \\ d\xi_H^2 \end{bmatrix} \quad (4.8)$$

Where

$dz_0$  = intrinsic time scale (deviatoric)

$dz_H$  = intrinsic time scale (volumetric)

$d\epsilon_0$  = path length in deviatoric strain space (distortion measure)

$d\epsilon_H$  = path length in volumetric strain space (volumetric measure)

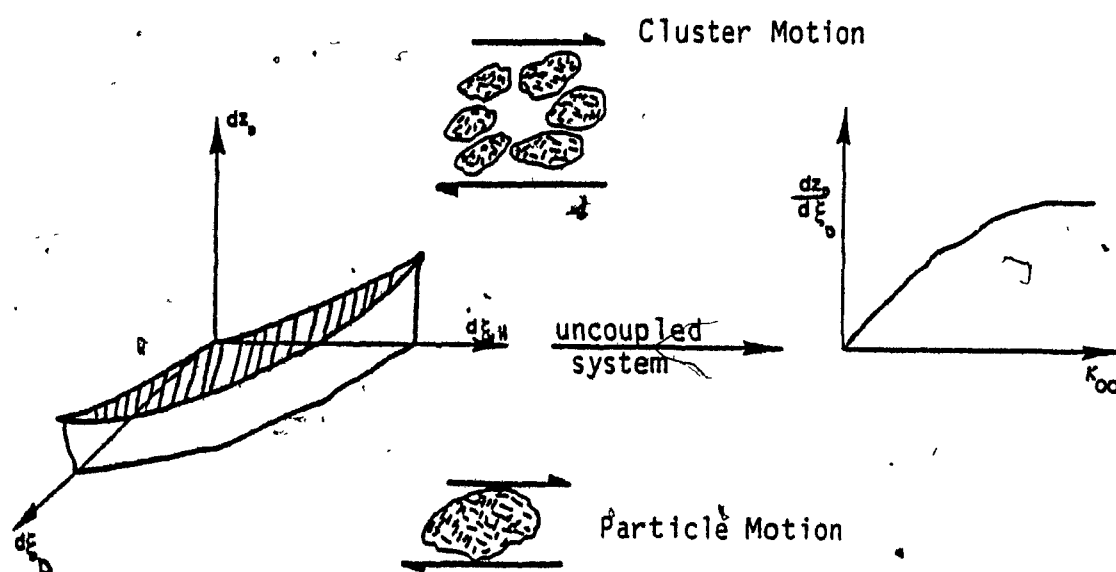
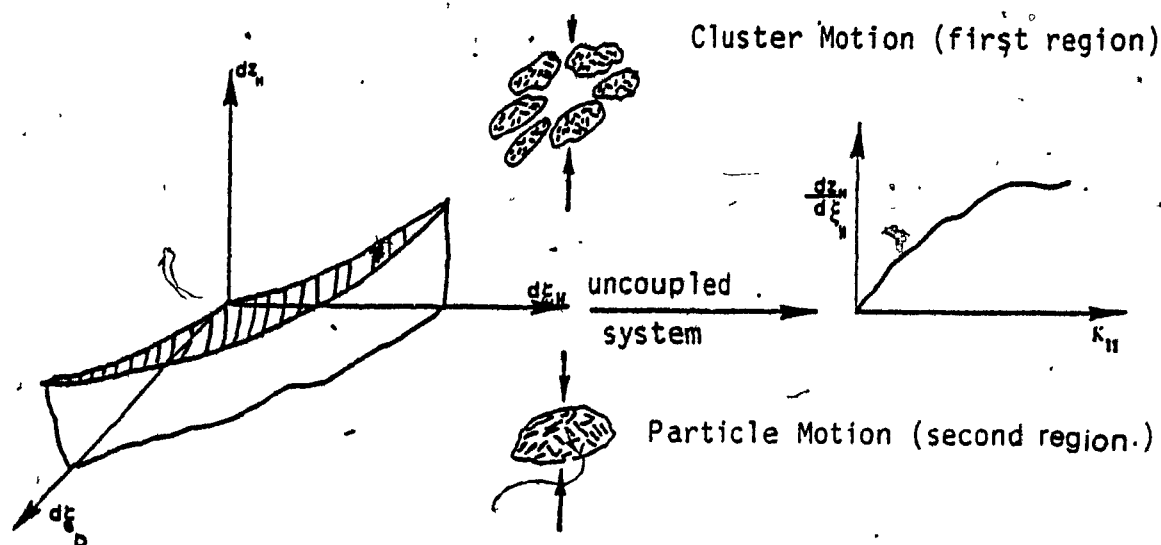
$\kappa_{ij}$  = material-dependent parameters ( $i=0,1$  and  $j=0,1$ ).

Note that the form of Eq.4.8 provides the theory with the provision for coupling between the deviatoric and volumetric components of deformation. In the present analysis, the volumetric intrinsic time measure will be addressed. Fig. 27 shows an artistic view of the intrinsic time measure.

#### 4-3-2-2 The First Region of The Compression:

We see that in this region the kinematics of deformation is represented by the microstrain of Eq. 3.17, i.e., the mechanics of clusters motion. As discussed in chapter two, the one aspect which causes the time-delay of the compression performance is the structural resistance of the clay skeleton. This is the time required for the cluster units to rearrange themselves under the imposed load. This rearrangement which depends on the surface condition of cluster units causes a permanent deformation. Hence, the volumetric microstrain space should simulate the above mechanism.

### a. Volumetric Intrinsic Time Measure



### b. Deviatoric Intrinsic Time Measure

Fig. 27 The Intrinsic Time Measure of the Macrostructural Unit

From Eq. 4.8, we can have the volumetric intrinsic time scale as follows:

$$(dz)_H^2 = \kappa_{10}^2 (dt)_D^2 + \kappa_{11}^2 (dt)_H^2 \quad (4.9)$$

Where,

$\kappa_{10}$  = The material properties which represent the volume changes due to over all shear (dilatancy)

$\kappa_{11}$  = The material properties which represent the cavity volume decreases due to shear at the contacts (overall volume change).

Eq. 4.9 represents greater generality in the description of the total phenomena of volume change. Since the volume changes due to shear and to hydrostatic stress have different microstructural sources, the form of  $\kappa_{10}$  and  $\kappa_{11}$  are different.

As has been stated in chapter three, only the one dimensional behaviour is being considered. Therefore, the coupling can be neglected as a first approximation, see Fig.27a. Hence:

$$\kappa_{10}^2 = 0$$

Hence,

$$(dz)_H^2 = \kappa_{11}^2 (dt)_H^2 \quad (4.10)$$

As has been discussed, the volumetric microstrain space should simulate the mechanism of the time-delay of the compression performance. Hence, in order to include the permanent deformation in the strain space, the volumetric measure should be set as equal to the volumetric strain.

Hence,

$$dt_H = |dc_v|$$

$$dz_H = \kappa_{11} |dc_v|$$

$\kappa_{11}$  represents an adjustment factor for the strain accumulation in strain space. The formulation and the characteristics of  $\kappa_{11}$  can be different for different clay materials. For our case, since the mechanics of deformation dictate that the time should implicitly be in the formulations, we will regard  $\kappa_{11}$  as a time rate dependent parameter. Hence, the material dependent parameter  $\kappa_{11}$  will be considered as a function of the volumetric time change of the cavity.

The correlation of the distance between particles with system void ratio (Bolt 1956) cannot take into consideration the presence of dead volume pore space (Mitchell 1976). However, the correlation between the directors and the volume of the system (MSU) can

consider the presence of dead volume pore space. Therefore,  $\kappa_{11}$  function can be established by using the concept of the compression zone. Hence, the compression zone of the spherical shaped clusters is

$$\frac{\partial \Sigma v}{\partial t} = \sum \frac{da_3}{dt} \cdot |a_1 \times a_2| + a_3 \cdot \left[ \left| \frac{da_1}{dt} \times a_2 \right| + \left| a_1 \times \frac{da_2}{dt} \right| \right] \quad (4.11)$$

Where,  $\sum$  = The summation over the number of the compression zones enclosed between the triad vectors within the macrostructural unit.

$a_1, a_2, a_3$  = The triad vectors (given in Chapter 3).

$v$  = The volume enclosed by the triad vectors.

If the cavity represents in one case a dead volume, the time rate of change of  $a_1, a_2$  and  $a_3$  is equal to zero, and hence  $\partial \Sigma v / \partial t = 0$ . If Eq. 4.11 is normalized by dividing it by total solids in the MSU (i.e., the number of the clusters in MSU), we get:

$$\frac{1}{\Sigma V_c} \frac{\partial \Sigma v}{\partial t} = \frac{\partial e_m(t)}{\partial t} \quad (4.12)$$

Hence,

$$\kappa_{11} = \Xi \left( \frac{1}{\Sigma V_c} \frac{\partial \Sigma v}{\partial t} \right) = \Xi \left( \frac{\partial e_m}{\partial t} \right) \quad (4.13)$$

where



$\Xi(.)$  = a function of the rate of change of the macrostructural void ratio.

$\Sigma$  = the summation over the number of the cluster units within the macrostructural unit (it was defined in Chapter 3).

The rate of change of the volume of the macrostructural unit depends on the condition of the cluster contacts. In order for the particles which belong to two cluster units in the region of the contact to move, (i.e., to slide and/or rotate), they must overcome an energy barrier. Once the energy barrier is overcome, and the particles begin to move this movement causes the cluster units to displace. This results in a volume change of the macrostructural unit.

This energy barrier depends on the thermal energy which is generated at the contact of the particles and also on the forces which exist at the cluster contacts. These forces are not constant, i.e., they increase as the excess pore water pressure decreases.

The form of the function  $\Xi(.)$  depends on the energy barrier generated at the contact region. Therefore, the rate process theory of Eyring (Eyring(1941)) can be used to establish the form of this function. The application of the rate process theory in the geotechnical engineering can be seen in.

the work of Mitchell et al.(1968), Mitchell (1976), Bazant et al.(1975), and Christensen et al.(1964) and Vyalov(1986).

Although we set the concept of the development strategy of the rate process theory, we will not pursue this development because it would require too many details which would detract from the main stream of establishing the micromechanics of clay compression performance under applied load. Hence, in the present analysis, we propose the following function:

$$\Xi(e(t)) = a \left( \frac{de}{dt} \right)^{\hat{a}} \quad (4.14)$$

Where  $a$  and  $\hat{a}$  are constants which can be found by simple optimization procedures on experimental test data. In actual fact these constants depend on a set of surface chemistry properties such as Plank's constant, Boltzman's constant, free energy of activation, temperature, etc. Eq. 4.14 represents the structural viscosity of the cluster interaction. The structural viscosity can be defined as the viscosity which depends on the fabric changes of the clay system.

The intrinsic time scale can have the following form:

$$dz_H = -\dot{a} (de_m/dt)^{\dot{a}} dc_v \quad (4.15)$$

The behaviour of Eq. 4.15 for a given set of values of  $\dot{a}$  and  $\dot{a}$  is given in Fig. 28.

#### 4-3-2-3 The Second Region Of Compression:

We see in this region that the kinematics of deformation is represented by the microstrain of Eq. 3.27, i.e., type B2 deformation. The cluster deformation is exhibited by the relative movement of the particles within this cluster. This motion depends on the viscous/friction between the particles as well as on the stress which is transmitted at the cluster contacts.

Since at the second region of compression the excess pore water pressure is equal to zero, the stresses induced on the clusters are constant. Hence, the volumetric microstrain space should simulate the mechanism of a creep phenomenon, i.e., the time is the most essential parameter in this space.

From Eq. 4.8, we have the volumetric intrinsic time scale as follows:

$$(dz_H)^2 = \kappa_{10}^2 (d\dot{\epsilon}_D^2) + \kappa_{11}^2 (d\dot{\epsilon}_H^2) \quad (4.16)$$

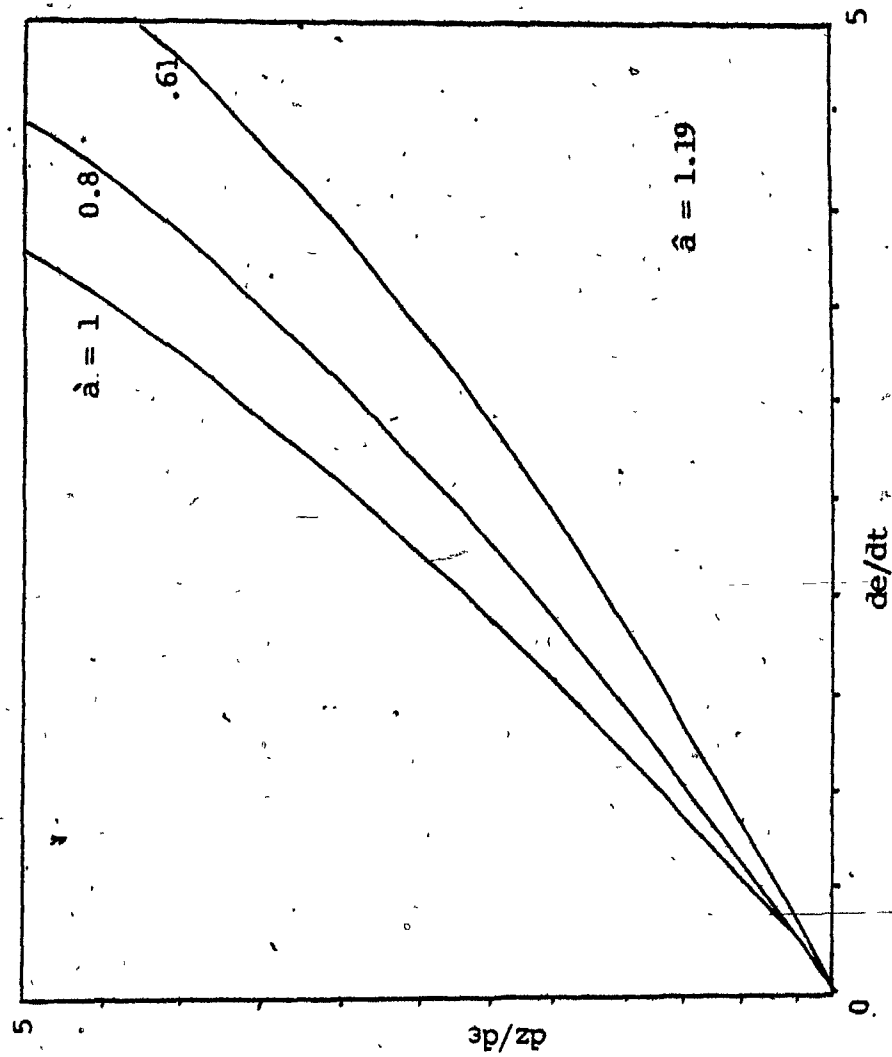


Fig. 28 The Intrinsic Time Scale for the First Region of Compression

where,  
 $\kappa_{10}$  = The material properties which represent dilatancy of the cluster units due to shear.

$\kappa_{11}$  = The material properties which represent the volumetric changes (change in the volume of the clusters), see Fig.27b

$$\text{Let } \kappa_{10}^2 = 0$$

$$dz_H^2 = \kappa_{11}^2 (d\epsilon_H^2) \quad (4.17)$$

We have already discussed that the volumetric microstrain space should simulate the time (creep process). Hence, we let the volumetric measure be equal to the time measure (o' clock time).

Hence

$$d\epsilon_H = dt \quad (4.18)$$

$\kappa_{11}$  is a function of volumetric time change of the cluster. It is an adjustment factor for the strain space; (i.e., for the time measure). Similar to the first region, the compression zone concept will be used here. However, this compression zone is considered for plate shapes.

Hence,

$$\kappa_{11} = \Xi \left( \frac{V}{V_s} (t) \right) = \Xi(\hat{e}_c(t) t) \quad (4.19)$$

$\Xi(\cdot)$  = a function of the updated cluster void ratio and the real time,

$V_s$  = the volume of solids(plates) within the cluster unit,

$V$  = the volume of water(intracluster)within the cluster unit,

$$V = \sum V$$

$V$  = the volume of water enclosed between triad vectors(see Table 2) for plate shape,

$\hat{e}_c(t)$  = the void ratio of the cluster unit (Eq. 3.31).

The summation  $\sum$  is performed over the number of volumes which is enclosed between the triad vectors.

When the energy barrier at the contacts between the particles within the cluster unit is overcome these particles will start moving and these movements will cause the volume of the cluster unit to change in time domain (t). Again, this energy barrier depends on the thermal energy and also on the forces generated within the cluster units. Although the forces transmitted at the cluster contacts are constant, the forces which exist within the cluster unit are not. This is so

because these forces depend on the fluid pressure build up inside the cluster unit.

Instead of using the rate process theory for the development of function  $\bar{z}(\cdot)$ , we consider the following exponential form:

$$\bar{z}(\hat{e}_c(t)) = sb_2 \exp (sb_1 \times \hat{e}_c(t) \times t) \quad (4.20)$$

$\hat{e}_c(t)$  will be updated for each time increment. The constants,  $sb_1$  and  $sb_2$ , can be found from simple optimization procedures on the experimental data. These constants depend on the surface chemistry of the particles.

The form of the intrinsic time scale is the following:

$$dz_H = sb_2 \exp( sb_1 \times \hat{e}_c(t) \times t) dt \quad (4.21)$$

Eqs. 4.15 and 4.21 represent the intrinsic time scales of the first region and the second region respectively. In the following section, we will develop the constitutive equations for both regions.

#### 4-3-3 Constitutive Equation:

For the development of the constitutive equation for the macrostructural unit, the following procedures are required (part of them have been established):

First, the kinematics of deformations: We established the kinematics of deformations which are represented by Eqs. 3.17 and 3.27 for the first and the second regions respectively. These two equations are generally of a three dimensional strain formulation.

Second, the stress field: We introduced the stress field which is represented by Eq. 4.1. Since we have two phase material, i.e., clay and water, the stress transfer mechanism is important.

Third, the fundamental concept of the constitutive equation: We established the fundamental concept for constructing the constitutive equation. This is done by introducing the intrinsic time measure. This measure takes care of the fabric changes which have been accumulated in the real time domain.

Finally, the type of the constitutive equation: In this section, we will introduce the type of the constitutive relation between the stress and the strain for the macrostructural unit.



The constitutive equation will take the integral type equation. This integral represents the total history of the deformation. The physical meaning of the integration is the summation over a sequence of intervals. In our analysis, this sequence of intervals is represented on the intrinsic time scale. Therefore, the applied stress is related to the history of the volumetric strain by a functional relationship. Hence, the volumetric constitutive equation can have the following form:

$$\sigma_v^m(z) = \int_0^\infty \mu(\bar{z}-\bar{z}) \frac{\partial c_v^m}{\partial z} dz \quad (4.22)$$

Where,  $\sigma_v^m$  is zero in the reference configuration,  $z=0$ ,

$\sigma_v^m(t)$  = the applied stress which is taken by the solid part of the MSU (effective stress),

$c_v^m$  = the volumetric strain of the MSU.

The kernel function  $\mu(\bar{z}-\bar{z})$  is defined according to the following:

$$\mu(\bar{z}-\bar{z}) = m \exp(-\nu (\bar{z}-\bar{z}))$$

Where,

$m$  = volumetric modulus,

$\nu$  = constant parameter.

The basic feature of Eq. 4.22 is that the actual time( $t$ ) has been replaced by a variable dependent on the strain, i.e., intrinsic time scale. It should be noted that the values of  $m$  and  $\nu$  will be different for different regions of compressions. In differential form, Eq. 4.22 can have the following form:

$$d\epsilon_v^m = \frac{\nu}{2m} dz \dot{\epsilon}^m + \frac{1}{2m} d\dot{\epsilon}_v^m \quad (4.23)$$

In the following, we keep the microstrain as  $\epsilon$ , i.e., without putting it in terms of the displacement. Eq. 4.23 will take different forms according to the compression regions.

---

a- In the first region of compression, we cast the volumetric constitutive equation by introducing Eq. 4.15 into Eq. 4.23 and rearranging the terms. Hence, we get:

$$d\dot{\epsilon}_v^m = (2m_1 + \nu_1 \Xi(e(t)) \dot{\epsilon}^m) d\epsilon_v^m \quad (4.24)$$

Let

$$\nu_1 = \nu_1 \Xi(e(t))$$

and

$$M_1 = 2m_1 + \nu_1 \Xi(e(t)) \dot{\epsilon}^m \quad (4.25)$$

Hence,

$$d\sigma_v^m = M_1 dc_v^n \quad (4.26)$$

Where

$m_1$  = the initial tangent modulus of the compressibility of the macrostructural unit,

$v_1$  = structural viscosity of the M.S.U, it is the structural viscosity of the cluster unit interaction,

$\sigma^m$  = the stress applied to the cluster units within the MSU. This stress depends on the pore water pressure  $P^n$  built up in the cavity. As  $P^n$  decreases, this stress increases.

In Eq. 4.24, the state of stress is generally a function of the current state of strain as well as the stress path followed to reach that state. Hence, the stiffness of the clay system increases as the process proceeds in time. The amount of increase in the stiffness depends on the level of the stress which is taken by the cluster units within the macrostructural unit, i.e.,  $\sigma^m$  in  $M_1$  (Eq.4.24). The rate at which this stiffness increase is considered by the intrinsic time scale, i.e.,  $dz$  in  $M_1$ .

b- For the second region of compression, the volumetric constitutive equation can have the following form:

$$d\epsilon_v^m = \frac{\nu}{2 m_2} dz \epsilon^m \quad (4.27)$$

Introducing Eq. 4.21 into Eq. 4.27, and rearranging, we get:

$$\frac{d\epsilon_v^m}{dt} = \frac{\nu_2}{2 m_2} \Xi(\hat{\epsilon}_c(t), t) \epsilon^m \quad (4.28)$$

Let

$$\nu = \nu_2 \Xi(\hat{\epsilon}_c(t), t)$$

Where

$\nu_{11}$  = structural viscosity of the MSU, it is the structural viscosity of the particle interaction within the cluster units in the MSU,

$\epsilon^m$  = the stress (effective) applied to the cluster units,

$2m_2$  = the initial tangent modulus of the compressibility of the macrostructural unit.

Eq. 4.28 contains the structural viscosity parameter  $\nu$ , in which  $\nu_{11}$  causes the rate of strain to be path dependent, and it contributes in decreasing the deformability of clay as the deformation process goes.

Hence, this microconstitutive equation has the ability to describe and model the microdeformation of the clay system in the second region (see Chapter 2).

### Discussion:

In this section, we will discuss the following fundamental points:

First, in chapter three, we established the state of the strain in the macrostructural unit (Eqs. 3.17 and 3.27). These strains are developed from director concept. Hence, Eqs. 4.26 and 4.28 can be formulated as follows:

$$d\epsilon_v^m = M_I d\epsilon(\underline{N}^m) \quad (\text{Eq. 4.26})$$

$$d\epsilon(\underline{N}^m)/dt = (\nu_2/2m_2)\Xi(\hat{e}(t), t) \epsilon_v^m \quad (\text{Eq. 4.28})$$

In the compression performance of the clay system under load, the volumetric strain accumulation which can be viewed from mechanics of cluster motion in the first region Eq. 3.17 (or the mechanics of cluster deformation in the second region, Eq. 3.27) can be found for a given stress applied. This is can be done by using Eqs. 4.26 and 4.28.

Once these strains are found from Eqs. 4.26 and 4.28, we can calculate and assess the mechanics of cluster motion and deformation by using Eqs 3.17 and

3.27 with the help of experimental data. This data should show the different stages of deformation observed on a test clay sample in scanning electron microscopy for a given stress applied.

Second, there is a unique relationship between the incremental change of the void ratio( $e_m$ ) and the volumetric strain( $\epsilon_v$ ). Therefore, we could use  $e_m$  in formulating Eqs. 4.26 and 4.28. However, in the following chapters we use  $\epsilon_v$  for both equations.

Third, from the mechanism of clay compression performance which is described in chapter two, and the constitutive modelling which is developed in this chapter, we can conclude that the structural viscosity of the first region will contribute relatively less than the structural viscosity of the second region in the total deformation process. This point will be considered in the following chapters.

#### 4-4 SUMMARY:

We considered the stress balance between the cluster units as opposed to the common practice which regrades the stress balance between the particles. At initial time ( $t=0$ ), uniform excess pore water pressure is assumed throughout the soil profile system. This assumption permits us to know the initial excess pore

water pressure in each cavity.

We developed a volumetric constitutive equation for both regions of compression by using the concept of the intrinsic time measure. The total constant parameters of the constitutive equations are eight (four for each region), i.e.,

First region:  $a$   $\hat{a}$   $v_1$  and  $m_1$

Second region:  $sb_1$   $sb_2$   $v_2$  and  $m_2$

One half of the task which has been set up in chapter one has now been accomplished—namely the work in the deterministic environments, i.e.,

- 1- the establishment of the microelement, and
- 2- the development of the law of performance which consists of three ingredients: the stress transfer, constitutive equation, and the flow equation.

The next half of the task will be accomplished in the next chapter.

## CHAPTER 5

### PASSAGE TO THE CONTINUUM (GLOBAL)

#### 5-1 GENERAL:

The performance prediction of the soil system under applied loads requires a mathematical model. To have this model reconcile to the actual soil constitution, the model should be based on micromechanics theory. The procedures for the development of this theory need work in two environments (see chapter one). The former one consists of two steps, which have been accomplished in chapters three and four.

In this chapter, we will establish the two steps in the probabilistic environment: the randomness of the law of performance and the passage to the global. It should be noted that there is a link between the two environments. This link gives one of the peculiar features of our micromechanics theory.



## 5-2 REVIEW:

Micromechanics theory is a relatively new field. Therefore, no standard method has been documented for the global passage. In this section, a critical review of the global passage will be addressed and an application of one of these approaches to our problem of clay compression will be demonstrated.

There are many possible approaches to pass to the global concept from microelement analysis. These approaches depend on the problem to be dealt with and what mathematical model is governing the behaviour of the microelement.

### In Geomaterials:

We will start with the approach which relates the internal change of the soil mass to its effects on the continuum. This approach can utilize the physico-chemical and biological analyses of a physical unit which consist of two to three clay particles or a cluster of particles. This utilization can be considered as a process of alteration of material properties and/or qualitative analysis.

A phenomenological test can be performed for the whole sample; and therefore, the continuum parameters of the soil can be measured from this experiment and an analysis of the effect of the local alteration on

the continuum parameters, can be done. See the work of Yong et al. (1985a,b) and Hoppe (1986) for detailed discussion of these procedures.

We will call the phenomenological approach a "continuum experimental approach". This approach has the advantage of being a quick analysis and of requiring no theoretical modelling. However, a valid conclusion from this analysis should be based on a critical review of the experiment boundary conditions and the local quantitative analysis. Fig.29 shows schematic view of this analysis.

In granular material, Oda (1972,1977), Oda et al. (1980,1982 a,b), Nemat-Nasser (1980), have considered an experimental and theoretical development of the granular material performance under different types of boundary stress conditions. The fundamental parameter which is considered in their development is the contact normal between the particles. From this parameter, they infer the so-called fabric ellipsoid, and they relate this ellipsoid with principle stress applied to the sample. It is worth mentioning that this concept can be characterized as an internal state parameters theory. However, it is a continuum theory, and its parameter is represented by contact normal.

Bazant et al. (1975), Bazant et al. (1986) and Zubelewicz et al. (1987) have used two concepts for

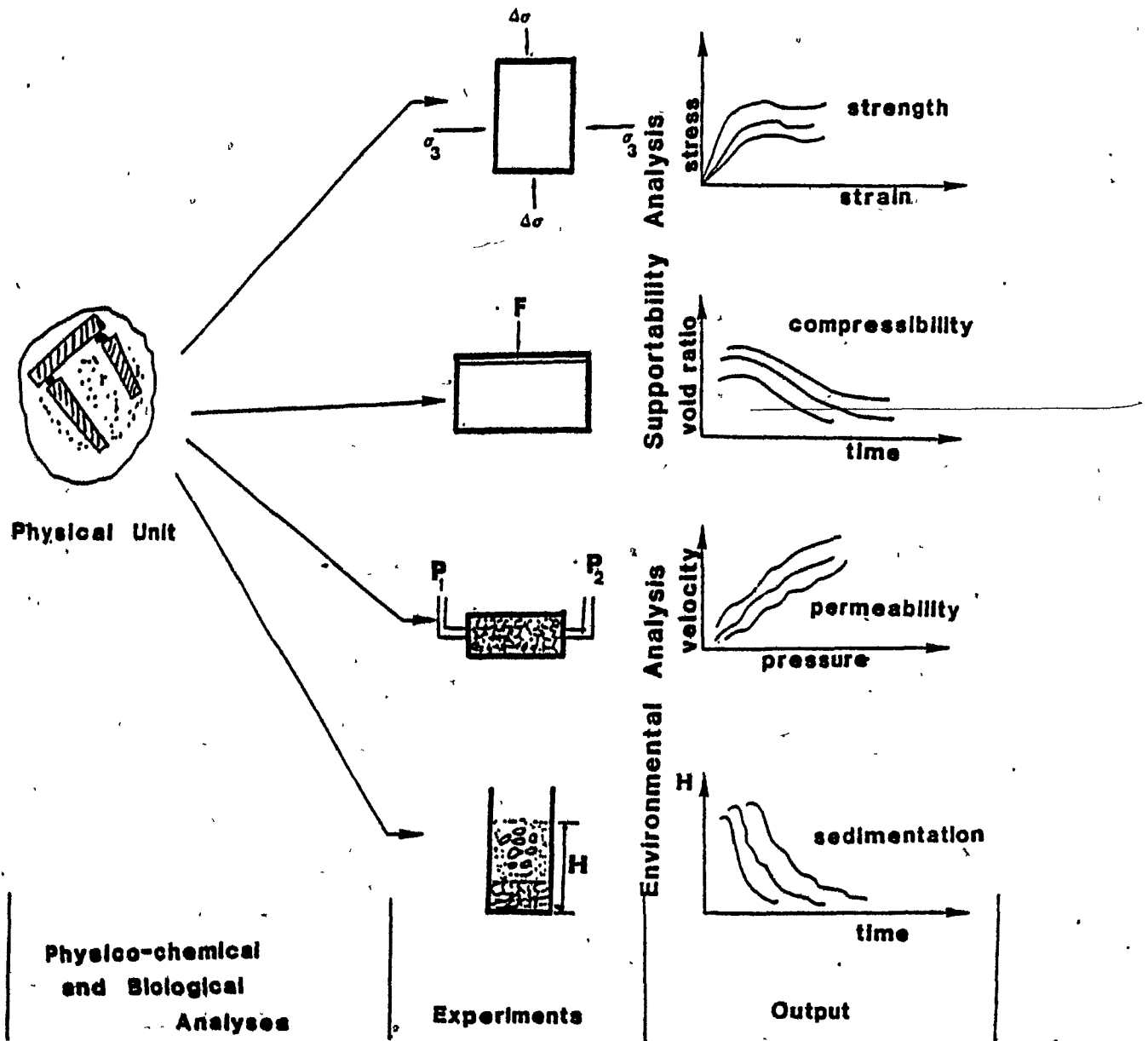


Fig. 29 Continuum Experimental Analysis

the passage to the global, namely:

1. the concept of matrix transformation which represents an analogue of the finite element passage from local coordinates to the global coordinates.

This concept has been used for the active plane in concrete (see discussion in chapter four). The disadvantage of this model for our purposes is that it does not discern between local properties and the global properties, i.e., the local properties are based on a piece of continuum material. This is one of the reasons that there is no need for micromechanics test for these models. (See our discussion of Zubelewicz et al. paper in chapter four.)

2. The concept of the virtual work is used in the papers by Bazant et al. (1985 and 1987). It stated that the work done by the global stresses under small variational global displacement is equal to the integral of the work done by the local stresses under variational local displacements on the microplanes.

The local parameter which is required for this passage is the orientation of the microplanes. Because it is difficult to find the orientation of these planes for concrete, Bazant et al. have assumed that these planes

exist in an isotropic condition.

On the other hand, for clay soil, they have used the X-ray scattering test to find the microplanes' orientations. Hence, The virtual work concept gives the same disadvantage as the matrix transformation concept. It should be noted that the application of the virtual work concept to the global formulation had been first introduced by Hill(1965), and then this procedure was used by Christoffersen et al.(1981) to find the global stresses in granular media by using the particle contact forces.

#### **In Theoretical Mechanics:**

Hill (1965 a,b), Bishop(1951,a,b), Batdorf and Budiansky(1949), Rice(1971), and Coleman and Gurtin(1967) have considered a continuum micromechanics theory in which the fundamental concept is to develop the internal state variable parameters. These parameters represent some physical characteristics of the material. Theories of macroscopic rate-dependency or rate-independent plasticity can be modelled by using the mechanism of slip for metal, with a single crystal or polycrystal.

Rice considered that the macroscopic yield surface can be regarded as the inner envelope of an unbounded number of planar yield surfaces representing critical shear conditions for each slip system at each element

of the material. Coleman et al. have worked out the thermodynamics of the internal state variable models.

From the theoretical mechanics point of view, Axelarad(1978) has used the concept of probability theory and functional analysis to develop the time evolution equation of the mechanical state of the material. This mechanical state is represented by the stress and strain vector space. This theory has been used both for polycrystal metal and for fibers. More detailed discussion of this theory is given in two books by Axelarad (1978,1984)

Beran and McCoy (1970), Kroner (1976,1980) and Mazilu(1976) have used the concept of statistical methods in order to formulate continuum theories for constitutive analysis. However, all of these authors have developed their concepts for small strain elastic theory in which the Green function plays an essential rule in their analyses. Furthermore, no microelement has been considered in these analyses, and for meaningful analysis, the ensemble average must be considered to be equivalent to the volume average.

Ericksen et al.(1958), Mindlin(1964), Eringen (1972), and Toupin(1964) have passed their systems of directors to continuum formulations by the assumption of the continuity of functions, assuming therefore, the mathematical point as the essential concept in their

theories.

Alblas (1976) has considered the ensemble theory for his analysis by introducing the concept of partition function. His formulation is for field equations only. The fundamental assumptions of the statistical mechanics are retained in his analysis.

Murdoch (1983,1984) used the volume average and time average of the quantities which represent the performance of a cell of size  $10^6 \text{ \AA}$ . He also developed field equations.

Muncaster (1983,a,b) has used the invariant manifolds for the development of relations between what he called fine theory and coarse theory. In addition, he applied his theory to the kinetic theory of gas, as fine theory and continuum gas dynamics as coarse theory. The concept of the invariant manifolds is considered from a deterministic point of view. Therefore, the continuity assumption plays a central role in the relation between the fine and coarse theories.

#### **Discussion:**

In most of the works discussed above, no microelement has been established. This has made it very difficult to consider all the relevant local parameters which are responsible for the actual

performance of the material. From the mathematical point of view, we conclude the finding of the above authors in the following fundamental points:

a- Authors who used statistical mechanics have found it difficult to develop the constitutive equations.

b- The use of functional analysis and measure theory in mathematical development of micromechanics models may limit the engineering applications of these models.

c- Authors who use internal state parameters accept the continuum concept.

All of these authors did not consider the basic axiomatic relations of the passage to the global. This problem will be discussed next.

### 5-3 AXIOMATIC RELATIONS FOR THE PASSAGE TO CONTINUUM:

In this section, we will try to establish an axiomatic structure which is necessary for constructing the principles of the passage from the performance of the microelement to the performance of the ensemble of microelements. First, we will outline the basic requirements for the microelement performance. Second,



we will discuss the basic requirements for the ensemble of microelements performance. Third, the condition of the passage to the global will be discussed.

### Microelement:

We write the evolution equation of the microelement (M S U) as follows:

$$Q(\dot{t}) = \mathcal{L}(\tau(\dot{t})) \quad (5.1)$$

where

$$\dot{t} \in R = [0, T]$$

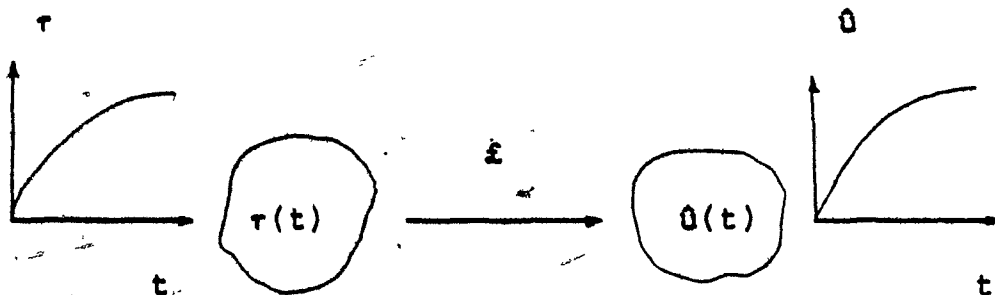
$\dot{t}$  = local time

$\tau(\dot{t})$  = input to the microelement system (e.g. stress)

$\dot{Q}(\dot{t})$  = response of the microelement system (e.g. strain)

$\mathcal{L}$  = mapping from the input to the response (transfer function). See Fig. below.

$\epsilon$  = Denotes element of.



This mapping can be represented in topological space as follows:

$\hat{x} : \tau \in \gamma \rightarrow \hat{u} \in \zeta$  as a function defined on an open subset of a Banach space.

Where

$$\gamma \cup \zeta = \Omega$$

$\gamma$  = subset in the Banach space (for the input)

$\zeta$  = subset in the Banach space (for the response)

$\Omega$  = the total subset in the Banach space

$\cup$  = denotes union.

We refer to Eq. 5.1 as the motion of the system (microelement) which the theory is meant to describe,  $t$  is the local time over which the microelement evolves.

### Time invariant

For each  $\theta \in \Omega$ , and  $\Delta t \in \mathbb{R}$

there is  $\theta' \in \Omega$  such that

$$\hat{u}_{\theta'}(t+\Delta t) = \hat{u}_{\theta}(t) \quad (5.2)$$

Where

$\theta$  = an element from the subset  $\Omega$  in the Banach space (e.g. microstrain at time  $t$ ).

$\theta'$  = an element from the subset  $\Omega$  in the Banach space (e.g. microstrain at time  $t+\Delta t$ ).

For all  $t$  and  $t+\Delta t$ , this condition states that any family of solutions of local state must be invariant with respect to translations of time.

### Ensemble of microelements:

We view the evolution equation of the collective or ensemble of microelements as follows:

$$\dot{u}(t) = \mathfrak{f}(\dot{\tau}(t)) \quad (5.3)$$

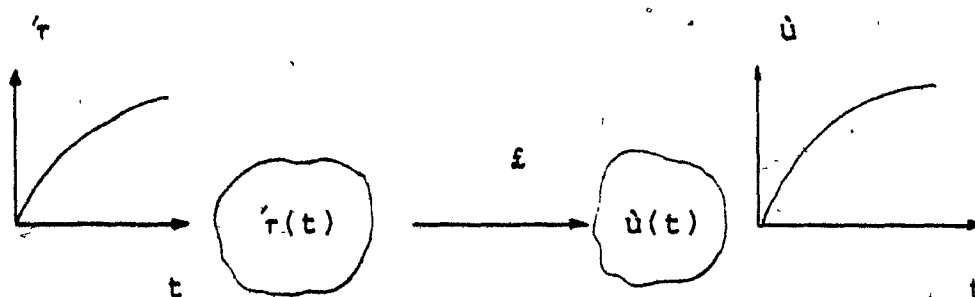
where

$t \in R = [0, T]$  as time interval, global time

$\dot{\tau}(t)$  = the input to the ensemble (e.g. stress)

$\dot{u}(t)$  = the response of the ensemble (e.g. strain)

$\mathfrak{f}$  = represents the mapping from the input to the response (transfer function). See Fig. below.



This mapping can be represented in the topological space as follows:

$\mathfrak{f}: \dot{\tau} \in \dot{\gamma} \longrightarrow \dot{u} \in \dot{\zeta}$  be a function defined on an open subset of a Banach space.

Where

$$\gamma \cup \xi = \Omega$$

$\gamma$  = subset in the Banach space (for the input)

$\xi$  = subset in the Banach space (for the response)

$\Omega$  = the total subset in the Banach space.

We refer to Eq. 5.3 as the motion of the system which the theory is meant to describe;  $t$  is the global time over which the ensemble of the microelements evolves.

#### Mapping to the global:

The mapping means the passage from the local to the global. This mapping can be represented by the following three cases:

##### Case 1

$$\xi = \Pi_1(\gamma) \quad (5.4)$$

In this case the input of the microelement is mapped onto the global response of the ensemble.

##### Case 2

$$\gamma = \Pi_2(\xi) \quad (5.5)$$

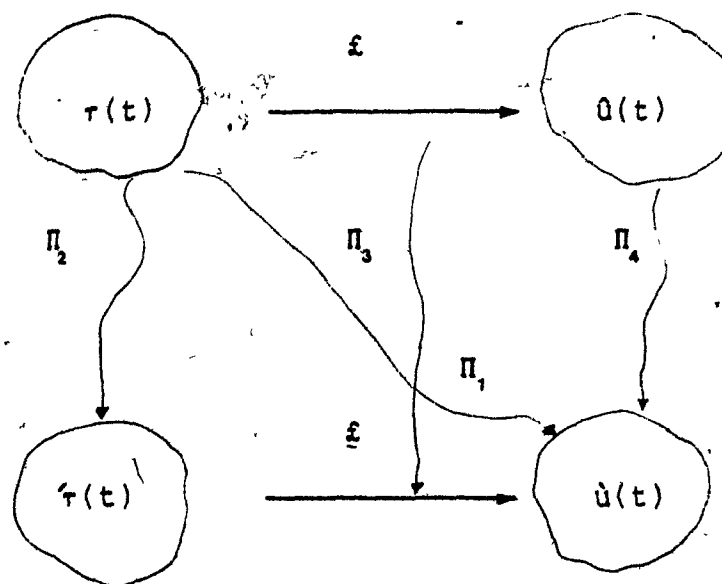
In this case the input of the microelement is mapped onto the global input of the ensemble.

##### Case 3

$$\underline{f} = \Pi_3(\underline{f}) \quad (5.6)$$

In this case the transfer function of the microelement is mapped onto the transfer function of the ensemble.

$\Pi$  (in Eq. 5.6) is the most essential function for the micromechanics development. In actual fact there are several mapping procedures, see Fig. below.



In words, with each state of the microelement, we can identify a state  $\hat{\epsilon} = \Pi(\epsilon)$  in a global sense. However, to each global state  $\hat{u} \in \hat{\epsilon}$ , generally, corresponds to many microstates due to the collective behaviour,  $\hat{u}_1 \hat{u}_2 \hat{u}_3 \hat{u}_4 \dots \in \hat{\epsilon}$ . The inverse mapping  $(\Pi^{-1})$  represents the behaviour of one microelement ( $\hat{u} \in \hat{\epsilon}$ ) which corresponds to one global behaviour. Therefore, the inverse mapping is a one-to-one mapping.

Thus the motion in Eq. 5.1 generally gives us a more detailed description of the system than does Eq. 5.3. Only when a clear distinction between the local and global time is established, are the two times considered identical. See Fig. 30.

**Initial state:**

We have the following condition for mapping:

For each  $x_i \in \Omega$

$$\Pi(Q(0)) = x_i$$

Where

$x_i$  = the global state corresponding to the initial state value (subscript refers to the initial time). It is an element from the subset  $\Omega$  in the Banach space (e.g. initial stress).

This condition suggests that there is no time delay (at  $t=0$ ) between the local and global performance. It has been applied for the initial excess pore water pressure establishment. See chapter four.

**Final state**

We have the following condition for mapping:

For each  $x_f \in \Omega$

$$\Pi(Q(t)) = x_f$$

Where

$x_f$  = the global state corresponding to the final state value (the subscript  $f$  refers to the final time).

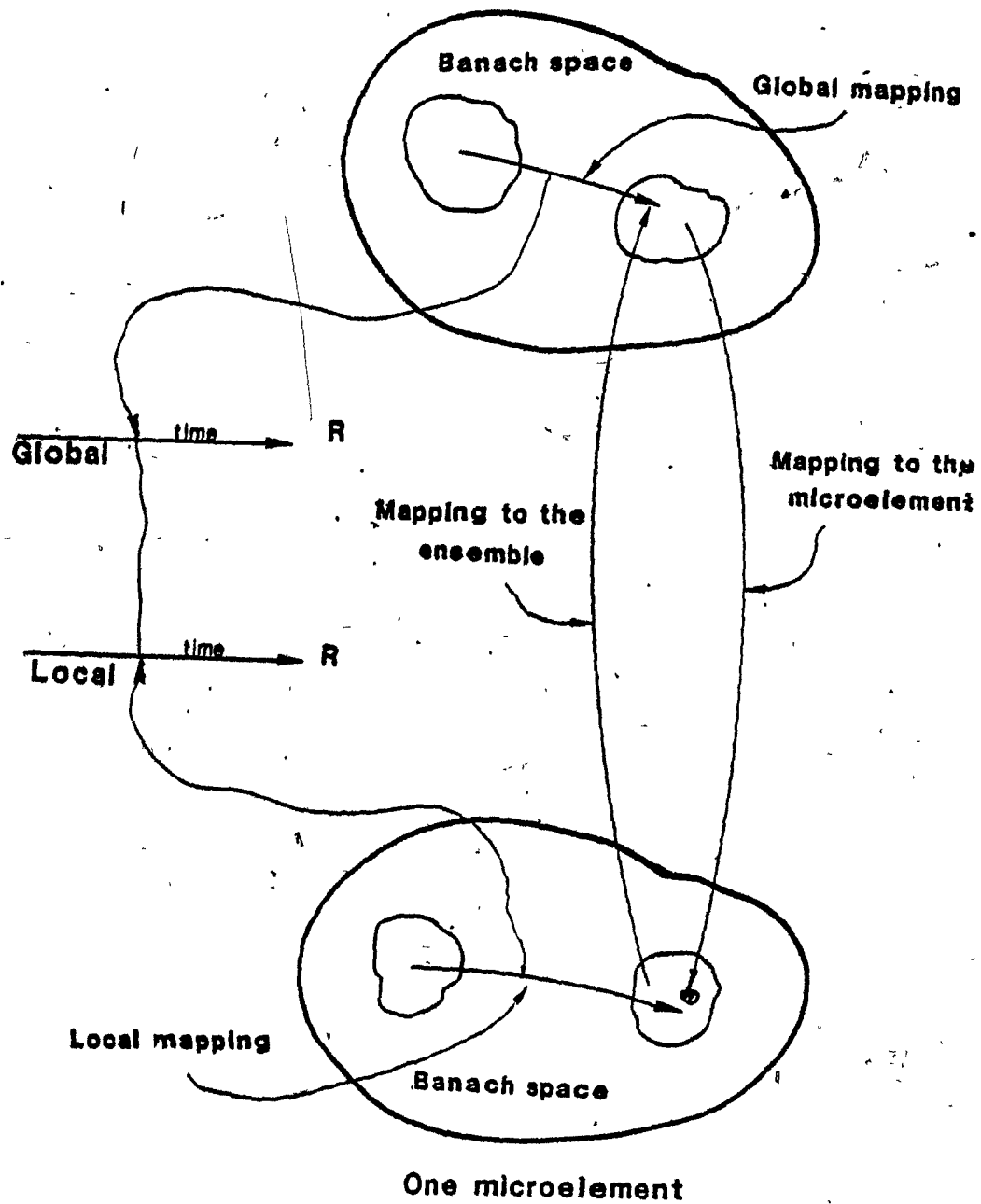


Fig. 30 Schematic view of the axiomatic structure of the passage to continuum

It is an element from the subset  $\Omega$  in the Banach space (e.g. final stress).

This condition suggests that there is no time delay (at  $t=t_0$ ) between the local and the global performance. This condition can be applied on the first region before the overlapped region and on the second region after the overlapped region, i.e., it cannot be applied for the transitional states as well as for the failure states.

These conditions and requirements are important elements in the mapping (passage) to the global. On the basis of the literature review in the preceding section, this mapping can be constructed by three different approaches. These are:

- a- Deterministic approach (with or without local scale).
- b- Statistical approach (with or without local scale).
- c- Probabilistic approach (with or without local scale).

These approaches are different in their basic structures and assumptions. In our analysis, we will consider the probabilistic approach for reasons which have been provided in the introduction. Since we shall adopt the probabilistic approach in this study, a more detailed discussion is desirable, which now follows.



#### 5-4 PROBABILISTIC APPROACH:

This approach can be considered to be developed in general by a stochastic measure theory. This development leads to the probabilistic functional relationship which connects the stochastic system analysis with that of semi-groups. Such mathematical analyses become so complex that their utility in the solution of an engineering problem is limited.

In the present work, we will not pursue this type of analysis. Instead, we will implement the conditions and the requirements of the preceding section in the manner which permits the prediction of the performance of clay system under compression loads.

In the following pages we will establish the two steps in the probabilistic environment: the randomness of the law of performance and the passage to the global. In order to establish the first step, some facts about the concept of probability should be addressed here. It has been noted that in general, the uncertainty can be classified in three types: the fundamental or intrinsic uncertainty, statistical uncertainty, and model uncertainty.

The fundamental uncertainty is intrinsic to the variability of the natural properties of the soil media, and cannot be reduced by repeated observation of

those properties. The two types of variabilites which can lead to fundamental uncertainty are local variability and global variability. Most of the applications of probability to geotechnical engineering consider only the global variability and not the local variability. See for example, Lumb (1966,1970 and 1975), Whitman (1984), Harr (1977), and others.

In the present analysis, we attribute the local variability to the variability in soil structure , i.e., "intrinsic soil structure variability". This intrinsic soil structure variability can be divided into two kinds: the fabric variability, and the potential variability

The fabric variability considers the size of cluster units, the neighbor distance  $D$ , the macrostructural void ratio, the triad vectors which enclose the compression zone, and so on. The variability in these parameters can be viewed from the perspective of their mean and standard deviations.

The potential variability considers several forces: the viscous force (mostly shear force) between clusters/ particles, and it depends on the viscosity parameter; the friction force (shear force) between clusters/particles, and it depends on the friction parameter and the normal forces; the electrostatic and electromagnetic forces between clusters/particles, and

they depend on the electrical and magnetical field generated in the region. The existence of all these forces in a specific clay system depends on the external applied forces, clay-water-electrolyte system, and on the bonds' (between clusters/particles) conditions. The variability in these parameters (forces) can be viewed also from their means and standard deviations. The intrinsic soil structure variability will be accounted for in the development of the evolution equations of the state functions.

It should be noted here that the global variability is a product of the local variabilites, and it can be viewed from the law of large numbers. There are very few studies which have modelled the local variability. See Yong et al. (1970); and in general, see the work of Axelrad(1984) for other materials.

Due to our imperfect knowledge of the probabilistic laws that govern the natural processes which we agree to handle as stochastic, statistical uncertainty arises from the limited extent of statistical samples. However, this uncertainty can be reduced by additional observations of either objective or subjective data.

Model uncertainty arises mainly because of simplification in physics predication algorithms in identification parameters of the problem, in model

analysis procedures, and in the probabilistic models themselves.

Some kinds of model uncertainty can be handled by modifying the probability distributions of some variables while others have to be accounted for by taking computed probabilities as estimates of imperfectly known "true" probabilities.

#### 5-4-1 Evolution Equation:

The passage from one microelement performance to the ensemble of microelements performance will be established by constructing the evolution equation. We will try to establish this equation from the physics point of view to give insight to the equation developed. From a pure mathematics point of view, see Gnedenko (1967).

Let us consider a system whose configuration and whose mechanical state are completely described by a set of  $n$  variables.

$$\{ 'w \} = \{ 'w_1, 'w_2, 'w_3, \dots, 'w_n \} \quad (5.7)$$

Examples of such variables are: an excess pore water pressure, macrostructural void ratio, microstrain and so on. On a microscopic level of description, the

variables  $\{w\}$  describe the state of the system. A more detailed description takes into account that the variables  $\{w\}$  are in fluctuating time dependent quantities. Thus,  $\{W(t)\}$  forms an  $n$ -dimensional random process. This process may be characterized in the usual way by a set of probability densities.

$$f_1(\{w^1\}, t_1) \cdot f_2(\{w^2\}, t_2; \{w^1\}, t_1) \quad (5.8)$$

Where  $f$  is the probability density for finding  $\{W(t)\}$ : near  $\{w\}$  at the time,  $t=t$  and so on.

As a first fundamental assumption, we introduce the Markov property of the random process  $W(t)$ , which is defined by the condition given in Eq. 5.9. The notion of a Markov process originated as a generalization of a sequence of trials connected into a chain which was studied by A. A. Markov. Unlike Bernoulli's scheme, Markov studied the case in which the probability of occurrence of an event in a subsequent trial depends on the outcome of previous trials.

$$\frac{f(\{w^v\}, t_v; \{w^{v-1}\}, t_{v-1} \dots \{w^1\}, t_1)}{f(\{w^{v-1}\}, t_{v-1} \dots \{w^1\}, t_1)} = \Pr(\{w^v\} | \{w^{v-1}\}, t_v, t_{v-1})$$

(5.9)

In Eq. 5.9 the conditional probability density  $\Pr(.|.)$  has been introduced. It only depends on the variables  $\{w^v\}$ ,  $\{w^{v-1}\}$ , and the two times  $t_v, t_{v-1}$ . From the Markov property Eq. 5.9, it follows immediately that the whole hierarchy of distribution, (Eq. 5.8), is given if  $w^1$  and  $\Pr(.|.)$  are known. This important feature of the Markov theory allows us to describe all the finite-dimensional distributions of the process in terms of a small number of constructively defined characteristics and thus allows us to evaluate the distribution of various functionals of the process.

As a consequence of Eq. 5.9, the probability density  $\{w\}$  obeys Eq. 5.10 which is obtained by integrating the expression for  $f(.)$ , following from Eq. 5.9:

$$f_2(\{w^2\}, t_2) = \int_0^\infty \{dw^1\} \Pr(\{w^2\} | \{w^1\}, t_1, t_2) f_1(\{w^1\}, t_1)$$

(5.10).

Eq. 5.10 contains the most important feature of the Markov process which is the evolutionary character

of its development: that is, the state of the process at the present completely determines its probabilistic behavior in the future. This allows us in our case, by appropriately extending the  $W$ -space of the process, to transform it into a Markov process. On the other hand, the evolutionary character of Eq. 5.10 permits us to derive an evolution equation for the determination of the probabilistic characteristics of the process.

A second fundamental assumption is the stationarity of the random process  $\{W(t)\}$ . This assumption implies that all external influences on the system are time independent on the adopted time scale of description. Owing to the assumption of stationarity the conditional distribution  $\text{Pr}(.|.)$  in Eqs. 5.9 and 5.10 depends only on the difference of the two times of its argument.

Eq. 5.10 has been simplified to a differential equation, see Van Kampen (1961,1983), Kramers (1940) and Moyal (1949), as follows:

$$\partial f(\{w\}, t) / \partial t = \sum_{s=1}^{\infty} \frac{(-1)^s}{s!} \frac{\partial^s K_{i_1, i_2, i_3, \dots, i_s}(\{w\}) f(\{w\}, t)}{\partial w_{i_1} \partial w_{i_2} \partial w_{i_3} \partial w_{i_4} \dots \partial w_{i_s}} \quad (5.11)$$

Where  $K_{i_1, i_2, i_3, \dots, i_s}$  = the coefficient of the differential equation.

Owing to the appearance of derivatives, it is in most cases too complicated to be solved in this form. Hence we consider the first and the second term of the equation. The higher order terms are in fact very small and add no physical and mathematical insight to the stochastic physics in general. See: Moyal (1949), Lax (1960) and Van Kampen (1961,1983)).

We rearrange the terms in Eq. 5.11 according to successive derivatives of  $f$ . Lax (1960) expanded Eq. 5.11 in orders of non-linearity. As a first derivative approximation we obtain from Eq. 5.11 the following equation:

$$\partial f / \partial t = \partial k_i(\{\dot{w}\}) f / \partial \dot{w} \quad (5.12)$$

This equation can easily be solved if the solution of its characteristic equations

$$\partial \dot{w} / \partial t = k_i(\{\dot{w}\}) \quad (5.13)$$

are known. Eq. 5.12 describes a drift of  $f$  in the  $\{\dot{w}\}$ -space along the characteristic lines given by Eq. 5.13. In this drift approximation fluctuations are introduced only by the randomness which is contained in the initial distribution.

In order to describe a fluctuation motion of the system, we have to include the second order derivative terms in Eq. 5.11; this leads to the evolution



equation:

$$\frac{\partial f}{\partial t} = -\partial k_1(\{w\}) f / \partial w + -\partial k_{12}(\{w\}) f / \partial w \partial w \quad (5.14)$$

The second order derivatives describe a generalized diffusion in  $\{w\}$ -space. The diffusion approximation Eq. 5.14 of Eq. 5.11 is adopted in all the following. We will use  $\text{Pr}(w, t)$  for  $f(w, t)$  and  $C$  for  $k$ . Hence:

$$\frac{\partial \text{Pr}(w, t)}{\partial t} = -\frac{\partial}{\partial w} \tilde{C} \text{Pr}(w, t) + \frac{1}{2} \frac{\partial^2}{\partial w^2} \tilde{\tilde{C}} \text{Pr}(w, t) \quad (5.15)$$

Eq. 5.15 represents the evolution equation of the parameters  $\{w\}$ , and  $\tilde{C}$  and  $\tilde{\tilde{C}}$  are the coefficients of this equation. Moyal (1949) called these coefficients the derivate moments of  $\dot{W}(t)$ . They have the following definitions (Moyal (1949) and Van Kampen (1983))

$$\tilde{C} = \left\langle \frac{\Delta \dot{w}}{\Delta t} \right\rangle \quad \text{Drift coefficient.}$$

$$\tilde{\tilde{C}} = \left\langle \frac{(\Delta \dot{w})^2}{\Delta t} \right\rangle \quad \text{Diffusion coefficient.}$$

Note: the angular brackets define the mean values of the enclosed quantities, and  $\Delta$  denotes increments.

These coefficients are fundamental for the evolution to take place. Hence, they are described by the physics of the process. In the next section, we introduce a state function. From this function, we can establish the two coefficients.

#### State Function:

The state function is a collection of parameters which are responsible for the transition from state  $i$  at time  $t$  to state  $j$  at time  $t + \Delta t$  due to applied load. Hence, it describes the "law of performance" of the microelement (the macrostructural unit) in a deterministic environment.

The randomness of the law of performance, as included in the probabilistic environment in chapter one, can be established by using the Monte Carlo simulation. This simulation technique has a capability to handle the variability of the parameters of the state function. It uses the random number generation in the computer code. A detailed discussion of the simulation technique is given in the appendix D.

The procedures for establishing the two coefficients of the evolution equation will be examined in the following sections.

### 5-4-2 Evolution Equation For the First Region:

There is "a physics-link" between the evolution parameter  $Pr(w, t)$  and the two coefficients  $(\tilde{C}, \tilde{\tilde{C}})$ . This link can be seen in the formulation of the state function. Therefore, it is essential to choose the right evolution parameter for the evolution equation because this parameter will bring the physics of the clay-water system into the coefficients of the evolution equation. In the following, we will cast the formulation of the state function.

The time rate of the stress balance can be as following:

$$\dot{\underline{\underline{\sigma}}}^m = \dot{\underline{\underline{\sigma}}}^m + P^r \underline{\underline{\sigma}} \quad \text{Let } \dot{\underline{\underline{\sigma}}}^m = \alpha_1 \dot{\underline{\underline{\sigma}}}^m \Rightarrow \alpha_1 \dot{\underline{\underline{\sigma}}}^m = \dot{\underline{\underline{\sigma}}}^m + P^r \underline{\underline{\sigma}}$$

Where  $\alpha_1 = \text{constant}$ .

Hence

$$P^r \underline{\underline{\sigma}} = (\alpha_1 - 1) \dot{\underline{\underline{\sigma}}}^m = \beta_1 \dot{\underline{\underline{\sigma}}}^m, \quad \beta_1 = \alpha_1 - 1$$

Thus, the applied volumetric stress on the MSU:

$$P^r = \beta_1 \dot{\underline{\underline{\sigma}}}^m_v \quad (5.16)$$

$\beta_1 = \text{constant}$  which relates the rate of change of the excess pore water pressure and the rate of change of the effective stress. Note for classical consolidation equation  $\beta_1=1$ , Terzaghi (1925).

From Eq. 4.26 and Eq. 5.16, we can develop the following equation:

$$\frac{\partial e_m}{\partial t} = \frac{(1 + e_m)}{M_I} \tilde{e}_v^m = \frac{(1 + e_m)}{M_I} \left( \frac{1}{\beta_1} \right) \frac{\partial P^r}{\partial t} \quad (5.17)$$

From Eq. 3.53, we have the following equation:

$$\frac{\partial e_m}{\partial t} = \frac{C_s \gamma_w D}{n} \frac{\sum R_i^2 a_i}{\sum V_c} \frac{\partial^2 P^r}{\partial x^2} \quad (\text{Eq. 3.53})$$

Hence

$$\frac{\partial P^r}{\partial t} = \frac{M_I}{n} \frac{C_s \gamma_w D \beta_1}{(1 + e_m)} \frac{\sum R_i^2 a_i}{\sum V_c} \frac{\partial^2 P^r}{\partial x^2} \quad (5.18)$$

Let

$$\tilde{C}_v = \frac{M_I}{(1 + e_m)} \frac{C_s \gamma_w D \beta_1}{n} \frac{\sum R_i^2 a_i}{\sum V_c} \quad (5.19)$$

$$\frac{\partial P^r}{\partial t} = \tilde{C}_v \frac{\partial^2 P^r}{\partial x^2} \quad (5.20)$$

Where

$\bar{C}_v$  = the microconsolidation coefficient.

The state function, Eq. 5.20, is a parabolic differential equation. It describes the excess pore water dissipation (in terms of  $P$ ) with time from the cavity formed by the macrostructural unit. This state function resembles the Terzaghi consolidation equation since there is a corresponding principle between the continuum physics and discrete physics. This is a good check for our modelling technique in discrete physics.

#### Microconsolidation coefficient:

As we see, the microconsolidation coefficient consists of the soil structure parameters, i.e., fabric parameters and stress-modulus parameters. Hence, the time delay of the clay compression due to low permeability can be represented by fabric parameters, (such as  $D, R, a, v_c, e_m$ ), and the time delay due to the structural resistance can be represented by stress-modulus parameters (such as  $M, n$ ).  $M$  includes the structural viscosity which produces the real time delay of the clay compression.

The average value of the microconsolidation coefficient can be equal to the classical consolidation coefficient. Hence, in mathematical form:

$$C_v = \langle \bar{C}_v \rangle$$

Where  $C_v$  = Terzaghi coefficient of consolidation.

The variability of the parameters ( $M$ ,  $e_m$ ,  $R$ ,  $a$ ,  $v_c$ , ....) of the microconsolidation coefficient will be examined by using the Monte carlo technique. In actual fact, the variability of these parameters represents the intrinsic soil structure variability. In modern probabilistic geotechnical engineering, the global variability of Terzaghi coefficient of consolidation is considered by Chang(1985).

From the law of large numbers, one can establish a link between the global variability of  $C_v$  and the intrinsic variability of  $\tilde{C}_v$ . This will not be presented in this research work. However, the microconsolidation coefficient and its variability will play a key role in the present analysis.

#### Final Equation:

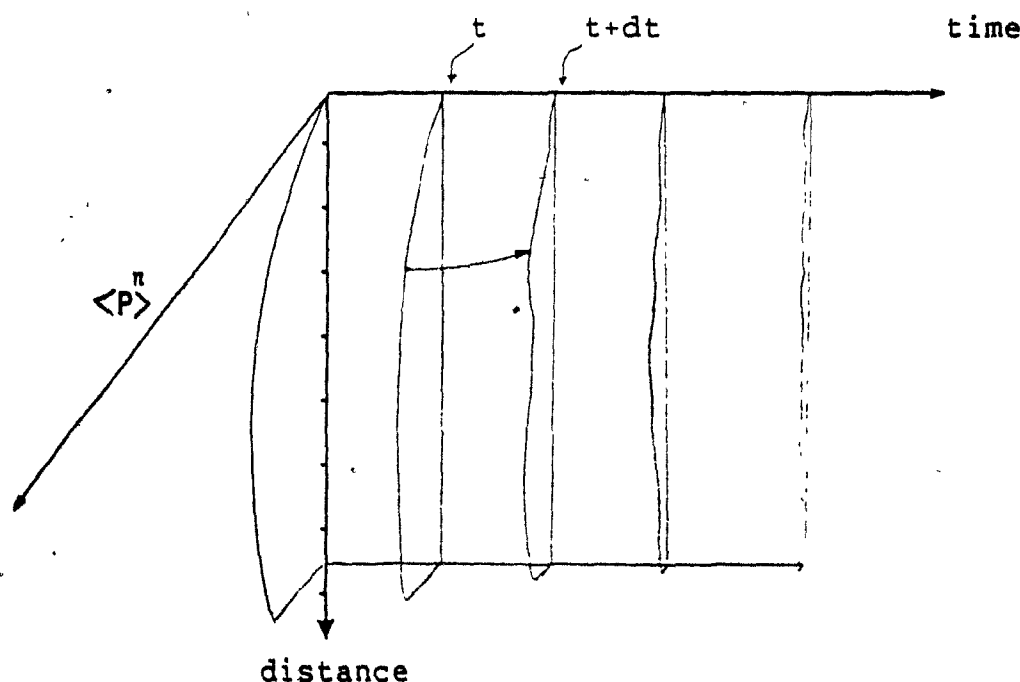
From Eq. 5.20, we can reveal that the excess pore water pressure is a very essential parameter for the evolution equation formulation. Therefore, Eq. 5.15 will take the following form:

$$\frac{\partial \text{Pr}(P', t)}{\partial t} = - \frac{\partial}{\partial P''} \left\langle \frac{\Delta P'}{\Delta t} \right\rangle \text{Pr}(P'', t) + \frac{1}{2} \frac{\partial^2}{\partial P''^2} \left\langle \frac{(\Delta P')^2}{\Delta t} \right\rangle \text{Pr}(P'', t) \quad (5.21)$$

$$\left\langle \frac{\Delta p'}{\Delta t} \right\rangle = \text{the drift coefficient,}$$

$$\left\langle \frac{(\Delta p')^2}{\Delta t} \right\rangle = \text{the diffusion coefficient.}$$

If we compare these coefficients with Eq.5.20, we can see that they include the parameters which are responsible for the physics of clay compression in the first region. Therefore, these coefficients are responsible for the transition of the clay system from state  $i$  at time  $t$  to the state  $j$  at time  $t+dt$ , i.e., in time increment  $dt$ . See Fig. below.



In order to solve Eq. 5.21 the following points are required: i) the calculation of its two

coefficients, ii) the initial condition of the probability distribution of the excess pore water pressure  $P_r(P^{\pi}, t=0)$ , iii) the boundary conditions, the position of the clay layer within the soil profile system, macrodimension (i.e., layer thickness), and microdimension (i.e.,  $D$  of MSUs). The last two points (ii and iii) will be examined in the appendix C and chapter six. However, the first point will be discussed in the following section.

#### 5-4-2-1 Calculation of The Coefficients:

Since the coefficient of the evolution equation should be found from the state function, the proper solution of this function must be sought. There are several methods to find the coefficients of the evolution equation. One example is the analytical method. It gives a close solution, and it can be used for simple state function. Another example is the correlation theory in which its integral should be solved numerically.

In the present analysis, the finite difference analysis will be used. The reason for using it lies in the following:

a- The nodes of the finite difference can be considered as "physical" nodes (i.e., they are not mathematical nodes) and hence the distances between the macrostructural units are involved as



node-to-node distances.

b- The finite difference analysis can synchronize the time increment of the state function with the time increment of the evolution equation since this equation will be solved by finite difference.

c- The finite difference analysis is simple and manageable in computer programming.

d- With the appropriate time increment, we can synchronize finite difference and finite element analyses in a mixed application (this will be discussed later).

#### **Finite Difference Analysis:**

For finite difference analysis, we feel that the control volume concept (Patankar (1980)) is more appropriate than using the Taylor-series formulation since in the control volume, the calculation domain is divided into a number of non overlapping control volumes. In our case, these volumes are the macrostructural units, such that there is one control volume surrounding each node point. Hence the nodes are in the centre of the macrostructural units, and the distance between nodes is equal to  $(D)$ . The numerical formulation is given in appendix C.

### Monte Carlo Simulation:

Essentially the Monte Carlo simulation technique generates the probability distribution of a function of several variables from the range of probability distribution of these variables. Each of these variables is regarded as a stochastic parameter.

For normal probability distribution, the computer simulation involves the use of an equation of the type:

$$X = Ma + Nr(S.D.) \quad (\text{Eq.D-2-3, App. D})$$

In which  $Nr$  is a standardized variate corresponding to the variable  $X$  with mean  $(Ma)$  and standard deviation  $(S.D.)$ . Independent standard uniform variate with range from 0-1 is used to obtain the standardized variate  $(Nr)$ , i.e., random number generation. See Appedix D.

Since there are a correlation among the parameters of the microconsolidation coefficient, multivariate probability distribution should be considered. We will assume for these parameters a normal distribution. Because the occurence of many individual effects and causes which cannot be treated seprately may lead to normal distribution.

If we generalize Eq. D-2-3 into multivariable form, we get the following:

$$\{X\} = \{Nr\}\{C.F.\} + \{Ba\}$$

Where  $\{C.F.\}$  is  $n \times n$  matrix with constant elements and is a function of the standard deviation of the variables and their correlation coefficients.  $\{Ba\}$  is a column vector with constant elements. The constant elements are the mean values of the random variables.

The following three parameters are considered correlated: The hydraulic radius( $R$ ), channel cross sectional area( $a$ ), and the macrostructural void ratio. The initial tangent modulus, and the effective stress are treated as single random variables, i.e., they follow Eq. D-2-3. Other parameters are considered from their mean values.

The steps for solving the evolution equation are:

1- find the probability distribution of the microconsolidation coefficient in each increment of time by using Monte Carlo simulation on the probability distribution of  $M, e, R, a, D, V_c$ , etc.

2- For each increment of time, solve the simultaneous equations which are produced from Eq. 5.20 (see Appendix C), with probability distribution of  $\tilde{C}_v$ .

3- For each increment of time, find the probability distribution of  $(\Delta P)^\pi$ .

4- Find the average of  $(\Delta P^\pi / \Delta t)$  and  $((\Delta P^\pi)^2 / \Delta t)$ , for each increment of time.

5- Solve the evolution equation by the finite

difference with time increments matching the time increments of the coefficients.

These steps are performed by 22 subroutines in the mainframe. Fig. 31 represents the computational flow scheme for finding the coefficients and the complete solution of the evolution equation. In the Appendix C, complete details of the formulation of different aspects of the computer program are given. The computer program is called Monte Carlo Finite Difference (MFD).

#### Discussion:

As we can see, the procedures for prediction of the excess pore water pressure dissipation in the micromechanics approach is entirely different from the procedures in the classical consolidation approach. The difference lies in the following items: 1. the introduction of the microelement and its properties, 2. the development and the finding of the consolidation coefficient.

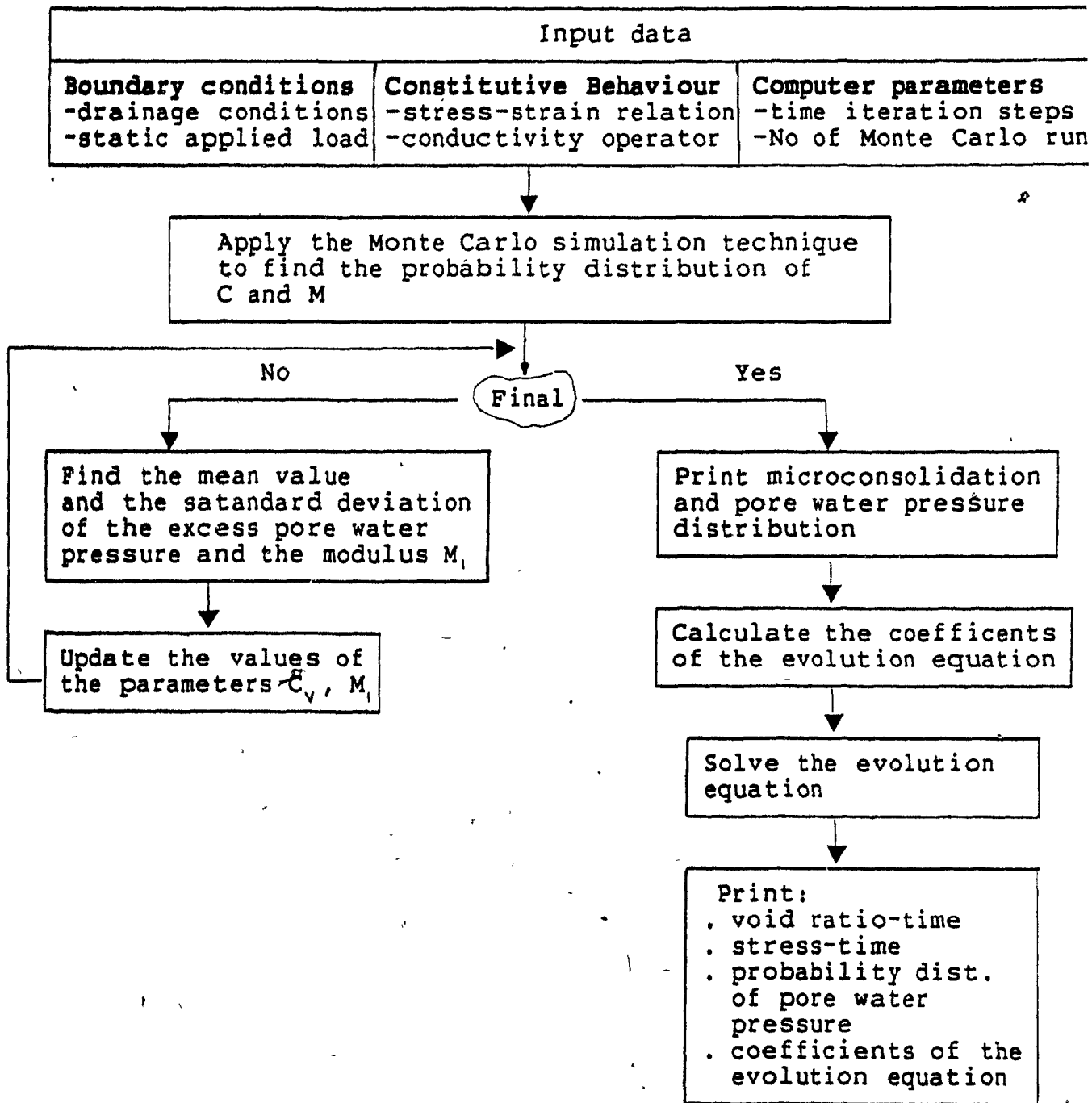


Fig. 31 Computational flow scheme of Monte Carlo finite difference analysis (MFD)

### 5-4-3 Evolution Equation For The Total Regions Of Compression:

The basic philosophy for developing the total region of compression is to choose an evolution parameter which is consistent for both regions. Furthermore, it has engineering applications. In the previous section, the excess pore water pressure was chosen for the first region. In itself it cannot be used for the development of the total region of compression since in the second region, the measureability and the calculation of this parameter are difficult if at all possible.

As discussed in the previous sections, the state function can dictate the type of evolution parameter which should be used. The constitutive equation normally describes the material state changes as the stress increases (or decreases). Therefore, the mechanical state of the material can be defined by the path of the strain accumulation in time domain (or in any domain) which corresponds to stress increase or (decrease).

Hence, the constitutive equations can be used for the state function formulations. In this section, the state functions for both regions will be addressed. However, the overlapped region will be treated in the next section.

In the first<sup>st</sup> region the state function is as follows:

$$d\sigma_v^m = M_I d\epsilon_v^m \quad (\text{Eq. 4.26})$$

This equation shows that as the stress increases (as excess pore water pressure decreases) with time, the strain path accumulation is in the time domain. Hence, the evolution parameter can be the strain. We will use the numerical technique, "mixed" finite element and finite difference, for calculating the two coefficients from the state function.

The reasons for using this mixed numerical technique are as follows:

a- Since there are two phenomena occurring at the same time, fluid flow (simulated by excess pore water pressure dissipation) and skeleton compression (simulated by strain accumulation in time), the stress transfer is the link between these two phenomena. Hence, the finite difference analysis will be used to update the excess pore water pressure (Eq. 5.20). Therefore, the effective stress at the nodes can be calculated at each node and at each time increment (Eq.4.1). Once this stress is known, the strain can be calculated at each node and at each time increment by using finite element analysis (Eq.4.26). It should be noted here that the time increments of both numerical

techniques are the same.

b- With the appropriate time increment, synchronization among the overlapped region, the first region, and the second region can be achieved.

The discussion of the formulation of the finite element code is given in appendix C.

In the second region, the state function is as follows:

$$\frac{\partial \epsilon_v(t)}{\partial t} = \frac{\nu_2}{m_2} sb_2 \exp(sb_1 \times \hat{e}_c \times t) \sigma_v^m \quad (\text{Eq. 4.28})$$

The evolution parameter is the strain. The finite element analysis will be used for calculating the first and second coefficients of the evolution equation from the state function presented above.

Hence, in general, the evolution equation can have the following form:

$$\frac{\partial \text{Pr}(\epsilon_v, t)}{\partial t} = - \frac{\partial}{\partial \epsilon_v} \left\langle \frac{\Delta \epsilon_v}{\Delta t} \right\rangle \text{Pr}(\epsilon_v, t) + \frac{1}{2} \frac{\partial^2}{\partial \epsilon_v^2} \left\langle \frac{(\Delta \epsilon_v)^2}{\Delta t} \right\rangle \text{Pr}(\epsilon_v, t) \quad (5.22)$$



For using this equation (Eq. 5.22), an appropriate strain for each region should be put in it. The finite difference analysis is used to solve Eq. 5.22. In the next section we will give the necessary steps for solving this equation for both regions.

#### 5-5 MATHEMATICAL MODELLING OF THE OVERLAPPED REGION:

In the previous section, the strain is considered to be the evolution parameter. Hence, a strain will be used for the overlapped region in order to be consistent in the prediction of the total region of compression.

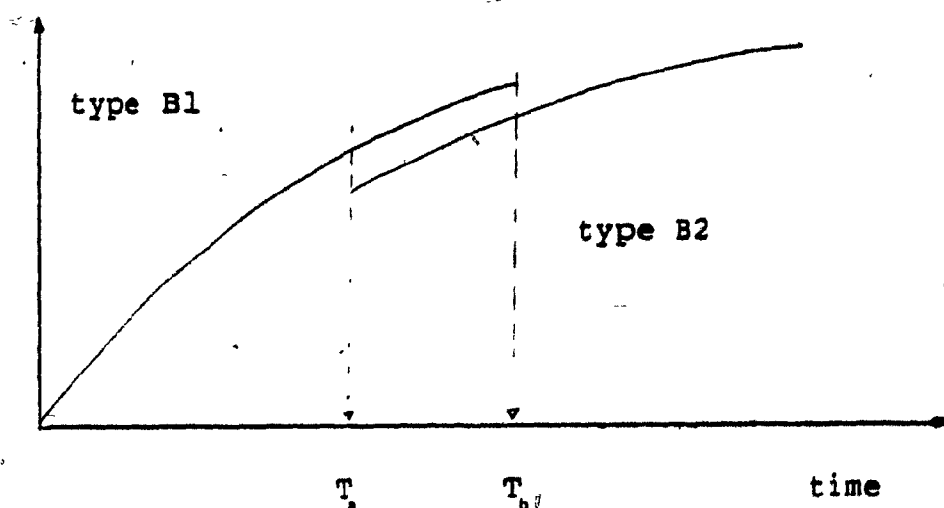
The description of the physics of the overlapped region in chapter two reveals that both mechanisms of deformation of the first and second region can occur at the overlapped region. This means that a number of macrostructural units will behave in one type of deformation and the rest of the macrostructural units will behave in the other type of deformation.

The overlapped region will occur between time  $t=T_a$  and time  $t=T_b$ . Before time  $T_a$ , most of the macrostructural units behave as the mechanism of type B1 deformation. As the process goes past  $T_a$ , the macrostructural units will pass to type B2 mechanism

until time  $T_0$  when all the macrostructural units will behave as the mechanism of type B2.

We would like to find the probability law which governs the number of the macrostructural units that will transfer to the mechanism of type B2 as the process takes place within the overlapped region.

The increasing number of macrostructural units that behave in type B2 (no. of MSUs which are transformed to behave into type B2) can be examined in another way. For example, the increasing number of the macrostructural units which are stopped to behave in type B1 may be considered. The term stop can be equivalent to death. Hence, the process can be regarded as death process in stochastic system analysis. Thus the Markov chain process is the building block for modelling the overlapped region. See Fig. below.



Consider a sequence of positive numbers  $\{\bar{C}_0\}$ . We



$$(1-x)^{-N} = \sum \binom{m+N-1}{m} x^m \quad (5.27)$$

and the concept of the generation function.

To obtain the following stochastic model, see the stochastic books of Samuel et al. (1981) and Cox and Smith(1961).

$$P_j(t) = \binom{N}{j} (\exp(-\bar{C}_0 t))^j (1 - \exp(-\bar{C}_0 t))^{N-j} \quad (5.28)$$

With simple mathematical manipulation observing the properties of binomial distribution, the mean and variance of the number of the macrostructural units that still behave in type B1 ( $X(t)$ ) are as follows:

$$E(X(t)) = N \exp(-\bar{C}_0 t) \quad (5.29)$$

$$\text{Var}(X(t)) = N \exp(-\bar{C}_0 t) (1 - \exp(-\bar{C}_0 t)) \quad (5.30)$$

where

$\bar{C}_0$  : It is an intensity parameter (it is a global parameter). In the next section we will give some detailed discussion about this parameter.

$N$  : the total number of macrostructural units (i.e., the number of trials in the binomial distribution).

$j$  : the number of MSUs which behave as type B1.

Figure 32 shows the plotting of Eq. 5.29 for different values of the intensity parameter ( $\bar{C}_0$ ). As can be seen the probability of the death process is very sensitive to the values of this parameter.

#### 5-5-1 The Intensity Parameter $\bar{C}_0$ :

The intensity parameter represents a key role in the evolution equation modelling of the overlapped region. It is generated from the physics of the compression process. The following points highlight some of the aspects of this physics:

a- The stress transfer which could be considered as a "physics-link" between the fluid flow (simulated by excess pore water pressure dissipation) and skeleton compression (simulated by strain accumulation) depends on the initial and boundary conditions as well as on the soil structure.

b- The intrinsic soil structural variability of the system as discussed previously is classified in two parts: fabric variability and potential variability. For example, in fabric variability, when the neighbor distance ( $D$ ) is very large ( $\langle D \rangle > 20 \mu\text{m}$ ), the clusters are small ( $\langle d_i \rangle < 5 \mu\text{m}$ ) and a large

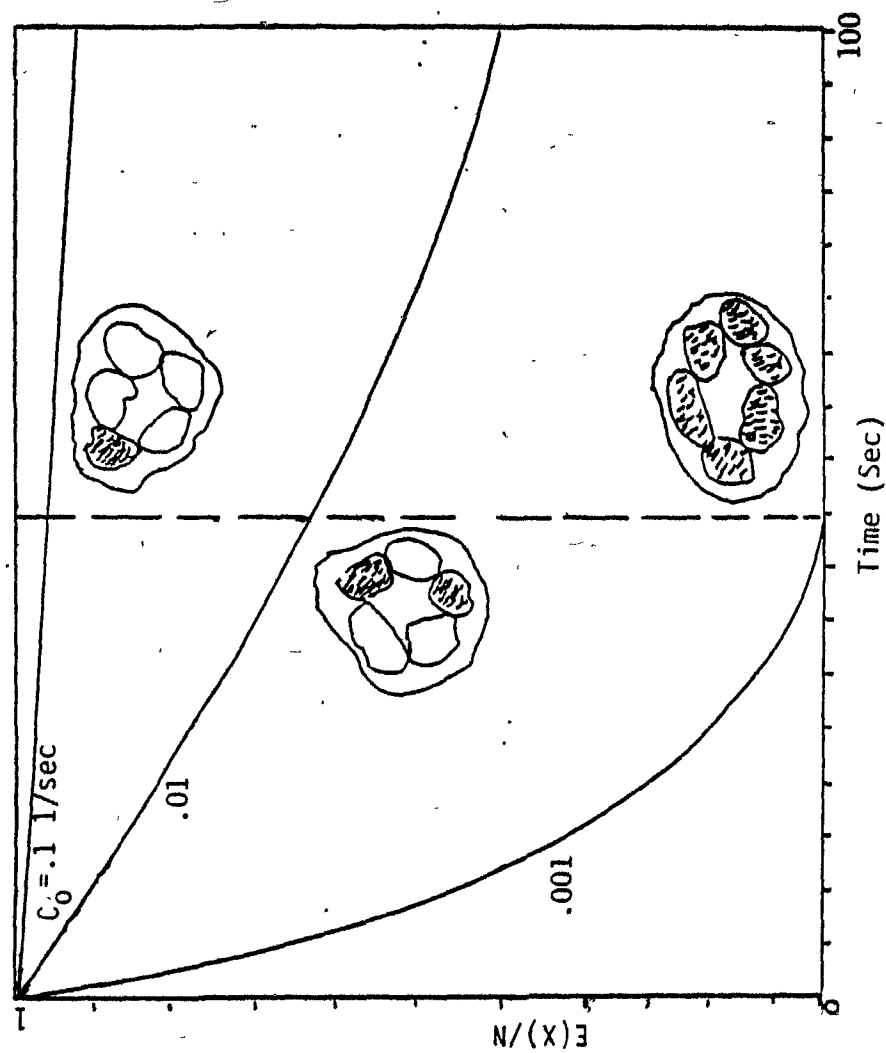


Fig. 32 The Plotting of Eq. 5.29 for Different Values of the Intensity Parameter ( $C_0$ )

motion of the clusters within the MSU will take place quickly (i.e., collapse condition-in short time). Hence, the type B2 deformation will take its place in several MSUs in a short time after the process gets started.

Another example is that in potential variability, when the integrity of the cluster units within the MSUs is weak compared with the rigidity of contacts (bond conditions) between these clusters, the type B2 deformation will take its place in several MSUs in a short time after the process gets started.

Hence, the intensity parameter( $\bar{C}$ ) links the consolidation process of the clay system on the first region to the creep process on the second region.

c- Some geometrical conditions which may have an effect on accelerating several MSUs to behave as type B2 are: the position of the macrostructural units in the clay layer, the position of this layer within the soil profile system, and the thickness of the clay layer.

#### **The concept of $\bar{C}$ modelling:**

On the basis of the above discussion, we can see that the intensity parameter depends on the fabric parameters and also on the stress-modulus parameters.

Hence, the intensity parameter can have the following form:

$$\tilde{C}_0 = C(D, m, R, e, v, \dots)$$

The physical form of the above equation can be established by using a Dimensional analysis technique (The II-theorem) Buckingham (1914).

Dimensional analysis is a mathematical method useful in determining a convenient arrangement of variables of a physical relation. Once orderly arrangement of the variable physical quantities has been established by Dimensional analysis, the experimental data must be used in order to obtain the necessary constants for a complete numerical expression.

If we assume that eight parameters are responsible for the phenomenon which is described by the intensity parameter, then we may put the above equation in the following form:

$$C(\tilde{C}_0, D, m, R, e, v, \sigma, \eta) = 0$$

From II-theorem, we have the following:

$$II(I_1, I_2, I_3, I_4, I_5) = 0$$

Therefore, we have five equations to be solved in order



to find the exponents of the parameters. Once the physical form of the equation is established, a numerical technique should be used on the experimental data so as to find the final expression. Further discussion on the intensity parameter modelling is given in the next chapter.

#### 5-5-2 Implementation-Evolution Equation of the Overlapped Region:

As discussed in the previous sections, the key concept of the evolution equation is the use of the state function. Since the two mechanisms of deformation work together in this region, its state function is represented partly by the state function of the first region and partly by the state function of the second region.

Therefore, as a first approximation we will use the following postulate: the state function of the first region works in the overlapped region with probability  $P(t)$ , and the state function of the second region works in the overlapped region with probability  $(1-P(t))$ . Hence, the format of the state function of the overlapped region can take the following:

$$\langle \Delta \epsilon_{ov}^m \rangle_j = P(t) \langle \Delta \epsilon_{v_I}^m \rangle_j + (1 - P(t)) \langle \Delta \epsilon_{v_{II}}^m \rangle_j \quad (5.31)$$

where

$\Delta \epsilon_{v_I}^m$  = the increment of volumetric strain of the type

B1 deformation, the subscript I refers to the first region.

$\Delta \epsilon_{vII}^m$  = the increment of volumetric strain of the type B2 deformation, the subscript II refers to the second region.

$\Delta \epsilon_{ov}$  = the increment of volumetric strain of the overlapped region, the subscript ov refers to the overlapped region.

After substituting Eq. 4.26 and Eq. 4.28 into Eq. 5.31, we get the following form for the overlapped region:

$$\langle \Delta \epsilon_{ov}^m \rangle = \langle M_{II} \rangle \langle \Delta \epsilon_v^m \rangle \quad (5.32)$$

Where:

$\langle \Delta \epsilon_v^m \rangle$  = the increment of stress which is considered in the overlapped region.

$$M_{II} = P(t) \langle 1/M_I \rangle + (1-P(t)) \langle M_2 \rangle \langle \epsilon_v^m \rangle / \langle \Delta \epsilon_v^m \rangle$$

$$M_{II} = \left( \nu_{22} s b / 2 m \right) \left( \exp s b \hat{\epsilon}(t) t \right) dt \quad (\text{see Eq. 4.28})$$

It should be noted that the value of  $\epsilon^m$  in the modulus  $M$  is updated with time, i.e.,  $\epsilon^m$  is not constant. Meanwhile, the stress in the second region for the

overlapped part is constant, i.e., the excess pore water pressure is equal to zero. Hence, at the end of the first region the average of  $\sigma^m$  in the modulus  $M$  is equal to the average stress of the second region.

Once the state function is established, the coefficient of the evolution equation can be found by using the numerical technique. The finite element analysis and the Monte Carlo simulation which have been used for both regions will be used here. It should be noted here that the time step which is used in the numerical technique should match the transition time step of the Markov chain process.

Hence, the procedures for development and calculation of compression evolution with time for the overlapped region can be as follows:

a- Find the probability distribution of the number of the macrostructural units that are converted to behave as type B2 deformation. The most essential parameter in this step is  $\bar{C}_0$ .

b- Find the state function by using the probability distribution developed in the first step together with the state functions developed in previous sections (Eq.5.31).

c- Find the coefficients of the evolution equation

and its solution by using numerical techniques, finite element analysis.

Four simple subroutines have been developed to perform the above steps.

The steps for the total region of compression prediction are:

1- Find the excess pore water pressure by repeating the same steps of the finite difference analysis for each increment of time.

2- Find the probability distribution of the effective stress in each node by using the balance equation with Monte Carlo simulation.

3- Solve Eq.4.26 by dividing it into two terms, i.e.,

$$d\sigma^n - d\sigma_v^n = 2m_1 d\epsilon_v^n \quad (\text{Eq.C-1-1, App. C})$$

or

$$\Delta\sigma^n - \Delta\sigma_v^n = 2m_1 \Delta\epsilon_v^n$$

Where

$$v_1 \sum (e_m(t)) \Delta\epsilon_v^n \sigma_v^n = \text{the nonlinear term.}$$

The finite element technique is used in such a way that the nonlinear term is added to each node by using iteration process within the finite element subroutine.

Note the parameters of this constitutive equation are random variables, i.e., Monte Carlo simulation should be performed. For each increment of time, find the probability distribution of the nodal displacements.

4- For each increment of time, find the average of  $\Delta \epsilon / \Delta t$  and  $(\Delta \epsilon)^2 / \Delta t$  from the probability distribution of the displacement.

5- Solve the evolution equation (Eq. 5.22) by using finite difference analysis.

By these above steps, the total deformation process of the first region can be calculated.

6- For the second region of compression, solve Eq. 4.28 by using finite element analysis, i.e., find the nodal displacement. The Monte Carlo analysis should be used to consider the variability of the parameters.

7- Find the average of  $\Delta \epsilon / \Delta t$  and  $(\Delta \epsilon)^2 / \Delta t$  for each increment of time.

8- Solve the evolution equation by finite difference analysis with the time increment matching the time increment of the coefficients.

By using the above steps, the total deformation of the second region can be calculated.

9- The steps for the overlapped region are given in the previous section.

By completing the above nine steps, the compression process of the clay system under applied load can be predicted. In chapter six, we will use these steps for deformation process prediction. Fig. 33 represents the computational flow scheme for finding the coefficients and the complete solution of the evolution equation for the total region of compression. These steps are performed by 30 subroutines in the mainframe. We call this program MFE.

#### 5-6 SUMMARY-THE EVOLUTION EQUATIONS:

For the first region of compressions alone, the excess pore water pressure has been chosen for the evolution equation. Finite difference analysis has been used for finding the two coefficients and also for finding the solution of this equation.

For the total region of compression the strain has been chosen for the evolution equation. In the first region, the finite difference and the finite element have been used for finding the two coefficients. In the second region, the finite element is used. In the overlapped region, after finding the probability distribution of the number of the macrostructural units which behave in type B2, both finite elements and finite difference have been used for solving the evolution equations.

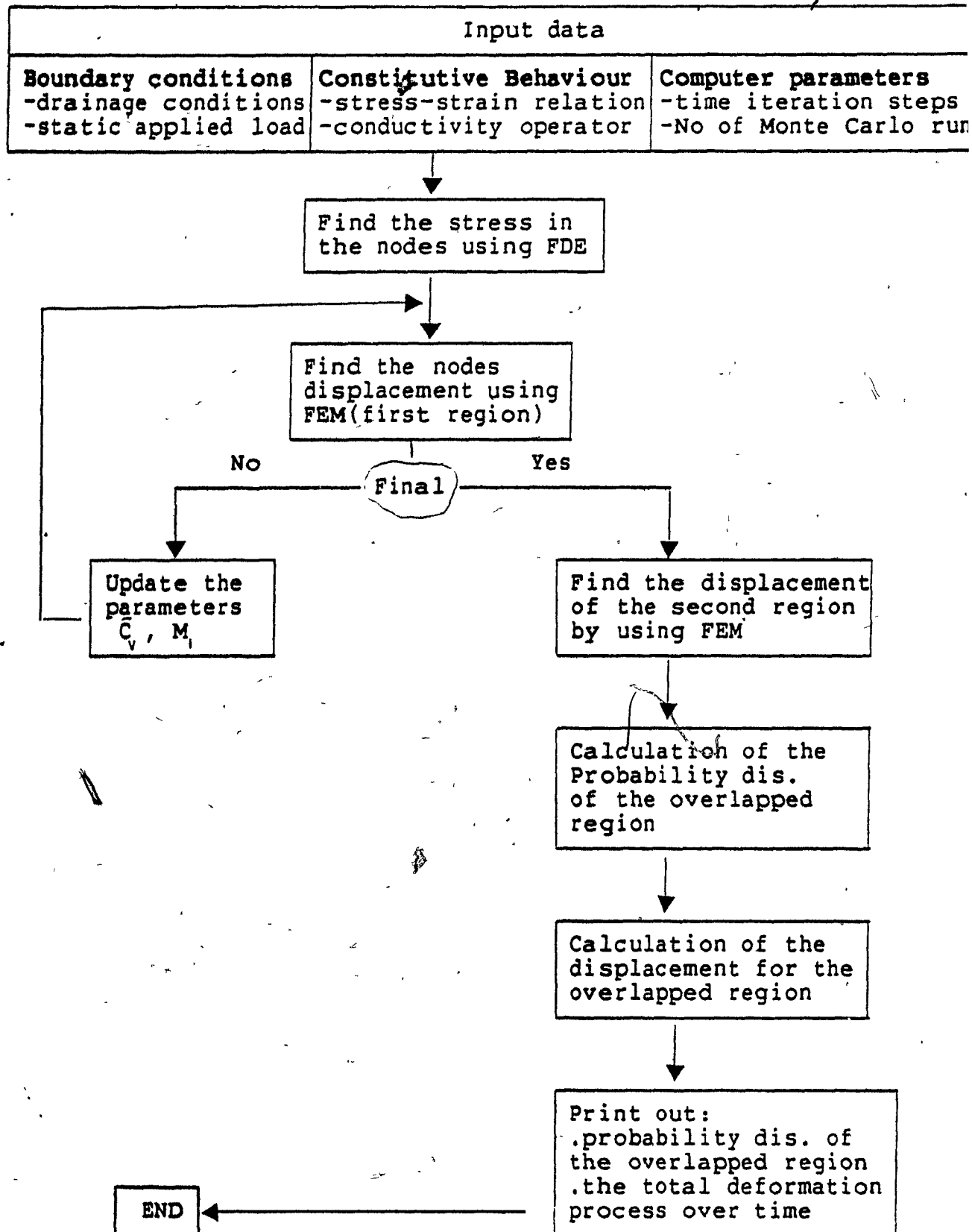


**Fig. 33 Computational flow scheme for modelling the total region of compression**

Table 4 shows the two steps in each environment (deterministic and probabilistic) for the development of the micromechanics theory of saturated clay soil performance under compression loading. As we can see the basic link between the two environments is the introduction of the intrinsic soil structure variability which is described in this chapter.



# Table 4 Summary-Evolution Equations

## DETERMINISTIC ENVIRONMENT:

a- Microelement: Macrostructural unit (MSU)

b- Law of performance: the state function of the MSU

i- First Region Alone:  
the basic parameter is the excess pore water pressure

$$\frac{\partial P'}{\partial t} = \bar{C}_v \frac{\partial^2 P'}{\partial x^2}$$

ii-Total Region of Compression:  
the basic parameter is the volumetric strain

First region,

$$d\epsilon_v^m = M_I d\epsilon_v^m$$

Second region,

$$\frac{\partial \epsilon_v^m(t)}{\partial t} = \frac{v_2}{m_2} s b_2 \exp(s b_1 x \hat{e}_c x t) \epsilon_v^m$$

Overlapped region,

$$\langle \Delta \epsilon_v^m(t) \rangle = \langle M \rangle \langle \Delta \epsilon_v^m \rangle$$

Table 4 Cont.

---

**PROBABILISTIC ENVIRONMENT:**

a- Randomness the state function: Monte Carlo analysis

b- Passage to the global: Evolution equation

i- First region alone:

$$\frac{\partial \text{Pr}(P^{\pi}, t)}{\partial t} = - \frac{\partial}{\partial P^{\pi}} \left\langle \frac{\Delta P^{\pi}}{\Delta t} \right\rangle \text{Pr}(P^{\pi}, t) + \frac{1}{2} \frac{\partial^2}{\partial P^{\pi 2}} \left\langle \frac{(\Delta P^{\pi})^2}{\Delta t} \right\rangle \text{Pr}(P^{\pi}, t)$$

ii- Total region of compression:

$$\frac{\partial \text{Pr}(c_v, t)}{\partial t} = - \frac{\partial}{\partial c_v} \left\langle \frac{\Delta c_v}{\Delta t} \right\rangle \text{Pr}(c_v, t) + \frac{1}{2} \frac{\partial^2}{\partial c_v^2} \left\langle \frac{(\Delta c_v)^2}{\Delta t} \right\rangle \text{Pr}(c_v, t)$$


---

## CHAPTER 6

### THE FEASIBILITY OF APPLICATION OF THE EVOLUTION MODELS

#### 6-1 FORWARD:

In the preceding chapters we have established the basic principles of micromechanics of soil and the prediction models for soil performance under compression loads. For these models, two large computer programs which make use of the numerical techniques (finite element and finite difference analyses), and Monte Carlo simulation have been written.

The experimental micromechanics is equally important. However, no standard test procedures have thus far been established. Moreover, working in small scale samples is a very difficult task. It requires skills and sophisticated equipment. The lack of standardized procedures of tests can be attributed to the lack of any link between micromechanics theory and the industrial applications.

It should be noted that the microelement and the ensemble of microelements scales should be the same for both the theoretical and the experimental developments.

Establishing the experimental micromechanics program is a lengthy process and it is beyond the scope of this study. Therefore, we are not going to compare between test data and our mathematical models' predictions. Instead, we will demonstrate the feasibility of the application of these models by using the experimental data of Turcott (Turcott, 1988). However, the discussion of this application has some merit in the overall analyses and prediction procedures in clay-compression solving program.

#### **6-2 SUMMARY-EVOLUTION EQUATIONS USED:**

In Table 5, the summary of the evolution equations are given. The parameters which are required for these evolution models can be divided into two sets: the first set can be the geometrical parameters, and the second set the stress-modulus parameters. The two sets actually represent the soil structure, and therefore, the first set represents the fabric and the second set represents the forces and the interaction potential.

##### **6-2-1 Geometrical Parameters:**

In this section, the list of the geometrical parameters will be given. Furthermore, the test technique used for obtaining these parameters is examined. The parameters are:

# Table 5 Summary-Evolution Equations

## DETERMINISTIC ENVIRONMENT:

a- Microelement: Macrostructural unit (MSU)

b- Law of performance: the state function of the MSU

i- First Region Alone:  
the basic parameter is the excess pore water pressure

$$\frac{\partial p'}{\partial t} = \bar{C}_v \frac{\partial^2 p'}{\partial x^2}$$

ii- Total Region of Compression:  
the basic parameter is the volumetric strain

First region,

$$d\epsilon_v^m = M_I d\epsilon_v^n$$

Second region,

$$\frac{\partial \epsilon_v(t)}{\partial t} = \frac{v_2}{m_1} s b_2 \exp(s b_1 x \hat{e}_c x t) \sigma_v^m$$

Overlapped region,

$$\langle \Delta \epsilon_v(t) \rangle = \langle M \rangle \langle \Delta \epsilon_v^n \rangle$$

Table 5 Cont.

**PROBABILISTIC ENVIRONMENT:**

a- Randomness the state function: Monte Carlo analysis

b- Passage to the global: Evolution equation

i- First region alone:

$$\frac{\partial \text{Pr}(P^v, t)}{\partial t} = - \frac{\partial}{\partial P^v} \left\langle \frac{\Delta P^v}{\Delta t} \right\rangle \text{Pr}(P^v, t) + \frac{1}{2} \frac{\partial^2}{\partial P^{v2}} \left\langle \frac{(\Delta P^v)^2}{\Delta t} \right\rangle \text{Pr}(P^v, t)$$

ii-Total region of compression:

$$\frac{\partial \text{Pr}(e_v, t)}{\partial t} = - \frac{\partial}{\partial e_v} \left\langle \frac{\Delta e_v}{\Delta t} \right\rangle \text{Pr}(e_v, t) + \frac{1}{2} \frac{\partial^2}{\partial e_v^2} \left\langle \frac{(\Delta e_v)^2}{\Delta t} \right\rangle \text{Pr}(e_v, t)$$

**Macrostructural Void Ratio Equation:**

$$e_m = \frac{V_m - \langle v \rangle_c n_c}{\langle v \rangle_c n_c}$$

$d_c$  : the diameter of the cluster units  
 $e_m$  : macrostructural void ratio. ( $e_{m_0}$  initial value)

$D$  : the distance between the two neighbor MSUs.  
 $f(y)$  : the observed radius of the cluster and the MSUs in probabilistic distribution form

$R$  : the hydraulic radius of the channels connecting the neighbor MSUs

$a$  : the cross-sectional area of the channels  
 $z^a$  : the distance between the centre of the MSU and the centre of the cluster

$z'$  : the distance between the centre of the MSU and the centre of the two neighbor clusters

$N_c$  : the number of cluster units per MSU

$N_m$  : the number of the MSUs within the ensemble

$e_c$  : the local void-ratio of the cluster unit.

There are several experimental techniques used for fabric parameters identification. These are: optical and scanning electron microscopy, X-ray diffraction, mercury intrusion porosimeter, acoustical velocity, Dielectric dispersion, electrical conductivity, and thermal conductivity. Since each of these techniques has its advantages and disadvantages, the combined use of a couple of them seems essential to obtain a reasonably comprehensive appraisal of the clay fabric analysis.

Of the methods listed above, the scanning electron

microscopy, mercury intrusion porosimeter and X-ray diffraction offer the advantages of getting the geometrical parameters. Detailed discussion of these techniques are given in Tovery(1973), Sridharan et al. (1971), Diamond (1970) and Krizek et al.(1973).

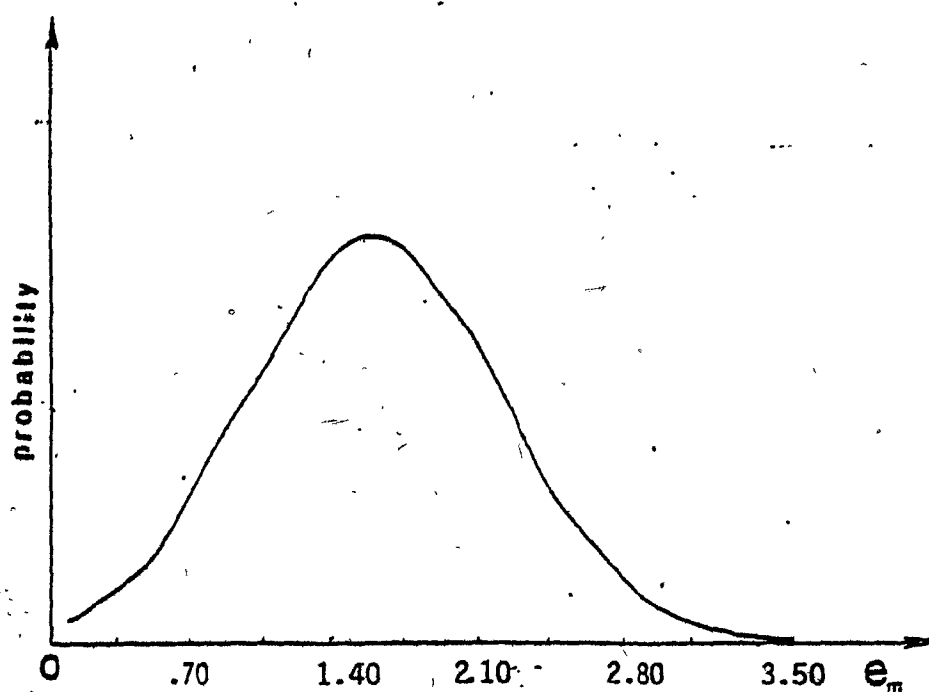
The scanning electron microscopy provides a three-dimensional image and allows direct observation of the clay particles (clusters) and their arrangement on a surface. From scanning electron microscopy, we can have the initial values of the above parameters. For example:

Synthetic clay (UF) (micrographs, from Turcott 1987): bulk void ratio= 2.65,  $\langle d \rangle = 4 \mu\text{m}$ ,  $\langle D \rangle = 15 \mu\text{m}$ ,  $\langle Z^a \rangle = 7 \mu\text{m}$ ,  $\langle Z \rangle = 7 \mu\text{m}$ , (note  $1 \mu\text{m} = .001\text{mm}$ ).

Natural clay (micrographs from Delage et al. 1984) bulk void ratio= 2.68,  $\langle d \rangle = 5 \mu\text{m}$ ,  $\langle D \rangle = 12 \mu\text{m}$ ,  $\langle Z^a \rangle = 4.5 \mu\text{m}$ ,  $\langle Z \rangle = 4.5 \mu\text{m}$ .

However, the void ratio of the macrostructural unit can be calculated from the information given by scanning electron microscopy. The computer program GME is used for these calculations. The prediction of the macrostructural void ratio is given in Fig. 34. And the parameters  $R$  and  $a$  can be modelled from the void ratio (see the derivations in appendix C-2) as follows:





$$\mu = \frac{1}{N_m} \left\{ \sum_i \frac{\langle A_c \rangle^i}{A_m^i} * n_c^i \right\}$$

$A_c$  = the area of the cluster unit (spherical shape)

$A_m$  = the area of the MSU (spherical shape)

$\sum$  = the summation over the number of MSU per ensemble

$N_m$  = the number of MSU per ensemble

$n_c$  = the number of cluster units per MSU

DATA:

$$\mu = 0.35$$

$$\langle V_c \rangle = 0.000064 \text{ mm}^3$$

Fig. 34 The Probability Distribution of Macrostructural Void Ratio (Photomicrograph from Turcott (1988))

The hydraulic Radius ( $R(t)$ ):

$$R(t) = e_m(t) \frac{4}{\pi} \frac{1}{S_v} \quad (6.1)$$

where:

$S_v$  = The specific surface area which is defined in chapter (3), Eq. 3.40.

$e_m$  = The void ratio of the macrostructural unit.

Hence, the mean value:

$$E(R) = (4/\pi) (1/S_v) E(e_m(t)) \quad (6.2)$$

The standard deviation

$$S.D._R = (4/\pi) (1/S_v) (S.D._e) \quad (6.3)$$

The channel cross-sectional area  $a(t)$ :

$$a(t) = e_m(t) (\pi d_1^2) \quad (6.4)$$

where

$d_1$  = the diameter of the cluster unit.

Hence, the mean value:

$$E(a) = (\pi d_1^2) E(e_m(t)) \quad (6.5)$$

and, the standard deviation:

$$S.D. = (\pi d_1^2) (S.D.) \quad (6.6)$$

It should be noted that the number of channels has been considered equal to the number of cluster units. As one can see, both the hydraulic radius and the channel cross-sectional area are functions of time. Hence they will be updated at each increment of time during the evolution.

#### 6-2-2 Stress-Modulus Parameters:

The stress-modulus parameters of clay performance under compression loads are listed as follows:

$\sigma^m$  = The stress applied to the macrostructural unit which is taken by the clusters only (effective stress). In our theory, each increment decrease of the excess pore water pressure,  $(P^m)$ , is considered equal to increment increase in  $(\sigma^m)$ , i.e.,  $\beta = 1$ .

$\eta$  = Absolute viscosity of the fluid.

$\nu$  = The structural viscosity modulus of the macrostructural unit when the MSU in the first region of the compression, i.e., it is the structural viscosity of the cluster interaction.

$\nu_{11}$  = Structural viscosity modulus of the MSU in the second region of the compression, i.e., it is the structural viscosity of the particle interaction within the cluster units in the macrostructural unit.

$m_1$  and  $m_2$  = The initial tangent modulus of the compressibility of the macrostructural unit.

$\hat{a}, \hat{a}$  = The parameters for  $\Xi(e_m(t))$ , first region of the compression.

$sb_1, sb_2$  = The parameters of  $\Xi(\hat{e}(t), t)$ , second region of the compression.

$\bar{C}_0$  = The intensity, parameter for the overlapped region.

### 6-3 APPLICATION-EVOLUTION EQUATIONS:

In the following, we will demonstrate the applications of the evolution equations. For the first region alone, the excess pore water pressure is the key parameter (Eq. 5.21). For the total region of compression the key parameter is the volumetric strain (Eq. 5.22).

### 6-3-1 Calculation Procedures of the Parameters:

a- Initial tangent modulus of the MSU: At the initial time, the response of the clay system due to applied load can be represented by the following equation:

$$d\sigma^m/d\epsilon_v^m = 2m_1$$

i.e., the term  $\hat{a}(d\epsilon_m/dt)\sigma^m = 0$ , see Eq. 4.26.

The initial tangent modulus is physically equal to the stress which produces unit strain. This strain is a result of "cluster movement" within the MSU at the instant of loading.

In order to find the value of the initial tangent modulus of the clay soil, we have to formulate  $\langle m \rangle$  as follows:

$$m_1 = \langle m_1 \rangle + m_1^* \quad (6.7)$$

Where,

$\langle m_1 \rangle$  = the average initial tangent modulus of the ensemble of MSUs which can be assumed equal to the average global initial tangent modulus, i.e.,  $\langle m_1 \rangle = \langle \bar{m} \rangle$ . And  $\bar{m}$  = the initial tangent modulus of the global test sample.

$m_1^*$  = The fluctuation over the average which can be related to the standard deviation of the ensemble modulus.

Fig. 35 shows the method of finding the initial tangent modulus from the experimental test program on saturated clay samples.

**b- The Constant Parameters of the First Region:**  
They have been obtained by using simple optimization procedures on three compression curves for different loads. These curves are produced from confined test on UF kaolinite clay which were performed by Turcott (1988). See his work for a detailed description of the intricate specimen preparation and the testing method, (see Figs.E-1, E-2, and E-3, App. E). The optimization procedures can be described as follows:

- 1- Formulate a simple error function.
- 2- Assume trial values of these parameters.
- 3- For three loads, run the computer program FDE for the first region. It should be noted that C will be updated each increment of time.
- 4- Compare the average predicted deformations with three experimental curves (E-1, E-2, and E-3).
- 5- If the error is large, select other values for the parameters in such a way as to minimize the error function.
- 6- Repeat these steps until the error is

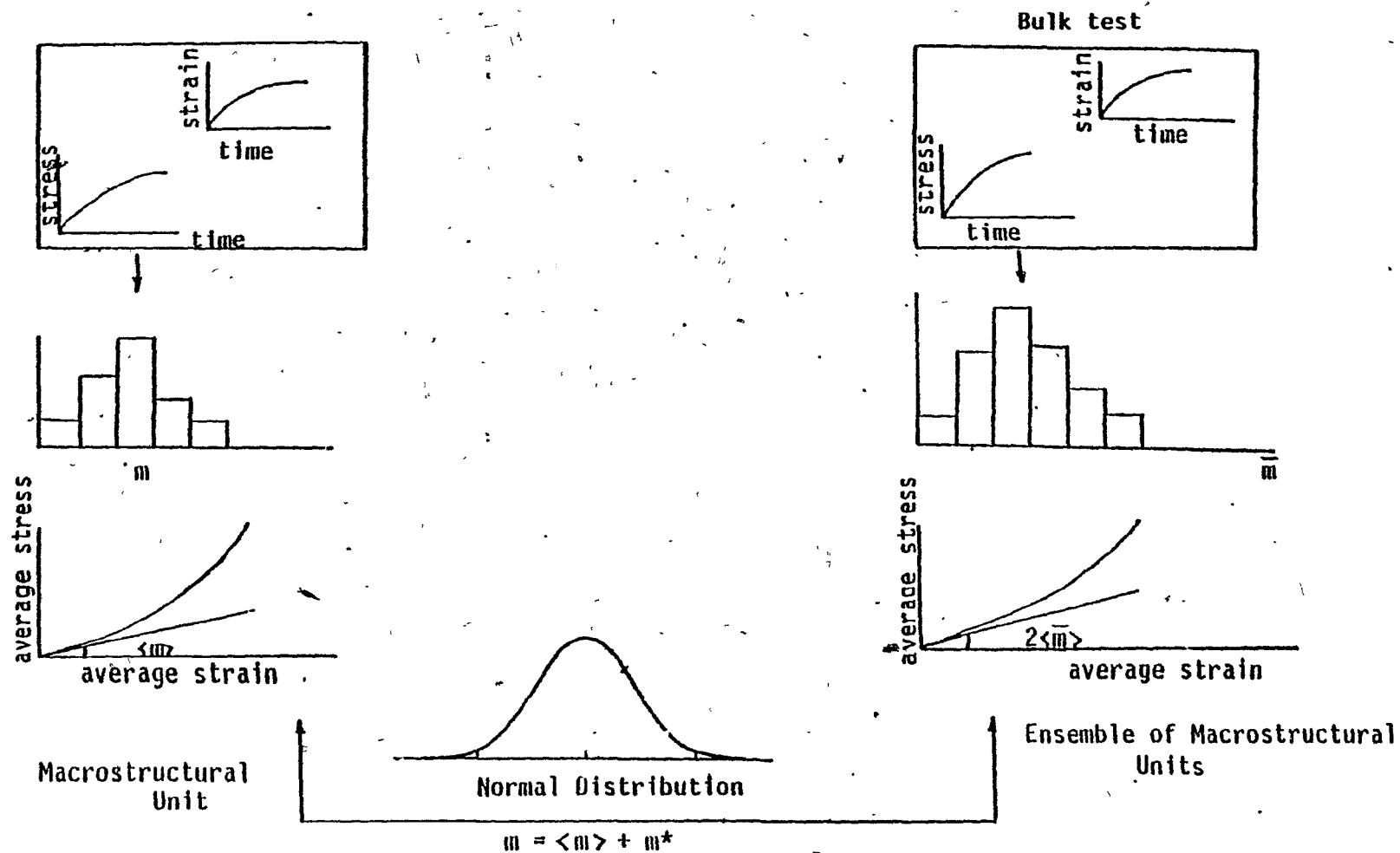


Fig. 35 Schematic View of the Method of Finding the Initial Tangent Modulus of the First Region

acceptable.

This procedure is not very different from the graphical matching technique.

c- The Constant Parameters of the Second Region:

If we take the log. of the both sides of Eq. 4.28 we get the following expression:

$$\log(\partial \hat{e} / \partial t) = \log(\hat{e}^m s b_2 v_2 / 2 m_2) + s b_1 \hat{e}_c(t) t \quad (6.8)$$

Fig. 36 shows the plot of Eq. 6.8. From the test data plotting, we can get the following:

The initial slope =  $s b_1 (\hat{e}_c(t=0))$

The intercept =  $\log(\hat{e}^m s b_2 v_2 / 2 m_2)$ .

We get the individual values of the parameters by using the optimization procedure which has been described above.

d- The Intensity Parameter( $\bar{C}_0$ ): since there is not enough experimental data, we will not use the dimensional analysis technique. Instead, since  $\bar{C}_0$  depends on the same parameters of  $\bar{C}_v$ , we will assume:

$$\bar{C}_0 = b \bar{C}_v$$



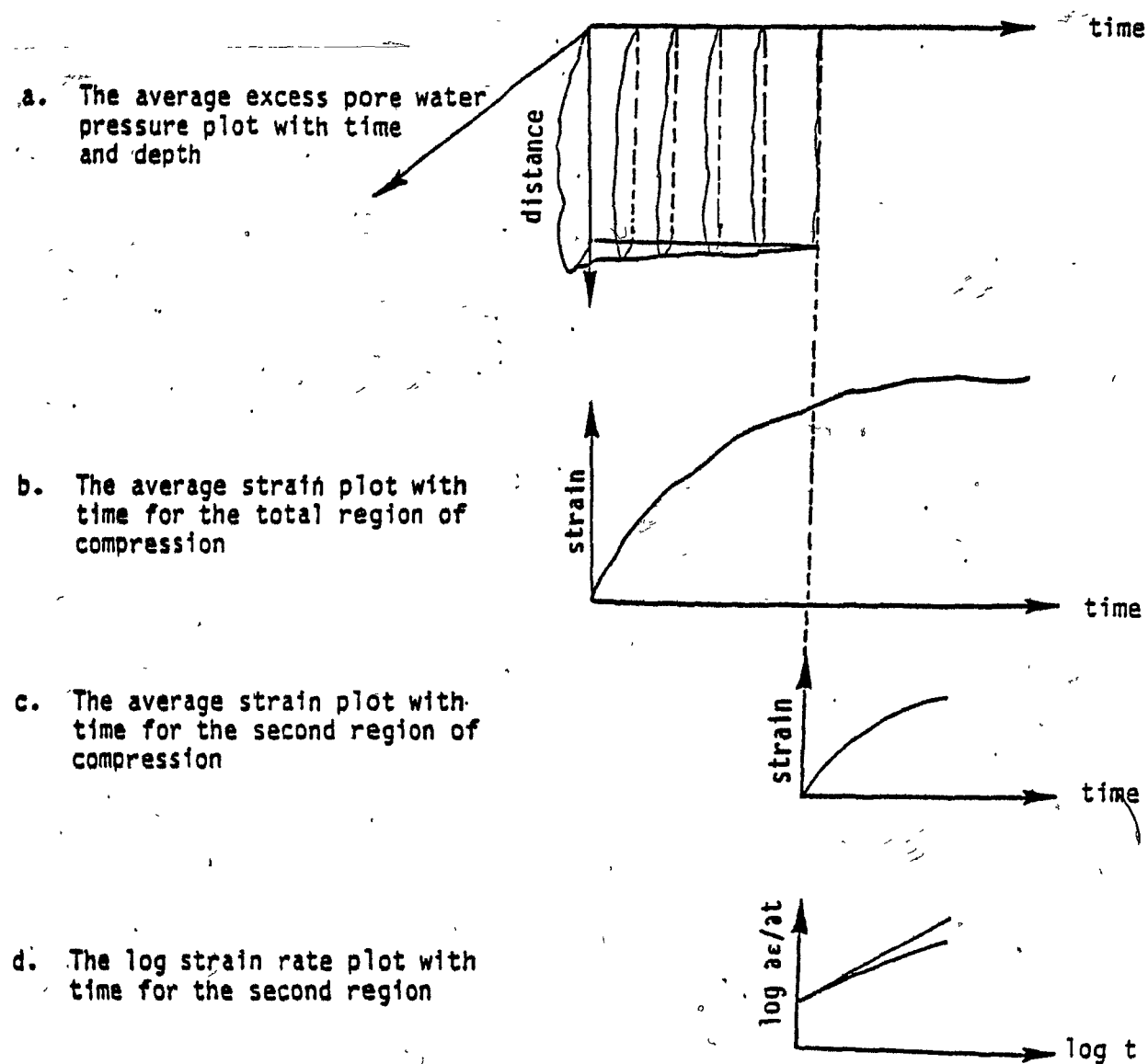


Fig. 36 The Steps for Finding the Parameters of the Second Region of Compression

The calculation of the constant  $b$  is done by the above optimization procedures but with condition of  $I_p=1$  is imposed at each increment of time in the two regions. It should be noted that for the overlapped region, we worked backward; i.e., from the end of the first region ( $P=0$ , at  $t=T_0$ ) to the beginning of the second region (at  $t=T_1$ ). Fig. 37 shows a schematic view of the solution technique for the overlapped region.

The input data for the evolution models are given in Table 6, and the computer output of the two programs, (i.e., MFD and MFE), is discussed in the next section.

### 6-3-2 Discussion:

The prediction of the evolution models are given in Figures 38 and 39, and it is worth considering their discussion in the following points:

a- The evolution models predictions are very sensitive to the values of the neighbor distance ( $D$ ), high excess pore water pressure dissipation and large deformation are caused by the greater value of this parameter. It is a collapse state parameter, and it describes the macropore collapse within the macrostructural unit.

b- The change in the microconsolidation value,  $\bar{C}_v$ , with time as opposed to the constant value, will

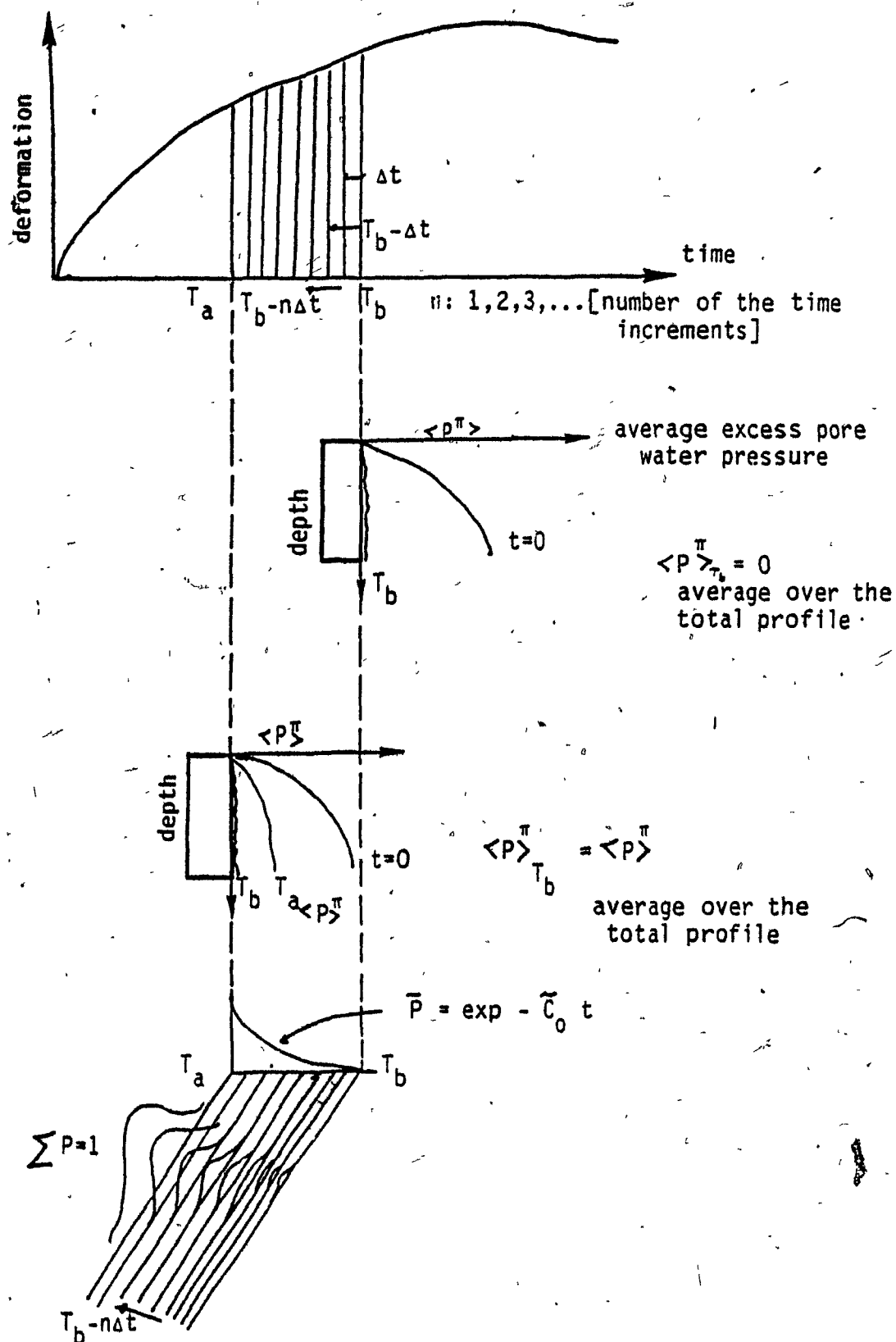


Fig. 37 Schematic View of the Solution Technique for the Overlapped Region

Table 6 Values for models prediction:

The paramter	Terminology used in computer	Value	Remarks
H	H	10.7mm	the height of the sample
T <sub>1</sub>	T	180 sec	the time for the first and the overlapped region, it is found by usig MFD program; i.e., to reach $\langle P \rangle = 0$ .
T <sub>2</sub>	T	120sec	the test time for second region
E(m)	RM4	2.1 kg/mm <sup>2</sup>	
S.D. of m	SGM4	.042	
a(v)	ALPH	1.15	
a	bi	1.20	
sb	sb	.3	
$v_2(sb_2)/m_2$	SGMH	2.5	
C <sub>0</sub>	ALAMDA	.1 (1/sec)	
E(e <sub>m</sub> )	Eo	1.56	the initial value of e <sub>m</sub>
S.D. of e <sub>m</sub>	SGMH	.5714	
E(R)	RM3	.001344	
S.D. of R	SGM(3,3)	.0000561	
E(a)	RMA	.0000196mm <sup>2</sup>	
S.D. of a	SGM(2,2)	.000072mm <sup>2</sup>	
d1	d1	.004mm	
$\beta_1$	BETA	1	
C	CS	.4	

E(.) = the average value  
S.D. of. = the standard deviation of

delay the consolidation of the layer, i.e., the excess pore water pressure dissipation for variable  $\tilde{C}_v$  will be slower than for constant  $\bar{C}_v$ . This has a significant effect on two stability calculations: i) the prediction of the effective stress, and hence the shear strength, and ii) the prediction of the differential settlement between two columns in a structural system.

c- The randomness in  $\tilde{C}_v$  has a significant effect on the prediction of the excess pore water pressure dissipation which supports the idea of Chang (1985) (in the continuum probability concept of the consolidation of clay, see chapter one). It should be noted that the intrinsic soil structure variability is reflected in the variability of the microconsolidation coefficient.

d- Using finite difference alone sometimes causes an overestimation in the prediction of the settlement of the clay layer. Hence, "mixed" finite difference and finite element should be considered together. The finite difference can be used for the prediction of the excess pore water pressure dissipation, and the finite element can be used for the calculation of the deformation in each node; and hence, the settlement.

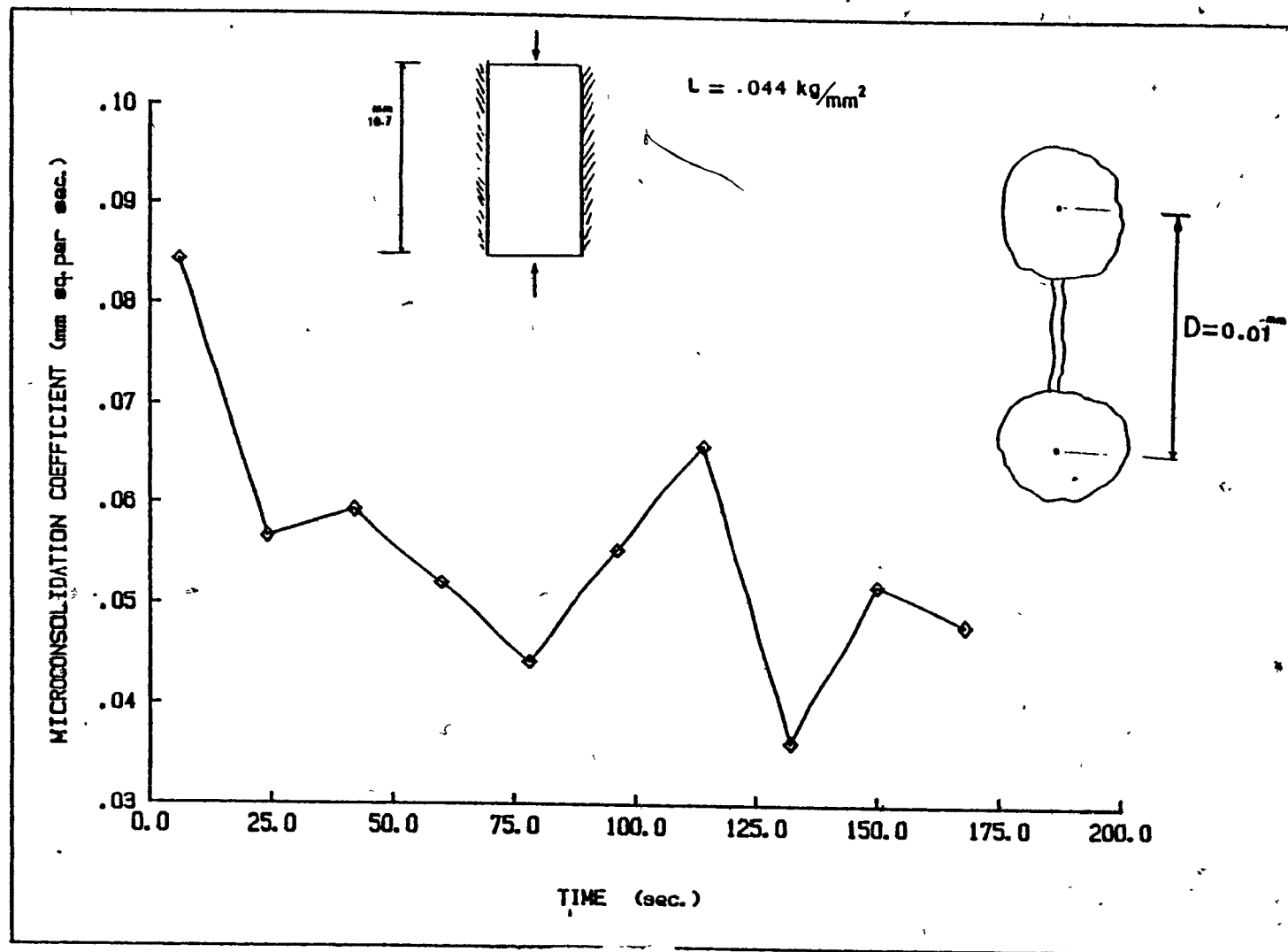


Fig. 38-a The average microconsolidation coefficient  
Monte Carlo Finite Difference Analysis(MFD)  
(100 Monte-Carlo run)

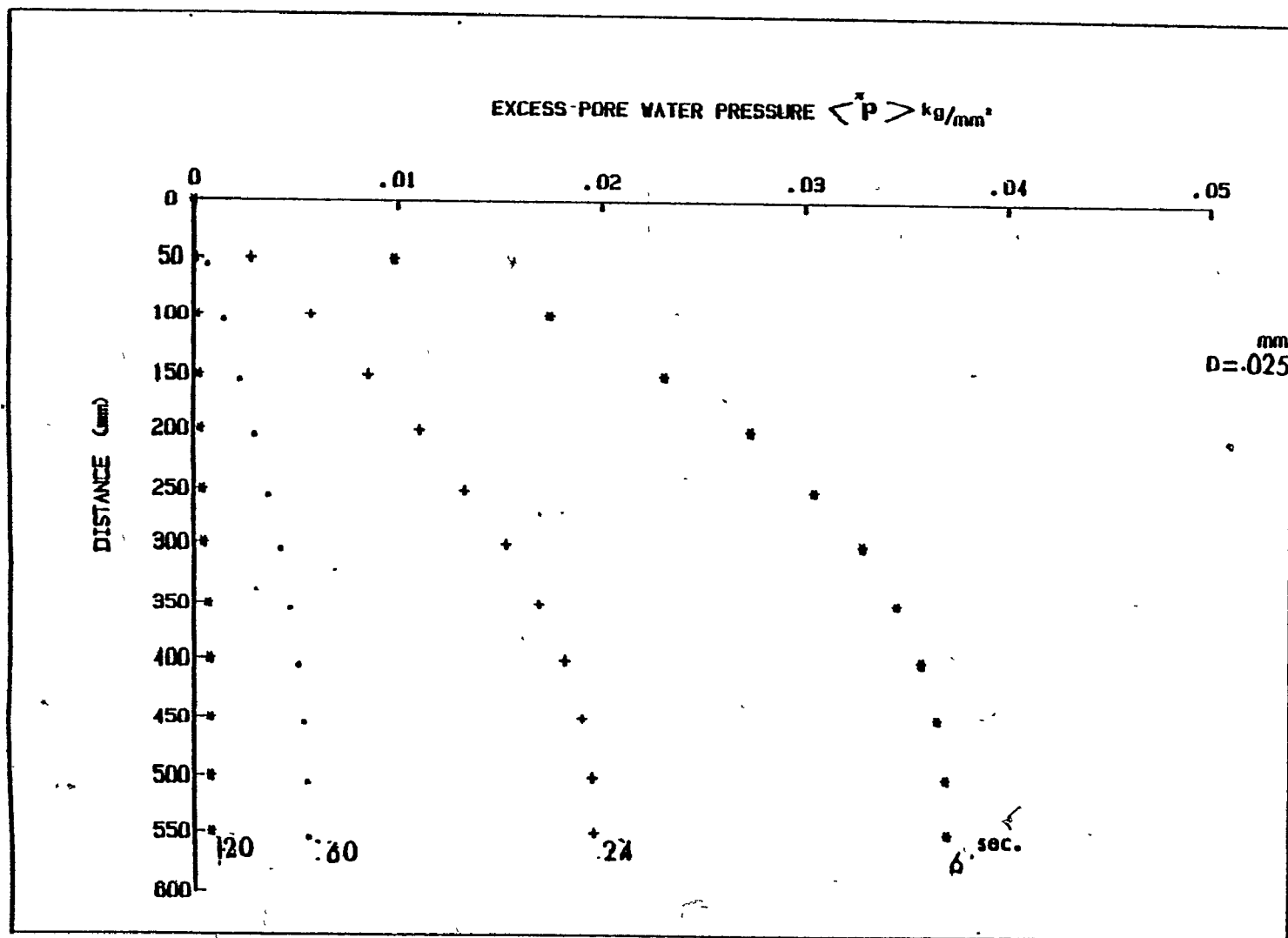


Fig. 38-b

The average excess pore water pressure  
(half length of the sample) MFD 100 run.

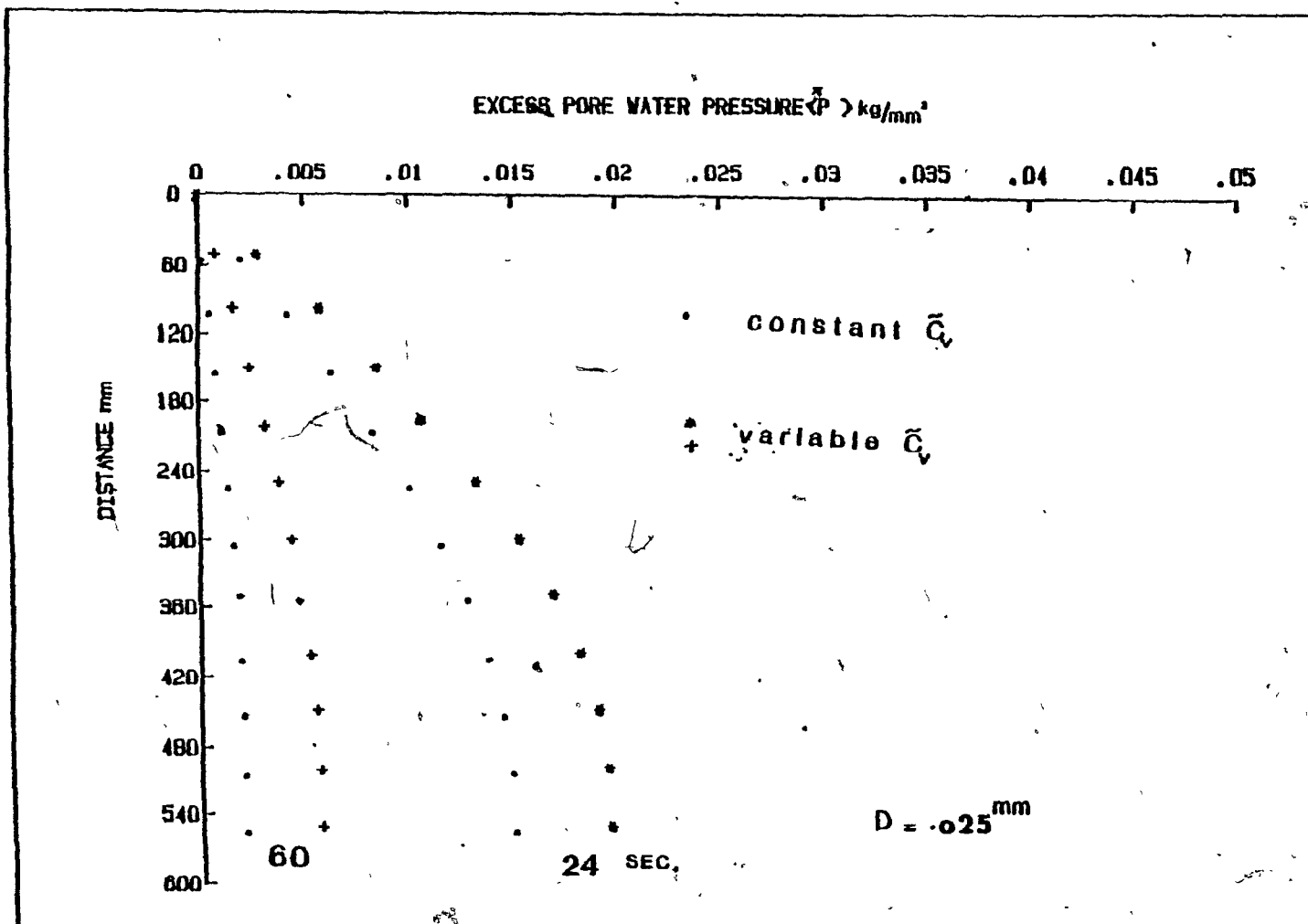


Fig. 38-c

The average excess pore water pressure for time-variable  $\bar{C}_v$  and constant  $\bar{C}_v$  (MFD, for constant  $\bar{C}_v$  the subroutine UPDATE is excluded, 100 run).



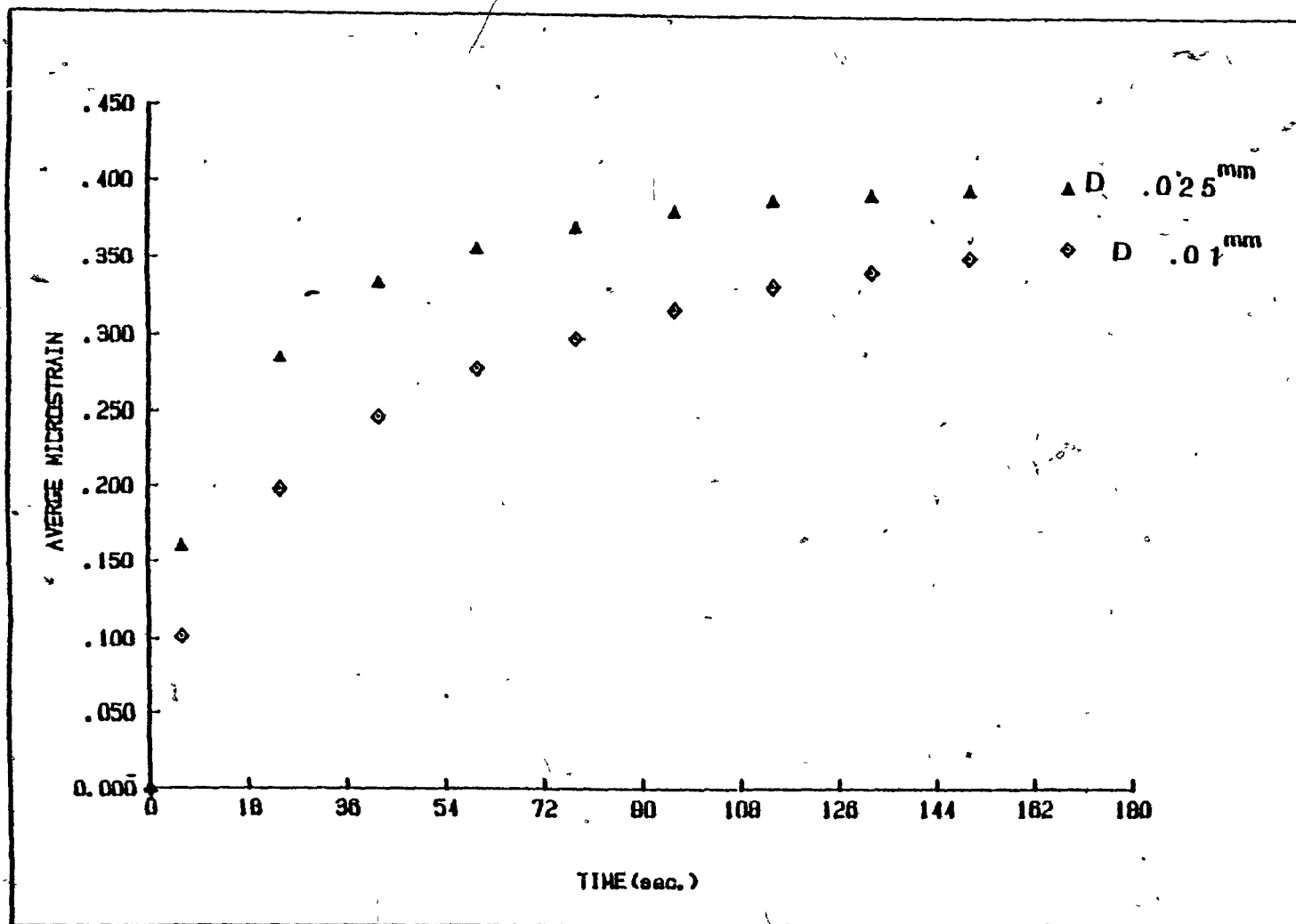


Fig. 38-d The average microstrain for different values of  $D$  (first region, MFD, 100 run)

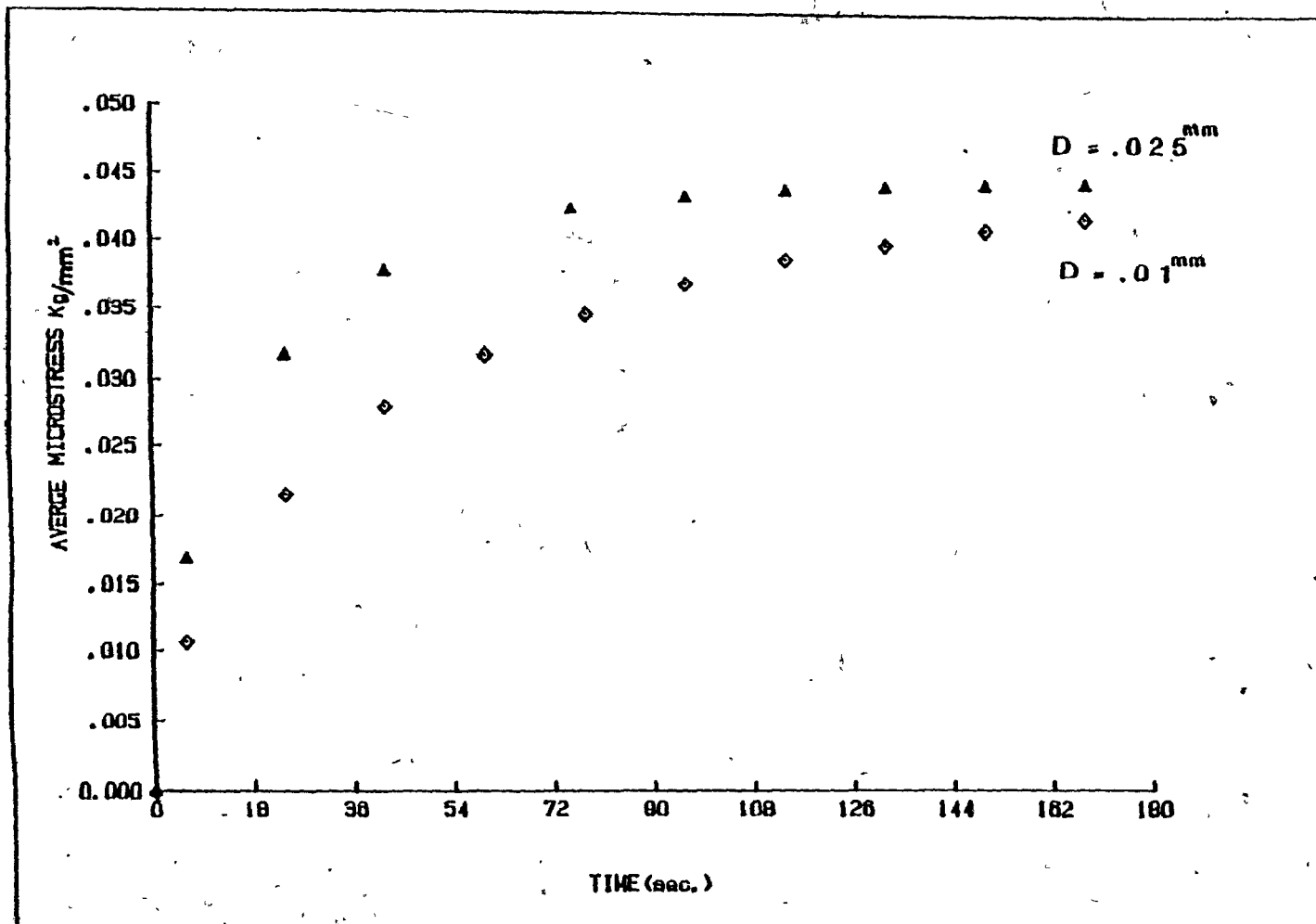


Fig. 38-e The average microstress for different values of D (MFD, 100 run)

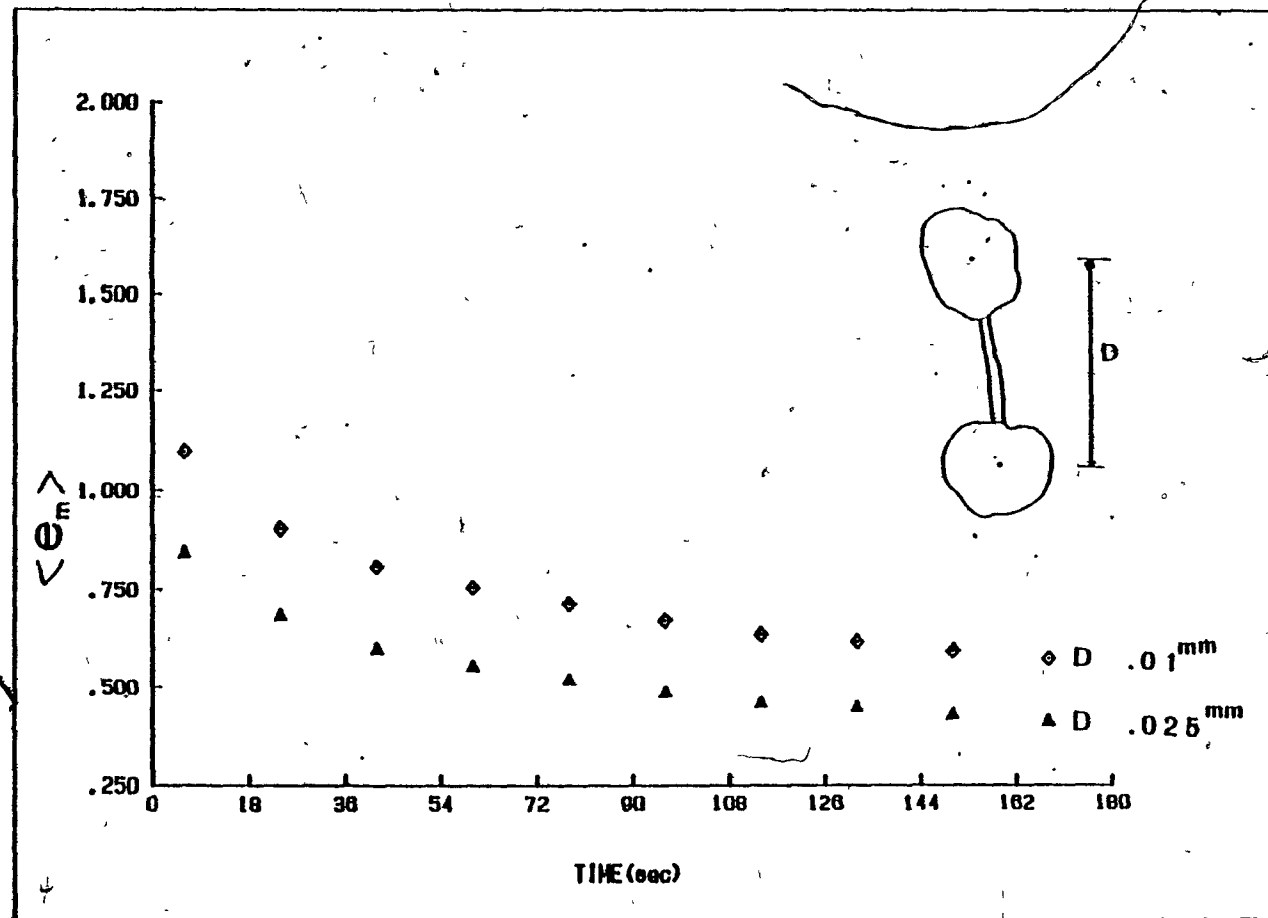


Fig. 39-a The average macrostructural void ratio for different values of  $D$ .

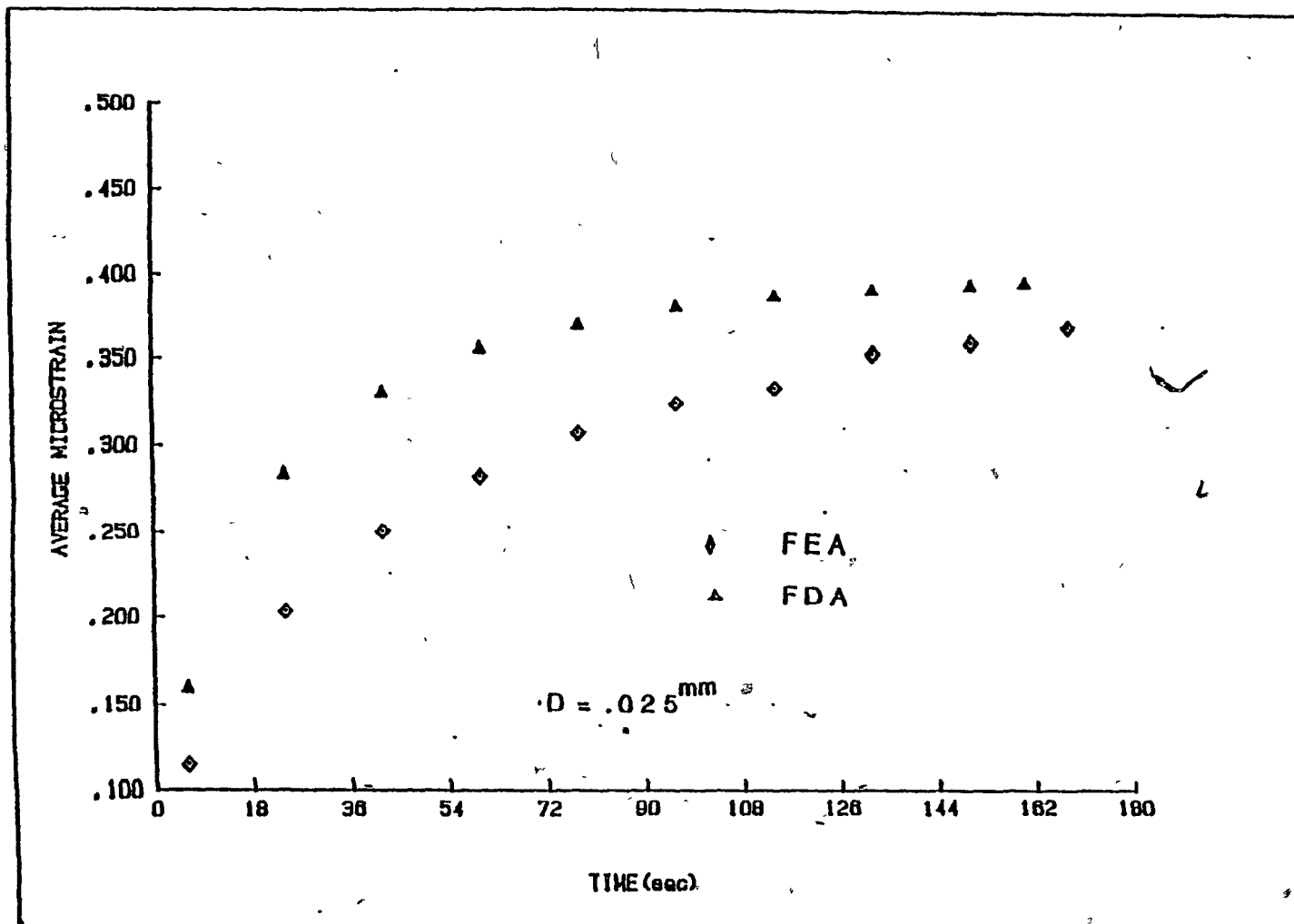


Fig. 39-b

The average microstrain (it is calculated by two different numerical techniques; finite difference and finite element. Note: the computer time for FE is relatively larger than FD time, 70 run).

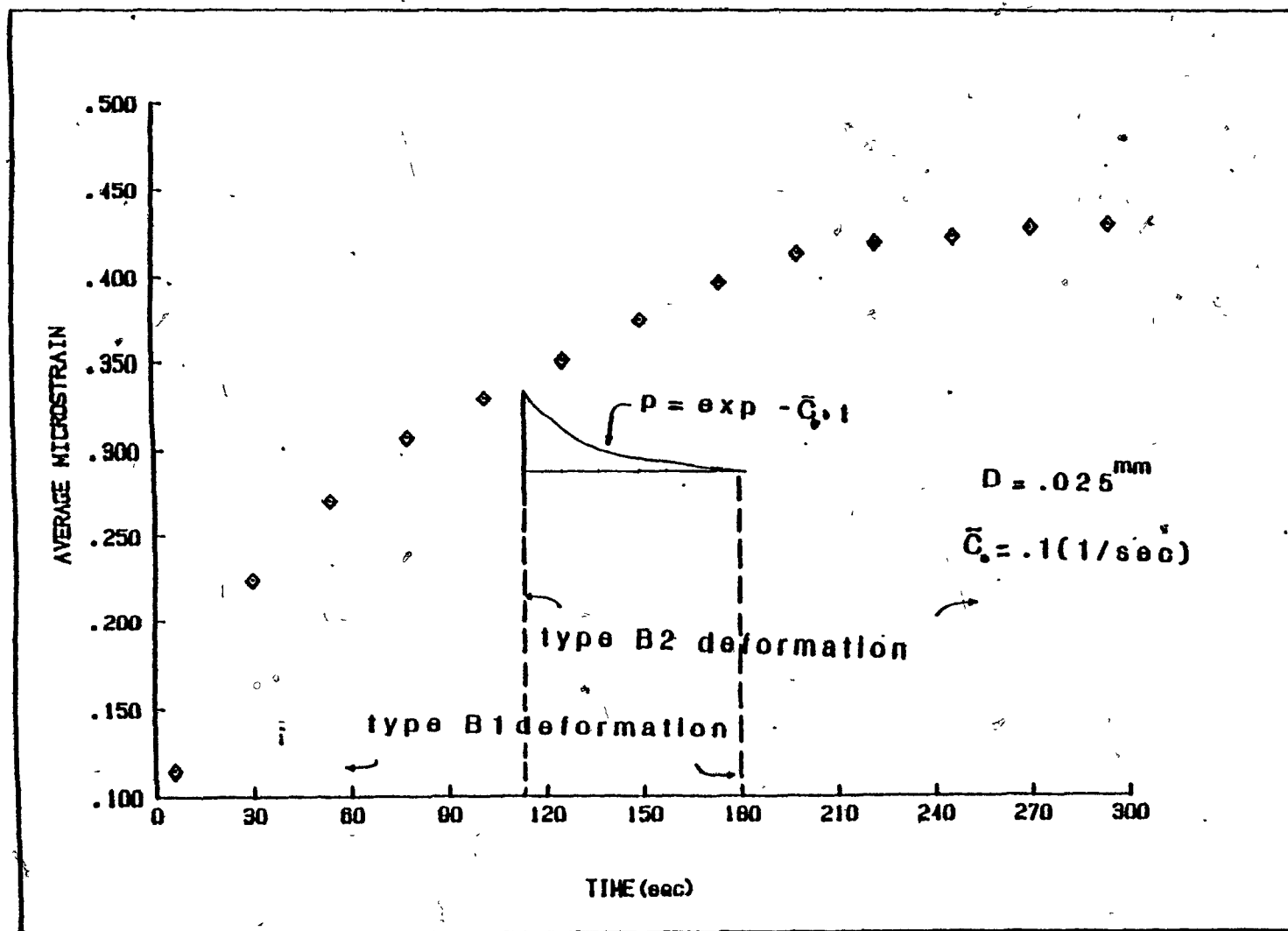


Fig. 39-c

The average microstrain for the total region of compression: first region, overlapped region and second region. Note: the computer time mainframe 25 minutes.

## CHAPTER 7

## CONCLUSION, CONTRIBUTION AND RECOMMENDATIONS

## 7-1 FORWARD:

There is, usually, a lag between a development in theoretical mechanics and its application in the engineering discipline. This is so especially in geotechnical engineering. This lag is usually due to the complexity of the model, the difficulty in doing experiments to characterize its parameters, the position of the theoretical mechanics research in open literature, and last but not least, it is due to the lack of mutual discussion and interaction between the researchers in different fields. An example of the lack of mutual discussion is that of the hypoelasticity model of Truesdell (Truesdell (1955)) which has only very recently been considered by geotechnical engineers, (albeit only in academia), for application in soil.

For an actual prediction of the soil performance under loads, the physics process of the soil (such as the mechanism of deformation, the mechanism of fluid flow, and the stress-deformation of the soil system) should be characterized and assessed. Once this characterization has been done, an analytical model can

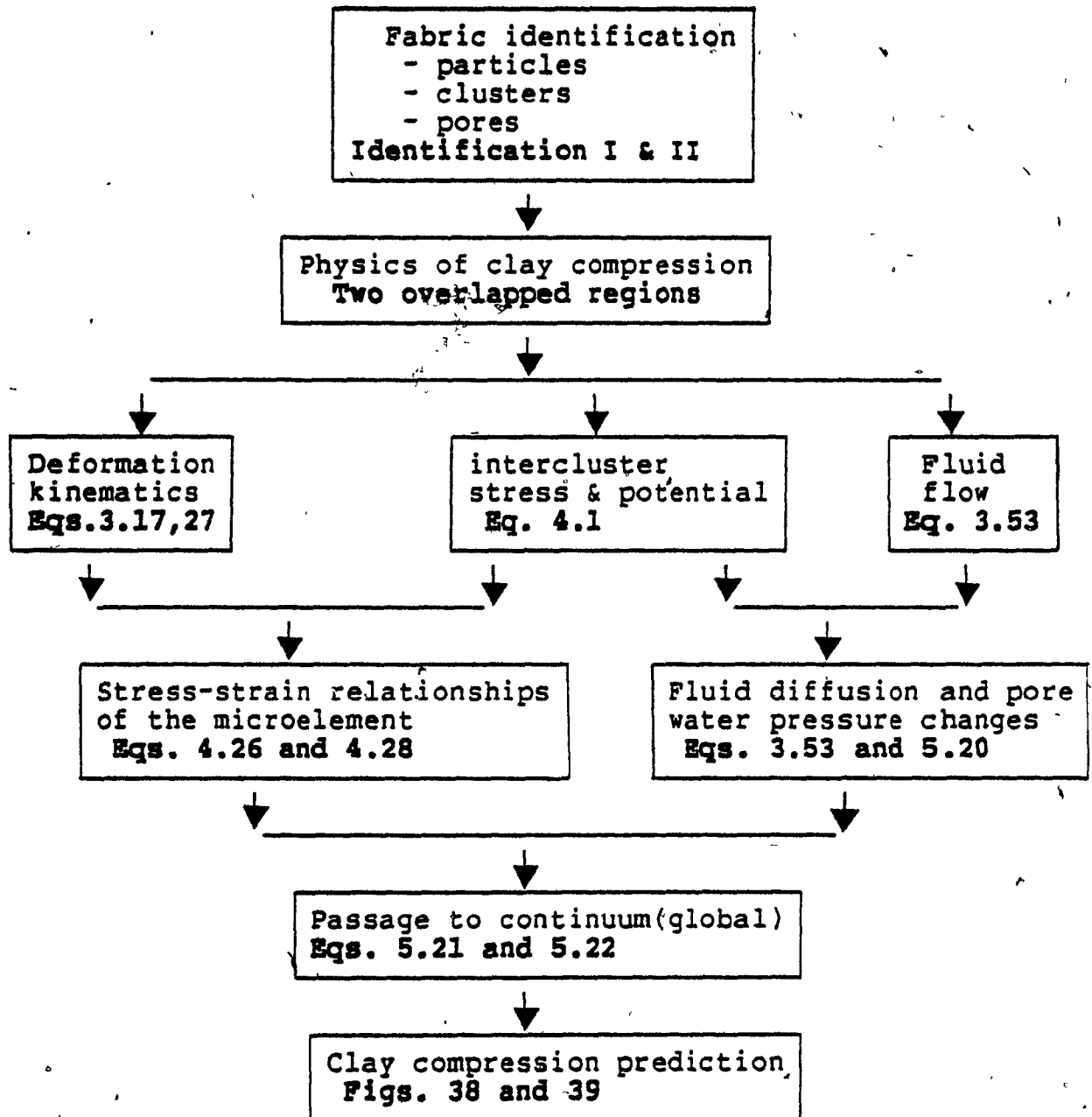
be established under premises clear to both Theoreticians who seek to ensure that the mathematics is rigorous, and also to the engineers who seek that the application of the model is feasible and practical. We have tried in this research work to follow the above proposition. This leads us naturally to the micromechanics approach.

## 7-2 SUMMARY:

By a comparison between the program strategy in the introduction (Flow Chart 1) and the development in the previous chapters, we can summarize this research work into the following points (Flow Chart 3):

### 1. Fabric analysis and the physics of clay compression:

We have reviewed fabric formation and we established the smallest scale for development of our analytical models (Table 1, chapter 2). We postulated that the mechanism of clay compression consists of two overlapped regions. In the first region, the clusters will move relative to each other and the fluid will move through macropores. In the second region, the clusters will not move but they will deform and the flow will be through the micropores. In the overlapped region, both mechanisms work together. This postulate has been substantiated by existing experimental



Flow Chart 3 The summary of the program strategy



programs and has been used for mathematical modelling in different chapters.

## **2. The Kinematics of deformation:**

2-a We described the types of deformation of the particulate system, in general (type A, B1, B2, and C). We reviewed the literature of the director theory and modified it to model the kinematics of deformation. Type B1 which represents the first region of compression is developed in chapter two. Type B2 which represents the second region of compression is developed also in chapter two.

2-b A probability distribution of the void ratio, water content and  $\rho$  were developed and a computer program was written, with input data, on the diameter of the cluster units and the macrostructural units.

2-c We discussed the physics of fluid movement from cavities and showed that there are two different types of fluid flow models: the conduit flow type and the flow around submerged object type. We have used the conduit type model with the concept of Hagen-Poiseuille and we established an analytical model for fluid flow from a given cavity to the adjacent ones.

## **3. Stress-Compressibility relationship:**

3-a We considered the stress balance between clusters as opposed to the common practice which considers the

stress balance between particles. The uniform pore water pressure is assumed throughout the soil profile system (at  $t=0$ ). This assumption permits us to know the initial excess pore water pressure in each cavity.

3-b We developed a volumetric constitutive equation for both regions of compression by using the concept of the intrinsic time measure.

#### 4- Passage to continuum:

4-a We reviewed the literature which attempts to construct the passage, and we established an axiomatic relation for the passage. The concept of intrinsic soil structural variability which consists of fabric variability and potential variability is introduced.

4-b The evolution equation was developed for the first region and its coefficients were found by using finite difference analysis. Also, for both regions, its coefficients were found by using finite element analysis and finite difference analysis.

4-c Stochastic model, binomial distribution, was developed to describe and predict the number of macrostructural units that will transfer to the mechanism of type B2 as the process takes place within the overlapped region.  $\bar{C}_0$  parameter plays a very essential role in the modelling of the overlapped region.

## 5- Computer programs:

We developed three computer programs:

a) GEM program for the probability distribution of void ratio, water content and  $\rho$ .

b) MFD program which describes the Monte Carlo finite difference program for solving the evolution equation of the first region.

c) MFE program which describes the Monte Carlo finite element program for solving the evolution equations of the total compression region.

### 7-3 CONCLUSION:

Besides the discussion which is considered in chapter six, the following conclusions are derived from this research work:

1. The micromechanics approach holds a promise in the future for solving various geotechnical engineering problems.
2. The mathematical point of the continuum theory can be substituted by the set theory in the case of the micromechanics approach.
3. One Kinematic parameter, surface deformation, in continuum theory may not be sufficient for a discrete system, and therefore, it is necessary to identify: i- the types of deformations (i.e. type B and C), ii- the development of the micro strain, and iii- the neighbor distance (D) and director parameters.
4. The identification of the geometrical structure of the soil medium is essential for a physical description and a mathematical model of fluid flow through this medium. Hence, the two classifications, (i- the conduit flow type, and ii- the flow around a submerged object type), are assets.
5. The macrostructural void ratio and the parameters of

the channels (R,D,a) connecting the cavities are important properties for fluid movement and are also important properties for the degree of the compressibility of the clay system.

6. The stress balance between the cluster units gives more realistic representation than the stress balance between clay particles since the modelling of stress between particles provides many details which may not be essential for global soil behaviour.

7. There are two structural viscosities which are partly responsible for time delay of the clay compression:

$\nu_1$  : For the first region

$\nu_{II}$  : For the second region

The  $\nu_1$  contribution to the time compression delay is less than  $\nu_{II}$ .

8. The axiomatic relations stated for the passage to global are essential to clarify the aspects of this passage.

9. The passage from the microelement to the global should be done without losing "soil structure" parameters which are essential in global clay compression performance.

10. The overlapped intensity parameter  $\bar{C}_0$  plays an

essential role in linking the process of consolidation in the first region with the creep effects in the second region.

11. The use of numerical techniques (finite difference FD and finite element FE) hold a promise in the future for solving problems in a micromechanics approach since they can be structured in a physical way (i.e., the nodes and the elements of FD and FE can be equivalent to a single microelement or several microelements).

#### 7-4 CONTRIBUTION:

The following points are believed to be original:

1. This is the first time a comprehensive work in micromechanics, in the field of geotechnical engineering, has been done to solve a particular problem. Furthermore, the problem which is addressed here is considered to be one of the important problems in the field of geotechnical engineering.

2- The description of the physics of clay performance under compression loads as a coherent picture of the entire process of compression ( i.e., skeleton compression, fluid flow process, and stress transfer) is original.

3. The development of the microstrains for type B1 and type B2, neighbor distance  $D$ , and the compression zone are original contributions not only in soil mechanics but also in theoretical mechanics.

4.. In this research, the macrostructural void ratio, water content and  $\mu$  are developed.

5. The fluid flow equation which considers the local parameters of the clay system is developed.

6. The stress balance of the macrostructural unit and simple constitutive equation are developed in chapter four.

7. The development of the microconsolidation coefficient( $\tilde{C}$ ) which is variable in time and random in space is an original contribution in the geotechnical engineering field.

8. The introduction of axiomatic relations of the passage is an original contribution in theoretical mechanics.

9. The stochastic passage from microelement to continuum is essential and original.

10. The introduction of the state function and the solution of the evolution equations by using finite element and finite difference are original.

11.  $\bar{C}_0$  parameter will play an essential role in modern soil mechanics since it provides a link between the consolidation and creep performance of the clay system under compression loads.

12. Introducing the concept of the intrinsic soil structure variability in chapter five is original and it will offer a new perspective to the school of probabilistic geotechnical engineering.



## 7-5 RECOMMENDATIONS FOR FUTURE RESEARCH:

### a. Fabric analysis and the physics of clay compression:

a-1 An extensive experimental program should be considered to: i) substantiate the postulated mechanisms for a given "site" condition, ii) identify different geometrical and stress parameters for the models given in this research work, iii) perform parameters-sensitivity studies for all models.

### b. Kinematics of Deformation:

b-1 Experimental: i) Simulate the kinematics of deformation of clusters movement by discrete particles (balls) and perform a compression test. ii) Simulate the condition of the clay system by mixing 50% silt with 50% clay, and perform creep test positioned in scanning microscopy equipment. Since the clay particles will cluster in groups, each cluster will have the same size of the silt, and therefore, tracing the movement of the silt and clay could be done.

b-2 Theoretical; develop a microstrain equation for type C deformation.

b-3 The flow equation for Case 2 and Case 3, (in Chapter three), can be developed for different chemical solutions. There can be a test program which accompanies the development.

b-4 The submerged object flow type can be developed for a sedimentation case.

**c. Stress compressibility relationship:**

c-1 The zeta potential analysis and other chemical tests can be used to develop the interaction potential between the cluster units and how this potential is significant for overall stress balance analysis.

c-2 The Extension of the developed constitutive model into three dimensional analysis can be done by identifying the parameters of the matrix in Eq.4.8.

**d. Passage to the continuum:**

d-1 Once the three dimensional constitutive equation is developed, the passage can be done by using the three dimensional evolution equation. Hence, the extension of the MFE program into three dimensional analysis can be established.

d-2 An explicit formulation of  $\bar{C}_0$  can be developed.

## REFERENCES

Abraham, R. and Marsden, J. E. (1978), "Foundations of Mechanics," Benjamin, London.

Abramowitz, M. and Stegun, I. A. (ed.) (1965), "Hand Book of Mathematical Functions," Dover Publications, New York.

Adams, J. (1965), "The Engineering Behaviour of a Canadian Muskeg," Proceedings, sixth International Conference on Soil Mechanics and Foundation Engineering, vol. 1, Montreal, Canada, 1965, pp3-7.

Aero, E. L. and Kuvshinskii, E. V. (1960), "Fundamental Equations of the Theory of Elastic Media with Rotationally Interacting Particles," Sov. Solid State 2, pp1272-1281.

Alblas, J. B. (1976), "A Note on the Physical Foundation Of the Theory of Multipole Stresses," Arch. Mech. Stos. 28, pp279-298.

Allen, S. J., Desilva, C. N. and Kline, K. A. (1967), "Theory of Simple Deformable Directed Fluids," Physics Fluids, 10, p2551

Alonso, E. E. and Krizek, R. J. (1975), "Consolidation of Randomly Heterogeneous Clay Strata," Transportation Research Record, No. 548, Washington, D. C., pp30-46.

Ang, H-S. and Tang, W. H. (1975), "Probability Concepts in Engineering Planning and Design," Volume I John Wiley & Sons, Inc.

Ang, H-S. and Tang, W. H. (1984), "Probability Concepts in Engineering Planning and Design," Volume II John Wiley & Sons, Inc.

Ansal, A. M. (1977), "A Endochronic Constitutive Law for Normally Consolidated Cohesive Soils." Ph.D. Civ. Eng. Dept. Northwestern University, Evanston, Illinois, p166.

Ansal, A. M., Bazant, Z. P. and Krizek, R. J. (1979), "Viscoplasticity of Normally Consolidated Clays," Proc. ASCE, J. Geotech. Eng. Div., 105 (GT4), pp519-537.

Athanasίου-Grivas, D. and Harr, M. E. (1978), "Consolidation-Probabilistic Approach," Journal of the Engineering Mechanics Division, ASCE, vol. 104, EM5, pp681-690.

Axelrad, D. R. and Yong, R. (1966), "On an Isothermal Flow Function for a Heterogeneous Medium," Modern Developments in the mechanics of continua, Academic Press, N. Y.

Axelrad, D. R. and Yong, R. N. (1970), "Micro-Rheology of the Yielding of a Heterogeneous Medium," Proc: 5th Int. Congress, Rheol. Kyoto University, Japan pp309-314.

Axelrad, D. R. (1978), "Micromechanics of Solids," PWN-Elsevier, Amsterdam.

Axelrad, D. R. (1984), "Foundations of the Probabilistic Mechanics of Discrete Media," Pergamon Press, Oxford.

Azzouz, A. S., Krizek, R. J. and Corotis, R. B. (1976), "Regression Analysis of Soil Compressibility," Soil and Foundations, Japanese Society of Soil Mechanics and Foundation Engineering, vol. 16, No. 22, p129.

Baker, R. (1971), "Mechanics of Soil With Structure A Continuum Approach Based on a Physico-Chemical Model" Ph. D. thesis submitted to Soil Science Department, McGill University, Canada.

Baker, R. (1986) Personal Communication.

Barden, L., and Berry, P. L. (1965), "Consolidation of Normally Consolidated Clay," Journal of the Soil Mechanics and Foundation Division, ASCE, vol. 91, No. SM5, pp15-53.

Barden, L. and Sides, G. (1971), "Sample Disturbance in the Investigation of Clay Structure," Geotechnique, vol. 21, No. 3, pp211-222.

Barber, E. S. (1961), "Notes on Secondary Consolidation" Proceedings, Highway Research Board; vol. 40 pp663-675.

Barden, L. (1965), "Consolidation of Clay with Non-Linear Viscosity," Geotechnique, London, England, vol. 15, No. 4 pp345-362.

Barden, L. (1968), "Primary and Secondary Consolidation of Clay and Peat," Geotechnique London, England, vol. 18, No. 1 pp1-24.

Barden, L. (1969), "Time Dependent Deformation of Normally Consolidation Clay," Journal of the Soil Mechanics and Foundation Division, ASCE, Vol. 95, No. SM1, pp1-31.

Barden, L. (1972), "The Influence of Structure on Deformation and Failure in Clay Soil," Geotechnique, Vol. 22, No. 1, pp159-163.

Batdorf, S. and Budiansky, B. (1949), "A Mathematical

Theory of Plasticity Based on the Concept of Slip," NACA TN 1871.

Bazant, Z. P. and Krizek, R. J. (1975), "Endochronic Constitutive Law for Liquefaction of Sand," Proc. ASCE, J. of Eng. Mech. Div., 102, pp225-238.

Bazant, Z. P., Ozaydin, K. and Krizek, R. J. (1975), "Micromechanics Model for Creep of Anisotropic Clay," J. of The Eng. Mech. Division, ASCE, Vol. 101, No. EM1, pp57-78.

Bazant, Z. P. and Kim, S. (1979), "Plastic-Fracturing Theory for Concrete," Journal of The Eng. Mech. Division, ASCE, Vol. 105, No. 3, pp407-428.

Bazant, Z. P., Ansal, A. M. and Krizek, R. J. (1982), "Endochronic Models for Soils," Soil Mechanics-Transient and Cyclic Loads, Edited by Pande G. N. and O. C. Zienkiewicz, John Wiley & sons Ltd.

Bazant, Z. P. and Chang, T. P. (1984), "Instability of Nonlocal Continuum and Strain Averaging," J. of The Eng. Mech. Division, ASCE, Vol. 110, No EM10, pp1441-1450.

Bazant, Z. P. and Oh, B. H. (1985), "Microplane Model for Progressive Fracture of Concrete and Rock," J. of The Eng. Mech. Division, ASCE, Vol. 111, No EM4, pp569-582.

Bazant, Z. P. and Kim, J-K. (1986), "Creep of Anisotropic Clay: Microplane Model," Journal of Geotechnical Eng. Vol. 112, No.4 pp458-467.

Benjamin, J. R. and Cornell, A. C. (1970), "Probability, Statistics, and Decision for Civil Engineers," McGraw-Hill Book Company.

Beran, M. J. (1968), "Statistical Continuum Theories," Interscience Publ., New York.

Beran, M. J. and McCoy, J. J. (1970), "Mean Field Variations in a Statistical Sample of Heterogeneous Linearly Elastic Solids," Int. J. Solid Structure, Vol. 6 pp1035-1054.

Berre, T. and Iversen, K. (1972), "Oedometer Tests with Different Heights on a Clay Exhibiting Large Secondary Compression," Geotechnique, London, England, vol. 22, No. 1 pp53-70.

Berry, P. L. and Poskitt, T. J. (1972), "The Consolidation of Peat," Geotechnique, London, England, vol. 22, No. 1 pp27-52.

Bishop, J. (1951 a,b), "A Theoretical Derivation of the Plastic Properties of a Polycrystalline Face-Centered Metal," Philos. Mag. 42, 414-427.

Bjierrum, L.(1967),"Engineering Geology of Normally Consolidated Marine Clays as Related to Settlement of Buildings," Geotechnique,London, England,vol. 17, No.2 pp83-118.

Bolt, G. H. (1956),"Physico-Chemical Analysis of the Compressibility of pure Clay," Geotechnique. 6 No.2, 86.

Borja, R. and Kavazanjian, E. (1985),"A Constitutive Model for the Stress-Strain-Time Behaviour of Wet Clay," Geotechnique 35, No. 3, 283-298.

Box, G. and Muller, M. E.(1958),"A Note on the Generation of Random Normal Deviates," The Annals of Math. Statistics, 29, p610.

Brown, C. B. (1978),"The Use of Maximum Entropy in the Characterization of Granular Media," Proceedings of the U.S.-Japan Seminar on Continuum- Mechanical and Statistical Approaches in the Mechanics of Granular Materials, Tokyo, Japan, pp98-108.

Buckingham, E. (1914),"On Physically Similar System," Phys. Rev. Vol. 4, pp354-376.

Capriz, G. and Guidugli, P. P.(1977),"Formal Structure and Classification of Theories of Oriented Materials" Ann. Mat. Pur Appl. (IV) 115,pp17-39.

Carroll, M. M. (1980),"Mechanical Response of Fluid-Saturated Porous Materials," Proc. of XVth Int. Congress of Theoretical and Applied Mechanics, Univ. of Tronto,(Ed. Rimrott and Tabarrok).

Carter, J. P., Small, J. C. and Booker, J. R. (1977),"A Theory of Finite ELastic Consolidation," In. J. Solids Structures, vol. 13, pp467-478.

Casagrande, A. (1932),"The Structure of Clay and its Importance in Foundation Engineering," Contributions to Soil Mechanics, Boston Society of Civil Engineering,1925-1940, pp72-112.

Casagrande, A. (1963),"The Detrmination of the Preconsolidation Load and its Practical Significance," Proceedings, First International Conference on Soil Mechanics and Foundation Engineering,Cambridge, Mass., vol.3, pp60-64.

Casagrande,A. (1939),"Notes on Soil Mechanics-First Semester," Pierce Hall, Harvard University, Cambridge, Mass., reprinted in 1967, p.118.

Chandrasekhar, S. (1943),"Stochastic Problems in Physics and Astronomy," Rev. Mod. Phy.,vol. 15, pp.1-89.

Chang, C. S. (1985), "Uncertainty of One Dimensional Consolidation," Journal of Geotechnical Engineering, vol. 111 No. 12, ASCE.

Chattopadhyay, P. K. (1972), "Residual Shear Strength of Some Pure Clay Minerals," Ph.D. Thesis, The University of Alberta, Edmonton, Canada.

Childs, E. C. and Collins-George N. (1950), "The Permeability of Porous Materials," Proc. of the Royal Society, London, England, Series A, Vol. 201, pp392-405.

Christensen, R. W. and Wu, T. H. (1964), "Analysis of Clay Deformation as a Rate Process," Journal of Soil Mechanics and Foundation Division, ASCE, vol. 90, No. SM6, pp125-157.

Christian, J. T. (1976), "Consolidation with Internal Pressure Generation," Journal of the Geotechnical Engineering Division, ASCE, vol. 102, no. GT10, pp1111-1115.

Christoffersen, J. , Mehrabadi, M. M. and Nemat-Nasser, S. (1981), "A Micromechanical Description of Granular Material Behaviour," J. Appl. Mech., Vol. 48, No. 2.

Coleman, B. D. and Gurtin, M. E. (1967), "Thermodynamics with Internal State Variables," J. Chem. Phys. Vol. 47.

Collins, K. and McGown, A. (1974), "The Form and Function of Microfabric Features in a Variety of Natural Soils," Geotechnique, 24, No. 2, pp223-254.

Cosserat, E. and Cosserat, F. (1909), "Theorie des corps Deformable," Hermann, Paris.

Cowin, S. C. (1978), "Microstructural Continuum Models for Granular Materials," Proc. U.S.-Japan Seminar on Continuum Mechanical and Statistical Approaches in the Mechanics of Granular Materials, Tokyo, Japan, pp162-170.

Cox, D. R. and Smith, W. L. (1961), "Queues," Wiley, New York.

Crawford, C. B. (1964), "Interpretation of the Consolidation Test," J. of The Soil Mechanics and Foundation Division, ASCE, Vol. 90, No. SM5 pp87-102.

Crawford, C. B. (1965), "The Resistance of Soil Structure to Consolidation," Can. Geotech. J. No. 2, pp90-97.

Davis, R. and Deresiewicz, H. (1977), "A Discrete Probabilistic Model for Mechanical Response of a Granular Medium," Acta Mechanica 27, pp69-89.

Debbas, S. and Rumpf, H. (1966), "On the Randomness of Beds Packed with Spheres or Irregular Shaped Particles," Chemical Engineering Science, vol. 21, pp583-607.

De Groot, S. R. (1951), "Thermodynamics of Irreversible Processes," Interscience Publisher, New York.

De Jong, J. (1968), "Consolidation Models Consisting of an Assembly of Viscous Elements or a Cavity Channel Network," Geotechnique, London, Vol.18.

De Jong, J. and Verruijt, A. (1965), "Primary and Secondary Consolidation of a Spherical Clay Sample," Proceedings, 6th International Conference on Soil Mechanics and Foundation Engineering Vol.1.

De Jong, J. (1971), "The Double Sliding, Free Rotating Model for Granular Assemblies," Geotechnique, Vol.21, pp155-163.

Delage, P. and Lefebvre, G. (1984), "Study of the Structure of a Sensitive Champlain Clay and of its Evolution During Consolidation," Can. Geotech. J. 21, pp21-35.

Desai, C. S. and Johnson, L. D. (1973), "Evaluation of Some Numerical Schemes for Consolidation," International Journal for Numerical Methods in Engineering, vol.7, pp243-254.

Diamond, S. (1971), "Microstructure and Pore Structure of Impact-compacted Clays," Clays and Clay Minerals, Vol.19, pp239-249.

Doob, J. L. (1961), "Stochastic Processes," Wiley, New York.

Ericksen, J. L. and Truesdell, C. (1958), "Exact Theory of Stress and Strain in Rods and Shells" Archive for Rational Mechanics and Analysis, vol.1 pp295-323.

Ericksen, J. L. (1961), "Conservation Laws for Liquid Crystals," Trans. Soc. Rheol., 23.

Eringen, A. C. (1962), "Nonlinear Theory of Continuous Media" McGraw-Hill, New York.

Eringen, A. C. (1964), "Simple Microfluids" Int. J. Eng. Sci. 2, 205.

Eringen, A. C. (1966), "Mechanics of Micromorphic Materials," Proc. Int. Congr. Appl. Mech., 11th. Springer-Verlag Berlin.

Eringen, A. C. (1972), "Theory of Micromorphic Material with Memory," Int. J. Eng. Sci. 10, 623.



Eringen, A. C., and Lee, J. D. (1971), "Wave Propagation in Nematic Liquid Crystals," J. Chem. Phys. 54, 5027.

Esteva, L. (1981), "Uncertainty, Reliability and Decisions in Structural Engineering," 3rd International Conference on Structural Safety and Reliability, Trondheim, Norway.

Eyring (1941), "The Theory of Rate Process," McGraw Hill, New York.

Field, W. G. (1963), "Towards the Statistical Definition of a Granular Mass," Proc. 4th A. and N. Z. Conf. on Soil Mech., pp143-148.

Flegmann, A. W., Goodwin, J. W. and Ottewill, R. (1969), "Rheological Studies on Kaolinite Suspensions," Proc. British Ceramic Society, Vol. 13, pp31-45.

Freeze, R. A. (1977), "Probabilistic One-Dimensional Consolidation," Journal of the Geotechnical Engineering Division, ASCE, vol. 103, No. GT7 pp725-742.

Garcia-Bengochea, I., Lovell, C. W. and Altschaeffl (1979), "Pore Distribution and Permeability of Silty Clays," Geotechnical Engineering Division, Vol. 105, No. GT7 p837.

Garlanger, J. E. (1972), "The Consolidation of Soils Exhibiting Creep Under Constant Effective Stress," Geotechnique, Vol. 22, No. 1, pp71-78.

Gelfand, I. and Shilov, G. E. (1964), "Generalized Functions," Vols 1 and 2, Academic Press, New York.

Gibson, R. E. and Lo, K. Y. (1961), "A Theory of Consolidation of Soils Exhibiting Secondary Compression," Acta Polytechnica Scandinavica, 296.

Gibson, R. E., England, G. L. and Hussey, M. L. (1967), "The Theory of One-Dimensional Consolidation of Saturated Clays," Geotechnique, London, Vol. 17.

Glannsdorff, P. and Prigogine (1970), "Non-Equilibrium Stability Theory," Physica 46, pp334-366.

Gnedenko, B. V. (1967), "The Theory of Probability," Chelsea Publishing Company, New York, N.Y.

Goldschmidt, V. M. (1926), "Undersokelser Ved Lersedimenter," Nordisk Fordbrugs forskning, Kongress 3, Kobenhavn, pp434-445.

Graham, R. (1973), "Statistical Theory of Instabilities in Stationary Non-Equilibrium Systems with Applications to Lasers and Nonlinear Optics," Springer Tracts in Modern Physics, 66 Springer Berlin, Heidelberg.

Graybill, F. A. (1961), "An Introduction to Linear Statistical Models," Vol. I, McGraw Hill Book Company, New York.

Gray, W. A. (1968), "The Packing of Solid Particles" Chapman and Hall Ltd.

Green, A. E. and Rivlin, R. S. (1964), "Multipolar Continuum Mechanics," Arch. Rat. Mech. Anal. 17, 113.

Hachich, W. (1981), "Seepage Related Reliability of Embankment Dams," Ph.D. Thesis, MIT, MA, USA.

Halmos, P. P. and Newmann, J. O. (1942), "Operator Methods in Classical Mechanics II," Ann. Math. 43 pp.322-350.

Hamaker, H. O. (1937), "The London-Van der Waals Attraction Between Spherical Particles," Physica 4, pp1058-1072.

Hansbo, S. (1960), "Consolidation of Clays with Special Reference to the Influence of Vertical Sand Drains." Swedish Geotechnical Institute, Proc. No. 18 Stockholm.

Harr, M. E. (1977), "Mechanics of Particulate Media-A probabilistic Approach," McGraw Hill International Book Co., Inc., New York, NY.

Hilliard, J. E. (1972), "Stereology; An Experimental Viewpoint," Advances in Appl. Probability, Spec. Suppl. pp92-111.

Hill, R. (1965a), "Continuum Micromechanics of Elastico-Plastic Polycrystals," J. Mech. Phys. Solids, 13, p89.

Hill, R. (1965b), "A Self-Consistent Mechanics of Composite Materials," J. Mech. Phys. Solids, 13, p213.

Hoppe, E. (1986), "The Influence of Acid Rain on the Engineering Properties of a Sensitive clay," M. Eng. Thesis, Civil Engineering and applied Mechanics Dept., McGill University.

Hull, T. E. and Dobell, A. R. (1962), "Random Number Generators," SIAM Reviw, 4 pp230-254.

Juang, C. , and Holtz, R. (1986), "A Probabilistic Permeability Model and the Pore Size Density Function," Inter. Journal Of Num. and Analy. Methods in Geomechanics Vol. 10 pp543-570.

Juarez-Badillo, E. (1981), "General Compressibility Equation for Soils," Tenth Int. Conference on Soil Mechanics and Foundation Engineerings, Stockolm, Sweden, Vol. 1, pp.171-178.

Juarez-Badillo, E. and Chen, B. (1983), "Consolidation Curves for Clays," ASCE, Journal of Geotechnical Engineering Division, 109(10), pp1303-1312.

Kachanov, L. M. (1971), "Foundation of the Theory of Plasticity," North-Holland, Amsterdam.

Kafadar, C. B. and Eringen, A. C. (1971), "Micropolar Media, I and II," Int. J. Eng. Sci. 9, pp272-307.

Kaloni, P. N. and Desilva (1970), "A Theory of Oriented Fluids," Physics Fluids, 13, 1708.

Kampe de Feriet (1962), "Statistical Mechanics of Discrete Media," Proc. Symp. Appl. Math., Amer. Math. Soc., Providence, R. L. pp165-198.

Kanatani, K. (1979), "A Micropolar Continuum Theory for the Flow of Granular Materials," Int. J. Eng. Sci., Vol. 17, pp419-432.

Kendell, M. G. and Moran, P. A. (1963), "Geometrical Probability," Griffin, London.

Kenney, T. C., Moum, J. and Berre, T. (1967), "An Experimental Study of Bonds in A Natural Clay," Proc. Geotech. Conf., Oslo, on Shear Strength of Natural Soils and Rocks, Vol. I, pp65-69.

Kitamura, R. (1978), "Deformation of Granular Soil as a Markov Process," Proc. of the U.S.-Japan Seminar on Continuum-Mechanical and Statistical Approaches in the Mechanics of Granular Materials, pp155-161, Tokyo, Japan.

Kitamura, R. (1981), "A Mechanical Model of Particulate Material Based on Stochastic Process," Soil and Foundations, Vol. 21, No.2 p63.

Kitamura, R. (1985), "A Markov Model for Deformation of Particulate Material," Fifth International Conference on Numerical Methods in Geomechanics, Nagoya. Japan, pp547-554.

Kline, K. A. and Allen, S. J. (1971), "A Thermodynamical Theory of Fluid Suspensions," Physics Fluids 14, 1863.

Kroner, E. (1976), "Ordered Versus Disordered Materials: Consequences for the Continuum Model," Archives of Mechanics 28,3, pp.455-465.

Kroner, E. (1980), "Graded and Perfect Disorder in Random Media Elasticity," The Eng. Mech. Division, Vol. 106, No. EM5.

Kubo, R. (1965), "Statistical Mechanics," North-Holland, Amsterdam.

Lafeber, D. (1966), "Soil Structure Concepts," Engineering Geology, 1(4) pp261-290.

Lamb, H. (1932), "Hydrodynamics," 6th Edition, Cambridge University Press.

Lambe, T. W. (1953), "The Structure of Inorganic Soil," ASCE, NO. 315 October.

Lambe, T. W. (1954), "The Permeability of Fine Grained Soils," ASTM special Publication 163, pp56-67.

Lambe, T. W. (1958), "The Structure of Compacted Clay," Journal of the Soil Mechanics and Foundations Division, ASCE, vol. 84, No. SM2 pp34.

Lambe, T. W. (1960), "A Mechanistic Picture of Shear Strength in Clay," Pro. of the ASCE Research Conference on the Shear Strength of Cohesive Soil," p437.

Landau, L. D. and Lifshitz, E. M. (1958), "Statistical Physics," Addison-Wesley Publishing Company, Reading, Mass., USA.

Lax, M. (1960), "Fluctuations from the Nonequilibrium Steady State," Rev. of Modern Physics Vol. 32 No. 33.

Lehmer, D. H. (1941), "Mathematical Methods in Large Scale Computing Units," Annals of Computation, Laboratory Harvard University, 26, pp144-146.

Leonards, G. A. and Girault, P. (1961), "A Study of the One-Dimensional Consolidation Test," Proceedings, Fifth International Conference on Soil Mechanics and Foundation Engineering, vol. 1 p213.

Leonards, G. A. (1962), "Engineering Properties of Soils; Foundation Engineering," McGraw-Hill Book Co. Inc., New York, pp107-139.

Leonards, G. A. and Altschaeffli, A. G. (1964), "Compressibility of Clay," J. of the Soil Mechanics and Foundation Division, ASCE, vol. 90, No. SM5, pp133-155.

Leroueil, S., Kabbaj, F., Tavenas, F. and Bouchard, R. (1985), "Stress-Strain Rate Relation for the Compressibility of Sensitive Natural Clays," Geotechnique 35, No. 2, pp159-180.

Lo, K.Y. (1961), "Secondary Compression of Clay," Proc. ASCE 87 SM4 pp61.

Low, P. F. (1961), "Physical Chemistry of Clay-Water Interaction," Advances in Agronomy, Vol. 13, pp269-327, Academic, New York.

Lumb, P. (1966), "The Variability of Natural Soils," Canadian Geotechnical Journal, vol. 3 No. 2, pp74-97.

Lumb, P. (1970), "Safety Factor and the Probability Distribution of Soil Strength," Canadian Geotechnical Journal, vol.7 No.3 pp225-242.

Lumb, P. (1975), "Spatial Variability of Soil Properties," Proc., Int. Conf. on applications of Statistics and Probability in Soil and Structural Engineering, Aachen, Germany, pp397-422.

Malvern, L. (1969), "Introduction to the Mechanics of Continuous Medium," Prentice-Hall, Inc. Englewood, Cliffs., N.J.

Marsal, R. T. (1965), "Stochastic Processes in the Grain Skeleton of Soil," Proc. 6th Int. Conf. on Soil Mechanics and Foundation Engineering, Canada, vol. 3, pp303-307.

Marshall, J. (1958), "A Relation Between Permeability and Size Distribution of Pores," Journal of Soil Science 9(1), pp1-8.

Matsui, T., Ito, T., Mitchell, K. and Abe, N. (1980), "Microscopic Study of Shear Mechanisms in Soils," Journal of the Geotechnical Engineering Division, Vol. 106, No. GT2.

Mazilu, P. (1976), "On the Theory of Linear Elasticity in Statistically Homogeneous Media," Archives of Mechanics 28, 3, pp517-529.

McConnachie, I. (1974), "Fabric Changes in Consolidated Kaolin," Geotechnique 24, No.2 pp207-222.

Mehrabadi, M. M., Nemat-Nasser, S. and Oda, M. (1982), "On Statistical Description of Stress and Fabric in Granular Materials," Int. J. for Numerical & Analytical Methods in Geomechanics, 6, No.1.

Mehrabadi, M. M. and Nemat-Nasser, S. (1983), "Stress, Dilatancy and Fabric in Granular Materials," Mechanics of Materials 2 pp155-161.

Mesri, G. and Olson, R. E. (1971a), "Consolidation Characteristics of Montmorillonite," Geotechnique, Vol. 21, No. 4 pp341-353.

Mesri, G. and Olson, R. E. (1971b), "Mechanisms Controlling the the Permeability of clays," Clays and Clay Minerals, 19, pp151-158.

Mesri, G., Rokhsar, A. and Bohor, B. F. (1975), "Composition and Compressibility of Typical Samples of Mexico City Clay," Geotechnique, London, England, vol.25, No.3, pp527-554.

Mesri, G. (1973), "Coefficient of Secondary Compression," Journal of the Soil Mechanics and

Foundations Division, ASCE, Vol.99 SM1, pp123-137.

Michael, A. S., and Lin, C. S. (1954), "The Permeability of Kaolinite," Industrial Engineering Chemistry, Vol. 46, pp1239-1246.

Mindlin, R. D. (1964), "Microstructure in Linear Elasticity," Arch. Rat. Mech. Anal. 16, 51.

Mitchell, J. K. (1962), "Components of Pore Water Pressure in Soils," Journal of the Soil Mechanics and Foundations Division, ASCE, vol.86, No.SM3, pp19-52.

Mitchel, J. K., Campanella, R. G. and Singh, A. (1968), "Soil Creep as a Rate Process," Journal of the Soil Mechanics and foundations Division, ASCE, vol.94, No.SM1, pp231-253.

Mitchell, J. K. (1956), "The Fabric of Natural Clays and its Relation to Engineering Properties," Proc. of the Highway Research Board, vol.35, pp693-713.

Mitchell, J. K. (1976), "Fundamentals of Soil Behaviour," John Wiley and Sons, New York, N.Y.

Monte, J. L. and Kriezsek, R. J. (1976), "One Dimensional Mathematical Model for Large Strain Consolidation," Geotechnique, Vol. 26, No.3, pp495-510.

Moran, P. A. P. (1966), "A Note on Recent Research in Geometrical Probability," J. Appl. Probability, 3, pp453-463.

Moran, P. A. P. (1972), "The Probabilistic Basis of Stereology," Advances in Appl. Probability, Spec. Suppl. pp69-71.

Moyal, E. (1949), "Stochastic Processes and Statistical Physics," Royal Statistical Society, No. 3 pp375-437.

Murayama, S. and Shibata, T. (1964), "Flow and Stress Relaxation of Clays," I.U.T.A.M. Symposium in Rheology and Soil Mechanics, Grenoble, France.

Murdoch, A. I. (1983), "The Motivation of Continuum Concepts and Relations from Discrete Considerations," Q.J. Appl. Math. 36, pp.163-187.

Murdoch, A. I. (1984), "A Corpuscular Approach to Continuum Mechanics: Basic Considerations," Archive for Rational Mechanics and Analysis, vol. pp291-319.

Nemat-Nasser, S. (1980), "On Behaviour of Granular Material in Simple Shear," Soils and Foundations, Vol 20, No.3, pp59-73.

Nemat-Nasser, S. and Mehrabadi, M. (1983), "Micromechanically Based Rate Constitutive Description

for Granular Materials," Proc. Internat. Conf. on Constitutive Laws for Engineering Materials: Theory and Application, Tucson, Az. Wiley, N.Y.

Newland, P. L. and Allely, B. H. (1960), "A Study of the Consolidation Characteristics of a Clay," Geotechnique, London, England, vol. 10, No. 1, pp 62-74.

Nicholson, W. L. (1970), "Estimation and Linear Properties of a Particle Size Distribution," Biometrika 57, pp 273-297.

Oda, M. (1972), "Initial Fabrics and Their Relations to Mechanical Properties of Granular Material," Soils and Foundations, Vol. 12, No. 1 pp 17-36.

Oda, M. (1977), "Co-ordination Number and its Relation to Shear Strength of Granular Material," Soils and Foundations, vol. 17.

Oda, M., Konishi, J. and Nemat-Nasser, S. (1980), "Some Experimentally Based Fundamental Results on The Mechanical Behaviour of Granular Materials" Geotechnique, 30, No. 4 pp 479-495.

Oda, M., Konishi, J. and Nemat-Nasser, S. (1982), "Experimental Micromechanical Evaluation of Strength of Granular Materials: Effects of Particle Rolling," Mechanics of Materials 1, pp 269-283.

Oda, M., Nemat-Nasser, S. and Mehrabadi, M. M. (1982), "A Statistical Study of Fabric in a Random Assembly of Spherical Granules," Int. J. for Numerical & Analytical Methods in Geomechanics, 6. No. 1.

Olsen, H. W. (1962), "Hydraulic Flow Through Saturated Clay," Proceedings of the Ninth National Conference on Clays and Clay Minerals, pp 131-161.

Olsen, H. W. (1965), "Deviations From Darcy's Law in Saturated Clays," Proc. of the Soil Science Society of America, 29(2), pp 135-140.

Olson, R. E. and Mesri, G. (1970), "Mechanisms Controlling Compressibility of Clays," J. of Soil Mech. and Found. Eng. Div. ASCE, Vol. 96, No. SM6, pp 1863-1878.

Olson, R. E. and Daniel, D. E. (1981), "Measurement of the Hydraulic Conductivity of Fine-Grained Soils," Permeability and Ground Water Contaminant Transport, ASTM, ST746, pp 18-64.

Oshima, N. (1953) Proc. 3rd Japan Nat. Congr. Appl. Mech. p 77.

Papoulis, A. (1967), "Probability, Random Variables and Stochastic Processes," McGraw Hill Book Co.

Patankar, S. (1980), "Numerical Heat Transfer and Fluid Flow," McGraw-Hill Book Company.

Perzyna, P. (1963), "The Constitutive Equations for Rate-sensitive Plastic Materials," Q. Appl. Math., 20, pp321-332.

Prigogine, I. (1980), "From Being to Becoming," W. H. Freeman and Co., San Francisco.

Provan, J. (1987) personal communication.

Pugachev, V. S. (1965), "Theory of Random Function," Pergamon Press, Oxford.

Pusch, R. (1966), "Quick Clay Microstructure," Engng Geol. 3 pp433-443.

Pusch, R. (1970), "Microstructural Changes in Soft Quick Clay at Failure," Canadian Geotechnical Journal, vol. 7, No. 1, pp1-7.

Pusch, R. (1973a), "Influence of Salinity and Organic Matter on the Formation of Clay Microstructure," Proc. Int. Symp. Soil Structure, Gothenburg, Sweden, pp161-167.

Pusch, R. (1973b), "Physico-Chemical Processes Which Affect Soil Structure and Vice Versa," Appendix to the Proc. Int. Symp. Soil Structure, Gothenburg, Sweden, pp27-37.

Pusch, R. (1973c), "Structural Variations in Boulder Clay," Proc. Int. Symp. Soil Structure, Gothenburg, Sweden.

Pusch, R. and Feltham, P. (1980), "A Stochastic Model of the Creep of Soils," Geotechnique, 30, No. 4. pp497-506.

Pusch, R. and Feltham, P. (1980), "Computer Simulation of Creep of Clay," J. Geotechnical Engineering Division, ASCE, Vol. 107, No. GT1

Rivlin, R. S. (1976), "The Passage from a Particle System to a Continuum Model," Arch. Mech. Stos. 28, pp549-561.

Rice, J. R. (1971), "Inelastic Constitutive Relations for Solids," J. Mech. Phys. Solids, Vol. 19 pp433-455.

Rice, J. R. (1975), "Continuum Mechanics and Thermodynamics of Plasticity in Relation to Microscale Deformation Mechanics," Constitutive Equations in Plasticity Edited by Argon, A. The MIT Press.

Reynolds, O. (1898), "On the Dilatancy of Media Composed of Rigid Particles in Contact," Philosophical Magazine,



Vol.20, pp469-481.

Rivlin, R. S. (1968), "Generalized Mechanics of Continuous Media," I.U.T.A.M. Symp. (E. Kroner, edit.) pp1-17.

Rosenquist, I. Th. (1959), "Physico-Chemical Properties of Soils," Journal of the Soil Mechanics and Foundation, ASCE vol.85, pp31-54.

Ross, S. (1983), "Stochastic Process," John Wiley, New York.

Rubinstien, R. Y. (1981), "Simulation and The Monte-Carlo Method," Wiley, New York.

Samarasinghe, M., Huang, H. and Dranevich, V. P. (1982), "Permeability and Consolidation of Normally Consolidated Soils," ASCE, Geotechnical Eng., Vol.108, No.GT6.

Samuel, K. and Taylor, H. M. (1981), "A Second Course in Stochastic Process," Academic Press.

Scheidegger, A. E. (1974), "The Physics of Flow Through Porous Media," 3rd Ed., University of Toronto Press, Toronto, Canada.

Schiffman, R. L., Ladd, C.C. and Chen, A. T. F. (1964), "The Secondary Consolidation of Clay," IUTAM Symp. (Kravtchenko, J. and Sirieys, P. M. editors), pp273-304.

Schlogl, F. (1967), "On the Statistical Foundation of The Thermodynamic Evolution Criterion of Glansdoff and Prigogine," Annals of Physics 46, pp334-366.

Schrodinger, E. (1952), "Statistical Thermodynamics," Cambridge University Press, Cambridge.

Schwartz, L. (1966), "Mathematics for the Physical Sciences," Addison-Wesley Publishing Company, Reading, Mass.

Scott, R. F. (1953), "Numerical Analysis of Consolidation Problems," M.Sc. Thesis, MIT, MA, USA.

Scott, R. F. (1985), "Plasticity and Constitutive Relations in Soil Mechanics," Journal of Geotechnical Engineering, ASCE, Vol. 111, No. 5 pp563-601.

Scott, R. F. and Michael, J. K. (1980), "Computer Modelling of clay Structure and Mechanics," Geotechnical Engineering Division, Vol. 106, No.GT1.

Silberstein, L. (1946), "Aggregates in Random Distribution of points," Phil. Mag. (2) 36, pp319-336.

Skempton, A. W. (1964), "Long Term Stability of Clay Slopes," *Geotechnique*, vol. 14, p. 77.

Smart, P. (1969), "Soil Structure in the Electron-Microscope," *Prco. Int. Conf. Struct., Solid Mech. Eng. Design, I*, Wiley-Interscience, New York, N.Y., pp 244-255.

Smith, W. O., Foote, P. D. and Busang, P. F. (1929), "Packing of Homogeneous Spheres," *Phys. Rev.*, vol. 34, pp 1271-1274.

Soderblom, R. (1969), "Salt in Swedish Clays and its Importance for Quick Clay Formation," *Swedish Geotechnical Proceedings*, No. 22, 63p.

Sridharan, A., Altschaeff, A. G. and Diamond, S. (1971), "Pore Size Distribution Studies," *Journal of the Soil Mechanics and Foundations Division, ASCE*, vol. 97, No. SM5, pp 771-787.

Sridharan, A. (1973), "Mechanisms Controlling Volume Change of Saturated Clays and the Role of the Effective Stress Concept," *Geotechnique* 23, No. 2 pp 359-382.

Sridharan, A. and Rao, V. G. (1979), "Shear Strength Behaviour of Saturated Clays and the the Role of the Effective Stress Concept," *Geotechnique*, 29, No. 2, pp 177-193.

Sridharan, A. and Rao, A. S. (1983), "Mechanisms Controlling the Secondary Compression of Clays," *Geotechnique*, London, vol. 32 No. 3, PP 249-260.

Tallis, G. M. (1970), "Estimating the Distribution of Spherical and Elliptical Bodies in Conglomerates from Plane Sections," *Biometrics* 26 pp 87-103.

Tan, T. K. (1957), "Report on Soil Properties and Their Measurement," *Proc. 4th Int. Conf. Soil Mech. Fd. Engng.* 3, pp 87-89.

Tan, T. K. (1964), "Detrmination of the Rheological Parameters and the Hardening Coefficients of Clays," *Symposium, International Union of Theoretical and Applied Mechanics, Rheology and Soil Mechanics, Grenoble*.

Tavenas, F., Leblond, P. and Leroueil, S. (1983), "The Permeability of Natural Soft Clays. Part I and Part II," *Canadain Geotechnical Journal*, Vol. 20. pp 629-644, pp 645-660.

Taylor, D. W. and Marchent, W. (1940), "A Theory of Clay Consolidation Accounting for Secondary Compression," *Journal of Mathematics and Physics*, vol. 9, pp 167-185.

Taylor, D. W. (1948), "Fundamentals of Soil Mechanics,"

Joh Wiley & Sons, New York, N. Y.

Taylor, G. I. (1938), "Plastic Strain in Metals," Journal of the Institute of Metals Vol. 62.

Taylor, T. R. and Schmidt, P. W. (1968), "Interparticle Potential Energies in Na-Montmorillonite Clay Suspensions," Clays and Clay Minerals, Vol. 19, pp77-82.

Terzaghi, K. (1925), "Erdbaumechanik," Vienna, F. Deuticke.

Terzaghi, K. (1943), "Theoretical Soil Mechanics" Wiley Publications, New York, N.Y.

Tonti, E. (1972), "On the Formal Structure of Continuum Mechanics Part I, Deformation Theory," Appl. Mech. Rev., 25, 7.

Tovery, N. K. (1973), "Quantitative Analysis of Electron Micrographs of Soil Structure," Proc. of the Int. Symp. of Soil Structure, Gothenburg, Sweden, pp50-57.

Toupin, R. A. (1964), "Theories of Elasticity with Couple-Stress," Arch. Rat. Mech. Anal. 17, p85.

Tovery, N. K. (1973), "Quantitative Analysis of Electron Micrographs of Soil Structure," Proc. of the Int. Symp. of Structure, Gothenburg, Sweden, pp50-57.

Tribus, M. (1969), "Rational Descriptions, Decisions and Designs," Pergamon Press.

Trollope, D. H. (1960), "The Fabric of Clays in Relation to Shear Strength," Proc. 3rd Australia-Newzealand Conf. on Soil Mechanics and Foundation Eng. pp197-202.

Truesdell, C. (1955), "Hypo-Elasticity," J. Rational Mech. Anal. 4, p83.

Truesdell, and Noll, W. (1963), "The Non-Linear Field Theories of Mechanics," Vol III/3, Handbuch der Physik, (Ed. S. Flugge), Springer Verlag Berlin.

Turcott, E. (1988), "Ph.D. Thesis to be submitted to the Mechanical Engineering Dept., McGill University.

Uhlenbeck, G. E. and Ornstein, L. S. (1930), "On Theory of the Brownian Motion," Physical Review, Vol. 36, p823.

Valanis, K. C. (1971), "A Theory of Viscoplasticity Without Yield Surface, Part I: General Theory, Part II: Application to the Mechanical Behaviour of Metals," Arch. of Mech., 23, p517 and p535.

Valanis, K. C. (1975), "On the Foundation of the

Endochronic Theory of Viscoplasticity," Arch. of Mech., 27,p857.

Valanis, K. C. and Read, H. E. (1979), "A New Endochronic Theory plasticity Model for Soils," Systems, Science and Software Report SSS-R-80-4294.

Valanis, K. C. and Read, H. E. (1982), "A New Endochronic Plasticity Model for Soils," Soil Mechanics- Transient and Cyclic Loads, Ed. by Pande, G. N. and Zienkiewicz, O. C. John Wiley & Sons Ltd.

Van Kampen, N. G. (1961), "A Power Series Expansion of the Master Equation," Can.J. Phys. Vol.39 pp551-567.

Van Kampen, N. G.(1983), "Stochastic Processes in Physics and Chemistry," North Holland, Amsterdam.

Vanmarcke, E. H.(1977a), "Probabilistic Modeling of Soil Profile," Journal of the Geotechnical Engineering Division,ASCE, vol.103, No. GT11, pp1227-1246.

Vanmarke, E. . H.(1977b), "Reliability of Earth Slopes," Journal of the Geotechnical Engineering Division, ASCE,vol.103,No.GT11, pp1247-1265.

Van Olphen, H.(1963), "An Introduction to Clay Colloid Chemistry," Wiley Interscience, New York.

Vyalov, S. S. (1986), "Rheological Fundamentals of Soil Mechanics," Elsevier, New York.

Wahls, H. E.(1962), "Analysis of Primary and Secondary Consolidation," Journal of the Soil Mechanics and Foundations Division,ASCE, vol.88, No.SM6, part 1, pp207-231.

Walker, L. K.(1969)"Secondary Settlement in Sensitive Clays," Canadian Geotechnical Journal, vol.6, pp219-222.

Walker, L. K. and Raymond, G. P.(1968), "The Prediction of Consolidation Rates in a Cemented Clay," Canadian Geotechnical Journal, vol.5 No.4, pp192-216.

Wicksell, S. D.(1925), "The Corpuscle Problem," Biometrika; Part I, 17, pp84-99.

Wicksell, S. D.(1926), "The Corpuscle Problem," Biometrika; Part II, 18, pp152-172.

Witt, K. J. and Brauns, J. (1983), "Permeability-Anisotropy Due to Particle Shape," Journal of Geotechnical Engineering, vol.109, No.9,ASCE pp1181-1187.

Whitman, R. V., Richardson, A. M. and Healy, K. A.(1961), "Time-Lags in Pore Pressure Measurements,"

Proc. Fifth Int. Conf. on Soil Mech. and Found. Eng., vol.1, pp407-411.

Whitman, R. V. (1984), "Evaluating Calculated Risk in Geotechnical Engineering," ASCE, Journal of Geotechnical Engineering, Vol. 110, No. 2 p.145.

Wong, E. (1971), "Stochastic Processes in Information and Dynamical Systems," McGraw Hill, New York.

Wu, T. H., Resendiz, D. and Neukirchner, R. J. (1966), "The Analysis of Consolidation by Rate Process Theory," Journal of the Soil Mechanics and Foundation Division, ASCE, vol.92 No. SM6, pp229-248.

Wu, T. H., Vyas, S. K. and Chang, N. Y. (1973), "Probabilistic Analysis of Seepage," Journal of the Soil Mechanics and Foundation Division, ASCE, vol.99, No. SM4, pp323-340.

Yong, R. N. and Chen, D. S. (1970), "Analysis of Creep of Clays Using Retardation Time Distribution," Proc. 5th Int. Congress Rheol. Kyoto University, Japan, pp501-513.

Yong, R. N. (1971), "General Report to Sessions Soil Technology and Stabilisation," Proc. 4th Asian Reg. Conf. Soil Mech., Bangkok.

Yong, R. N. and Sheeran, D. E. (1973), "Fabric Unit Interaction and Soil Behaviour," Proceedings of the International Symposium on Soil Structure, Gothenburg, Sweden, pp176-183.

Yong, R. N. and Warkentin, B. (1975), "Soil Properties and Behaviour," Elsevier Scientific Publ. Comp. New York.

Yong, R. N., Sethi, A. J., Ludwig, H. P. and Jorgenson, M. A. (1978), "Physical Chemistry of Dispersive Clay Particle Interaction," ASCE, Convention, Chicago, pp1-21.

Yong, R. N., Sethi, A. J. and LaRoche, P. (1979), "Significance of Amorphous Material Relative to Some Champlain Clays," Canadian Geotechnical Journal, No.16, pp511-520.

Yong, R. N., Sadana, M. and Gohl, W. (1984), "A Particle Interaction Energy Model for Assessment of an Expansive Soil," Fifth International Conference on Expansive Soils, Adelaide South Australia.

Yong, R. N., Elmonayeri, D. and Chong, T. S. (1985a), "The Effect of Leaching on the Integrity of a Natural Clay," Engineering Geology Vol. 21, pp279-299.

Yong, R. N. (1985b), "Interaction of Clay and and

Industrial Waste-A Summary Review," Second Annual Canadian/American Conference on Hydrogeology Hazardous Wastes in Ground Water-A Soluble Dilemma, Banff.

Yvon, J. (1969), "Correlations and Entropy in Classical Statistical Mechanics," Pergamon Press, Oxford.

Zeevaert, L. (1960), "Consolidation Theory for Materials Showing Intergranular Viscosity," Proceedings, 3rd Pan American Conference, Soil Mechanics and Foundation Engineering, vol.1 Caracas, Venezuela.

Ziegler, H. (1965), "Some Extremum Principles in Irreversible Thermodynamics, With Application to Continuum Mechanics," In Progress in Solid Mechanics, Ed. Sneddon, I. N. and Hill, R. Vol. 4, pp91-193.

Zienkiewicz, O. C. (1971), "The Finite Element Method in Engineering Science," McGraw-Hill, New York.

Zubelewicz, A. and Bazant, Z. (1987), "Constitutive Model with Rotating Active Plane and True Stress," Journal of The Eng. Mech., ASCE, Vol. 113, No.3 pp398-412.

## APPENDIX A

## A-1 THE RELATION BETWEEN THE MOMENTS OF OBSERVED AND CALCULATED CLUSTER SIZE DISTRIBUTION:

From chapter three, we have the following equation:

$$F(y) = \frac{y}{E(r)} \int_y^{\infty} \frac{g(r)}{(r^2 - y^2)^{1/2}} dr \quad \text{A-1-1 (repeated)}$$

The n-th moment can have the following definitions:

$$E(y^n) = \int_0^{r_{\max}} y^n f(y) dy$$

$$E(r^n) = \int_0^{r_{\max}} r^n g(r) dr$$

Substituting the value of  $f(y)$  from Eq. A-1-1

$$E(y^n) = \frac{1}{E(r)} \int_y^r \left( y^n \int_r^{\infty} \frac{g(r)}{(r^2 - y^2)^{1/2}} dy \right) dy$$

The solution of the above equation leads to

$$E(y) = \frac{E(y)^{2n+1}}{E(r)} \frac{2.4.6....2n}{3.5.7....(2n+1)}$$

$$E(y) = \frac{E(y)^{2n}}{E(r)} \frac{1.3.5....(2n-1)}{2(2.4.6.....2n)} \pi/2$$

It follows that:

$$E(y) = (\pi/4) \frac{E(r^2)}{E(r)}$$

$$E(y^2) = (2/3) \frac{E(r^3)}{E(r)}$$

For equal size clusters

$$E(y) = (\pi/4) r$$

$$E(y^2) = (2/3) r^2$$

Where  $E(y)^n$  = the  $n^{th}$  moment of the function  $f(y)$

$E(r)^n$  = the  $n^{th}$  moment of the function  $g(r)$

**The average specific surface area:**

If a sample of clay soil contains clusters with projected diameters  $d_1, d_2, \dots, d_k$  and the corresponding number of the clusters  $N_1, N_2, \dots, N_k$  the total surface area can be approximated (Harr 1977) by

$$\bar{S} = \pi \sum_{i=1}^k d_i^2 N_i$$

and their volume by

$$\bar{V} = \pi/6 \sum_{i=1}^k d_i^3 N_i$$



Hence, average of the total surface area can be expressed

$$\langle \bar{S} \rangle = \pi N \langle d^2 \rangle$$

where  $N$  = the total cluster units.

And the average of their volume

$$\langle \bar{V} \rangle = \pi/6 N \langle d^3 \rangle$$

The surface area per unit volume (Harr 1977):

$$\bar{S}_v = 6 \sum d_i^2 N_i / (\sum d_i^3 N_i)$$

It follows that

the average specific surface area of the cluster is

$$S_v = 6 \frac{E(d^2)}{E(d^3)} = 3 \frac{E(r^2)}{E(r^3)}$$

For equal size clusters

$$S_v = 3/r$$

## A-2' NUMERICAL TECHNIQUE FOR SOLVING EQUATION 3.37:

The integral equation which is given in Chapter 3, is as follows

$$F(y) = \frac{y}{E(r)} \int_y^{\infty} \frac{g(r)}{(r^2 - y^2)^{1/2}} dr \quad \text{A-2-1}$$

It should be put in a form suitable for the calculation of the probability distribution of the diameter of the cluster units. Hence, by using Tonelli's theorem (Tallas(1969)), and some other integration properties, the solution of the Equation A-2-1 can be written as follows:

$$G(r) = 1 - \frac{\int_0^{\infty} f(y) (y_i^2 - y^2)^{-1/2} dy}{\int_0^{\infty} y^{-1} f(y) dy} \quad \text{A-2-2}$$

Given the distribution of observed radius of cluster units, we cannot solve equation A-2-2 in close form, and hence we will solve it numerically. (Where  $y_i$  = observed radius of a given cluster unit).

Let  $y_i, i=1,2,3,\dots,n$  represent the class boundaries, then  $G(r)$  can be calculated as follows:

$$G_1 = \int_0^{\infty} \frac{f(y)}{y} dy$$

$$G_2 = \int_{y_1}^{\infty} f(y) (y_1^2 - y^2)^{-1/2} dy$$

Hence,

$$G_1 = \sum_i^n \frac{\left( \frac{f_i}{y_{i+1}} - \frac{f_{i+1}}{y_i} \right)}{(y_{i+1} - y_i)} \text{Log} \frac{y_{i+1}}{y_i}$$

$$G_2 = \sum_i^n \frac{\left( \frac{f_i}{y_{i+1}} - \frac{f_{i+1}}{y_i} \right)}{(y_{i+1} - y_i)} \left( (y_{i+1}^2 - y_i^2)^{1/2} - (y_1^2 - y_i^2)^{1/2} \right)$$

$$+ \left( \frac{\frac{f_i}{y_{i+1}} - \frac{f_{i+1}}{y_i}}{(y_{i+1} - y_i)} \right) \text{Log} \frac{y_{i+1} + (y_{i+1}^2 - y_i^2)^{1/2}}{y_i + (y_1^2 - y_i^2)^{1/2}}$$

There are seven subroutines written in Fortran language for the development of probability distribution of void ratio, water content and density.

## APPENDIX B

## B-1 THE DEVELOPMENT OF THE CONDUIT FLOW EQUATION:

In this section, we will develop the conduit flow equation under the basic assumption of viscous flow mechanism.

From Newton's law, we have the following expression:

$$\tau = \eta \frac{dv_x}{dy} \quad \text{B-1-1}$$

where

- $\eta$  = coefficient of absolute viscosity
- $\tau$  = the shear stress around fluid element
- $v_x$  = the velocity of the fluid in direction of flow.

The force equilibrium; see Fig. B-1

$$F_H = \pi y (P_2 - P_1) - 2 \pi y \tau \Delta x = 0 \quad \text{B-1-2}$$

where  $P_1$  and  $P_2$  are the pressures at the edge of the element. Introducing Equation 1 into 2, we get

$$y (P_2 - P_1) \tau_w + 2 \eta \frac{dv_x}{dy} \Delta x = 0$$

$$\frac{dv_x}{dy} = - \frac{\tau_w}{2 \eta} \frac{(P_2 - P_1)}{\Delta x} y$$

integrating

$$v_x = - \frac{\tau_w}{2 \eta} \frac{(P_2 - P_1)}{2 \Delta x} y^2 + \text{const.} \quad \text{B-1-3}$$

It is assumed that there is no slip along the walls of the channel (i.e.,  $v = 0$ ,  $y = R$ ). Introducing the boundary conditions in Eq. 3, we get:

$$v_x = \frac{\tau_w}{2 \eta} \frac{(P_1 - P_2)}{\Delta x} (R^2 - y^2)$$

$$v_{\max} = \frac{\tau_w}{4 \eta} \frac{(P_1 - P_2)}{\Delta x} (R^2)$$

$$q = \int v_x dA = 1/2 a v_{\max}$$

$$q = \frac{\gamma_v}{8n} \frac{(P_1 - P_2)}{\Delta x} \quad (Ra)^2$$

Generally, for any cross sectional shape and  $D=\Delta X$  (where D is the distance between two neighbor MSUs), we have the following relation:

$$q = \frac{C_s \gamma_v}{n} \frac{(P_A^\pi - P_r^\pi)}{D^{Ar}} \quad (Ra)^2$$

where  $C_s$  = shape factor

$R$  = hydraulic radius = area/wetted perimeter

$a$  = cross sectional area of the channel

$P_A^\pi$  = pore water pressure which builds in the cavity of MSU A

$P_r^\pi$  = pore water pressure which builds in the cavity of the MSU r

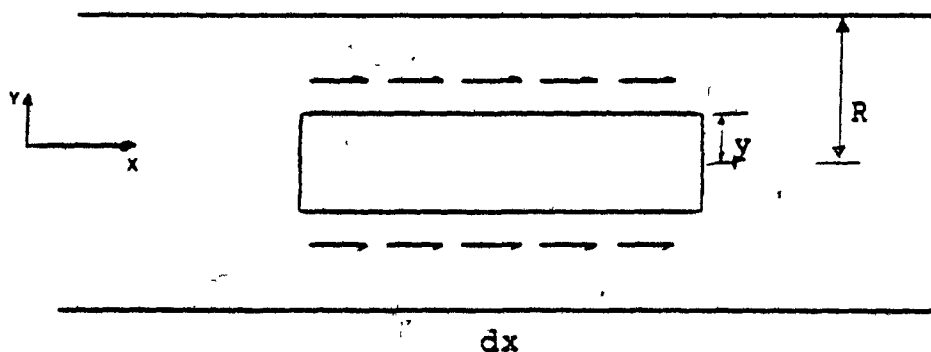


Fig. B-1 Fluid element

## B-2 THE DEVELOPMENT OF THE HYDRAULIC RADIUS (R):

From moment analyses(A-1), we have the following equations

$$E(y) = (\pi/4) \frac{E(r^2)}{E(r)} \quad B-2-1$$

$$E(y^2) = (2/3) \frac{E(r^3)}{E(r)} \quad B-2-2$$

The average area  $E(A)$  of all the circles appearing in the macrostructural unit is given by

$$E(A_c) = (\pi/4) E(y^2) = (\pi/4)(2/3) \frac{E(r^3)}{E(r)} \quad B-2-3$$

and we have

$$E(A_c) n_c = A_t (1-n) \quad B-2-4$$

Where

$n$  = total number of clusters in the MSU

$A_t$  = total area of the MSU

$$R = \frac{\text{cross section normal to flow}}{\text{perimeter normal to flow}} = \frac{A_t n}{P_y}$$

$P_y$  is the perimeter of the sectioned voids in the cross-sectional area and is equal to the perimeter of the sectioned clusters  $P_c$  in the same area  $A_t$ . Hence,

$$P_y = P_c = n_c E(y)$$

B-2-5

Combining Eqs B-2-1, 2, 3, 4 and 5, we get:

$$P_y = (3/2) \pi A (1-n_c) \frac{E(r^2)}{E(r^3)}$$

Where  $n_c$  = the porosity of the MSU

$$R = \frac{n_m}{1-n_m} \frac{4}{\pi} \frac{1}{3 (E(r^2)/E(r^3))}$$

$$R = \frac{n_m}{1-n_m} \frac{4}{\pi} \frac{1}{S_v}$$

Hence,

$$R = \frac{e_m}{\pi} \frac{4}{S_v}$$

B-2-6



## APPENDIX C

### C-1 THE COMPUTER PROGRAM FOR THE EVOLUTION MODEL OF THE FIRST REGION:

The strategy which is used in developing of the computer programs is to put all the calculations and cyclic updating in several subroutines, and therefore the main program consists of only calling and executing of these subroutines in DO loops. We call this program as MFD.

The advantages of this strategy is that the program can be extended by adding other subroutines, generalizing or updating the existing subroutines. For one reason or another, the main program can be easily changed into Pascal language and linked with the Fortran subroutines.

In the following, we will discuss the theories supporting these subroutines and the position of these subroutines in the main program logic.

#### C-1-1 READ DATA:

The data is given in read format statement. However, the initial excess pore water pressure and the initial probability distribution are given in the subroutine IPP(PRI,ZP,ZPI).

PRI : Initial Probability distribution function of the excess pore water pressure which can be represented by Derac Delt function.

ZP : The initial excess pore water pressure ( $\bar{P}$ )

ZPI : The value of this excess pore water pressure in all the cavities. See Fig. C-1 below.

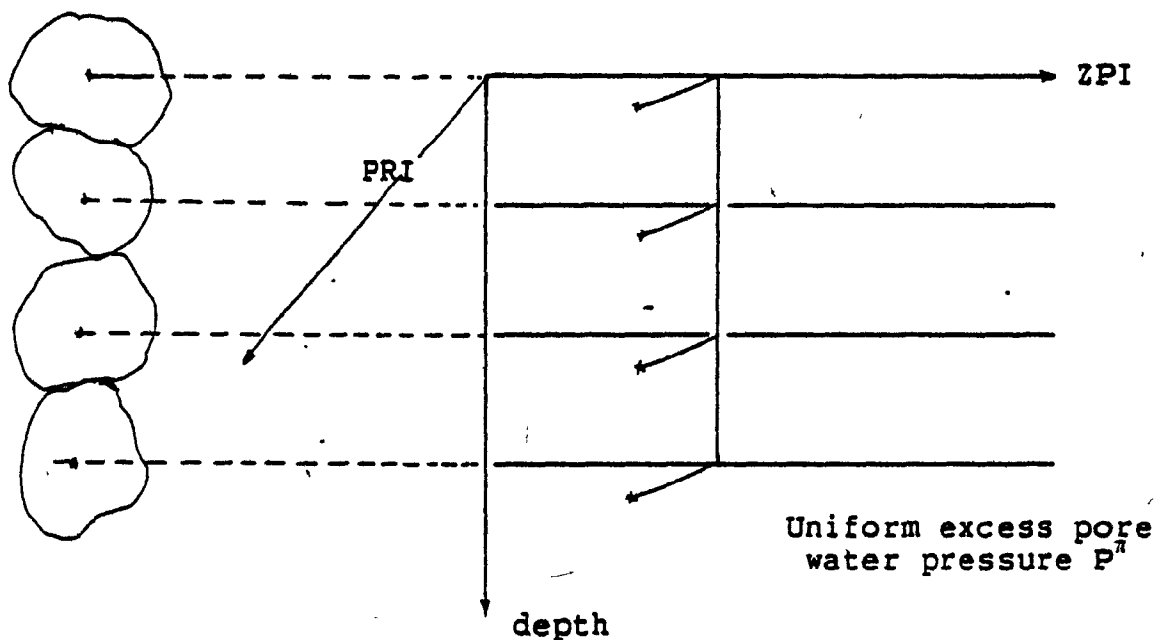


Fig. C-1 The initial excess pore water pressure

**C-1-2 SUBROUTINE MONTD:**

We are using the Monte-Carlo analysis to find the probability distribution of the microconsolidation coefficient ( $\bar{C}_v$ ) and the compressibility parameter ( $M$ ). We have considered the parameters of the ( $\bar{C}_v$ ) as normal distribution. Hence  $R$ ,  $a$  and  $e_m$  are dependent multivariate normal distribution. The Monte-Carlo simulation is given in Appendix E. The subroutine logic within the main program is given in the next subroutine.

**C-1-3 SUBROUTINE FINITD:**

Subroutine FINITD is using finite difference method to solve the state function. The concept of control volume of Patanker (1980) will be used here. For more details about this concept and the mathematical derivations, see Patanker (1980).

The fully implicit scheme is selected for discretization of the equation. Hence:

$$\frac{1}{\Delta t} \left( \frac{z_{i+1}^{j+1}}{1} - \frac{z_i^j}{1} \right) = \frac{k}{(\Delta x)^2} \left( \frac{z_{i+1}^{j+1}}{1+1} - 2\frac{z_i^{j+1}}{1} + \frac{z_{i-1}^{j+1}}{1-1} \right)$$

$$\frac{\Delta x}{\Delta t} \left( \frac{z_{i+1}^{j+1}}{1} - \frac{z_i^j}{1} \right) = \frac{k}{(\Delta x)} \left( \frac{z_{i+1}^{j+1}}{1+1} - 2\frac{z_i^{j+1}}{1} + \frac{z_{i-1}^{j+1}}{1-1} \right)$$

$$\left( \frac{\Delta x}{\Delta t} + \frac{2k}{\Delta x} \right) \frac{z_i^{j+1}}{1} = \left( \frac{k}{\Delta x} \right) \frac{z_{i+1}^{j+1}}{1+1} + \left( \frac{k}{\Delta x} \right) \frac{z_{i-1}^{j+1}}{1-1} + \left( \frac{\Delta x}{\Delta t} \right) \frac{z_i^j}{1}$$

Whence

$$a \frac{z_i^{j+1}}{1} = a \frac{z_{i+1}^{j+1}}{1+1} + a \frac{z_{i-1}^{j+1}}{1-1} + S$$

Where

$z$  = the excess pore water pressure

$k$  = the microconsolidation coefficient

$$a = \frac{\Delta x}{\Delta t} + \frac{2k}{\Delta x}$$

$$a = \frac{k}{\Delta x}$$

$$S = \frac{\Delta x}{\Delta t} z_i^j = a \frac{z_i^j}{1}$$

$$a_i^j = a_{i-1}^j + a_{i+1}^j + a_i^j$$

Hence

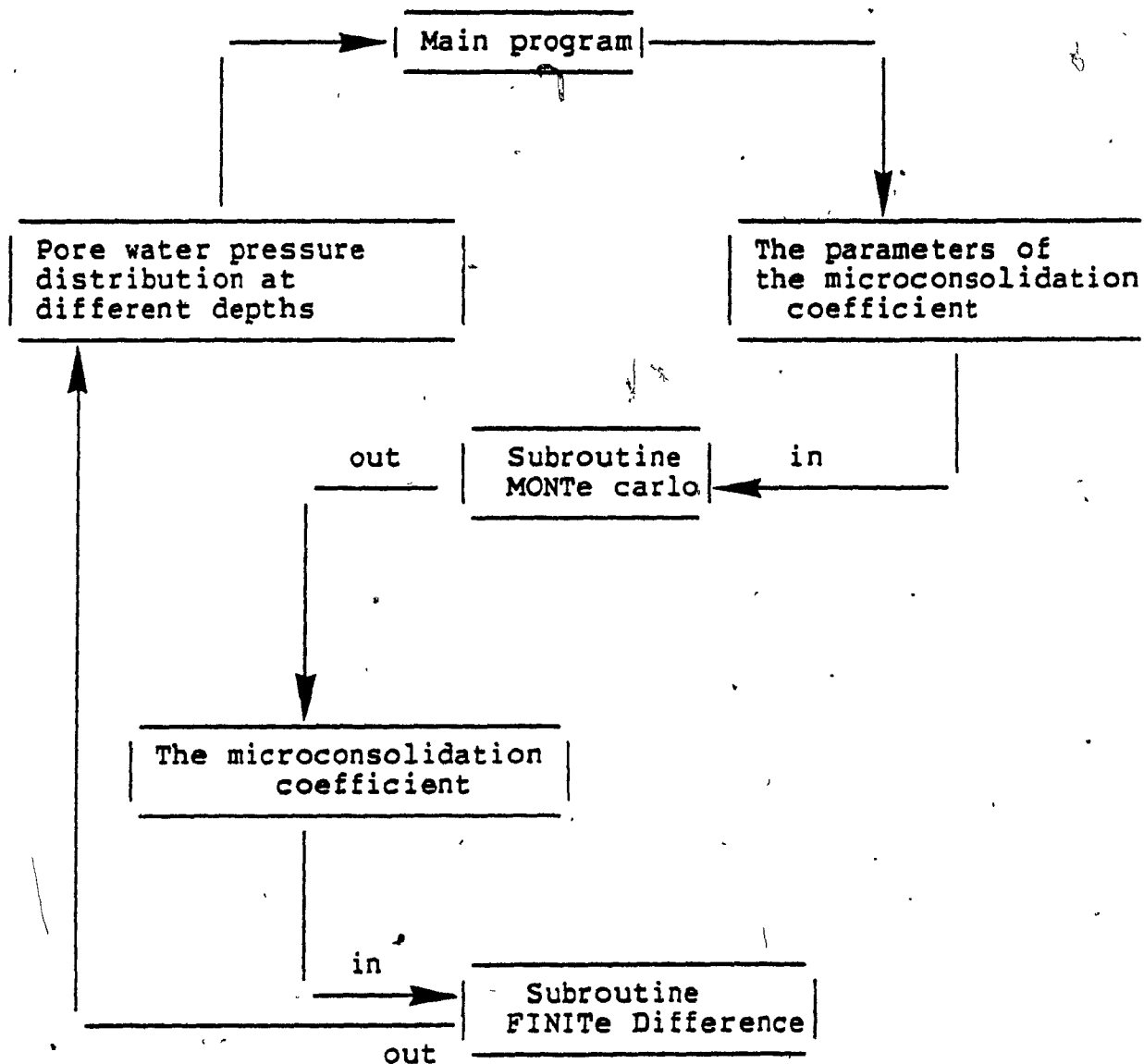
$$a(I) z^{j+1} = C(I) z^{j+1}_{(I-1)} + b(I) z^{j+1}_{(I+1)} + D(I)$$

Therefore, the coefficients of the equation are:

$$a(I) = \left( \frac{\Delta x}{\Delta t} + \frac{2k}{\Delta x} \right), \quad C(I) = \frac{k}{\Delta x}, \quad b(I) = \frac{k}{\Delta x}, \quad D(I) = \frac{\Delta x}{\Delta t} z_i^j$$

Gaussian elemention technique is used for solving n simultaneous equations.

The logic of the subroutines MONTD and FINITD within the main program are given below:



note; the two subroutines are in one Do loop.

Fig C-2 The Logic of MONT and FINITD  
within the Main Program

**C-1-4 SUBROUTINE SECMNT:**

The purpose of this subroutine is to find the mean and the standard deviation of the excess pore water pressure  $p^\pi$ , the compression modulus ( $M$ ) and the microconsolidation coefficient.

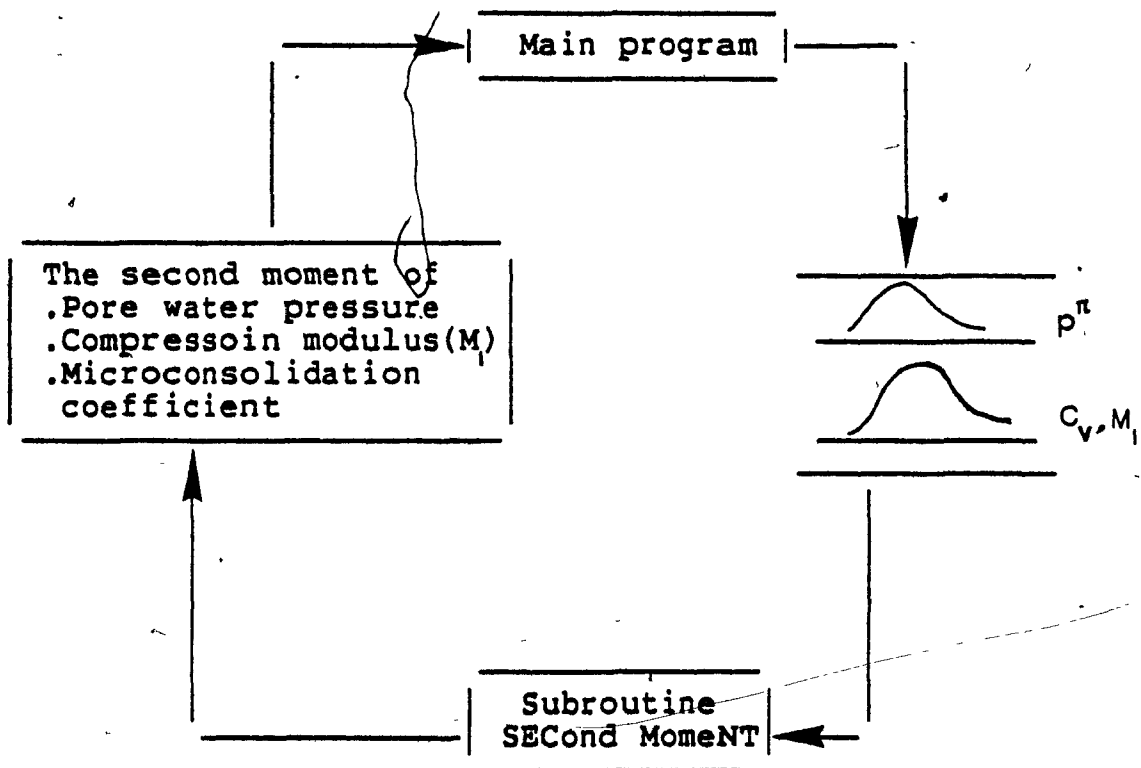


Fig C-3 The Logic of the Subroutine SECMNT within the main program

### C-1-5 SUBROUTINE UPDATE:

The routine of this program is to update the values of the parameters in each increment of time. The updated values of the parameters of the previous time step will be an input to the second increment of time. It is difficult to input probability distribution, see the discussion in chapter one. Hence, we input the means and the standard deviations of these parameters, and therefore the second moment analysis is used to find the mean and the standard deviation.

#### Theory:

For a given function  $y = g(x_1, x_2, \dots, x_n)$ , it is possible to find the moments of the dependent variables in terms of functions of moments of the independent variables, Papoulis (1967) and Benjamin et al. (1970). By using multidimensional Taylor-series expansion, we can have the following approximation for equation C-1-1.

$$y = g(x_1, x_2, x_3, \dots, x_n)$$

C-1-1

$$E(y) = g(m_{x_1}, m_{x_2}, m_{x_3}, \dots, m_{x_n}) + 1/2 \sum_{i,j} \frac{\partial^2 g}{\partial x_i \partial x_j} \Big|_m \text{cov}(x_i, x_j)$$

Where  $(\partial^2 g / \partial x_i \partial x_j)_m$  is the mixed second partial derivative of  $g(x_1, x_2, \dots, x_n)$  with respect to  $x_i$  and  $x_j$



evaluated at  $m_{x_1}, m_{x_2}, \dots, m_{x_n}$

The first order approximation to the variance of  $y$  is

$$\text{var}(y) = \sum_{i,j} \left. \frac{\partial g}{\partial x_i} \right|_m \left. \frac{\partial g}{\partial x_j} \right|_m \text{cov}(x_i, x_j)$$

which, if the  $x_i$  are uncorrelated, is simply

$$\text{var}(y) = \sum_i \left( \left. \frac{\partial g}{\partial x_i} \right|_m \right)^2 \text{var}(x_i)$$

To be noted that if any one of the independent variables is deterministic rather than as probabilistic, it will not contribute in the variance of  $y$ . Hence, if all the independent variables are deterministic, the variance of  $y$  equal to zero and there will be no uncertainty in the value of the dependent variable  $y$ .

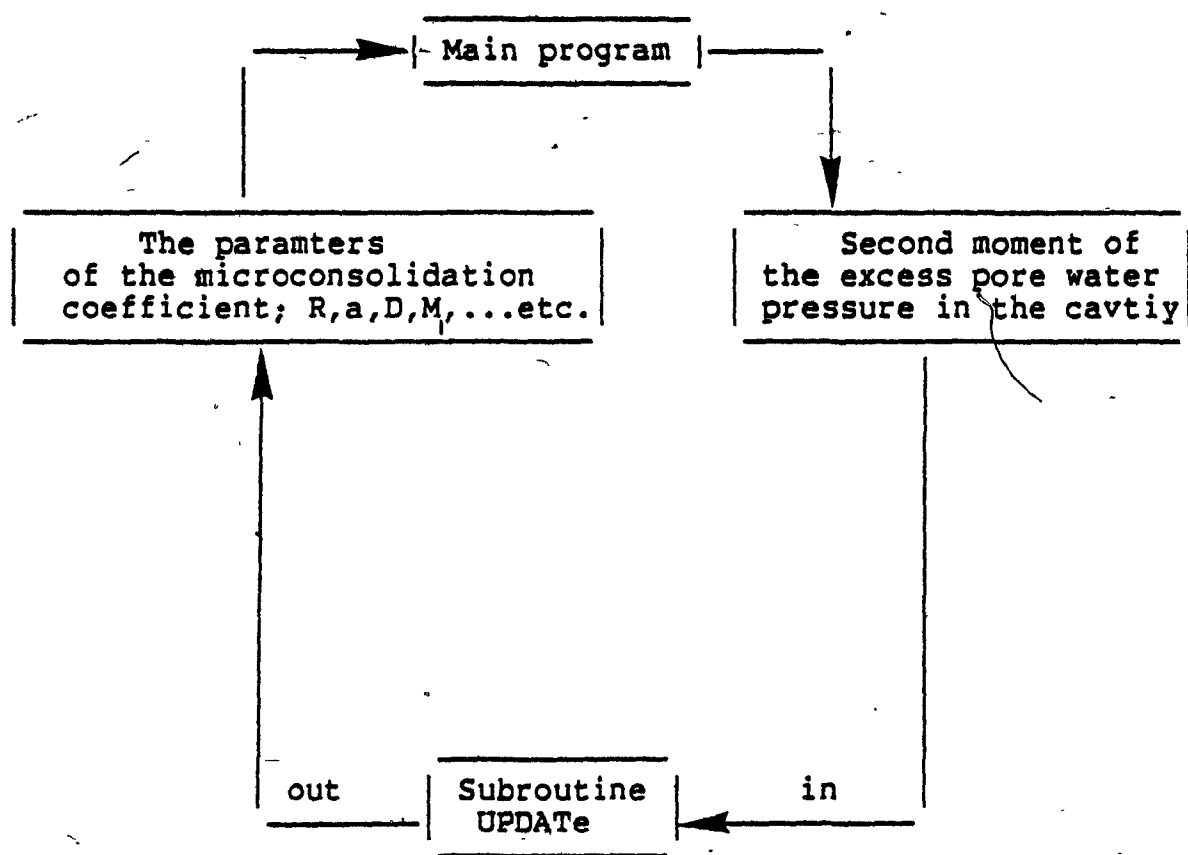


Fig C-4 The Logic of **UPDATE** within the Main Program

**C-1-6 SUBROUTINE FINPR:**

The routine of this program is to solve the evolution equation. Finite difference analysis is used in this subroutine program. The same technique which has been used in the subroutine FINITD is used here. The logic is given below.

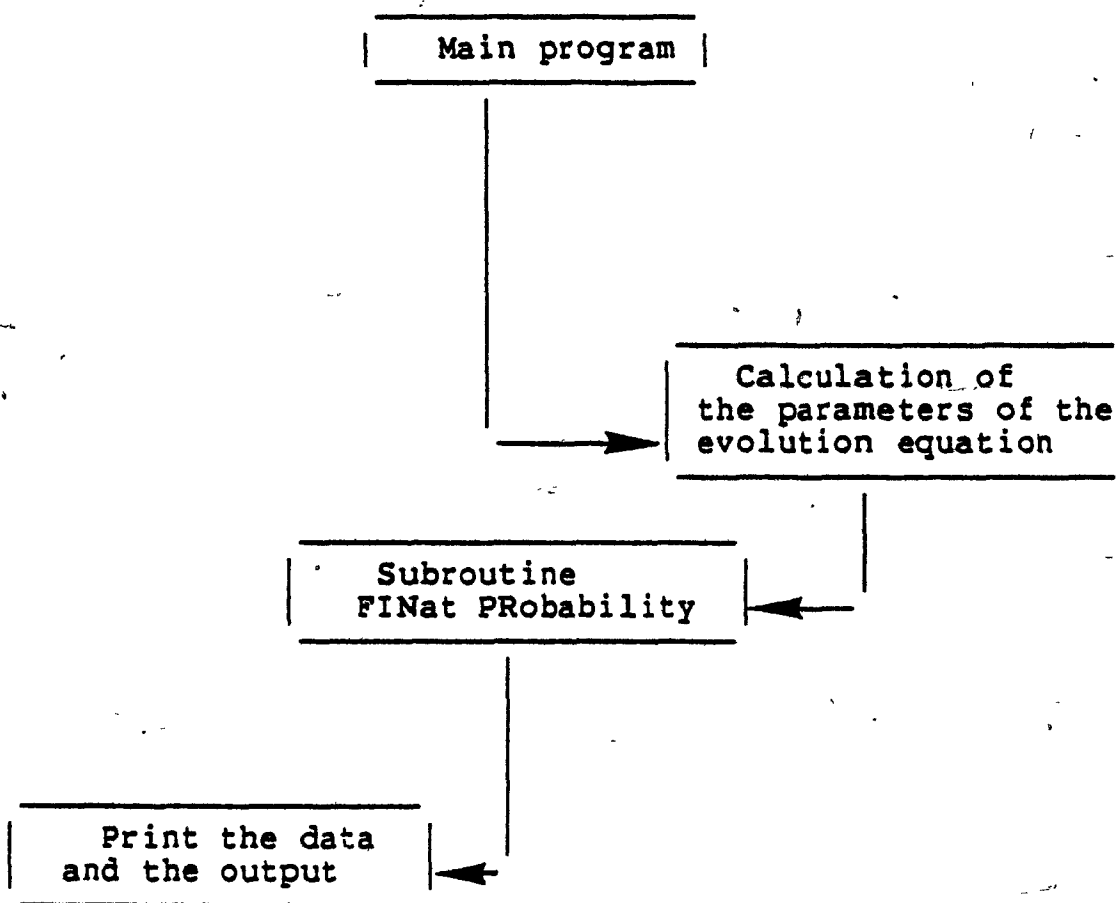


Fig C-5 The Logic of FINPR in the Main Program

## C-2 THE COMPUTER PROGRAM FOR THE EVOLUTION MODEL OF THE TOTAL REGION OF COMPRESSION:

The same strategy which is used in previous section will be used here, we call this program as MFE. In the following, we will discuss the theory supporting the FINLEM subroutine.

### C-2-1 READ DATA:

The data is given in read format statement. Besides the data given from MFD, we have the following data:

$m_2, \nu_2, sb_1$  and  $sb_2$  = constant parameters  
 $\tilde{C}_0$  = The intensity parameter for the overlapped region

### C-2-2 SUBROUTINE FINLEM:

For the first region, we update the effective stress at each node, by using the finite difference analysis program coupled with Monte Carlo technique. Once we have these stresses, we will use the finite element analysis on the constitutive equation developed in chapter four.

we will consider the grid system in one dimensional form; for the first region, the basic structure of the finite element analysis will be as

follows:

$$d\sigma^m - d\sigma''^m = 2m_1 d\epsilon_v^m$$

or

$$\Delta\sigma^m - \Delta\sigma''^m = 2m_1 \Delta\epsilon_v^m$$

where

$$\Delta\sigma''^m = \text{the nonlinear term and equal to } \Xi(\epsilon_c(t)) \Delta\epsilon_v^m$$

Hence, the finite element formulation from strain energy concept can be casted as follows:

$$\begin{aligned} \text{Increase in strain energy} &= \int \{\dot{\epsilon}\}^T \{\Delta\sigma\} dL \\ &= \int \{\delta\}^T \{B\}^T \left\{ \{C\} \{\Delta\epsilon\} + \{\Delta\sigma''\} \right\} dL \\ &= \int \{\delta\}^T \{B\}^T \left\{ \{C\} \{B\} \{\Delta\delta\} + \{\Delta\sigma''\} \right\} dL \end{aligned}$$

Where

$\delta$  = virtual displacement

$\epsilon$  = virtual strain

$dL$  = incremental length of the bar element

$$\text{Additional external work} = \{\delta\}^T \{\tilde{\Delta}P\}$$

$$\Delta P = \int \{B\}^T \left\{ \{C\} \{B\} \{\Delta\delta\} \right\} dL + \int \{B\}^T \{\Delta\sigma''\} dL$$

$$\tilde{\Delta}P = \int \{B\}^T \{\Delta\sigma''\} dL$$

$$\Delta P - \dot{\Delta P} = \int \{B\}^T \{C\} \{B\} dL \{\Delta \delta\}$$

Hence

$$\Delta P - \dot{\Delta P} = [K] \Delta \delta \quad C-2-1$$

Where

$$K = \int \{B\}^T \{C\} \{B\} dL$$

and

B = mode shape for bar element = ( 1/2 ; -1/2 ).

C = m<sub>1</sub> (Eq. 4.25).

Subroutine FINELM is utilizing four subroutines which are routines to solve Eq.C.2.1

## APPENDIX D

## D- Monte Carlo Simulation:

Monte carlo simulation is required for problems involving random variables with known probability distributions. This simulation which involves repeating of operations, uses in each operation a particular set values of the random variables. These random variables are generated in accordance with the corresponding probability distribution.

One of the main concepts in a Monte Carlo Simulation is the generation of random numbers from a prescribed probability distribution. Hence, first we will consider the generation of uniformly distributed random numbers. Let  $U$  a random variable with uniformly distributed function take the following form:

$$\Pr(u_i) = \begin{cases} 0 & , u_i < 0 \\ u_i & , 0 < u_i < 1 \\ 1 & , u_i > 1 \end{cases} \quad D-1$$

We consider the generation of such random numbers ( $U$ ) in the range (0,1). An often used formula for the generation of the "pseudorandom" sequence is given by

the recurrence relation (Lehmer 1963):

$$U_n = a U_{n-1} \pmod{m}$$

This relation is called the multiplicative congruential method for the generation of pseudorandom numbers. Here  $m$  is a large integer determined by the design of the computer (a large power of two in the case of binary computers) and  $a$ ,  $U$  are integers between 0 and  $(m-1)$ .

The corresponding pseudorandom numbers  $U$  are then obtained from the relation:

$$U_i = \frac{R_i}{m}$$

D-2

The proper choice of the constants  $a$ ,  $U$  and the starting value of  $R$  (seed) is discussed by Hull (1963). Such a sequence will repeat itself after at most  $m$  steps and will, therefore, be periodic. Hence, we must ensure the period is longer than the number of random numbers required in any single experiment.

The actual program used for generation of random numbers in  $(0,1)$  takes the following steps:

```
SUBROUTINE RAN(K,IR,N1,N2)
```

```
PI= 3.14
```

```
IR=IR*K
```

```
IF(IR.LT.0)IR=IR+2*(2**30-1)+2
```



```

R=DFLOAT(IR)/2.**31
U1=R
IR=IR*K
IF(IR.LT.0)IR=IR+2*(2**30-1)+2
R=DFLOAT(IR)/2.**31
U2=R
RETURN
END

```

Note the seed chosen in the program was ( $5^{**12}$  and  $7^{**11}$ ). These two seeds are recommended to us by Professor Bach (1985).

There are several methods to convert the generated random numbers in  $(0,1)$  into different probability distributions. In the following, we will consider the methods which have been used in this research work.

#### D-1 Inverse Transform Method:

The application of the inverse transform method is most effective, if the inverse of the probability distribution of the random variable,  $X$ , can be expressed analytically.

Let  $F(x)$  be a probability distribution. Then at a given probability  $F(x) = u$ , the value of  $x$  is

$$x = F_x^{-1}(u)$$

D-1-1

We have,  $u$ , is a value of the standard uniform variate,  $U$ , as given before. Hence,

$$\Pr(X < x) = \Pr\left[F_x^{-1}(u) < x\right]$$

D-1-2

$$= \Pr\left[u < F_x(x)\right]$$

$$= F_u\left[F_x(x) = F_x(x)\right]$$

which means that if  $(u_1, u_2, \dots, u_n)$  is a set of values from  $U$ , the corresponding set of values obtained through Eq.D-4, that is

$$x_i = F_x^{-1}(u_i) \quad i=1,2,3,\dots$$

Hence, when the probability distribution has the following form,

$$F_x(x) = a_1 \exp - a_2 x$$

D-1-3

$$x_i = - \frac{1}{a_2} \ln \frac{u_i}{a_1}$$

D-1-4

Eq. D-6 has been used in computer program GME

## D-2 Box and Muller Method:

### D-2-a Normal distribution:

Box and Muller (1958) have shown that if  $U_1$  and  $U_2$  are two independent standard uniform variates, then the following functions

$$N_1 = (-2 \ln U_1^{1/2}) \cos 2 \pi U_2 \quad \text{D-2-1}$$

$$N_2 = (-2 \ln U_1^{1/2}) \sin 2 \pi U_2 \quad \text{D-2-2}$$

constitute a pair of statistically independent standard normal variates. See Box et al. (1938) for derivation. Therefore, if  $U_1$  and  $U_2$  are a pair of independent uniformly distributed random numbers, a pair of independent random variables from a normal distribution  $N(\mu, \sigma)$  may be generated by

$$X_1 = \mu_1 + N_1 \sigma_1 \quad \text{D-2-3a}$$

$$X_2 = \mu_2 + N_2 \sigma_2 \quad \text{D-2-3b}$$

These formulations have been used in the computer program MFD and MFE.

### D-2-b Multi-Normal Random Distribution:

In this section, we will define the multi-normal distribution and describe the way to find its distribution. Multivariate normal density function for trivariate can be defined as follows:

$$f(z) = \frac{1}{|V|^{1/2} (2\pi)^{p/2}} \exp - 1/2 (z - \mu)' V^{-1} (z - \mu) \quad D-2-4$$

$$z = \begin{pmatrix} z_1 \\ z_2 \\ z_3 \end{pmatrix} \quad \mu = \begin{pmatrix} \mu_1 \\ \mu_2 \\ \mu_3 \end{pmatrix}$$

$$V = \text{covariance matrix} = \begin{pmatrix} \sigma_{11} & \sigma_{12} & \sigma_{13} \\ \sigma_{21} & \sigma_{22} & \sigma_{23} \\ \sigma_{31} & \sigma_{32} & \sigma_{33} \end{pmatrix}$$

It is a symmetric matrix with  $\sigma_{ii}$  = the variance and  $\sigma_{ij}$  = the covariance

The correlation coefficient:

$$\rho_{jk} = \frac{\sigma_{jk}}{\sqrt{\sigma_{jj} \sigma_{kk}}}$$

D-2-5,

We consider a general equation of the following form (see Mood and Graybill(1963)):

$$Z = \mu + N S.F$$

D-2-6

Where S.F 3x3 matrix which is function of mean values and the covariance matrix and the matrix N is the standard normal variate. By using the concept of the mathematical statistics (see Mood and Graybill(1963)), we can generate the values of  $Z_1, Z_2$ , and  $Z_3$  from Eq. D-2-6.

$$Z_3 : N(\mu_3, \sigma_{33})$$

D-2-7

$$Z_2 : N(E(Z_2 | Z_3), \sigma_{22})$$

D-2-8

$$E(Z_2 | Z_3) = \mu_2 + \frac{\rho_{23} \sigma_{23}}{\sigma_{33}} (Z_3 - \mu_3)$$

D-2-9

$$\sigma_{22|3} = \sigma_{22} \sqrt{1 - \rho_{23}^2}$$

D-2-10

$$Z_1 : N(E(Z_1 | Z_2, Z_3), \sigma_{11|2,3})$$

D-2-11

$$E(Z_1 | Z_2, Z_3) = \mu_1 + \frac{(\rho_{12} \sigma_{23} + \rho_{13} \sigma_{22})}{(1 - \rho_{23}^2) \sigma_{22}} (Z_2 - \mu_2)$$

$$+ \frac{(\rho_{13} - \rho_{12}\rho_{23}) \sigma_{11}}{2} (z_3 - \mu_3) + \frac{(1 - \rho_{23}^2) \sigma_{33}}{2} (z_3 - \mu_3) \quad \text{D-2-12}$$

$$\sigma_{z_1, z_2, z_3} = \sigma_{11} \sqrt{1 - \frac{(\rho_{13}^2 - \rho_{12}\rho_{23})^2}{(1 - \rho_{23}^2)}} \quad \text{D-2-13}$$

Hence, we can generate the normal variates of  $z_1, z_2$ , and  $z_3$  as same procedures as the single normal variable, i.e., by using their means and standard deviations (Eqs.9,10 for  $z_2$ , Eqs. 12, 13 for  $z_3$ ). Therefore if we input the means and standard deviations of the  $z_3, z_2$ , and  $z_1$  in Eqs.7,8 and 11 we can define their normal distribution. These formulations will be used in the computer programs MFD and MFE.

### D-3 Discrete Random Variable:

The uniformly distributed random numbers will be also used for generating the discrete probability distribution. The discrete probability distribution can be developed from the following equation, Abromowizz (1965) and Ang et al. (1983).

$$F(x_{j-1}) < u < F(x_j)$$

D-3-1

Hence for Poisson-distributed random variable  $X$  with parameter  $\mu$ , we can have the following form:

$$\exp(-\mu) \sum_{i=0}^{j-1} \frac{(\mu)^i}{i!} < u < \exp(-\mu) \sum_{i=0}^j \frac{(\mu)^i}{i!}$$

D-3-2

Where  $j$  is the value of the random variable.

There is another method (Rubinstein (1981)) for large  $\mu$ ; the Poisson distribution may be approximated by the Normal distribution with mean  $\mu - (1/2)$  and standard deviation  $\sqrt{\mu}$ . Hence, to generate a poisson distributed random variable, a value  $x$  may first be generated from normal distribution  $N(\mu-1/2, \sqrt{\mu})$  as described before and round off  $x$  to the nearest integer, and set Poisson distribution parameter equal to that integer. We have used this approximation for our analysis in computer program GEM.

**APPENDIX E****E- EXPERIMENTAL DATA:**

We have used the experimental program of Turcott(1988) for the models applications, see Turcott(1988) for detailed description and discussion of this program. However, we will give a very brief account of the experiment.

The clay used in this study was a kaolinite clay identified as hydrite UF from Georgia Kaolin.

Some of its engineering properties were as follows,

L.L. : 67.7 %

P.L. : 32.7 %

P.I. : 35.0 %

Size of particles: .2  $\mu$ m  $\rightarrow$  .6  $\mu$ m.

**Equipment:** Confined compression (oedometer test) non-standard, i.e., it has diameter of 6.25 mm and height range from 10mm  $\rightarrow$  11mm.

**Test condition:** Fully saturated sample, double drainage (top and bottom), and each test runs under constant load. It should be noted that all three tests were



incremented from zero load.

The test output which are represented by bulk strain-time are given in Figs. E-1, 2, and 3.

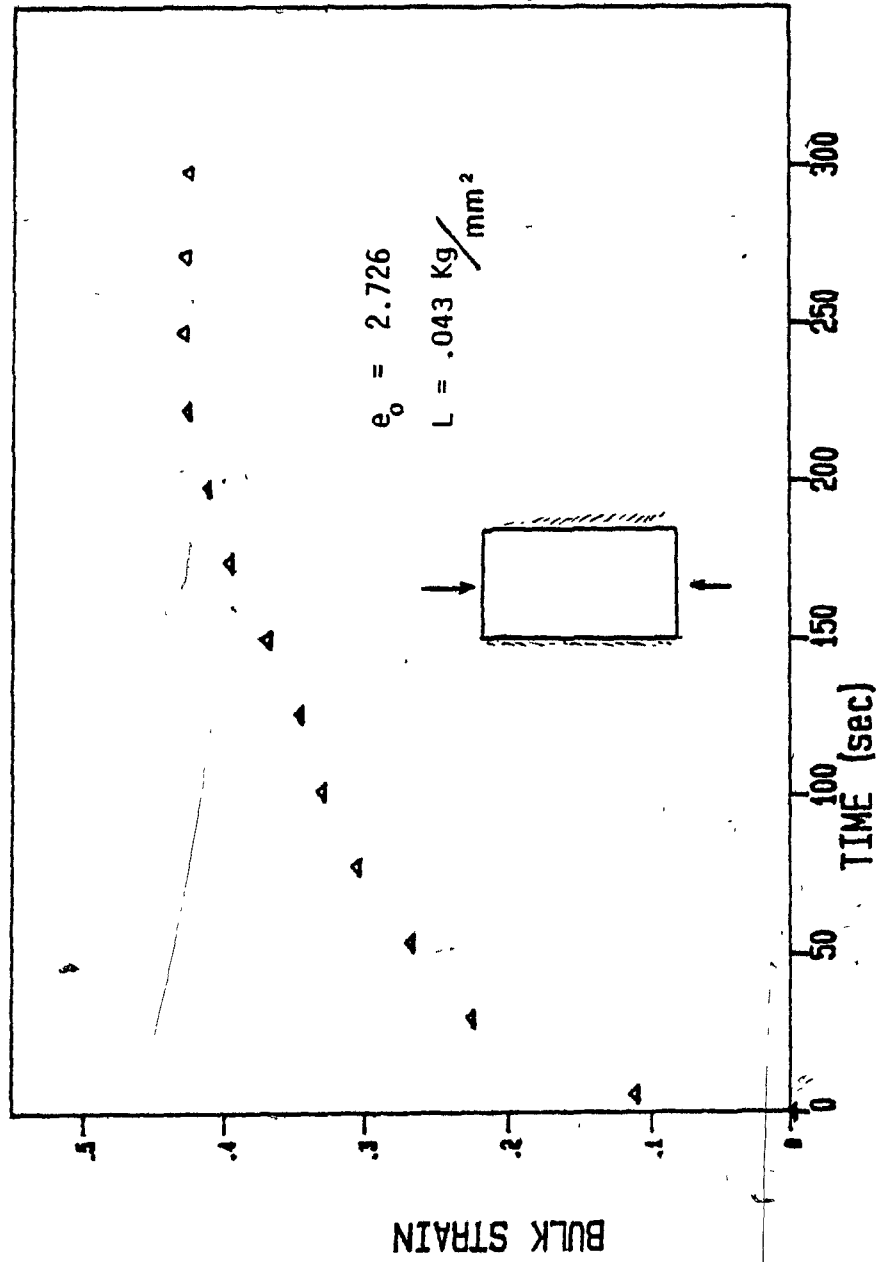


Fig.E-1 Bulk strain versus time

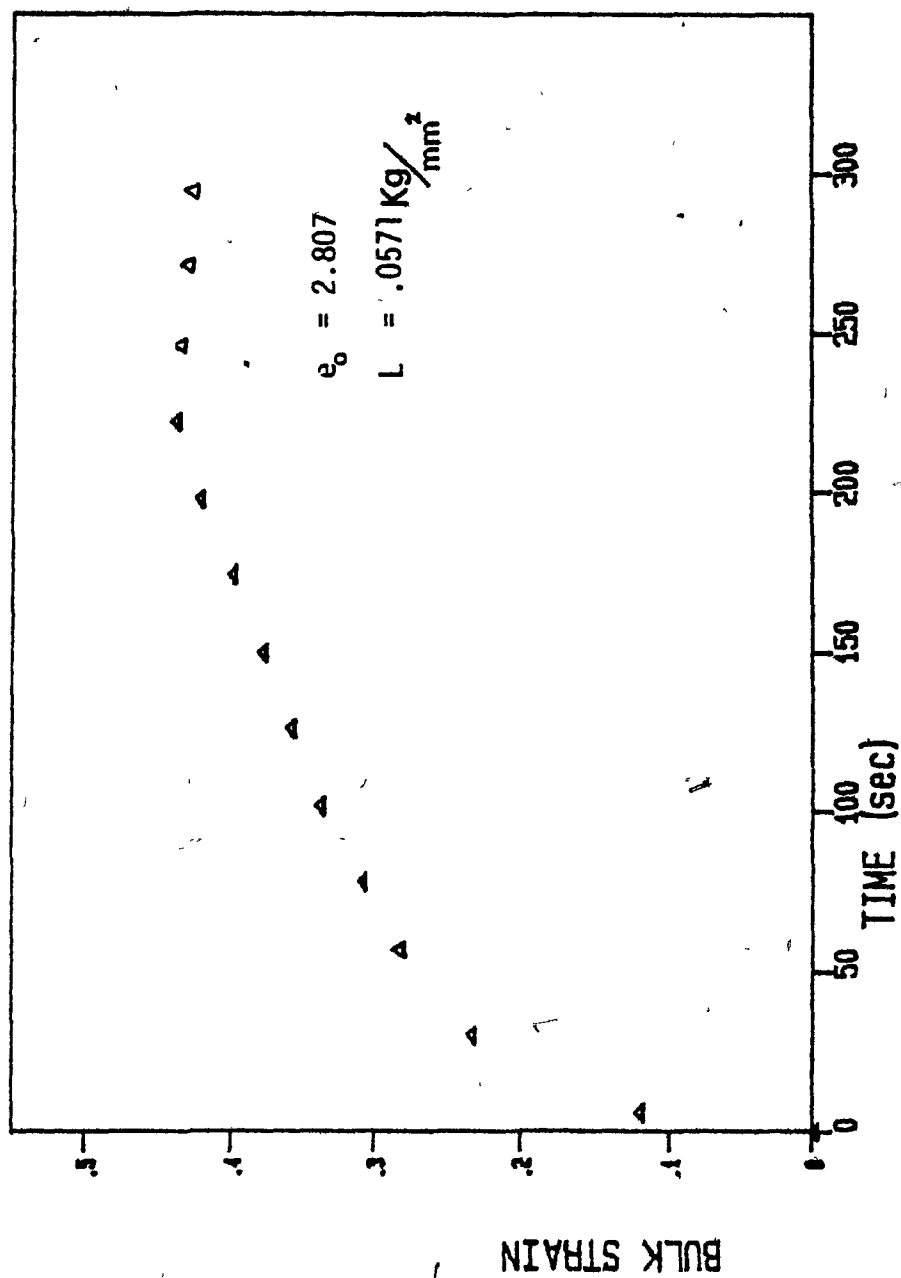


Fig.E-2 Bulk strain versus time

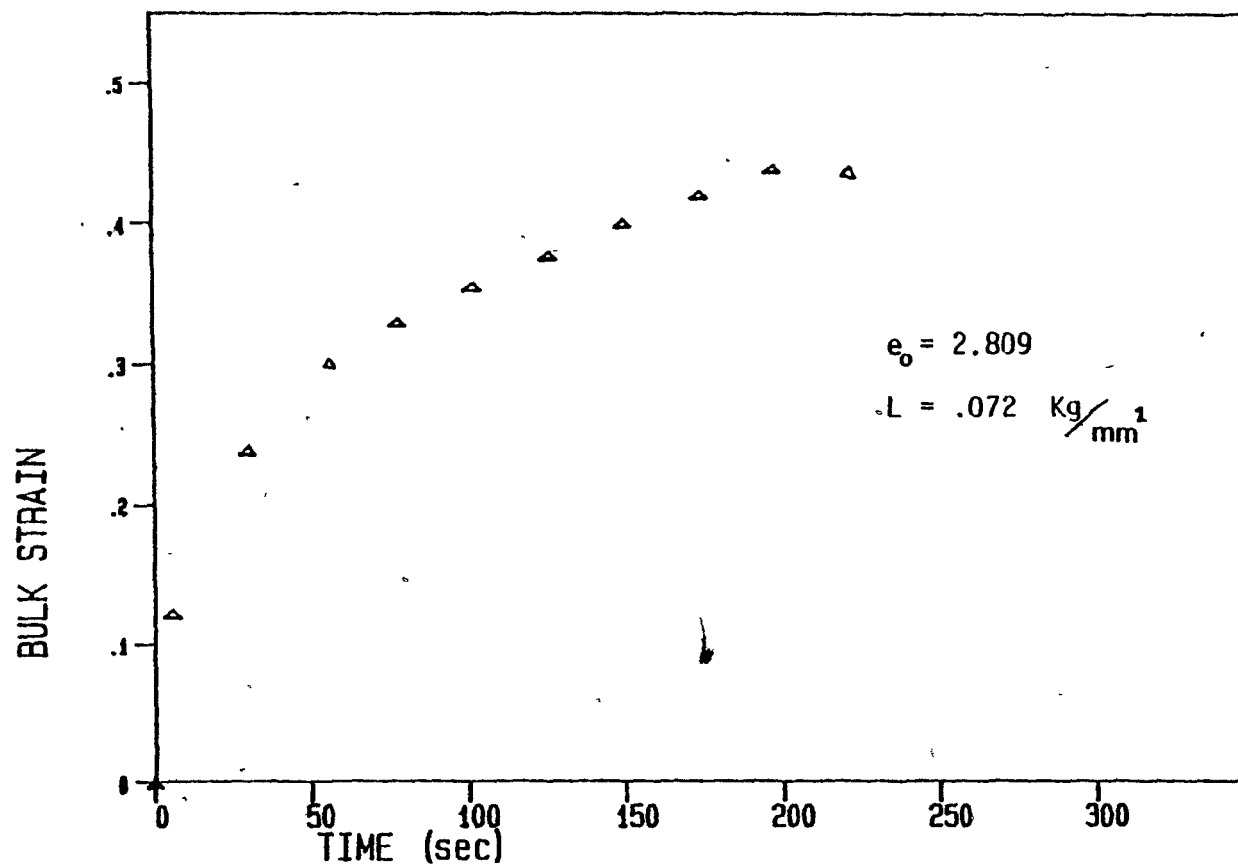


Fig.E-3 Bulk strain versus time

**END**

**20·1|0·|89**

**FIN**

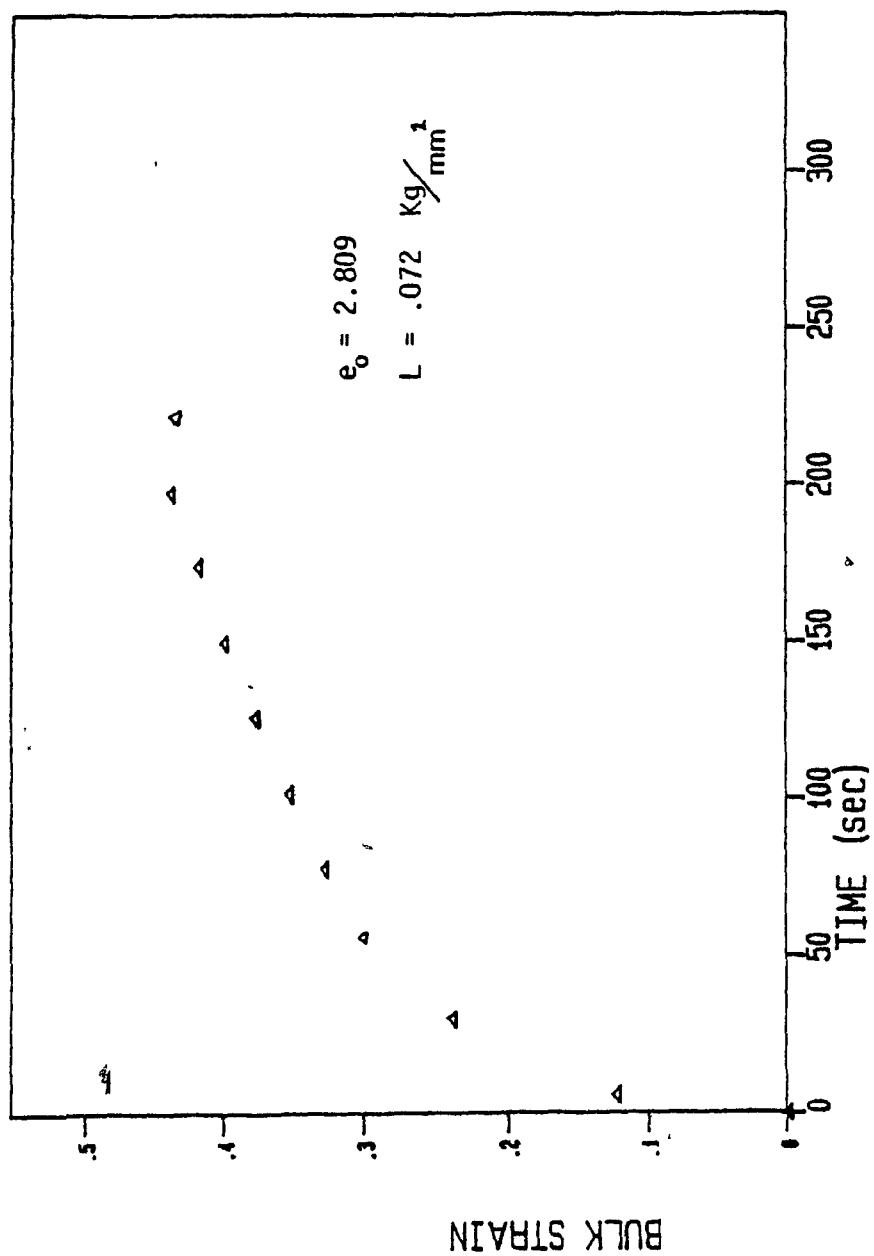


Fig.E-3 Bulk strain versus time